During the past few decades, there has been quite some development and increased professional use of tools to simulate the processes that are involved in analysis of the heat, air and moisture (HAM) conditions in buildings. Researchers are striving to advance the possibilities to calculate the integrated phenomena of heat, air and moisture flows in the buildings while including the interactions that take place between the various building materials, components, and room air, as well as the influences due to occupants and Heating, Ventilation and Air-Conditioning (HVAC) systems.

In this thesis, a more accurate assessment of HAM conditions in the building is obtained by modeling and coupling a sub-zonal airflow model, which describes the varying, non-uniform indoor environmental conditions near a building component with a HAM component model.

DTU Civil Engineering
Department of Civil Engineering
Technical University of Denmark

Brovej, Building 118
2800 Kgs. Lyngby
Telephone 45 25 17 00

www.byg.dtu.dk

ISBN: 9788778772954
ISSN: 1601-2917

Paul Steskens

Modelling of the hygrothermal interactions between the indoor environment and the building envelope

Report R-216 2009

DTU

Modelling of the hygrothermal interactions between the indoor environment and the building envelope

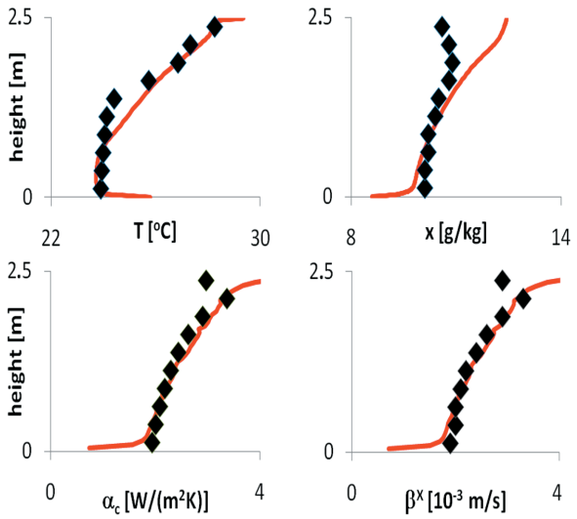

Paul Steskens

PhD Thesis

Department of Civil Engineering
2009

DTU Civil Engineering Report R-216 (UK)
December 2009

DTU Civil Engineering
Department of Civil Engineering

Modelling of the Hygrothermal Interactions between the Indoor Environment and the Building Envelope

Paul Steskens

BYG·DTU – Department of Civil Engineering
Technical University of Denmark

2009

Supervisors: Carsten Rode
Hans Janssen
Morten Hjorslev Hansen
Birgitte Dela Stang

Preface

This PhD thesis is part of the project *Model for Multidimensional Heat, Air and Moisture (HAM) Conditions in Building Envelope Components*, and has been initiated by Professor Carsten Rode, and Senior Researchers Morten H. Hansen and Birgitte Dela Stang. The project was a cooperation between the Department of Civil Engineering (BYG) of the Technical University of Denmark, and the Danish Building Research Institute (SBi) with financial funding by the Danish Council for Independent Research | Technology and Production Sciences (Det Frie Forskningsråd | Teknologi og Produktion (FTP)), which is gratefully acknowledged. The project has been supervised by Professor Carsten Rode (BYG ·DTU) and Associate Professor Hans Janssen (BYG ·DTU), and Senior Researchers Morten H. Hansen and Birgitte Dela Stang.

The thesis is a monograph, which served as a basis for a journal paper and three conference papers. Moreover, during the project it was possible to cooperate with the Building Energy and Environmental Systems Laboratory at the Syracuse University. The research presented in this thesis contributed to the development of the CHAMPS software for Combined Heat, Air, Moisture and Pollutant Simulations in buildings.

The international collaboration and academic discussions with other members, who participated in the development of the software for Combined Heat, Air, Moisture and Pollutant Simulations (CHAMPS) are highly appreciated and have certainly contributed to improve the project. Within this group special thanks go to Professors Jianshun Zhang and John Grunewald, as well as to Andreas Nicolai from Syracuse University and Dresden University of Technology, for hosting my 6 month research stay at the Building Energy and Environmental Systems Laboratory with fruitful supervising. The research stay was supported by private funds Larsen & Nielsen Fonden, Otto Mønsteds Fond, Poul V. Andersen Fond, E. Hegenthofts Legat, and Lemvigh-Müller & Much Fonden, and their funding is thankfully appreciated.

This study could not have been completed without help from a number of people, and I would like to express my gratitude to all who in one way or another have contributed. Special thanks go to my supervisors Carsten Rode and Hans Janssen, who guided and encouraged me and always generously shared both time and knowledge with me. I would like to thank my co-supervisors Morten H. Hansen and Birgitte D. Stang for their valuable advice, guidance and discussions. Furthermore, I would like to acknowledge Ernst Jan De Place Hansen for his technical and scientific advice as a collaborator in our common project.

I will also express my gratitude to all my colleagues at the Department of Civil Engineering and particularly the section of Building Physics and Services for the nice working and social environment. They always made work and life more enjoyable especially due to the traditional coffee breaks and social events.

At last I want to thank the people, with whom I have a very close relationship. Thanks to all my friends and my family for your love, trust, and support.

Lyngby, August 2009

Paul Steskens

Summary

Within building physics, it is generally accepted that moisture and temperature levels – and their variations in time and space – play a crucial role in the degradation processes of building components, in the (perceived) quality of the interior environment in a building and the energy used by the heating, ventilation, and air-conditioning (HVAC) system. During the past few decades, there has been quite some development and increased professional use of tools to simulate the processes that are involved in analysis of the heat, air and moisture (HAM) conditions. Currently, researchers are striving to advance the possibilities to calculate the integrated phenomena of heat, air and moisture flows in the buildings while including the interactions that take place in buildings between the various building materials, components, and room air, and the influences due to occupants and Heating, Ventilation and Air-Conditioning (HVAC) systems.

The heat, air and moisture conditions in a building component are dependent of the boundary conditions, i.e. the indoor and outdoor climate conditions. Due to the spatial variability of these climatic conditions, caused by local heat and moisture sources, imperfect mixing and microclimatic effects, the temperature and relative humidity in the neighbouring air are seldom uniform. Similarly, the convective surface heat and moisture transfer coefficients vary in space, due to their strong dependence on for example the local air velocity and the local temperature. The main requirement for a successful modelling of the hygrothermal interaction between the building component and the indoor environment is the correct treatment of the interfacial flows at the boundaries.

Current HAM component models consider the indoor environmental conditions and surface transfer coefficients to be uniform. In order to get a better prediction of the interaction between the indoor environment and the building component, different options with respect to the modelling of the local indoor environmental conditions and local convective surface transfer coefficients are available: a first of option is a nodal or multi-zone model, which considers the indoor environmental conditions to be uniform. Second, a computational fluid dynamics models (CFD) model, which is capable of predicting the local temperature and relative humidity near a building component as well as the local surface transfer coefficients, can be used. However, detailed CFD models cannot easily and quickly solve time-dependent hygrothermal interactions across the boundaries of a building model, are computational intensive and not suitable for transient HAM calculations over a longer period of time. Third, sub-zonal airflow models, which describe the airflow in the zone of a building, can be used. Sub-zonal models are able to perform transient calculations over a relatively long period of time, while the computational effort is relatively small. However, the models are in general not capable of providing very detailed information about the local conditions in the room compared to CFD.

The main objective of the research presented in this thesis is to obtain a more accurate assessment of the heat, air and moisture conditions in the building component and the zone by modelling and coupling a sub-zonal airflow model, which describes the varying, non-uniform indoor airflow near a building component with a HAM component model. Compared to the multi-zone/nodal airflow models, a sub-zonal model may lead to a relatively accurate prediction of the local temperature and relative humidity near the building component and convective surface transfer coefficients. Similarly, the relatively short computation time still enables an efficient coupling with the HAM component model.

First of all, a literature study focussing on the modelling of the hygrothermal interaction between the HAM transport in the building component and the indoor environment near the component was carried out. Approaches to model the non-uniform indoor airflow near the building component have been evaluated and compared. Advantages, disadvantages and limitations of the developed models were examined. The literature review showed that CFD applications for indoor airflow simulation have achieved considerable successes and serve as a valuable tool for predicting airflow, temperature and relative humidity distributions in enclosed environments as well as the local convective surface transfer coefficients. However, there are many factors influencing the results predicted. CFD results should be analyzed with care, and validation with experimental results is always required. Nevertheless, detailed airflow models cannot easily and quickly solve time-dependent hygrothermal interactions across the boundaries of a building model. In practice, only steady-state simulations of the airflow in a single room at a specific time, and/or transient simulations over a relatively short period of time, for example a diurnal cycle, are feasible. And, since these calculations are relatively computational intensive, transient calculations over a longer period of time are currently not

possible. In addition, the review of the literature demonstrated that the sub-zonal modelling approach can be a suitable method to estimate temperature and relative humidity fields in a room with reasonable accuracy. However, studies on the ability of sub-zonal airflow models to provide an accurate prediction of the local indoor environmental conditions near a building component and of the local convective surface transfer coefficients have not been reported so far.

Second, the influence of the non-uniform surface transfer coefficients, due to local indoor environmental variations, was analyzed. A parameter study has been used to investigate how the magnitude of the surface transfer coefficients - resulting from the air velocity near the surface of a building component - influences the hygrothermal conditions in the building component and the indoor environment. Three building component configurations (calculation objects) were selected for analysis: two insulated wall elements and a thermal bridge. The study resulted in the following conclusions:

- While the influence of the convective surface transfer coefficients on the HAM conditions on the surface of the insulated walls was limited, this influence was relatively large when considering a thermal bridge.
- Focusing on the hygrothermal performance of the walls, the analysis showed that the influence of the convective surface heat transfer coefficient on the hygrothermal performance is relatively large compared to the influence of the convective surface moisture transfer coefficient. With respect to the analyzed building components, the investigations showed that assuming an average value for the convective surface moisture transfer coefficient is acceptable, while assuming an average value for the convective surface heat transfer coefficient is not acceptable.
- With respect to the hygrothermal performance of the thermal bridge, the influence of both the convective surface heat and moisture transfer coefficient on the hygrothermal performance is relatively large. The analysis showed that assuming an average value for these coefficients is not acceptable.
- The influence of both the surface heat transfer coefficient and the surface moisture transfer coefficient on the heat and vapour exchange between the building component and the indoor environment as well as the buffering capacity of the building component is relatively large. Assuming average values for the surface transfer coefficients may introduce relatively large errors in the prediction of these fluxes and the prediction of the indoor environmental conditions.

Third, the capability and applicability of the sub-zonal airflow model to predict the local indoor environmental conditions near the building component as well as the local non-uniform surface transfer coefficients has been investigated. Three test cases for respectively natural, forced and mixed convection in a room have been analyzed. The indoor environmental conditions in the room predicted from the sub-zonal airflow models have been compared to experimental results and numerical results obtained from CFD. Moreover, the predicted surface transfer coefficients are compared with numerical results from CFD. The sub-zonal models have been compared to CFD models based on two criteria: First, the ability of the model to predict the local air velocity, temperature and relative humidity near the building component. Second, the capability of the model to predict the local convective surface transfer coefficients. Furthermore, the efficiency, accuracy, computational effort (or simulation time), and flexibility of the models is evaluated. The following has been concluded from this work:

- For natural convection, the sub-zonal model is able to give a prediction of the temperature and vapour content distribution in the room, with a maximum relative deviation between approximately 10% and 15% compared to the temperatures and vapour contents predicted by CFD. (The relative maximum deviation is defined as the maximum deviation between a quantity predicted by the sub-zonal model and the quantity predicted by CFD, divided by the quantity predicted by the CFD model).
- Regarding forced convective airflow, the model showed to be applicable to give a rough prediction of the global temperature and vapour content distribution in the room with a maximum relative deviation of approximately 10%. If local recirculation of the airflow is present, the relative deviation increases up to 25% for the local temperature and 30% for the local vapour content. The surface transfer coefficient model gave relatively good results for regions where

recirculation does not take place, while the relative deviation is approximately 30%. The model cannot be applied in regions where local recirculation of the airflow takes place.

- For mixed convection, the application of a sub-zonal airflow model to predict the indoor environmental conditions and surface transfer coefficients showed to be limited. Relatively large deviations up to 40% regarding for both the global and local conditions in the room have been observed. It was possible to give a relatively accurate prediction of the local convective surface transfer coefficients with a maximum relative deviation of 20% in the part of the room where natural convection is dominating. However, where forced convective airflow was dominating locally, it was not feasible to predict the local convective surface transfer coefficients and deviations up to factor 2 and higher have been observed.

The study showed that sub-zonal models combined with an appropriate surface transfer coefficient model are able to give a prediction of the indoor environmental conditions in a room under natural or forced convective conditions. However, one important remark should be made. In the case studies, reference conditions, for example experimental data or numerical results from CFD, have been used for the development of a reliable sub-zonal airflow model. The availability of such reference conditions is a prerequisite for the development of a reliable sub-zonal model. In addition, the main advantage of the sub-zonal model is a significant reduction in computational effort compared to CFD. The computation time of a sub-zonal airflow model with a surface transfer coefficient model implemented generally varies between a few seconds up to 20 seconds, compared to several hours up to a few days for a CFD simulation.

Fourth, the hygrothermal performance of a building zone and building envelope was investigated using a coupled whole-building HAM simulation. The sub-zonal airflow model is coupled to a HAM building component model. A case study has been used for analysis: four models have been applied to model the indoor environmental conditions and the convective surface transfer coefficients in the room. The predicted hygrothermal conditions on the internal surface of the building components predicted by the different models have been compared. Based on the investigations it is concluded that:

- Regarding the surface temperature and relative humidity on the surface of the building component, a relatively large relative difference up to approximately 10% has been observed between the separate HAM component models with lower and upper limits for the convective surface transfer coefficients.
- Considering the hygrothermal conditions predicted by the coupled HAM component and sub-zonal model and the coupled HAM component and nodal model smaller differences with a maximum relative difference of 5% have been observed.

The differences between the nodal model and the sub-zonal model showed to be relatively small and the case study showed to be less suitable for demonstrating the influence of the varying local indoor environmental conditions and surface transfer coefficients on the hygrothermal conditions on the surface of and in the building component. It is recommended for future research to apply the coupled HAM component model and sub-zonal airflow model for investigations considering other cases which may result in larger excitations of the indoor environmental conditions.

It is concluded that the coupled HAM component model and sub-zonal model provided detailed information of the local environmental conditions in the building zone near the building component, i.e. the local air temperature, and relative humidity, of the local conditions in the building component, and detailed information regarding the local convective surface transfer coefficients. Moreover, the model showed to be suitable for transient heat, air and moisture simulations of the component-indoor air interaction.

Resumé

Inden for bygningsfysikken accepteres det sædvanligvis, at fugt- og temperaturniveauer – og deres variation i tid og rum – spiller en afgørende rolle for byggekomponenters nedbrydningsprocesser, for den (opfattede) luftkvalitet i bygninger, og for den energi, der bruges til opvarmning, ventilation og køling (på engelsk forkortet HVAC: Heating, Ventilating and Air-Conditioning). I løbet af de seneste årtier har der været en udvikling og øget professionel brug af værktøjer til at simulere og analysere processer for varme-, luft- og fugtforhold (HAM: Heat, Air and Moisture). Aktuel forskning drejer sig om at fremme mulighederne for at beregne integrerede varme-, luft- og fugtstrømme i bygninger og samtidig inkludere de vekselvirkninger, der finder sted imellem byggematerialer, byggekomponenter og rumluft, såvel som påvirkninger fra brugere og fra varme-, ventilations-, og kølesystemer. Gængse beregningsmodeller for varme-, luft- og fugttransport i konstruktioner forudsætter ensartede klimamæssige betingelser indendørs og ensartede overgangskoefficienter for den konvektive varme- og fugttransport ved overfladerne. For at få en bedre forudsigelse af vekselvirkningen mellem indeklimaet og byggekomponenterne, er der flere forskellige valgmuligheder med hensyn til, hvordan de lokale indeklimabetingelser og de lokale overgangskoefficienter kan modelleres: Der kan benyttes knudepunkts- eller multi-zone modeller, CFD-modeller (Computational Fluid Dynamics) og subzone-modeller. Med subzone-modeller kan der foretages instationære beregninger over lange tidsperioder, selvom beregningsarbejdet er relativt begrænset. Imidlertid er disse modeller, sammenlignet med CFD, i almindelighed ikke egnede til at skaffe meget detaljerede informationer om de lokale forhold i rummet.

Hovedformålet med undersøgelsen, der er præsenteret i denne afhandling, er at opnå en nøjagtigere vurdering af de hygrotermiske forhold i bygningsdele og rum ved at koble en model for varme-, luft- og fugttransport i konstruktioner med en subzone-luftstrømningsmodel, der beskriver de uensartede indeklimabetingelser nær bygningsdelene.

Denne rapport omfatter:

- en litteraturundersøgelse, der fokuserer på modellering af den hygrotermiske vekselvirkning mellem varme-, luft- og fugttransport i en byggekomponent og i indeklimaet nær ved komponenten;
- en parameterundersøgelse for at undersøge, hvordan størrelsen af overgangskoefficienterne påvirker de hygrotermiske forhold i byggekomponenten og i indeklimaet;
- en undersøgelse af ydeevne og anvendelighed af subzone-luftstrømningsmodellen til at forudsige de lokale indeklimabetingelser nær ved byggekomponenten såvel som de lokale variationer i overgangskoefficienterne;
- en koblet varme-, luft- og fugttransportmodel for hele bygningen, hvormed der kan udføres en samlet analyse af den hygrotermiske tilstand i rum og klimaskærm.

Undersøgelsen har vist at subzone-modeller kombineret med en passende model for overgangs-koefficienterne kan give en forudsigelse af indeklimabetingelserne i et rum under betingelser med både naturlig og tvungen konvektion. Der skal dog tilføjes en vigtig kommentar: I de casestudier, der er arbejdet med i projektet, er der brugt referencebetingelser, fx forsøgsdata eller numeriske resultater fra CFD, til at udvikle subzone-luftstrømningsmodellen med. Tilgængeligheden af sådanne referencebetingelser er en forudsætning for at udvikle en pålidelig subzone-model. Hovedfordelen ved subzone-modellen er en betydelig reduktion i beregningsarbejdet sammenlignet med CFD.

Contents

1 Introduction

The global climate is changing: measurement data over the last centuries indicate that the global climate is changing, and scientific research predicts that this change will continue, albeit with ongoing discussion on the predicted rate of change [1]. Concern over climate change has reached the highest levels of government, with nations trying to address climate change at international level as exemplified by the Kyoto Protocol, calling 'climate change the world's greatest environmental challenge'. Amongst many other impacts, climate change will undoubtedly impact the hygrothermal performance of buildings, having an effect on the durability of the building envelope, the comfort and quality of the indoor environment, as well as on the energy consumption for the heating, cooling and ventilation needed to maintain this environment.

Most effort concerning the built environment and climate change has focused on actions and measures for climate change mitigation, by making buildings more energy efficient, thus reducing the production of greenhouse gasses. Given the long lifespan of buildings, it is certain that today's building stock and the projects currently under design and construction will be operating under different climate conditions in 40–70 years from now [2]. Building architects and engineers have a strong need to predict the influence of these climatic conditions on the building performance, the building's energy consumption and production of green house gasses over this relatively long period of time.

A major source of new information on the performance of building design could be provided by simulation models. Computer simulation might be the most appropriate technique to study the hygrothermal behaviour of buildings in the climate of the future. It allows the performance assessment of a complex system like a building under predicted operational conditions, and allows the investigation of the impact of individual factors, such as the building's configuration and parameters, operational regimes, occupant behaviour, and climate conditions, on the overall hygothermal behaviour.

1.1 Background

Within building physics, it is generally accepted that moisture and temperature levels – and their variations in time and space – play a crucial role in the degradation processes of building components, in the (perceived) quality of the interior environment in a building and the energy used by the heating, ventilation, and air-conditioning (HVAC) system. Research has shown that the temperature and relative humidity in a building influence the deterioration of furnishings, the mould growth on building surfaces, and the durability of building components. The Danish Building Defects Fund's annual reports (e.g. [3]) shows that most building damages are related to moisture such as due to the insufficient performance of vapour barriers [4], rot decay in outdoor wooden constructions, wetting from thermal bridges, and a lack of ventilation. Generally, the list of damages clearly points out that the local hygrothermal conditions play an important role. Similarly, it has been shown that the interior moisture and temperature levels are essential factors in the occupants' comfort and the perception of indoor air quality (IAQ). High relative humidity favours house dust mites, moulds and bugs [5]. Moreover, the temperature and relative humidity in a building influences the energy consumed for air-conditioning, i.e. the HVAC system controls the indoor environmental conditions in such a way that a comfortable indoor climate is maintained. However, the HVAC system may consume a significant part of the total building energy consumption.

The moisture and temperature conditions inside a building are highly dependent on the material combinations, the climate conditions on both sides of the construction and of building usage. The heat, air and moisture flows that are generated inside a building, that traverse the enclosure and the flows injected by the HVAC system continuously interact with each other. Airflows, generated by air pressure differences inside and outside buildings, may impact the ingress of harmful gasses such as radon and change the heat, air and moisture (further-on called HAM) response of the envelope. Resulting moisture deposits in the envelope may negatively affect energy consumption. Moisture from inside and heat and moisture from outside attack the envelope's durability.

Previous research has shown that the accurate assessment of hygrothermal conditions in building zones and components is highly dependent on the description of the heat and moisture exchange between zones and components [6]. More concretely, it has been demonstrated that the local indoor environmental

conditions and local surface transfer coefficients are important with respect to the hygrothermal response of building components [7] [8], the annual heating load predictions of a building [9], local microclimatic conditions [10], heat and moisture buffering of internal surfaces [10] [11], historic brick wall buildings [12], and conservation of culturally valuable objects in historical buildings [13]. The observations and conclusions from these studies served as an important motivation for the research presented in this thesis. Therefore, these findings are summarized shortly.

Regarding the hygrothermal response of building components, Holm [7] numerically investigated the influence of the indoor and outdoor climatic conditions through a sensitivity analysis. The author concluded that the moisture content in the building component, and thus the component's performance, is directly susceptible to the assumed surface conditions and surface transfer coefficients. Similarly, Janssen et al. [8] indicated that the hygrothermal conditions in building components are sensitive to the model applied for the external surface heat and moisture transfer coefficient.

Beausoleil-Morrison [9] reviewed the impact of the convective surface heat transfer coefficients in a building on the annual heating load predictions. He reported that numerous researchers have examined the sensitivity of simulation predictions to the modelling of internal convection. They have demonstrated that predictions of building energy demand and consumption can be strongly influenced by the choice of the convective surface heat transfer coefficient. The author [9] developed a method that is able to resolve the impact that HVAC systems have upon room convective regimes. Two case studies were used to investigate this influence. It is concluded that the total annual heating load predictions of an energy efficient house were found to increase by up to 3.3%, while the method had an even greater impact on the simulation of a typical office building conditioned with an air-based heating and cooling system. In this case, the method increased the predicted annual heating load by 9% and the cooling load by 19%.

Mortensen [10] demonstrated that the local indoor environmental conditions and local surface transfer coefficients are important in microclimates, such as a local area within a room where the climate varies from that of surrounding areas due to a variety of influencing factors. Critical microclimates are often found near thermal bridges, like corners or behind furniture placed close to poorly insulated walls.

Other investigations [10] [11] concluded that the influence of the local indoor environment and convective surface transfer coefficient is relatively large when considering the moisture buffering effect of internal surfaces. Roels *et al*. [11] determined the influence of the surface film resistance on the Moisture Buffer Value (MBV) for several building materials. The authors demonstrated a significant influence on the obtained results: a lower surface film resistance resulted in a higher MBV. The biggest influence was found for the most permeable materials and for very high values of the surface film resistance.

Furthermore, Abuku *et al*. [12] presented the hygrothermal simulation of a (historical) tower with brick walls of 29 cm thickness susceptible to German climatic conditions and wind driven rain loads. In the study, wind-driven rain formed the key moisture supply source for permeable building facades, with only a (very) secondary role for vapour supply. The main removal role, on the other hand, was taken up by evaporative drying: the convective water vapour transport from the surface to the air. The major uncertainty when modelling evaporative drying is the surface moisture transfer coefficient. The authors exemplified the sensitivity of the moisture responses to the surface moisture transfer coefficient and showed that the moisture responses of historic brick facades are sensitive to the modeling of evaporative drying. Abuku showed that drying of the building component via the internal surface forms an important moisture source for the building zone. The description of the moisture exchange will thus affect both the building component and the building zone.

In addition, Steeman [13] presented the analysis of the local hygrothermal conditions and interactions between a historical building and culturally valuable objects, which are part of the building. The conservation of culturally or historically valuable objects sensitive to moisture related damage, poses a complex problem. To maintain these objects in good condition it would be best to store them in a climate which is as constant as possible, for instance in a depot. Yet typically these objects are located in museums or historical, often free-floating or free-running, buildings where they are exhibited or part of the interior. As a result, the objects are exposed to variations in the indoor climate caused by for example moisture loads induced by visitors or temperature loads generated by the heating systems. An accurate prediction of the local climatic conditions near the object enables the analysis of the impact of these conditions on the object itself and may prevent possible damage.

Finally, within the framework of the present study, a parameter study [14] was used to investigate how the hygrothermal conditions of the building component and environment varied with the magnitude of the surface transfer coefficients - resulting from the air velocity near the surface of the building component. From this work, it was concluded that while the influence of the convective surface transfer coefficients on the HAM conditions on the surface of insulated walls was limited, this influence was relatively large when considering a thermal bridge. Different surface temperature, relative humidity, and vapour pressures were predicted when different convective surface transfer coefficients were applied. The influence of both the surface heat transfer coefficient and the surface moisture transfer coefficient on the heat and vapour exchange between the building component and the indoor environment as well as the buffering capacity of the building component is relatively large. In consequence, when performing a hygrothermal performance analysis and simulation, it is important to take the local airflow velocity near the component into account. Assuming average values for the surface transfer coefficients may introduce relatively large errors in the prediction of these fluxes and the prediction of the indoor environmental conditions.

The studies that have been mentioned above indicated that the local environmental conditions and local surface transfer coefficients play an important role when considering the hygrothermal performance of building components and building zones. In the next section, the different methodologies and models with respect to the modeling of the local environmental conditions near a building component and the local surface transfer coefficients are considered. Moreover, the advantages, disadvantages and limitations of current models are discussed.

1.2 State-of-the-Art

During the past few decades, there has been quite some development and increased professional use of tools to simulate the processes that are involved in analysis of HAM conditions. Currently, researchers are striving to advance the possibilities to calculate the integrated phenomena of heat, air and moisture flows in buildings while including the interactions that take place between the various building materials, components, and room air, the influences due to occupants and Heating, Ventilation and Air-Conditioning (HVAC) systems. For example, researchers developed integrated simulation software by coupling a HAM component model with a multi-zone airflow model [15] [16], building energy simulation software and computational fluid dynamics (CFD) [17] [18], or a HAM component model with CFD [10][13][19].

The main requirement for a successful modelling of the hygrothermal interaction between the building component and the indoor environment is the correct treatment of the interfacial flows at the boundaries [6]. The heat, air and moisture conditions in a building component are dependent of the boundary conditions, i.e. the indoor and outdoor climate conditions. Due to the spatial variability of these climatic conditions, caused by local heat and moisture sources, imperfect mixing and microclimatic effects, the temperature and relative humidity in the neighbouring air are seldom uniform. Similarly, the convective surface heat and moisture transfer coefficients vary in space, due to their strong dependence on for example the local air velocity and the local temperature.

A general overview of the main features of current building simulation tools, focusing on the hygrothermal modelling and on the interactions between heat, air and moisture transfer mechanisms in buildings, has been reported by Woloszyn et *al*. [6]. The authors report a number of models, available for the simulation of the heat, air and moisture response of buildings and building components. While engineers have the option to use a whole building energy simulation (BES) model to investigate the thermal behaviour of the building, mainly focusing on the prediction of the annual energy consumption of a building, the building energy simulation tools have so far not been well suited to predict moisture transfer processes in buildings. With respect to the modelling of the indoor environment, three levels of granularity are available (Table 1).

In a first approach, the indoor environmental conditions are considered to be uniform, and represented by nodal or multi-zone models. The air in the building is considered to be well mixed. Such models are in general not suitable for obtaining information regarding the local conditions near the building component and an accurate prediction of the interaction between the indoor environment and the building component.

Second, when highly detailed simulations of airflow and hygrothermal conditions within a zone of a building are desired, the option consists of using computational fluid dynamics (CFD). CFD models are capable of predicting the local temperature and relative humidity near a building component as well as the local surface transfer coefficients. However, detailed airflow models cannot easily and quickly solve time-dependent hygrothermal interactions across the boundaries of a building model. In practice, only steady-state simulations of the airflow in a single room at a specific time, and/or transient simulations over a relatively short period of time, for example a diurnal cycle [20], are feasible. And, since these calculations are relatively computational intensive, transient calculations over a longer period of time are currently not possible.

Third, as an alternative for the use of CFD models, which are strongly limited by computer capacity, sub-zonal airflow models, which describe the airflow in the zone of a building, for example the airflow in a room, in part of the room, or the airflow near a building component, can be used. Sub-zonal models are able to perform transient calculations over a relatively long period of time, while the computational effort is relatively small. However, the models are in general not capable of providing very detailed information about the local conditions in the room compared to CFD.

Table 1: Granularity of airflow modeling

Nodal /multi-zone models	Sub-zonal models	Computational Fluid Dynamics
• Average temperature and relative humidity in a room. • No information about local quantities. • Transient • Short computation time • Average, uniform surface transfer coefficients	• Information about local conditions in the room. • Simplified airflow modeling • Transient • Short computation time • Average, uniform surface transfer coefficients	• Very detailed information about local conditions in the room. • Solving of Navier-Stokes equations • Steady-state • Long computation time • Local, non-uniform surface transfer coefficients

In conclusion, Section 1.1 indicated that the local environmental conditions and local surface transfer coefficients play an important role when considering the hygrothermal performance of building components. However, current HAM component models consider the indoor environmental conditions and surface transfer coefficients to be uniform. In order to get a better prediction of the interaction between the indoor environment and the building component, a different approach is needed. While computational fluid dynamics could be applied to get detailed predictions of the local environmental conditions and convective surface transfer coefficients, this approach is not (yet) feasible given the computational effort of such models. In this thesis, the applicability of sub-zonal airflow modelling for the prediction of the local environmental conditions and surface transfer coefficients is investigated.

1.3 Research Objectives and Methodology

The main objective of the work presented in this thesis is to obtain a more accurate assessment of the heat, air and moisture conditions in the building component and the zone by modelling and coupling a sub-zonal airflow model, which describes the varying, non-uniform indoor airflow near a building component with a HAM component model. Compared to the multi-zone/nodal airflow models, a sub-zonal model may lead to a relatively accurate prediction of the local temperature and relative humidity near the building component and convective surface transfer coefficients. At the same time, the relatively short computation time still enables an efficient coupling with the HAM component model.

The following methodology has been applied: First of all, a literature study focussing on the modelling of the hygrothermal interaction between the HAM transport in the building component and the indoor environment near the component was carried out. Approaches to model the non-uniform indoor airflow near

the building component have been evaluated and compared. Advantages, disadvantages and limitations of the developed models were examined.

Second, the influence of the non-uniform surface transfer coefficients, due to local indoor environmental variations, was analyzed. A parameter study has been used to investigate how the magnitude of the surface transfer coefficients - resulting from the air velocity near the surface of a building component - influences the hygrothermal conditions in the building component and the indoor environment.

Third, the capability and applicability of the sub-zonal airflow model to model the local indoor environmental conditions near the building component as well as the local non-uniform surface transfer coefficients has been investigated. Three test cases for respectively natural, forced and mixed convection in a room have been analyzed. The indoor environmental conditions in the room predicted from the sub-zonal airflow models are compared to experimental results and numerical results obtained from CFD. Moreover, the predicted surface transfer coefficients are compared with numerical results from CFD. The sub-zonal models have been compared to CFD models based on two criteria: First, the ability of the model to predict the local air velocity, temperature and relative humidity near the building component. Second, the capability of the model to predict the local convective surface transfer coefficient. Furthermore the efficiency, accuracy, computational effort (or simulation time), and flexibility of the models is evaluated.

Fourth, the hygrothermal performance of a building zone and building envelope is investigated using a coupled whole-building HAM simulation. The sub-zonal airflow model is coupled to a HAM building component model. A case study has been used for analysis. The model should provide detailed information of the local indoor environmental conditions in the building zone near the building component, and the conditions in the building component. In general, the model should be suitable for transient heat, air and moisture simulations of the component-indoor air interaction, provided the computation time is relatively short.

1.4 Outline

The outline of this thesis is as follows:

Section 2 presents a literature study that has been carried out. The study focused on the modelling of the hygrothermal interaction between the HAM transport in the building component and the indoor environment near the component. Approaches to model the non-uniform indoor airflow near the building component have been evaluated and compared. Advantages, disadvantages and limitations of the developed models were examined.

In Section 3, the influence of the non-uniform surface transfer coefficients, due to local indoor environmental variations, was analyzed. The results of a parameter study to investigate how the magnitude of the surface transfer coefficients - resulting from the air velocity near the surface of a building component - influences the hygrothermal conditions in the building component and the indoor environment are presented.

Section 4 describes the numerical modelling that has been applied for the modelling of the indoor environmental conditions and the local convective surface transfer coefficients. Moreover, numerical details and considerations considering the modelling of the indoor environmental conditions using sub-zonal airflow modelling are presented.

Section 5 presents the study of the capability and applicability of the sub-zonal airflow model to predict the local indoor environmental conditions near the building component as well as the local non-uniform surface transfer coefficients. Three test cases for respectively natural, forced and mixed convection in a room have been analyzed. The results from the sub-zonal airflow models have been compared to experimental results and numerical results obtained from CFD. Furthermore, the efficiency, accuracy, computational effort (or simulation time), and flexibility of the different models is evaluated.

In Section 6, the hygrothermal performance of a building zone and building envelope using a coupled whole-building HAM simulation was investigated. The sub-zonal airflow model is coupled to a HAM building

component model and a case study has been used for analysis. The results of a transient simulation of the heat, air and moisture transport in the building zone and the building component and the component-indoor air interaction are presented.

Section 7 presents the general conclusions and discussion.

2. Literature

The hygrothermal behaviour of buildings and building components has been researched for many years. The temperature and humidity of the indoor air are important factors influencing energy consumption of buildings, durability of building components, and comfort and health of building occupants. Indoor humidity depends on several factors, such as moisture sources, airflows, and moisture exchange with materials (Figure 1). All these phenomena are strongly dependent of each other. Researchers used both experimental methods and numerical modelling to investigate the interaction between the building envelope and the indoor and outdoor environment.

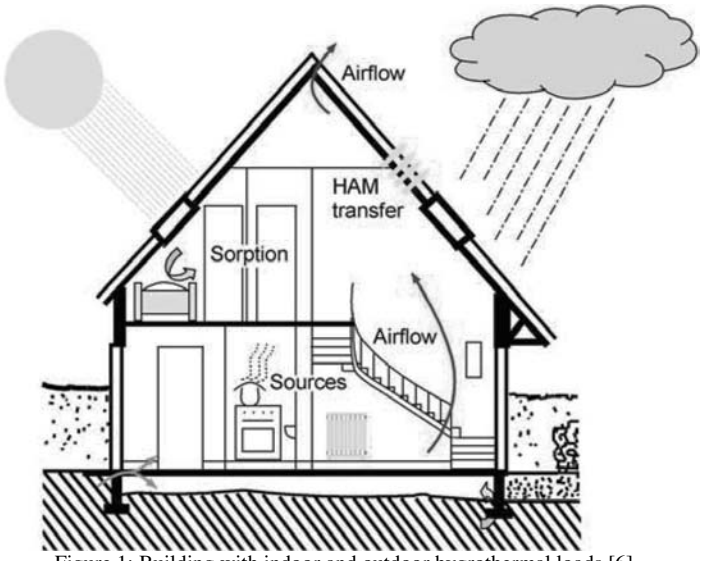

Figure 1: Building with indoor and outdoor hygrothermal loads [6]

Section 2.1 presents the state-of-the-art of the modelling of the whole building heat, air and moisture conditions. Three classes of building simulation models are distinguished and categorized.

In Section 2.2, the different modelling techniques to describe heat and moisture transport in indoor air are discussed. Additionally, the background and fundamentals of CFD and sub-zonal modelling are discussed in more detail in respectively Section 2.3 and Section 2.4.

In Section 2.5, the concept of convective surface transfer coefficients is presented. Previous research that focussed on the determination of the convective heat and moisture transfer coefficients is evaluated.

Section 2.6 presents the state-of-the-art in modelling and coupling the indoor airflow and HAM component models. Moreover, coupling strategies and data exchange methods are evaluated.

The conclusions from the literature review are presented in Section 2.7.

2.1 Hygrothermal modelling

In engineering practice, the hygrothermal performance of building components is often evaluated based on the Glaser method [21]. Due to its restrictions - stationary, no liquid transfer, no air transfer, etc. - it is considered to be only rarely reliably applicable. In research, the application of numerical simulation models for heat and moisture transfer in building components is more common. Hygrothermal simulations of building components have been applied for evaluation of the hygrothermal performance of building components [22], the risk of algae formation and mould growth on exterior and interior surfaces [12] [23],

the effect of rain buffering on the occurrence and intensity of runoff on brick facades [24], the effect of interior moisture buffering on the interior relative humidity [10].

During the past few decades, the development and professional use of tools to simulate some of the processes that are involved in analysis of whole building heat, air, and moisture (HAM) conditions increased. In general, these tools can be distinguished in three main classes: building energy simulation software tools, airflow simulation tools, and HAM component models. Each class can be subdivided based on the spatial discretisation or granularity of the model. In this section, these three classes and the subdivision by granularity is discussed briefly.

Fairly comprehensive tools for the prediction of the energy consumption of an entire building have been developed for more than a decade. An intensive overview of such building energy simulation (BES) tools has been documented by Crawley *et al*. [25]. The development of building energy simulation models mainly focussed on the analysis of the energy consumption used for heating, ventilation, and air-conditioning of the building. Though, the building energy simulation tools have so far not been well suited to predict moisture transfer processes in buildings. Moreover, airflows in the building are analyzed on a simplified, macroscopic scale, mainly based on the pressure differences between the inside and outside environment and/or the different zones within the building.

Airflow simulation tools and Computational Fluid Dynamics (CFD) software tools are available for the simulation of the airflow within a room or zone of a building. These models focus on the accurate prediction of the local airflows on a relatively small scale, for example in a room or part of a room. The airflow between the zones of a building, as well as air exchange with the outdoor environment is predicted at a bulk level. Some of the tools deal with airborne moisture transport and also represent the heat transfer in the air and in the building envelope. However, in general these tools cannot be used to predict moisture exchange between the air in a zone and its adjacent porous walls.

HAM component models have been developed for the detailed assessment of the time-dependent hygrothermal conditions within a building component. Dynamic heat, air and moisture (HAM) model are applicable to perform transient calculations of the heat, air, and moisture conditions in a building component over a relatively long period of time, for example over several years. The indoor and outdoor environmental conditions serve as boundary conditions for the model and are usually considered to be uniform. Interactions between the building component and the indoor environment within the building are not considered.

The three classes of building simulation models can be distinguished based on the spatial discretisation (granularity) of the room air volume on the one hand and, and the building envelope on the other hand [6] [26]:

<u>INDOOR ENVIRONMENT</u>

- Coarse-grained models: mono-zone models for air volumes, where the whole building is represented as one perfectly mixed zone and the same temperature and relative humidity is assumed for all rooms.
- Intermediate-grained models: multi-zone models for a combination of well-mixed air volumes, that allow several rooms or groups of rooms, each with different characteristics, to be simulated. Heat and mass transfer is not only modelled between the indoor and outdoor environments but also between different zones inside one building. This includes transfer in walls and also airflows, that can be computed using for example pressure network modelling.
- Fine-grained models. In fine-grained models, the air in each room is subdivided into several control volumes (typically between ten and a few hundred). These sub-zonal models can also be used to represent several adjacent rooms connected by openings.
- Very fine-grained models: computational fluid dynamic (CFD) modelling of room air, enabling detailed calculations of temperature, velocity and concentration fields in a room. Typically a room is divided into thousands to millions of control volumes and the conservation equations are solved for each control volume e.g. by using control volume or finite element techniques.

<u>BUILDING ENVELOPE</u>

For the building envelope the main difference in HAM-transfer modelling is made by the dimension of the represented phenomena. Therefore, granularity refers here to the dimension of spatial discretisation used:

- Coarse-grained models: transfer function models for the envelope, where the dynamic heat and possible mass fluxes are determined without investigating conditions within the envelope.

- Intermediate-grained models: one-dimensional models for the envelope.
- Fine-grained models: two-dimensional models for the envelope.
- Very fine-grained models: three-dimensional for the envelope, using control volume or finite element techniques to calculate the heat and mass fluxes, as well as the temperature and concentration fields in the envelope parts, including three-dimensional thermal bridges or similar singular geometries.

Currently, researchers are striving to advance the possibilities to calculate the integrated phenomena of heat, air and moisture flows in buildings while including the interactions that take place in buildings between the various building materials, components, and room air, and the influences due to occupants and Heating, Ventilation and Air-Conditioning (HVAC) systems. The main requirement for a successful modelling of the hygrothermal interaction between the building component and the indoor environment is the correct treatment of the interfacial flows at boundaries between the control volumes of different type (interface between air and material) [6]. The prediction of the heat and moisture fluxes between the building component and the indoor environment depends, first of all, on the prediction of the local temperature and relative humidity of the air near the component. Second, an accurate prediction of these fluxes is dependent of the description of the convective surface transfer coefficients. In addition, the prediction of the local conditions and surface transfer coefficients is directly influenced by the airflow model that describes the indoor airflow in the building near the component.

In the following sections, an overview of the current modelling which focuses on the room-component interaction is presented. As has been demonstrated previously, the accurate prediction of the room-component interaction depends on the local near-component conditions, and the convective surface transfer coefficients. The quality of these local conditions and coefficients is directly influenced by the airflow model that describes the indoor airflow in the building near the component. The next section presents the different airflow models that are applied in current building simulation software with decreasing granularity of the model: nodal models, mutizone models, sub-zonal models and computational fluid dynamics (CFD) models. The main advantages, disadvantages and limitations are discussed.

2.2 Indoor Airflow model

In this section, the different modelling techniques to describe heat and moisture transport in indoor air are discussed. In general four levels of granularity are distinguished: nodal models, multizone models, sub-zonal models, and computational fluid dynamics. Additionally, the background and fundamentals of sub-zonal modelling and CFD are discussed in more detail, since these models have been applied in the present work.

2.2.1 Nodal models

In the nodal approach, a building or a collection of rooms is represented by a single calculation node. The node is considered to be perfectly homogenous. This means that inside the zone uniform properties are assumed, i.e. the air in the zone is considered to be well mixed. The model is not suitable for obtaining information regarding the local conditions near the building component. Figure 2 shows a schematic representation of a nodal model. The indoor environment in the building is represented by one node. Each node exchanges heat and moisture with its surrounding building components and the outdoor environment. With respect to the convective surface transfer coefficients, average and uniform coefficients are used to model the heat and moisture transfer between the air in the room and the corresponding building component.

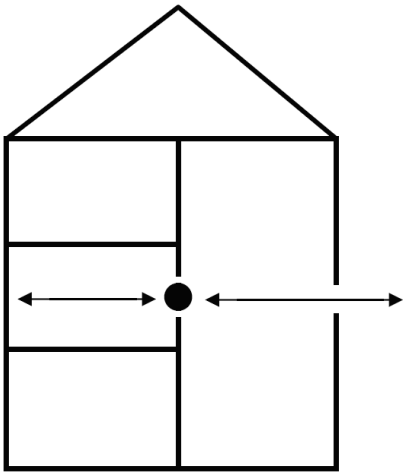

Figure 2: Nodal airflow model

The main advantage is that such models are suitable for the efficient building energy simulation of a relatively large building. The model requires solving only a relatively small number of equations, i.e. an energy balance equation, and moisture balance equation in each node. Moreover, this approach is suitable for design and system sizing since it provides a rapid solution. However, the main limitation is that nodal models do not provide any information regarding the local indoor environmental conditions near a building component. Such models are not applicable for obtaining a more accurate prediction of the local indoor climatic conditions and coupling to a HAM component model.

2.2.2 Multi-zone models

In multizone models, a similar approach as in the nodal models is applied. The entire zone is represented by a single calculation node with uniform properties describing the air in the room. However, interaction between the different air nodes in the different zones is accounted for in the model (Figure 3). Multizone models treat heat transfer and airflow between different zones of a building. Such models use average or representative values for the parameters describing the conditions in a single zone (pressure, temperature, etc.). The links between zones, which include windows, doors, cracks, ventilation ducts, etc., are specified by their flow (or resistance) properties and flow rates through them are determined by the differential pressure across the links. The network of links is then described by a series of flow equations, which are solved simultaneously to provide a mass conserving solution.

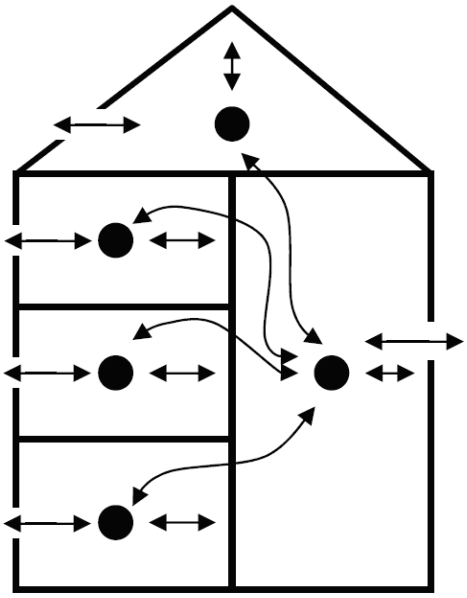

Figure 3: Multi-zone model for the airflow in a building

Multizone models can be used with time-varying input or boundary conditions to predict variations in conditions over the period of interest. Calculation of the mass and energy balances in each zone at each time step is included to predict the variation of the quantities with time. While they may be used to predict airflows into and out of a room and the mean quantities within a room, they cannot resolve airflow patterns or variations in temperature or relative humidity within a room. Multi-zone models do not treat local phenomena within a room, such as stratification. If knowledge of local variations is important, then multizone models are not suitable.

In general, the model has limited capabilities to cope with variations in air velocities, temperatures or contaminant concentrations within rooms. The user is required to identify and describe all the zones (rooms) of interest and the links or flow paths between those zones (and with the outside air). The program is then used to calculate flows and contaminant transport between the zones.

With respect to the modelling of the interaction between the building component and surrounding indoor environment, few numerical models are able to provide a two-dimensional prediction of the heat and moisture conditions in the building component taking into account the near component conditions and interaction. Coupled models have been presented by Nicolai et *al*. [16] and Holm et *al*. [27]. An average temperature and relative humidity for the indoor environment is assumed, while the influence of the heat and moisture conditions in the building component on the indoor air conditions is taken into account. However, it should be noticed that the surface heat and moisture transfer coefficients are fixed and an average uniform value is applied for the entire building component. Hence, time-variant and spacial variations of the convective surface transfer coefficients are not accounted for.

With respect to the room-component interaction modelling, multizone models have similar advantages and disadvantages as the nodal models. The computational performance is relatively good, while no information regarding the local indoor environmental conditions is provided.

2.2.3 Sub-zonal airflow models

In the sub-zonal modelling approach, a room or a space in a building is sub-divided into a relatively small number of discrete control volumes or cells (subzones) (Figure 4). Within a sub-zone, temperature and concentration regimes are considered to be fairly uniform. In the subdivided rooms, two types of sub-zones are used: standard sub-zones and flow element (or mixed) sub-zones. Standard sub-zones are assumed to have a representative air temperature which does not differ markedly from their immediate neighbouring subzones. The important characteristic of these sub-zones is that flow velocities (and momentums) between them are small and primarily driven by pressure differences. A flow element sub-zone or mixed sub-zone is under the direct influence of the flow driver (fan, heaters, etc.). The flow element parts are treated as isolated volumes where the air movement is controlled by a restricted number of parameters, and the air movement is fairly independent of the general flow in the enclosure.

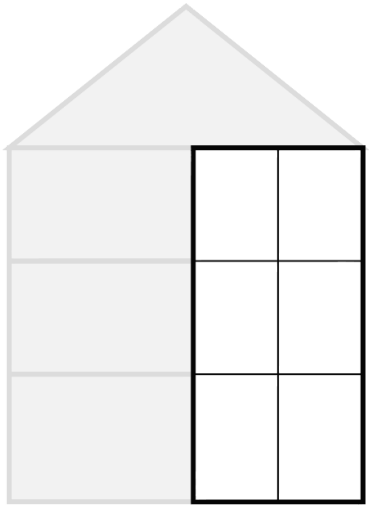

Figure 4: Sub-zonal model

Sub-zonal models are able to perform transient calculations over a relatively long period of time, while the computational effort is relatively small. However, the models are in general not capable of providing very detailed information about the local conditions in the room compared to CFD. For additional information on the background, fundamentals and comparative studies regarding sub-zonal models is the reader referred to Section 2.4.

2.2.4 Computational fluid dynamics

When highly detailed simulations of airflow and hygrothermal conditions within a zone of a building are desired, the option consists of using computational fluid dynamics (CFD). CFD solves the equations by discretization of the equations. The spatial continuum is divided into a finite number of discrete cells (Figure 5), and finite time-steps are used for dynamic problems. the mathematical equations describing the airflow are solved in each cell. CFD models are capable of predicting the local temperature and relative humidity near a building component as well as the local surface transfer coefficients.

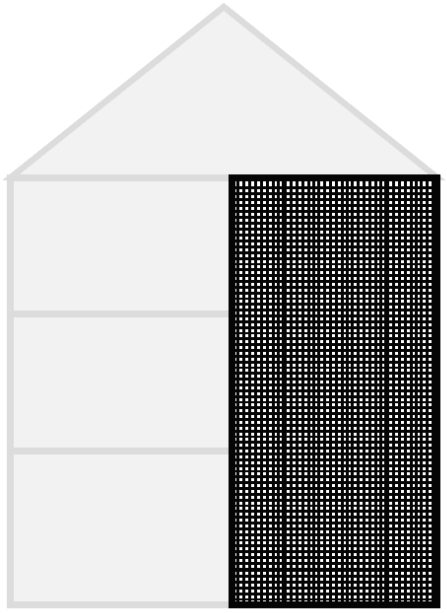

Figure 5: Computational fluid dynamics.

However, detailed CFD models cannot easily and quickly solve time-dependent hygrothermal interactions across the boundaries of a building model. In practice, only steady-state simulations of the airflow in a single room at a specific time, and/or transient simulations over a relatively short period of time, for example a diurnal cycle [20], are feasible. And, since these calculations are relatively computational intensive, transient calculations over a longer period of time are currently not possible. Additional information on the numerical techniques, background and fundamentals of CFD models is presented in Section 2.3.

2.3 Computational Fluid Dynamics Modeling

In computational fluid dynamics (CFD) numerical techniques to solve the Navier-Stokes (N-S) equations for fluid flow are applied. CFD also solves the conservation equation of mass for the contaminant species and the conservative equation of energy for building thermal comfort and indoor air quality analysis. All the governing conservation equations can be written in the following general form:

$$\frac{\partial \Phi}{\partial t} + (\underline{u} \bullet \nabla)\Phi - \Gamma_{\phi} \nabla^2 \Phi = S_{\phi} \qquad (1)$$

Eq. (1) presents the transport equation for property Φ, where Φ is 1 for mass continuity, T for temperature [K], C for gas contaminant concentrations [mol mol^{-1}], X for moisture content [kg kg^{-1}]. Moreover, t is the time [s], $\underline{u}$ is the velocity vector [m s^{-1}], and S_{ϕ} is the source term. For buoyancy-driven flows, the Boussinesq approximation, which ignores the effect of pressure changes on density, is usually employed. The buoyancy-driven force is treated as a source term in the momentum equations.

With respect to the airflow in a building, the flow in rooms is usually turbulent. The flow fluctuations associated with turbulence give rise to additional transfer of momentum, heat and mass. These changes to the flow character can be favourable (efficient mixing) or detrimental (high energy losses) depending on one's point of view.

Building engineers are mainly interested in the prediction of mean flow behaviour, but turbulence cannot be ignored, because the fluctuations give rise to the extra Reynolds stresses on the mean flow. These extra stresses must be modelled. What makes the prediction of the effects of turbulence so difficult is the wide range of length and time scales of motion, even in flows with relatively simple boundary conditions.

In general, researchers applied methods, which can be grouped into four categories, to capture the effects due to turbulence [28]:

- Direct numerical simulation: these simulations compute the mean flow and all turbulent velocity fluctuations. The unsteady Navier-Stokes equations are solved on spatial grids that are sufficiently fine that they can resolve the Kolmogorov length scales at which energy dissipation takes place and with time steps sufficiently small to resolve the period of the fastest fluctuations. These calculations are very costly in terms of computing resources and in general not applicable for solving the airflow in rooms.
- Large eddy simulation (LES): This is an intermediate form of turbulence calculations which tracks the behaviour of the larger eddies. The method involves space filtering of the unsteady Navier-Stokes equations prior to the computations, which passes the larger eddies and rejects the smaller eddies. The effects on the resolved flow (mean flow plus large eddies) due to the smallest, unresolved eddies are included by means of a so-called sub-grid scale model. Unsteady flow equations must be solved, which means that the demands on computing resources in terms of storage and volume of calculations are relatively large.
- Reynolds-averaged Navier-Stokes (RANS) equations: Attention is focused on the mean flow and the effects of turbulence on mean flow properties. Prior to the application of numerical methods the Navier-Stokes equations are time averaged (or ensemble averaged in flows with time-dependent boundary conditions). Extra terms appear in the time-averaged (or Reynolds-averaged) flow equations due to the interactions between various turbulent fluctuations. These extra terms are modeled with classical turbulence models. The most common RANS turbulence models are classified on the basis of the number of additional transport equations that need to be solved along with the RANS flow equations.
- Detached eddy simulation models: The detached eddy simulation (DES) method presents the most recent development in turbulence modelling [29], which couples the RANS and LES models to solve problems when RANS is not sufficiently accurate and LES is not affordable. In DES a one-equation eddy-viscosity model (Spalart-Allmaras model) is used for the attached boundary layer flow while LES is used for free shear flows away from the walls. In practice, the switch between the RANS and

LES models requires more programming and computing efforts rather than simply changing the calculation of the length scale. Recent studies [29] [30] [31] indicated that DES appears a promising model, giving the best velocity agreement and overall good agreement with measured Reynolds stresses. However, they also mentioned that the eddy resolving approaches (LES and DES) demanded extremely high computational costs and computer power. As an emerging technology, DES still needs more studies before it can be applied for predictions of air distributions in enclosed environments.

Near-wall treatment

The accuracy of CFD prediction is highly sensitive to the boundary conditions assumed by the user. The boundary conditions for CFD simulation of indoor airflows relate to the inlet (supply), outlet (exhaust), enclosure surfaces, and internal objects. The temperature, velocity, and turbulence of the air entering from diffusers or windows determine the inlet conditions, while the interior surface convective heat and moisture transfers in terms of surface temperatures or heat fluxes, surface relative humidity or moisture fluxes respectively relate to the enclosures. Focussing on the local near component conditions these boundary conditions are crucial for the accuracy of the results.

Near a solid wall, the flow behaviour and turbulence structure of the flow are considerably different from free turbulent flows, due to the presence of the solid boundary. In flows along solid boundaries, there is usually a substantial region of inertia-dominated flow far away from the wall and a thin layer within which viscous effects are important [28]. In general the turbulent boundary layer adjacent to a solid surface is composed of two layers (Figure 6):

- The inner layer: 10-20% of the total thickness of the wall layer; the shear stress is (almost) constant and equal to the wall shear stress. Within this region there are three zones, in order of increasing distance from the wall:
  - The viscous sublayer: viscous stresses dominate the flow adjacent to the surface.
  - The buffer layer: viscous and turbulent stresses are of similar magnitude.
  - The log-law layer: turbulent (Reynolds) stresses dominate.
- The outer layer or law-of-the-wake layer: characterized by an inertia-dominated core flow far from the wall and free form direct viscous effects.

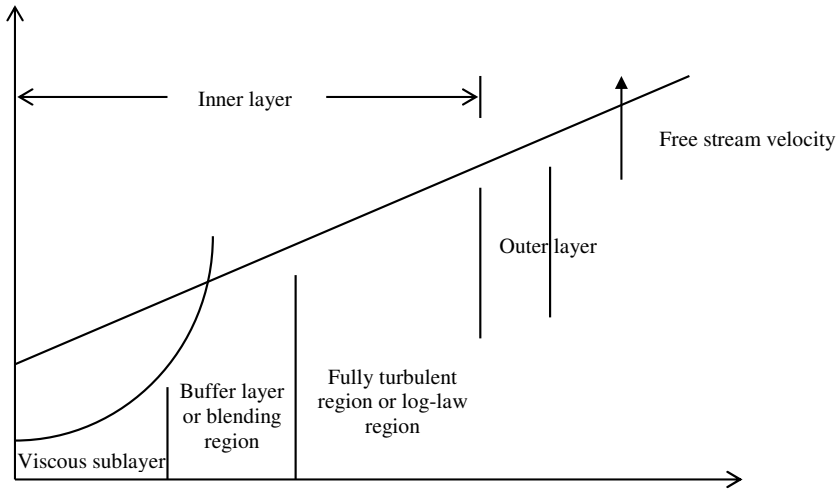

Figure 6 : Subdivision of the near-wall region.

Traditionally, there are two approaches to modeling the near-wall region (Figure 7). In one approach, the viscosity-affected inner region (viscous sublayer and buffer layer) is not resolved. Instead, semi-empirical formulas called wall functions are used to bridge the viscosity-affected region between the wall and the fully-turbulent region. The use of wall functions obviates the need to modify the turbulence models to account for the presence of the wall.

In another approach, the turbulence models are modified to enable the viscosity-affected region to be resolved with a mesh all the way to the wall, including the viscous sublayer. This approach is usually referred to as the "near-wall modeling" approach.

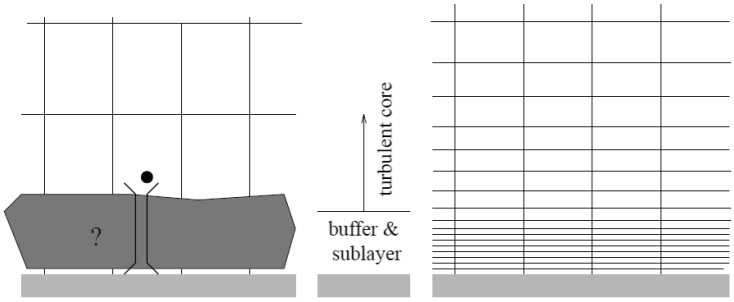

Figure 7: "Wall function" approach (left) and "near-wall modeling" approach (right)

The selected approach is dependent of the kind of turbulence model, which is used for the modelling of the airflow in the room. Considering engineering applications, the use of the standard k-ε model with standard wall functions [30] is common practice. In this model, the wall functions relate the local wall shear stress to the mean velocity, turbulence kinetic energy, and the rate of dissipation by a logarithmic function or log-law. However, it should be noticed that the log-law is not valid at low Reynolds numbers. This means that if the focus lies on the local conditions near a wall and the local surface heat and moisture transfer coefficients, the model should be adapted to be valid for low Reynolds number flow. Another option is to use another turbulence model, for example the k-ω turbulence model, which uses near-wall modelling.

Evaluation of Turbulence Models for Indoor Airflow

RANS turbulence models succeed in expressing the main features of many turbulent flows by means of one length scale and one time scale defining variable. Among the best known ones are the k-ε model and the Reynolds stress model (Table 2). The standard k-ε model is valued for its robustness, and is still widely preferred in internal flow computations [28]. The computing resources required for reasonably accurate flow computations are modest. This approach has been the mainstay of building engineering flow calculations over the last decades.

Table 2: Turbulence models [28]

Number of extra transport equations	**Name**
Zero	Mixing length model
One	Spalart-Allmaras model
Two	k-ε model
	k-ω model
	Algebraic stress model
Seven	Reynolds stress model

With respect to the application of CFD for predicting natural convection, forced convection, and mixed convection in rooms, five k-ε two-equation models have been studied by Chen [32]. The performance of the standard k-ε model, a low-Reynolds-number k-ε model, a two-layer k-ε model, a two-scale k-ε model

and a renormalization group (RNG) k-ε model is evaluated. The models have been compared to corresponding experimental data from literature.

The main conclusion that is presented in the paper is that the prediction of the mean velocity in the room by the five models is generally satisfactory, but the predicted turbulent velocity does not agree with the experimental data. Since all these models use the assumption of isotropic turbulence, they also fail to predict correctly the anisotropic turbulence found in indoor airflow. These models are unable to catch the secondary recirculation observed in the flows studied.

Moreover, in the paper, it is found that some models perform better in one case but more poorly in another; while the standard k-ε model gives stable results, the predictions do not always agree with the experimental data. The RNG k-ε model performs slightly better than the standard k-ε model, and the stability of the two models during the computations is similar. The application of the low-Reynolds-number k-ε models does not need the conjunction to wall functions with which the location of the first grid point from the wall is sufficiently large. However, the models are less stable numerically and, as a very fine grid distribution is required in the near-wall region, the computing cost is significantly higher than when using high-Reynolds-number models. If the low-Reynolds-number models are applied to study practical problems with complicated geometry, the high computing cost may be unacceptable to engineers.

In a more intensive study [33], the performance of an even wider range of turbulence models potentially suitable for indoor airflow has been evaluated in terms of accuracy and computing cost. These models cover a wide range of computational fluid dynamics (CFD) approaches including Reynolds averaged Navier-Stokes (RANS) modeling, hybrid RANS and large eddy simulation (or detached eddy simulation, DES), and large eddy simulation (LES). The RANS turbulence models tested include the zero-equation model, three two-equation models (the RNG k-ε, low Reynolds number k-ε, and SST k-ω models), a three-equation model ($v^2 - f$ model), and a Reynolds stress model (RSM). The investigation tested these models for representative airflows in enclosed environments, such as forced convection and mixed convection in ventilated spaces, natural convection with a medium temperature gradient in a tall cavity, and natural convection with large temperature gradient in a model fire room. The predicted air velocity, air temperature, Reynolds stresses, and turbulent heat fluxes by the models were compared against the experimental data from the literature. The study also compared the computing time used by each model for all the cases. The results reveal that LES provides the most detailed flow features while the computing time is much higher than RANS models and the accuracy may not always be the highest. Among the RANS models studied, the RNG k-ε and a modified $v^2 - f$ model have the best overall performance over the four cases studied. Meanwhile, the other models have superior performance only in some particular cases.

In conclusion, it should be noticed that both studies [29] [32], [33] have reported similar observations. While each turbulence model has good accuracy in certain flow categories, each flow type favours different turbulence models. Moreover, CFD applications to airflow simulation for enclosed environments have achieved considerable successes, as reviewed by Zhai [29]. Zhai [29] concluded that CFD is a valuable tool for predicting air distribution in enclosed environments. However, there are many factors influencing the results predicted. Different users may obtain different results for the same problem even with the same computer program. The accuracy of the simulation heavily depends on a user's knowledge of fluid dynamics, experience and skills using numerical techniques. Among various CFD influential factors proper selection of a turbulence modelling method is a key issue that will directly affect simulation accuracy and efficiency. The reader should be aware, that, however the availability of a large number of CFD software packages makes the application of these CFD models common, CFD results should be analyzed with care, and validation with experimental results is always required.

As an alternative for the use of CFD models, which are strongly limited by computer capacity, sub-zonal airflow models can be used. The next section proceeds with the background, fundamentals and comparative studies of sub-zonal models.

2.4 Sub-zonal airflow modelling

The sub-zonal model approach is based upon the partitioning of a room into a limited number of sub-zones (Figure 4); it can be considered as an intermediate approach between a one-node (single-zone) model and a CFD model. The first sub-zonal model scheme was developed in the 1970s [34] from observations realized in a test cell. Lebrun proposed an airflow and heat transfer model for a six-zone configuration with a heating system. Later on, the model has been authenticated by extensive experimental studies, such as the research reported by Inard et *al*. [35], measuring the distribution of temperature within a controlled environment, a MINIBAT cell. A category of sub-zonal models has been developed driven by these experimental studies. The majority of these studies are motivated initially by the quantification of the temperature stratification within a single room with a heating system. Gradually, the goal has been extended to study the performance of various systems and the level of thermal comfort they produce.

After the development of airflow modelling approaches for single-zone and multi-zone configurations, researchers strived to develop a general sub-zonal model, which is independent of any assumptions for airflow directions. This resulted in the actual sub-zonal models, which are based on the corresponding an air mass balance equation and the energy conservation equation in different zones. Later on, other balance equations have been added to these equations, such as the moisture balance [36][37].

An intensive summary of the development and applications of the sub-zonal approach as well as critical reviews of the sub-zonal models is presented in literature [38] [39]. In this section, the main principles and fundamentals of the sub-zonal approach that have been used in this study, are presented.

As has been mentioned earlier, in the sub-zonal approach, a room or a space in a building is sub-divided into a relatively small number of discrete control volumes or cells (subzones) (Figure 4). Within a sub-zone, temperature and concentration regimes are considered to be fairly uniform. Two types of subzones are used: standard subzones and flow element (or mixed) subzones. Standard subzones are assumed to have a representative air temperature and vapour pressure, which do not differ markedly from their immediate neighbouring subzones. The important characteristic of these sub-zones is that flow velocities (and momentums) between them are small and primarily driven by pressure differences. Mass flows between adjacent sub-zones are calculated in different ways for horizontal and vertical interfaces.

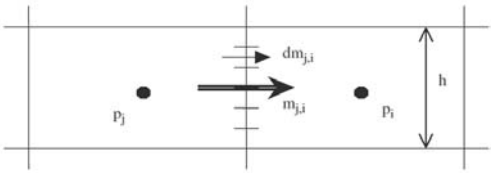

Figure 8: Mass flow between two adjacent sub-zones.

Standard sub-zones, as presented in Figure 8, are identified as those where the driving forces are pressure differences and air velocities are relatively low. A power-law relation is assumed to govern the differential mass flow. The differential mass flow $dm_{j,i}$ through differential area dA (the adjoining face area) is expressed as:

$$dm_{j,i} = C_d \rho (\Delta p_{j,i})^n dA \tag{2}$$

and, for airflow from j to i, the mass flow rate $m_{j,i}$ through the cross-sectional area A is

$$m_{j,i} = \int dm_{j,i} = C_d \rho (\Delta p_{j,i})^n A \tag{3}$$

where C_d is an empirical 'permeability' constant, analogous to the orifice discharge coefficient, that is assumed to have a value less than 1. In literature [40], it has been concluded that a value of 0.83 m s^{-1} Pa^{-n} is

most appropriate. The power-law exponent n is often taken as $n = 0.5$ which corresponds to the orifice equation and ρ refers to the density of the incoming air.

For airflow through a vertical interface the driving pressure, $\Delta p_{j,i}$ is given by:

$$\Delta p_{j,i} = p_j - p_i \tag{4}$$

For airflow through a horizontal interface, the hydrostatic variation of pressure is taken into account.

$$\Delta p_{j,i} = (p_j - p_i) - \frac{1}{2}(\rho_i g h_i + \rho_j g h_j) \tag{5}$$

Where p is the pressure [Pa], ρ the air density [kg m^{-3}], g the gravitational acceleration [m s^{-2}], and h is the height [m].

Substituting Eq. (4) and Eq. (5) into Eq. (3) taking into account the sign of airflow rate, the subzone-to-subzone mass flow rate $m_{j,i}$ is presented by Eq. (6) and Eq. (7) for horizontal and vertical interfaces respectively.

$$m_{j,i} = C_d \rho A \left| p_j - p_i \right|^n \left(\frac{p_j - p_i}{\left| p_j - p_i \right|} \right) \tag{6}$$

$$m_{j,i} = C_d \rho A \left| p_j - p_i - \frac{g}{2}(\rho_i h_i + \rho_j h_j) \right|^n \left(\frac{p_j - p_i - \frac{g}{2}(\rho_i h_i + \rho_j h_j)}{\left| p_j - p_i - \frac{g}{2}(\rho_i h_i + \rho_j h_j) \right|} \right) \tag{7}$$

In literature, the sub-zonal model, represented by Eq. (7), is referred to as the standard or power-law sub-zonal model (PLM).

A flow element sub-zone or mixed sub-zone is under the direct influence of the flow driver (fan, heaters, etc.). However, the volume of the sub-zone may not entirely be under the direct influence of the flow driver. The sub-zone therefore requires two approaches: one for the air belonging to the flow element and one for the air not directly under the influence of the flow element (named as non-flow element air). The flow element parts are treated as isolated volumes where the air movement is controlled by a restricted number of parameters, and the air movement is fairly independent of the general flow in the enclosure. The driving forces of flow elements are jets, thermal plumes, boundary layers, fans, etc. Specific models have been developed to describe flows for some typical examples [38] [41] .

Limitations and Improvements

The power law sub-zonal model has limitations, which are inherent to the very features of the model. A review of the sub-zonal models and its applications [38] showed that the sub-zonal model yielded reasonably good predictions for natural convection. Nevertheless, for forced convection it was found that the sub-zonal models fail to predict recirculation loops reasonably.

Researchers have tried to improve the quality of the prediction of the power-law model. The sub-zonal models use the power law model (PLM) with a constant and identical flow coefficient (C_d) for each cell. First of all, attempts to improve the power-law model focussed on optimization of the flow coefficient (C_d). Often, the value for the flow coefficient C_d is 0.83, however Wurtz et *al.* [40] showed that the PLM's prediction does not depend on this C_d value. However, other authors [42] showed discrepancies from applying the PLM with a constant flow coefficient for predicting indoor airflow distribution. To improve the quality of PLM predictions, they proposed using a given C_d value for each cell. A CFD simulation is used for the C_d value for each cell. The new model provided an appropriate and variable flow coefficient in each cell for the case of forced convection and predicted the recirculation in the standard zone reasonably. However, it should be mentioned that this type of optimisation is case-specific.

A second alternative approach has been taking the surface drag into account in the sub-zonal model. The power-law sub-zonal model implicitly demands that all changes in kinetic energy in a control volume are dissipated. Axley [43] showed that such an assumption in general cannot be satisfied. The assumption corresponds to a static fluid, which is not a reasonable assumption given that the purpose of the macroscopic model is to predict airflow. Alternatively, a surface-drag flow relation was developed by considering the transfer of shear stress near wall surfaces using the momentum balance on differential flow conduits linking neighbouring cells. The benefit offered by this more physically consistent model is, however, dependent on the cell subdivision used for any given sub-zonal model as relative difference between near-surface and central flow resistance will be greater for finer subdivisions.

The review presented by Teshome et *al*. [38] showed that several models either based on the surface drag (SD) model or a combination of the power law model and the surface drag model (PLM-SD), have been developed. This literature review showed that despite the widespread implementation of sub-zonal models for different applications, no thorough investigation was made which resulted in a successful improvement of the sub-zonal model's capabilities. An important problem in the power law model is that the flow has been considered to be only driven by the thermal pressure gradient. This could be a reasonable approximation for natural convection since the driving pressure results from the temperature gradient (buoyancy). Furthermore, the influence of upstream/downstream convection and diffusion on the flow might be less important. However, this might not be the case for forced ventilation and one has to take into account the effect of the thermal pressure gradient as well as upstream and downstream convection and diffusion on the flow. Hence, the influence of flow from upstream and downstream neighbouring zones on a given zone needs to be considered. Alternatively, in order to provide an accurate prediction of the airflow in a room in case of forced convection, the power law model requires the inclusion of flow element sub-zones for those sub-zones which are under the direct influence of a flow driver (fan, heaters, etc.).

Evaluation of sub-zonal models

Simulation results obtained from sub-zonal models have been evaluated and verified, often based on a comparison with experimental data and CFD results. Comprehensive reviews of the literature on sub-zonal models have been carried out by Teshome and Haghighat [38] [42], and Megri and Haghighat [39]. The evaluations focussed on the developments and applications over the last three decades. Sub-zonal models have been used for the simulation of the airflow, temperature and relative humidity field in a room under natural, mixed and forced convective conditions. For additional information on specific studies, the reader is referred to these reviews. Only the most important observations and conclusions with respect to the present study are presented here. These observations have been categorized based on the flow regime: natural, mixed, and forced convection.

Wurtz [44] demonstrated the use of sub-zonal models for the simulation of natural convection in two- and three-dimensional enclosures. The author compared the predicted temperature distributions with experimental results and numerical results obtained from CFD. It is concluded that the air temperature distribution calculated by the sub-zonal model lies between the experimental and CFD results. The sub-zonal model gave a good prediction of the qualitative behaviour of the airflow in the room, but quantitatively, differences up to 25% relative to the measurements were observed.

Several researchers [37] [45] compared the ability of sub-zonal models and a standard k-ε model to predict airflow and temperature distributions in a two-dimensional ventilated room under mixed convection conditions. In this configuration, sub-zonal models gave a satisfactory estimate of airflow patterns, provided specific laws to model momentum were implemented. The sub-zonal models gave a rough estimate of the structure of the recirculation in the room. The sub-zonal models were able to predict the temperature profiles in the room. The authors [37] [45] concluded that sub-zonal models could be a suitable tool to estimate thermal comfort in a ventilated room, when details of airflow are required one may use a standard k-ε model to simulate the airflow in the room.

Mora *et al*. [46] conducted simulations of airflow in a full-scale test-room equivalent to Nielsen's experiments [47], which served as a validation Benchmark for isothermal forced convection within the framework of the project IEA Annex 20. Four different formulations of the standard sub-zonal model taking into account the surface drag were used. As an alternative simplified method to predict airflows in large

spaces the authors [46] also explored the possibility of applying a conventional standard k-ε CFD model to this configuration. The predictions of the airflow patterns and velocity profiles were compared and the ability of each class of models to predict the total pressure drop across the test room (i.e. from the inlet to the outlet) was analyzed. It was observed that the CFD models predicted a large recirculation loop around the center of the room, and significant entrainment of the room air in the inlet jet. While slight differences among the four sub-zonal formulations did exist, none predicted the recirculation loop around the geometric center of the room; this was true even for those sub-zonal models for which the specific driven flow model patch predicts the jet itself. Moreover, the analysis showed that the sub-zonal model was not able to predict the air velocity in the room accurately, while the pressure difference between the inlet and the outlet of the room predicted by CFD was approximately six times larger compared to the sub-zonal model. However, measurements of the pressure drop over the room have not been carried out.

Applications have shown that the sub-zonal modelling approach can be a suitable method to estimate temperature and relative humidity fields in a room with reasonable accuracy. Adding specific laws to describe momentum-driven flows, such as jets, improved the airflow pattern predictions. Sub-zonal models can give a satisfactory estimate of airflow patterns but not highly detailed information on air speed magnitude. Nevertheless, this approach showed to be adequate to estimate indoor thermal comfort.

Moreover, a significant reduction in computational effort has been observed with respect to the simulation of a sub-zonal model compared to CFD [38] [39] [42]. Sub-zonal models have proven to be a suitable tool for annual thermal comfort analysis studies with a few minutes computation time [37]. The ability of the sub-zonal model to provide a relatively accurate prediction of the temperature and relative humidity field in a room as well as the short computation time makes the application of the sub-zonal model attractive for the transient simulation of heat, air and moisture in buildings.

2.5 Convective surface transfer coefficients

As has been mentioned earlier, the quality, accuracy and efficiency of numerical simulation of moisture and heat transfer inside building components is dependent of the description of the internal boundary conditions. Except for the airflow model that describes the local temperature and relative humidity near the building component, the prediction of the heat and moisture fluxes between the building component and the indoor environment depends on the accurate prediction of the convective surface transfer coefficients.

2.5.1 Convective surface heat transfer coefficient

Transfer coefficients are widely used in building engineering for the prediction of heat and mass fluxes between a surface and an adjacent fluid. The concept of transfer coefficients for heat transfer was introduced by Newton (Eq. (8)).

$$q = \alpha_c \Delta T \tag{8}$$

where q is the heat flux [W m^{-2}] from the surface to the fluid, ΔT the driving force, being the temperature [K] difference between the surface and the zone, and α_c the convective surface heat transfer coefficient [W m^{-2} K^{-1}]. Knowing the heat transfer coefficient, the heat flux associated with any given driving force can be calculated. Hence, Eq. (8) is not a physical law, but is in general considered as a definition of the surface transfer coefficient. In some cases the surface transfer coefficient can be linked to the physical concept of boundary layers. For instance, when considering forced convection over a flat plate.

Most software tools which are currently available for the simulation of heat and moisture transport in buildings use simplified models, both for forced and buoyancy-driven flows. In addition, the flow type

along a given element of the building is supposed unchanged during the whole simulation despite the possibility of changing air flow conditions by means of the ventilation, for example. As a consequence, either a time-invariant convective surface heat transfer coefficient is used, or some refinement is obtained by recalculating the coefficient during the simulation but always by using the same correlation for a given surface. Most software tools use average and uniform surface heat transfer coefficients for each building component. Therefore, the lack of accuracy in the modeling of the convective phenomena might be an explanation for the high sensitivity of simulation predictions to the modeling of internal convection shown by several authors [48].

In addition, despite the numerical evidence that the accuracy in the modelling of the convective surface transfer coefficient influences the heat and moisture flows through and from the component, experimental research [49] showed that the variation of the local convective surface heat transfer coefficient at the surface of a building component is relatively large. The authors [49] measured local surface heat and moisture transfer coefficients at different locations in a room and concluded that for the accurate prediction of the local temperature and relative humidity in a (micro-)climate near a building component, it is not acceptable to assume an average value for the entire building component.

2.5.1.1 CHTC Correlations

The formulae for the convective heat transfer coefficients can be determined analytically, experimentally or numerically. The literature study showed that few experimental investigations focus on the measurement of the convective surface heat transfer coefficient (CHTC) in rooms, such as presented by Erhorn et *al*. [49]. Various experimental studies focus on the measurement of the average CHTC of a building element and are often carried out in laboratory conditions.

Analytical approach

The theoretical formulae for the convective heat transfer coefficients are derived from boundary layer theory [50] from a vertical or horizontal heated plane in an undisturbed surrounding. Figure 9 presents the airflow over a horizontal plate, which is kept at a surface temperature T_s, while heated with a heat flux q [W m^{-2}]. The air velocity and temperature in the room at a reference distance from the plate are considered to be the reference velocity and temperature, indicated by the subscript ∞.

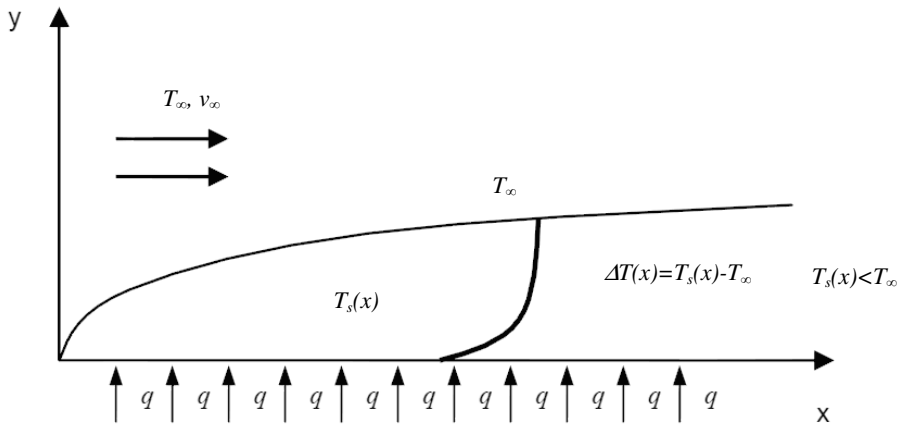

Figure 9: airflow over a horizontal plate with a surface temperature T_s and heat flux q [W m^{-2}].

The local CHTC (Eq. (9)) is dependent on the local Nusselt number, which describes the ratio of convective and conductive heat transfer across the boundary.

$$\alpha_c = \frac{Nu_x x}{L} \tag{9}$$

where α_c is the local surface heat transfer coefficient [W $m^{-2}K^{-1}$], Nu_x is the local Nusselt number [-], x is the coordinate along the plate [m], and L is the length of the plate [m].

The flow at the beginning of the plate is laminar, resulting in the development of a laminar boundary layer. After a certain distance $x = x_{critical}$ (from the leading edge), the boundary layer becomes turbulent. The transition from laminar to turbulent flow usually occurs at a critical Reynolds number ($Re_{x, critical}$) of $5 \cdot 10^5$. Although the transition from laminar to turbulent occurs over a region of finite length, a transition point is used for simplicity and it is frequently assumed that the transition is sudden. The numerical value of $Re_{x, critical}$ is strongly dependent on how free from perturbation the outer flow is.

The application of Eq. (9) to compute the local convective surface heat transfer coefficient α_c is illustrated using a small example for forced convection along a flat plate (Figure 9). Air with a velocity v_∞ and temperature T_∞ is flowing over a horizontal flat plate, uniformly heated with heat flux q. Under these conditions Churchill [50] determined the local Nusselt number Nu_x from boundary layer theory analytically (Eq. (10)). The relationship represented by Eq. (10) is used to calculate the local convective surface heat transfer coefficient (α_c).

$$Nu_x = \frac{0.3387\,\mathrm{Re}_x^{0.5}\,\mathrm{Pr}^{0.33}}{\left[1+\left(\frac{0.0468}{\mathrm{Pr}}\right)^{0.667}\right]^{0.25}} \tag{10}$$

where Re_x is the local Reynolds number and Pr is the Prandtl number.

Experimental Work

Experimental work focussing on the determination of the convective heat transfer coefficients in a building under real conditions is rare. Wallentén [51], for example, presented the measurement of the convective heat transfer coefficient at the outer ambient wall of a room with a window exposed to a natural climate. However, most measurements have been carried out in special environments with, for example, metal-coated insulated plates or walls.

The formulae obtained from experiments are derived from a wide range of situations where the reference temperature T_∞ typically is chosen at a position close to the wall or in the middle of the test room. Numerous authors suggested relationships for the mean convective surface heat transfer coefficient on a wall. An intensive review of the mean convective surface heat transfer coefficients for natural convection on isolated vertical and horizontal surfaces with special interest in their application to building geometries [52], and on surfaces in two- and three-dimensional enclosures [53]. Comparison between the correlations for the heat transfer coefficient showed that large discrepancies could occur. The discrepancies are found to be up to a factor 5 for vertical surfaces, up to a factor 4 for horizontal surfaces facing upward, and up to a factor 8 for horizontal surfaces facing downward. It is not the objective of the present work to repeat or evaluate this review. However, two issues resulting from the review are important:

- A clear conclusion is that a correlation obtained for an isolated surface is not suitable for a surface in a real sized enclosure, especially for buildings, where the location and type of heating source and ventilation may influence the flow pattern in the enclosure and, hence, the heat transfer coefficient.
- Noting that the values of the heat transfer coefficients in many present dynamic simulation models are based on those evaluated for isolated surfaces, building modellers should consider carefully the basis for the heat transfer coefficient computed in their present models.

Although the studies [52] [53] presented an intensive comparison, the authors did not conclude on what approach to apply for implementation in numerical tools.

Similarly, Beausoleil-Morrison [9] classified the principal convective regimes found in buildings according to the driving force and its cause. The main objective of the work was the implementation of an algorithm in a building energy simulation program. Five main convective regimes have been distinguished: two buoyancy-driven flow regimes, two mechanically driven ones and one mixed flow regime. The correlations have been created by combining the correlations for natural convection [54] and for forced convection where the air is supplied by a ceiling diffuser [55]. For vertical surfaces, the program calculates convection coefficients for forced and natural convection by assigning appropriate equations to each internal surface each time-step of the simulation. Depending on the air movement, both heat transfer mechanisms are combined and result in one convective surface heat transfer coefficient.

The main advantage of the study reported by Beausoleil-Morrison [9] was the reduction of the large variety of CHTC correlations to a relatively small number (six), which made the dynamical choice of a convective model adapted to the time-evolving type of flow during the simulation possible. However, the current limitations are best described in [56]:

- The accuracy of the simulation results will still depend on the accuracy of the convective models implemented.
- Numerous correlations have been proposed for CHTC values for various flow types, but large uncertainties are still associated with them.
- Most correlations are abruptly separated in two parts with one relation for the laminar regime and a second one for the turbulent regime. The location of the transitional zone is generally arbitrary and correlations are less accurate for this region. Therefore, most of these correlations may only be used for conditions not too much different from those for which they have been derived. For a general use in building engineering, a better accuracy or reliability would be necessary, especially in the transitional region between the laminar and the turbulent regimes.
- Most investigations considered an isothermal plate (or wall) although other boundary conditions may also be of interest for various situations encountered when simulating building interiors.
- Even if averaged heat transfer coefficients are generally required, a better knowledge of the local characteristics of the convective phenomena should bring some additional refinement to building simulations.

Additionally, especially within the present study, it should be mentioned that a majority of the studies focuses on the determination of a correlation for the average CHTC on a building element, while correlations for the local CHTC are also needed to improve the hygrothermal simulations in a building.

Computational Fluid Dynamics

While computational fluid dynamics modelling has become more common, CFD tools to model heat transfer in building enclosures have been applied widely. A comparison of the models, which are currently available, for modelling heat transfer in a building is presented in [29] [32] [33]. Moreover, Awbi et *al*. [57] compared experimental results for natural convective heat transfer coefficients for heated room surfaces with CFD calculations. The standard k-ε model using standard wall functions and a low-Reynolds-number k-ε model were used. The authors [57] concluded that, since these wall functions are empirically derived for forced convection in pipes and over flat plates, the prediction of the CHTC is extremely sensitive to the distance of the point from the surface at which the wall function is applied. Furthermore, the investigation showed that, if a more accurate prediction of the convective surface heat transfer coefficient is desired, the low-Reynolds-number k-ε model is suitable, but computationally very expensive.

CHTC modelling considerations

The models for the local convective surface transfer coefficients for natural convection are based on the analytical boundary layer theory for a flat plate and experimental work. Similarly, the local convective surface heat transfer coefficient for forced convection is based on the boundary layer theory (flat-plate analogy) and correlations determined by Beausoleil-Morrison [9] applied locally. With respect to the

boundary layer theory for a flat plate, this theory may not be entirely transferrable to building components, for example a wall in a room.

Several assumptions are considered: temperature boundary conditions, geometrical influences, entrance velocity and leading edges, surface roughness. The validity of the assumptions is discussed based on the analysis presented by Erhorn *et al.* [49] and Khalifa *et al.* [52]. Erhorn *et al*. [49] measured the local surface heat and moisture transfer coefficients at different locations in a room. Khalifa *et al.* [52] reported an intensive review of the convective surface heat transfer coefficients on isolated vertical and horizontal surfaces with special interest in their application to building geometries, and on surfaces in two- and three-dimensional enclosures.

The example presented in Figure 10 is used for the illustration of the problem. The figure presents the airflow over a vertical plate, which is kept at a surface temperature T_s [°C], while heated with a uniform heat flux q [W m^{-2}]. The air velocity and temperature in the room at a reference distance from the plate are considered to be the reference velocity and temperature, indicated by the subscript ∞.

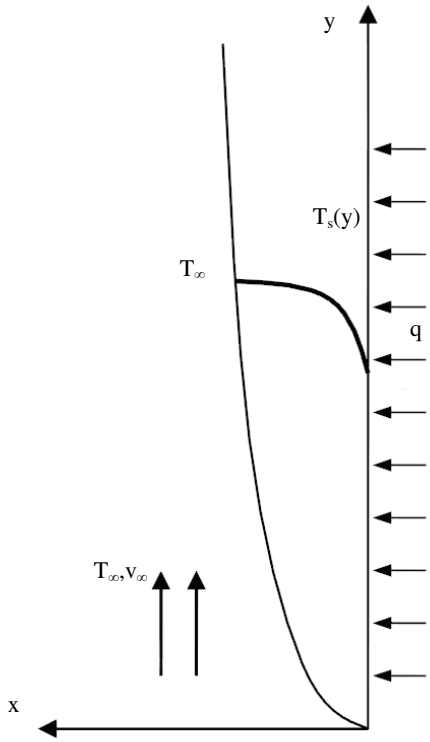

Figure 10: Airflow over a vertical flat plate with a surface temperature T_s and heat flux q [W m^{-2}].

With respect to the assumed boundary conditions for the temperature and heat flux along the plate, the boundary layer theory [50] assumes an isolated surface with either a constant surface temperature or uniform heat flux along the plate. The study reported by Erhorn [49] showed that neither the surface temperature along a wall in the building is constant nor the heat flux along the wall is uniform. However, the variation in the surface temperature of the plate and the non-uniformity of the heat flux may be relatively small, resulting in only a relatively small deviation in the local surface heat transfer coefficient prediction.

At the beginning of the flat plate, the velocity and temperature distributions of the airflow are assumed to be uniform with a velocity v_∞ and temperature T_∞. Furthermore, a sharp edge (or leading edge) located at

the beginning of the plate. The flow at the beginning of the plate is laminar, resulting in the development of a laminar boundary layer. After a certain distance $x = x_{critical}$ (from the leading edge), the boundary layer becomes turbulent. The transition from laminar to turbulent flow usually occurs at a critical Reynolds number ($Re_{x,\,critical}$) of $5 \cdot 10^5$. Although the transition from laminar to turbulent is a region of finite length, a transition point is used for simplicity and it is frequently assumed that the transition is sudden. The numerical value of $Re_{x,\,critical}$ is strongly dependent on how free from perturbation the outer flow is.

In building enclosures, it may not be valid to assume a leading edge, since the beginning of the building component is often located in a corner. Similarly, the assumption that the velocity and temperature distributions in the corner are constant and uniform may also be discussible. Khalifa et al. [52] showed that, in real sized enclosure, especially in buildings, where the location and the type of heating source and ventilation may influence the flow pattern in the enclosure, this may result in deviations between the CHTC predicted by boundary layer theory and the measured CHTC. It is also difficult to predict the flow pattern in the corner of the enclosure, since the airflow pattern in the corner is directly influenced by the indoor environmental conditions in the room. In general, the boundary layer near the corner may be less smooth compared to the boundary layer for a flat plate, while transition to a turbulent boundary layer occurs at a relatively short distance from the edge of the component.

Furthermore, the surface roughness of the building component may result in a more turbulent airflow along the building component compared to the airflow observed along a flat plate. The increased turbulence of the airflow may result in a higher Nusselt number, resulting in an increased convective surface heat transfer coefficient.

In conclusion, comparing the relationships based on the boundary layer theory [50], the experimental work from Erhorn *et al.* [49] and the review by Khalifa *et al.* [52], the analysis showed that values of the heat transfer coefficients based on the boundary layer theory and related assumptions should be considered carefully. The boundary layer theory for a vertical or horizontal flat plate may only be rarely applicable for building components and building enclosures.

2.5.2 Convective surface moisture transfer coefficient

The surface moisture transfer coefficient can be defined in an analogous way as the surface heat transfer coefficient, yet several options are available for the choice of the driving force. First of all, the difference between the vapour density at the interface and in the gas free stream is used (Eq. (11)), while a second option is the difference in mass fractions (Eq. (12)). Third, in building engineering it is common practice to use the difference in vapour pressure as a driving force for mass transfer (Eq. (13)). A fourth option to express the driving force is the use of mole fractions (or ratio of vapour pressure to total pressure) described by Eq. (14).

$$g = \beta^{\rho}(\rho_{v,s} - \rho_{v,\infty}) \tag{11}$$

$$g = \beta^{X}(X_s - X_{\infty}) \tag{12}$$

$$g = \beta^{P}(P_{v,s} - P_{v,\infty}) \tag{13}$$

$$g = \beta^{Z}(Z_s - Z_{\infty}) \tag{14}$$

where the subscripts ‘s’ and ‘∞’ respectively represent the surface and free stream conditions, g represents the mass flux [kg m^{-2} s^{-1}] at the interface between the gas and liquid or solid, β the surface mass transfer coefficient related to respectively the vapour density (ρ), the mass fraction (X), the partial vapour pressure (P_v), and the mole fraction Z. Moreover, ρ_v represents the vapour density (species mass per volume) [kg m^{-3}], X the mass fraction of the vapour (species mass per mixture mass) [kg kg^{-1}], P_v the vapour pressure (partial pressure of the species) [Pa], and Z the mole fraction (moles of species per mole mixture) [mol mol^{-1}].

The motivation for mentioning these definitions, presented by Eq. (11) – Eq. (14), here that the different definitions of the mass transfer coefficient are not (entirely) valid when describing convective mass transfer under changing ambient conditions in buildings. A theoretical and numerical study [13] on the validity of the different definitions of mass transfer coefficient showed that convective mass transfer

coefficients related to vapour pressure (Eq. (13)) as driving force is only applicable to isobaric systems and should be corrected by the static pressure when used under a different ambient pressure. Moreover, convective mass transfer coefficients related to vapour density (Eq. (11)) are only allowed under the condition of constant density. If this condition is not fulfilled, the values of the coefficient are dependent of the ambient conditions such as temperature, relative humidity and pressure. Hence, if the coefficient is used in non isothermal conditions an accurate prediction of the mass flux is only possible under exactly the same ambient conditions as those for which the mass transfer coefficients were originally determined.

When using mass fractions as driving force (Eq. (12)), the mass transfer coefficients are independent of the ambient temperature, relative humidity, and total pressure. Thus, from [13], it is concluded that the mass fraction as driving force is preferred.

2.5.2.1 CMTC correlations

Similarly as for the convective surface heat transfer coefficient (α_c), the formulae for the convective surface moisture or mass transfer coefficients (β) can be determined analytically, experimentally or numerically. A theoretical determination of the convective moisture transfer coefficient is based on the analogy of heat and mass transfer. Alternatively, experimental studies have been carried out to determine the CMTC in wind tunnels and in rooms.

Heat and Mass Transfer Analogy

The use of the heat and mass analogy for the calculation of average mass transfer coefficients inside buildings is common practise and is prescribed in a European Standard [58]. The Chilton-Colburn analogy [59] is probably the most successful and widely used analogy from heat, momentum, and mass transfer analogies. The basic mechanisms and mathematics of heat, mass, and momentum transport are considered to be essentially the same. Before the fundamentals and limitations of the analogy are discussed, the following dimensionless numbers, which are used for the characterization of the flow or heat/mass transfer regime are recalled:

$$\mathrm{Pr} = \frac{\nu}{\alpha} \tag{15}$$

where *Pr* is the Prandtl number which describes the ratio of the kinematic viscosity ν [$m^2 s^{-1}$] of the fluid and the thermal diffusivity α [$m^2 s^{-1}$].

$$\mathrm{Sc} = \frac{\nu}{D} \tag{16}$$

where *Sc* is the Schmidt number expressing the relation between the kinematic viscosity ν [$m^2 s^{-1}$] of the fluid and the mass diffusivity *D* [$m^2 s^{-1}$] of the species in the fluid.

$$\mathrm{St} = \frac{\alpha_c}{\rho c_p v_\infty} \tag{17}$$

St is the Stanton number for heat transfer, which measures the ratio of heat transferred into a fluid to the thermal capacity of the fluid, where α_c is the convective surface heat transfer coefficient [W m^{-2} K^{-1}], ρ the density of the fluid [kg m^{-3}], c_p the fluid's thermal capacity [J kg^{-1} K^{-1}], and v_∞ the free stream velocity [m s^{-1}] in external flow and the bulk mean fluid velocity in internal flow.

$$\mathrm{St_m} = \frac{\beta^\rho}{v_\infty} \tag{18}$$

Similarly, St_m is the Stanton number for mass transfer, representing the ratio of species transferred into a fluid, where β^ρ is the convective surface mass transfer coefficient [m s^{-1}] related to the vapour density, and v_∞ the free stream velocity [m s^{-1}] or bulk mean fluid velocity.

Combining the expressions presented by Eq. (15) – Eq. (18), this results in the Chilton-Colburn analogy:

$$St\, Pr^{2/3} = St_m\, Sc^{2/3} \tag{19}$$

Using the definition of heat and mass Stanton numbers, Eq. (19) can be expressed more conveniently:

$$\frac{St}{St_m} = \left(\frac{Sc}{Pr}\right)^{2/3} \tag{20}$$

$$\frac{h}{h_m} = \rho c_p \left(\frac{Sc}{Pr}\right)^{2/3} = \rho c_p \left(\frac{\alpha}{D}\right)^{2/3} = \rho c_p Le^{2/3} \tag{21}$$

where *Le* is the Lewis number, defined as the ratio of thermal diffusivity α [m^2s^{-1}] to mass diffusivity *D* [m^2s^{-1}]. Additionally, it should be mentioned that in a special case in which the molecular diffusivities of momentum, heat, and species are identical, i.e. $\nu = \alpha = D$, and thus $Pr = Sc = Le = 1$, Eq. (21) reduces to the Reynolds analogy:

$$\alpha_c \cong \rho c_p \beta^\rho \tag{22}$$

The main requirement for the Reynolds analogy to be valid is: $Pr = Sc = Le = 1$. In practice, this condition is never fulfilled in buildings, since the Prandtl number for air is approximately 0.713. Therefore, the Chilton-Colburn analogy is preferred for applications in buildings.

The Validity of the Chilton-Colburn Analogy in Buildings

The Chilton-Colburn analogy (Eq. (21)) is a convenient relationship, since the convective surface heat and mass transfer coefficients are directly related to each other. The analogy has been observed to hold quite well in laminar and turbulent flow over plane surfaces. But this is not always the case for internal flow and flow over irregular geometries. In general, this equation, relating convective heat and mass transfer, is valid for gases and liquids within the ranges, $0.6 < Sc < 2500$ and $0.6 < Pr < 100$ [60]. The analogy is valid for smooth surfaces and is based on the assumption that respectively the dimensionless velocity and temperature profiles and the dimensionless velocity and species concentration profiles are similar.

Recently, the validity of the heat and mass analogy for airflows inside buildings has been studied by Steeman [13]. Despite the frequent use of the heat and mass transfer analogy, the author investigated whether the relationship is applicable for the determination of average and local convective surface mass transfer coefficients inside buildings, where natural and mixed convection occurs over complex geometries. The study analyzed the performance of the Chilton-Colburn analogy for 80 scenarios, representing natural and mixed convection in a room, including scenarios with simultaneous heat and maas transfer, with a Lewis number equal to one (Le = 1), uniform and discrete moisture sources and non-analogous boundary conditions.

The conclusions [13], which are most important for the present study are summarized briefly:

- For the scenarios with simultaneous heat and mass transfer and with Le = 1, the over and under prediction of both the average and local surface mass transfer coefficient is limited to respectively 14% and 3%. The relatively good results prove the capability of the heat and mass transfer analogy to accurately predict mass transfer coefficients for natural and mixed convection in these cases. The mutual influence of heat and mass transport appeared to be small in humid air at ambient condition, and does not affect the validity of the analogy.

- With respect to the cases with moisture sources in the room, a relatively large over- and under-prediction of the local surface mass transfer coefficient may occur locally near the moisture source itself.
- The study showed that problems can arise due to the choice of the reference condition, especially considering the cases with non-analogous boundary conditions for heat and mass transport. In many applications one single reference is chosen to calculate the transfer coefficient at different positions. It is however not always possible to relate all local fluxes to a single reference. As a result it may occur that the difference between the reference condition and the surface condition is nearly zero, while non-zero flux exists. In that case, it has been recommended to choose a different set of reference conditions, preferably the mass averaged indoor condition.

Regarding the research presented by Steeman [13], one important remark should be made. In practical cases, the requirement, that all boundary conditions for heat and mass transfer inside buildings should be analogous, is rarely fulfilled. If the boundary conditions are not analogous, the accurate prediction of local mass fluxes using the analogy is no longer guaranteed when one single reference value is used. (The prediction of average mass flow rates using one single reference is less sensitive to dissimilarities in the boundary conditions). Consequently, the author [13] concluded that it is not recommended to use the analogy for the prediction of local mass transfer coefficients and to determine the local mass transfer coefficients directly, for instance with a computational fluid dynamics model. However, a more intensive examination of the study [13] showed that it is not necessarily required to discard the Chilton-Colburn analogy, but, hence, use computational fluid dynamics to choose the correct reference condition for the analogy. In this way, the determination of local surface mass transfer coefficients in case of non-analogous boundary conditions by means of the Chilton-Colburn analogy is applicable, but should be done carefully.

Experimental Work

Compared to the experimental work that focuses on the determination of the local convective surface heat transfer coefficients in buildings, measurements that have been carried out to determine the relationship between the convective surface moisture transfer coefficients are limited. While some researchers, such as Schwarz [61], measured convective surface moisture transfer coefficients on external building surfaces, others used measurements in full-scale test facilities [62] [63] [64] [65], or wind-tunnel experiments [64] [66], focussing on internal building surfaces.

In [65], data for vapour transfer resistances for flows in natural and forced convection in and around buildings has been published. Bednar et *al*. [62] measured surface transfer coefficients for indoor environments under non-stationery conditions, for example in a room with still air and during short term airing. Similarly, an investigation of the relationship between the surface vapour transfer resistance and the airflow velocity above a material sample in a test room is reported by Mortensen et *al*. [63]. The experiments are performed by use of the ordinary cup method for permeability tests.

Focussing on the determination of the local surface moisture transfer coefficient in a wind-tunnel, Talev et *al*.[64] used three horizontal water cups, placed inline after each other in the tunnel. Moreover, the convective moisture transfer coefficient between a forced convective airflow (at relatively low Reynolds numbers) and a free water surface in a rectangular duct was reported in [66].

Figure 11 [67] shows a comparison of the results from [61] [63], and [66]. The results obtained from the studies show that the surface resistance decreases, as expected, for increasing airflow velocity above the boundary layer of the material surface. All experiments were carried out under forced convective conditions. Only Iskra and Simonson [66] make a clear distinction between data obtained for laminar or turbulent flow and present their data as function of the Reynolds number. Figure 11 presents the laminar flow regime results [66]. These are clearly situated in the low velocity range.

Mortensen [63] measured a slightly larger velocity range which resulted in approximately 50% higher mass transfer coefficients compared to [66]. Talev et *al*. [64] reported surface moisture transfer coefficients, which are approximately a factor two larger compared to the data presented by Schwarz [61] and Worch [65]. However, only the data reported in [66] seems to be useful, as only this experiment is well documented at the moment.

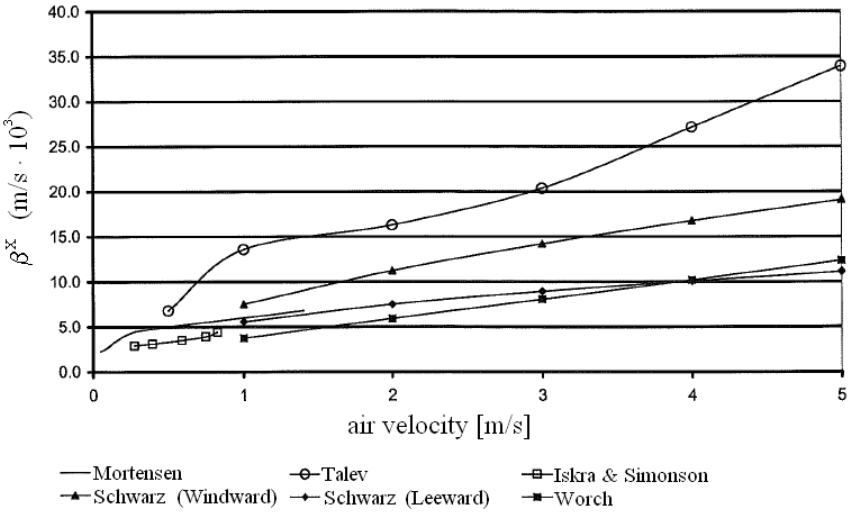

Figure 11: Experimental results for the surface moisture transfer coefficient (SMTC) as a function of the air velocity [67]

Computational Fluid Dynamics

As an alternative to the limited number of relationships obtained from experimental investigations, researchers used CFD simulation to get a more accurate prediction of the convective surface moisture transfer coefficients near the building component. Most researchers used CFD not only for the modelling of the surface moisture transfer coefficients, but also for the modelling of the hygrothermal interaction between the local indoor environment and the building component [13] [19] [68]. A summary of the modelling of this hygrothermal environment-component interaction is presented in the next section.

2.6 Coupling airflow and HAM model

Section 2.2 showed that several options for the modelling of the heat and moisture transport in indoor air are available. Nevertheless, only sub-zonal airflow models and computational fluid dynamics are capable of providing a prediction of the local temperature and relative humidity in a room. With the availability of sub-zonal models and CFD, two options are possible for the calculation of the local convective surface transfer coefficients. First of all, CFD could be used directly to calculate the local convective surface heat and moisture transfer coefficients. Second, in Section 2.5, it was demonstrated that relationships for the convective surface heat and moisture transfer coefficients could be used, if information regarding the local environmental conditions in the room resulting from the sub-zonal airflow model is available. This enables the calculation of the heat and moisture flows between the building zone and the building component, which serve as boundary conditions for the HAM component model.

Both options have been investigated by other researchers and both CFD models and sub-zonal airflow models have been coupled to HAM component models previously. Section 2.6.1 presents a literature review of the research that focussed on the coupling between CFD and HAM models. In Section 2.6.2, the studies that aimed at the coupling between sub-zonal airflow and HAM models are reviewed. In Section 2.6.3, coupling strategies and data exchange methods to couple airflow models and HAM component models are evaluated.

2.6.1 Coupling CFD-HAM

In general, two approaches are available to couple CFD with HAM simulation. The first one is to extend the CFD domain to solve heat and moisture transfer in solid materials. In literature, this approach is often referred to as internal coupling. Previous studies on the coupling of CFD and building energy simulation (BES) [69] [70] indicated that this approach is very computationally expensive and would not become a design tool in the near future. However, researchers have applied this approach for solving combined HAM transport in buildings.

Mortensen et *al*. [68] modelled both the airflow and its interactions with constructions in the commercial CFD tool Fluent. The constructions are modelled as immobile fluids having ordinary building material characteristics. A diffusion model to model the vapour diffusion within the wall was used. The walls have been declared as laminar zones with zero velocity. The author [68] showed that it is possible to investigate the microclimates in rooms with the described CFD model. Two particular cases with different moisture sources have been simulated. The numerical results have been compared to Particle Image Velocimetry (PIV) measurements [10]. It was found that the simulations gave reasonable results for the average flow in the room, however some discrepancies have been observed in the microclimatic environments, for example behind the furniture.

Similarly, Steeman [13] extended the commercially available CFD package Fluent with the effective moisture penetration depth (EMPD) model [71], describing the moisture buffering of the wall. The CFD model has been validated using experimental results. Furthermore, the results from the CFD-EMPD model have been compared to the simulation results obtained with a nodal model using a similar EMPD approach. Steeman concludes that the well-mixed sub-zonal model was able to predict the average indoor water vapour pressure with good accuracy. The accuracy of the well-mixed sub-zonal model could be further improved by using CFD generated surface transfer coefficients. The author showed that it is not always necessary to use the fully coupled CFD–EMPD model to predict the average indoor climate. It can be sufficient to determine the average surface transfer coefficient with CFD for one relevant situation, which significantly reduces the computational cost. In case of multi-zone building simulation, it can thus be recommended to only use CFD for those zones with a geometry substantially different from the standard cases with well known surface transfer coefficients (or for those zones where the micro-environment has to be known). For those cases, the use of CFD for the prediction of average surface transfer coefficients can improve the accuracy of the (de)humidification loads predicted by building energy codes.

Moreover, Steeman [13] developed the CFD-EMPD model into a fully coupled CFD-HAM model, which is able to predict the hygrothermal conditions in the porous building material as well as the surrounding indoor environment. The microclimate in a showcase for the protection of paintings was used to demonstrate the capabilities of the CFD-HAM model with respect to the simulation of the interaction between the velocity, temperature and relative humidity of the air inside the showcase and the hygrothermal response of the painting. The author concluded that the developed model is capable of predicting the effect of air distributions on the hygrothermal behaviour of porous objects in practical cases and is a valuable tool for the study and prevention of moisture related damage in valuable objects.

Both authors [13] [68] successfully modelled the interaction between the indoor environment and the HAM transport in the building component. While both models predict the velocity, temperature and relative humidity distribution in the room, the main disadvantage of both models is that the computational effort is relatively large.

A second alternative approach is to couple a CFD program with a HAM component simulation program, where the HAM simulation program handles the heat and moisture transfer in enclosures with a large time step (a few minutes to an hour), while CFD simulates the airflow at a specific time step. Such a coupling procedure largely reduces computing time because it does not solve the flow field during the transition from one time step to another. This coupling approach has been widely applied in building energy simulation, often referred to as external coupling, and has shown improved accuracy in both the energy simulations and indoor airflow computations [72]. Though, few researchers have applied such an approach when modelling the indoor environment and the HAM conditions in the building envelope.

In [19], a model that couples CFD with an external vapour transport model in order to simulate vapour transfer between air and porous materials was presented. A transient case of turbulent air flow over a drying wood sample, and a transient case of transitional air flow over gypsum samples were simulated. The author concluded that time discretization appeared to have an important impact on the results. Importance should be placed on the time stepping scheme used to discretize the simulation. Moreover, further work, such as the validation of the numerical results with experimental data and the implementation of adaptive time stepping, was recommended.

Clovis [73] indicated that CFD seems to be a complex package to be integrated with a whole building simulation package and a careful approach must be exercised when coupling CFD tools with other systemic simulation tools. The author pointed out that computing time used by CFD as well as stability and convergence of numerical methods are two major issues associated with the integration of CFD and energy simulation. Similar issues are important when considering the coupling of CFD and HAM component modelling. In addition, it should be noticed that the mathematical equations describing the moisture transport in porous building materials are strongly non-linear. Thus, not only the numerical stability and convergence of the CFD model is important, but also the stability and convergence of the HAM component model.

Moreover, both systems, i.e. room air and building, have a different characteristic time. While room air has a characteristic time of a few seconds, the characteristic time of the building envelope usually lies between a few hours up to a few days. CFD simulation must be performed over a long period for the hygrothermal performance of the building envelope, but it must use a small time-step to account for the room air characteristics.

2.6.2 Coupling sub-zonal-HAM

A number of sub-zonal models, which are capable to predict the velocity, temperature and relative humidity field in a room, has been reviewed and compared in literature [38] [39] [42]. However, only few models incorporate the interaction between the HAM conditions in the building and the building envelope. Currently, the most detailed model to consider this interaction has been presented in [36] and [45]. The airflow in a test room [74] has been modeled using a standard sub-zonal model with a jet model. The heat and moisture transport in the building envelope was modelled using a one-dimensional envelope model, which treats coupled heat and moisture transfers in structural materials and considers that moisture migrates through the porous material in both liquid and vapour phases. In this way, the moisture buffering effects in construction materials were taken into account. Furthermore, radiation exchange between the building components was modelled. The predicted velocity and temperature fields have been compared to experimental data, and the authors conclude that the model gives reliable results. However, the predicted relative humidity has not been validated against experimental data.

The models described in [36] and [45] have two main limitations:

- The model does not take into account the heat and moisture distribution in the building component. Since the HAM component model is only one-dimensional, the model is not capable of predicting local variations in temperature and relative humidity in the component, for example due to thermal bridges.
- The convective surface heat and moisture transfer coefficients are modelled as average coefficients based on the research presented in [9]. Therefore, the model is not able to model local indoor environmental variations, for example due to a corner or micro-climatic conditions behind furniture.

2.6.3 Coupling strategies and data exchange methods

CFD models and sub-zonal airflow models have been coupled to HAM component models. However, coupling of the building zone and the component is not straight-forward. While the characteristic time with respect to the HAM flows in a building component is relatively long, usually between a few hours up to a few days, the characteristic time of the airflow in a room varies between a few minutes and a few hours. The difference between these characteristic times makes a transient simulation of both systems inefficient. While the airflow simulation requires the model to take relatively small time steps, calculation of the heat and moisture flows in the building component at these steps would result in small deviations of the flows over time, and in principle in unnecessary computations. Or, in other words, CFD simulation must be performed over a long period for the hygrothermal performance of the building envelope, but it must use a small time-step to account for the room air characteristics. Therefore, the room model and the component model should be coupled in such a way that a simulation can be carried out efficiently. The efficiency, accuracy, computational effort (or simulation time), and flexibility of the data exchange methods between the envelope and room model are important.

Strategies [75] [16], approaches [17] [70], and guidelines [18] [72] for the coupling between airflow and building envelope models have been reported. Basically, two coupling strategies are distinguished (Figure 12): internal coupling, i.e. the equations describing the HAM transport in the building envelope model and the room model are solved in the same domain, and external coupling, where both models are solved in different domains, while information between the domains is exchanged at different times. Regarding external coupling of the domains, static coupling and dynamic coupling can be distinguished. While the static coupling process has occasional (static) information exchange for a simulation, the dynamic coupling process performs continuous (dynamic) information exchange between the room and the envelope model.

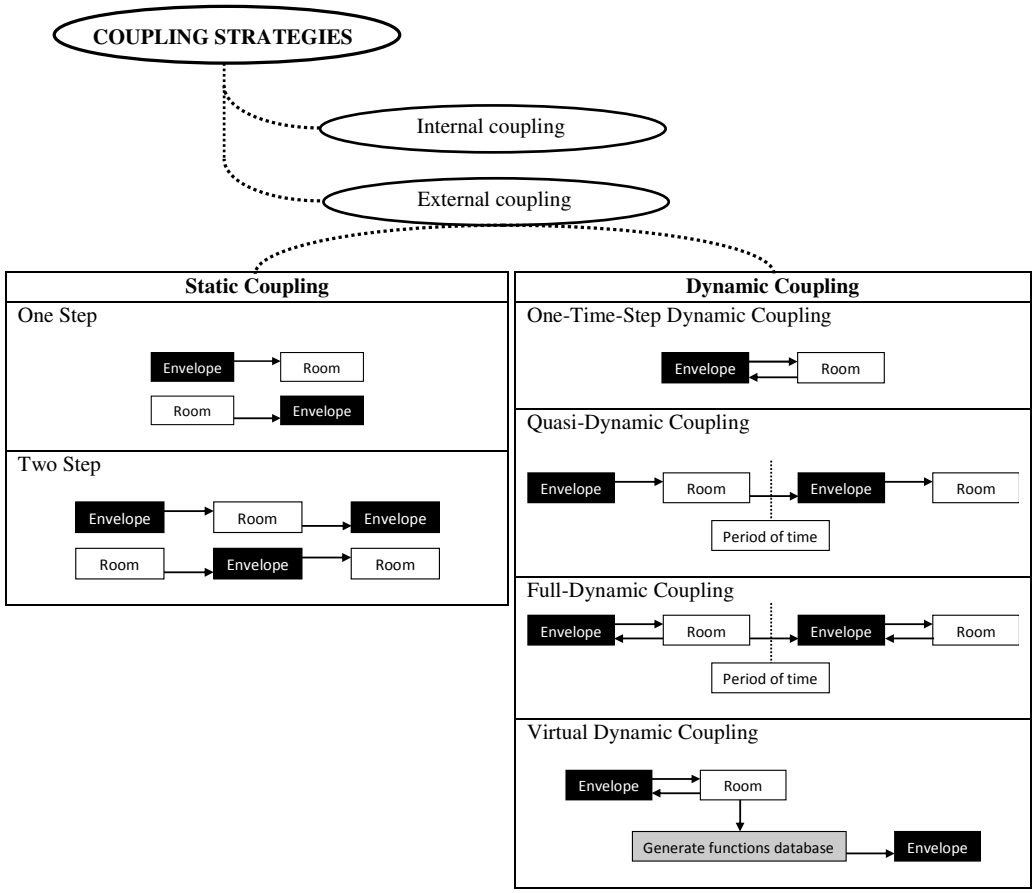

Figure 12: Illustration of the coupling strategies between the building envelope model and the room airflow model.

Figure 12 shows that the static coupling involves one-step or two-step information exchange between the envelope and the room model, depending on the sensitivity of the building HAM performance and user's accuracy requirement on solutions. With only a few coupling steps, the static coupling can be performed manually. Generally, the one-step coupling is good in cases where the stability of the domains is not very sensitive to the exchanged variables [70]. The two-step static coupling is a good coupling strategy for buildings with little changes in the exchanged information, and where the results of the HAM component model do not strongly depend on the exchanged data.

Dynamic coupling, which involves coupling between the two domains at every time-step, is needed when both models are sensitive to the transient boundary conditions. Figure 12 presents four types of dynamic coupling:

- One-time-step dynamic coupling, which is focuses on the envelope/room coupling at one specific time-step of interest. At that time-step, the iteration between both domains is performed to reach a converged solution. This coupling is applied in cases in which a designer is interested in only a

few typical scenarios (design conditions) and both domains are very sensitive to the exchanged information.

- Quasi-dynamic means that the envelope/room model is not coupled at every time step. Many building designs require the airflow, heat and moisture flows over a period of time, such as start-up and shutdown periods. The envelope/room coupling may be conducted at every time-step over this period. When the time-step is relatively small, it may not be necessary to couple the two programs at every time-step because the changes of the required information may not be significant. In this case, the coupling requires no iteration between the two domains.
- Full dynamic coupling involves the iteration between the two domains for a couple of times at each time-step to reach a converged solution. This coupling strategy is undoubtedly the most accurate, but also the most computationally intensive. Full dynamic coupling may for example be necessary for poorly insulated buildings with dynamical loads.
- Virtual dynamic coupling might be an efficient way to reduce the computational costs. This coupling strategy is often applied with respect to the use of CFD models for the prediction of the indoor environmental conditions in the room. Complete models, based on computational fluid dynamics (CFD) are time-consuming for real-time applications. In this approach, a reduced model is needed. When the air temperature has negligible variations, the velocity field may be considered fixed. In this case, the size of a CFD model may be reduced by solving only the energy balance equation, then putting this equation in the form of state-space and finally by reducing its order by proper orthogonal decomposition (POD). In [76], such an algorithm was applied to a room equipped with a fan coil. Four fixed airflow fields, corresponding to negligible air temperature variation, were considered, resulting in four airflow patterns. The reduced model obtained from these airflow patterns was validated by comparison with CFD results.

Apart from the coupling algorithm that determines the efficiency, accuracy, computational effort (or simulation time), and flexibility of the data exchange methods between the envelope and room model is important. In [72], three feasible data exchange methods were evaluated and compared for the coupling between energy simulation (ES) and CFD.

Table 3 presents a comparison of the data exchange methods evaluated based on stability and computational effort. The table shows that method-1, which transfers enclosure interior surface temperatures (T_s) from ES to CFD and returns convective heat transfer coefficients (α_c) and indoor air temperature gradients ($\Delta T_{room,a}$) from CFD to ES, is more stable than method-2, which transfers enclosure interior surface temperatures (T_s) from ES to CFD, but returns convective heat fluxes (Q_{conv}) from CFD to ES. Method-1 showed to be unconditionally satisfy the convergence condition when the heat transfer coefficient is larger than zero. Meanwhile, the computing cost of method-2 is most expensive, sine it runs an explicit iteration scheme in ES while the others are implicit. Comparing data exchange method-1 and method-3, the computational effort of method-3 is relatively high, which results in a recommendation of the authors [72] to use method-1 for coupling ES and CFD.

Table 3: Data exchange methods [72]

Data exchange method	ES → CFD	CFD → ES	Stability	Computational effort
1	T_s	α_c, $\Delta T_{room,a}$	high	Low
2	T_s	Q_{conv}	low	high
3	Q_{conv}	α_c, $\Delta T_{room,a}$	high	high

Where α_c is the convective heat transfer coefficients [W $m^{-2}K^{-1}$] , $\Delta T_{room,a}$ the indoor air temperature gradient [K], and Q_{conv} the convective heat flux [W m^{-2}]

2.7 Summary and Conclusions

Current software for the simulation of the heat, air, and moisture conditions in a building have been categorized in three classes and it has been demonstrated that it is common to subdivide these tools based on the spatial discretisation or granularity of the model. Focusing on the room-component interaction, the accurate prediction of this interaction depends on the local near-component conditions, and the convective surface transfer coefficients. The prediction of the local conditions and coefficients is directly influenced by the airflow model that describes the indoor airflow in the building near the component. With respect to the modelling of the airflow in a room, several options are available, though only computational fluid dynamics and sub-zonal airflow models are capable of providing a prediction of the local temperature and relative humidity in a room.

The literature review showed that CFD applications for indoor airflow simulation have achieved considerable success and serve as a valuable tool for predicting airflow, temperature and relative humidity distributions in enclosed environments as well as the local convective surface transfer coefficients. However, there are many factors influencing the results predicted. CFD results should be analyzed with care, and validation with experimental results is always required. Nevertheless, detailed airflow models cannot easily and quickly solve time-dependent hygrothermal interactions across the boundaries of a building model. In practice, only steady-state simulations of the airflow in a single room at a specific time, and/or transient simulations over a relatively short period of time, for example a diurnal cycle, are feasible. And, since these calculations are relatively computational intensive, transient calculations over a longer period of time are currently not possible.

As an alternative for the use of CFD models, which are strongly limited by computer capacity, sub-zonal airflow models can be used. The review demonstrated that the sub-zonal modelling approach can be a suitable method to estimate temperature and relative humidity fields in a room with reasonable accuracy. Adding specific laws to describe momentum-driven flows, such as jets, may improve the quality of the airflow pattern predictions. Compared to CFD, sub-zonal models can give a satisfactory estimate of airflow patterns, but cannot give highly detailed information on air speed magnitude. Moreover, the local conditions predicted by the sub-zonal model could be used for the prediction of the local convective surface transfer coefficients. The main advantage of the sub-zonal model is a significant reduction in computational effort compared to CFD. The ability of the sub-zonal model to provide a relatively accurate prediction of the local conditions in a room as well as the short computation time makes the application of the sub-zonal model attractive for the transient simulation of heat, air and moisture in buildings.

In this thesis, the applicability of sub-zonal airflow modelling for the prediction of the local environmental conditions and surface transfer coefficients is investigated. The main objective is to obtain a more accurate assessment of the heat, air and moisture conditions in the building component and the zone by modelling and coupling a sub-zonal airflow model, which describes the varying, non-uniform indoor airflow near a building component with a HAM component model. Since both systems, i.e. the room air and the building envelope, have a different characteristic time, both models should be coupled in an efficient way, regarding efficiency, accuracy, computational effort (or simulation time), and flexibility. In the present study, strategies, approaches, and guidelines are analyzed. It is the objective to develop an efficient and flexible model, which is applicable for the assessment of the heat, air and moisture transport in the indoor environment and within the building envelope as well as the interaction between both domains. More specifically, the model should provide detailed information of the local environmental conditions in the building zone near the building component, i.e. the local air temperature, and relative humidity, of the local conditions in the building component, and detailed information regarding the local convective surface transfer coefficients. Moreover, the model should be suitable for transient heat, air and moisture simulations of the component-indoor air interaction, provided the computation time is relatively short.

3 Influence of Hygrothermal Interactions

The main objective of the work presented in this thesis is to obtain a more accurate assessment of the heat, air and moisture conditions in the building component and the zone by modelling and coupling a sub-zonal airflow model, which describes the varying, non-uniform indoor airflow near a building component with a HAM component model. Compared to the multi-zone/nodal airflow models, a sub-zonal model may lead to a relatively accurate prediction of the local temperature and relative humidity near the building component, and convective surface transfer coefficients. At the same time, the relatively short computation time still enables an efficient coupling with the HAM component model.

This section focuses on the magnitude of the surface heat and moisture transfer coefficients, and investigates how the magnitude of these coefficients may affect the hygrothermal performance of building components and building zones. For the building components, the analysis particularly emphasizes the surface relative humidity and temperature and the formation of surface moulds. For the building zones, the analysis studies the interior temperature and relative humidity and the heat and moisture buffering in the building zone.

The literature study showed that current simulation models to predict heat, air and moisture conditions in buildings assume average and constant surface transfer coefficients for convective heat and moisture transfer. An overview of the research that focused on the modelling of the convective surface heat and moisture transfer coefficients has been presented in Chapter 2. A parameter study has been used to investigate how the magnitude of the surface transfer coefficients - resulting from the air velocity near the surface of a building component – influences the hygrothermal conditions in the building component and the indoor environment is presented. Three building components have been selected as calculation objects for the analysis. Different values for the surface heat and moisture transfer coefficients have been applied. The hygrothermal response of the building has been simulated and the simulation results are presented and discussed.

Section 3.1 presents the methodology that has been applied to investigate the influence of the surface transfer coefficients on the hygrothermal conditions in the building component and the building zone. The results of the study are presented in Section 3.2. Section 3.3 presents the conclusions of the parameter study.

3.1 Analysis and Methods

A parameter study was used to investigate how the magnitude of the surface transfer coefficients – resulting from the air velocity near the surface of a building component – influences the hygrothermal conditions in the building component and the indoor environment. Three building components were selected as calculation objects for the analysis. Different values for the surface heat and moisture transfer coefficients were applied. Next, the hygrothermal response of the building was simulated and the simulation results are presented and discussed.

3.1.1 Simulation strategy

A parameter study was used to investigate how the magnitude surface transfer coefficients - resulting from the air velocity near the surface of a building component - influences the hygrothermal conditions on the building component and in the indoor environment. The simulation strategy which was applied is as follows:

The hygrothermal performance of a building zone and building components has been investigated using a coupled whole-building HAM simulation. First of all, the geometry of a building (Figure 13) which is defined along the lines of Common Exercise 1 of the IEA-ECBS Annex 41 [77], was selected for analysis. The properties of the building are presented in Table 4. The geometry of the building is coupled to the calculation objects which are presented in the following sub-section.

Second, the geometry of the building was defined in CHAMPS-Multizone [16], a multizone/network model for inter-zonal air and pollutant transport. The geometry of the calculation objects is defined in CHAMPS-BES [78], which is an envelope model for the coupled simulation of heat, air, moisture and

pollutant transport in a building component. Both models are coupled in order to solve the governing equations in the different domains, i.e. in the zone and in the component, simultaneously.

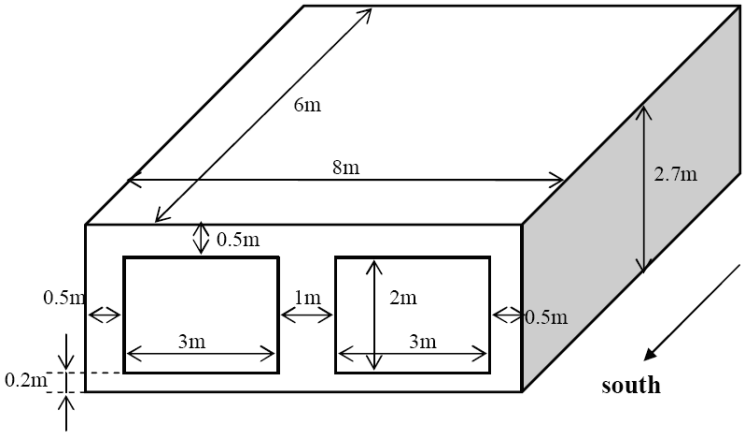

Figure 13: Geometry of the building [77]

Third, external boundary conditions were applied using the Test Reference Year (TRY) for Danish (Copenhagen) outdoor climatic conditions. The building is exposed to the TRY outdoor air temperature and relative humidity, while solar radiation is not accounted for in the simulation of the calculation objects. Since the surface conditions on the internal side of the building component, and the interaction between the indoor environmental conditions in the room and the building component are the main focus, the modelling of solar radiation has been omitted.

Fourth, the indoor environmental conditions were applied. According to the requirements of Common Exercise 1 [77] the temperature in the building is controlled to be between 20 - 27 °C during the entire year. However, within the CHAMPS software environment it is not possible to control the indoor air temperature directly. To obtain comfortable indoor environmental conditions, a separate prediction of the required heating and cooling load is needed. An estimate of the required heating/cooling power can be obtained using a whole building simulation in HAMBASE [79]. The resulting heating/cooling power is supplied to the building configured in CHAMPS-Multizone. In this way, the indoor air temperature is found to be between 20 - 27 °C during the entire year. Internal heat gains and moisture sources are applied according to the figures, presented in Table 4.

Table 4: Building properties

Volume [m^3]		129.6
Air change rate [1 h^{-1}]	Constant	0.75
Internal gains [W]	Constant	200.0
Moisture source [g h^{-1}]	9.00h – 17.00h	792

Fifth, different values for the surface heat and moisture transfer coefficients were applied. Lower and higher limits for the surface transfer coefficients were applied as well as a combination of a standard surface heat transfer coefficient with a lower and a higher limit for the moisture transfer coefficient.

Then, an initial temperature and relative humidity of 20 °C and 50% RH respectively were applied throughout the entire building. The hygrothermal performance of the building was simulated for one year. The investigations showed that a transition period may be neglected using these initial conditions of 20 °C and 50% RH, which are average conditions, representative for the entire year.

3.1.2 Calculation objects

This section presents the building components that were analysed to investigate the influence of the surface transfer coefficients on the hygrothermal response of the building components and the building zone. It was our objective to compare the influence of the convective heat and mass transfer coefficients near the component using two wall elements and a concrete floor penetrating the external wall of a building. Figure 14 and Figure 15 present the geometry of the calculation objects. The composition of the wall elements is presented in Table 5. The material properties for the corresponding materials are presented in Table 6.

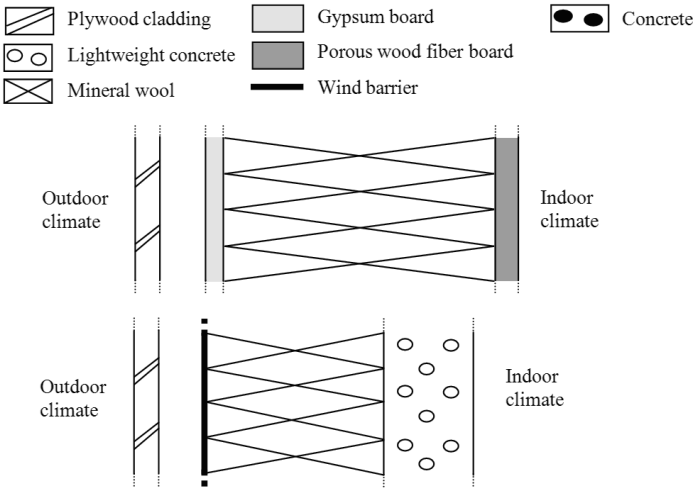

Figure 14: Composition of the timber frame and lightweight concrete wall.

Besides the wall elements, a floor penetrating the external wall of a building was analysed. Two rooms (on top of each other) were connected by a concrete floor. Both rooms were connected to the outdoor climate by the lightweight concrete wall, consisting of a plywood cladding, a wind barrier, mineral wool insulation and a lightweight concrete layer. The construction is presented in Figure 15. The reader should notice that the original geometry of the building (Figure 13) has been extended. For this analysis, the building could be considered as two original buildings on top of each other (Figure 15). Moreover, a one-dimensional model in CHAMPS-BES [78] has been used to simulate the HAM transport in the wall elements (Figure 14), while the building corner (Figure 15) has been modelled two-dimensionally.

It was the objective to investigate the influence of the surface heat transfer coefficients on the hygrothermal performance in the component when considering a thermal bridge, such as a balcony. Due to inertia effects, the air velocity near the corners was relatively low compared to the average air velocity in the room. Lower air velocities result in relatively low convective surface heat and mass transfer coefficients near the corner compared to the surface transfer coefficients in the centre of the components.

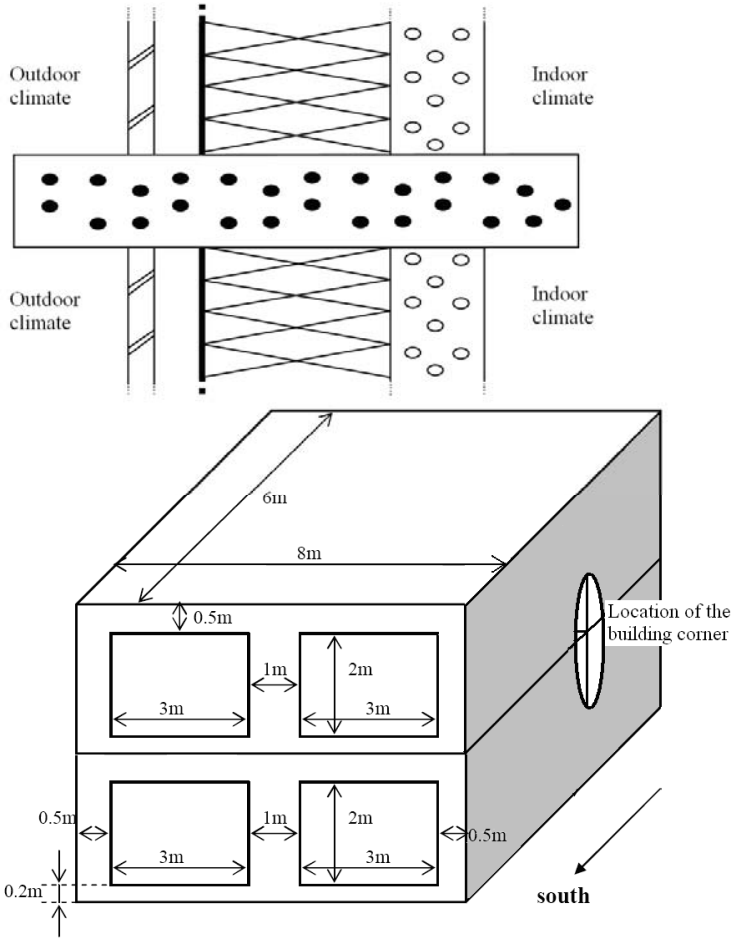

Figure 15 Building detail selected for analysis.

Table 5: Wall elements

Timber frame wall element	Lightweight concrete wall element
▪ 15 mm plywood cladding ▪ 25 mm air cavity ▪ 9 mm gypsum board wind barrier ▪ 150 mm glass mineral wool ▪ Vapour barrier ▪ 13 mm porous wood fibre board	▪ 15 mm plywood cladding ▪ 25 mm vented cavity ▪ wind barrier ▪ 100 mm glass wool ▪ 50 mm lightweight concrete

Table 6: Material Properties

	Porous wood fibre	Lightweight concrete	Concrete
d [mm]	13	50	300
λ [W m^{-1} K^{-1}]	0.13	0.45	1.5
ρ [kg m^{-3}]	450	1250	2200
c_p [J kg^{-1} K^{-1}]	2500	1050	840
δ [s]	$4.5 \cdot 10^{-12}$	$1.8 \cdot 10^{-11}$	$2 \cdot 10^{-12}$
ξ [kg m^{-3} Pa^{-1}]	0.0507	0.044	0.046

3.1.3 Parameter analysis

Several indoor environmental conditions, presented in Table 7, were investigated. Based on the observations obtained from the literature study [60] [80], typical values for the convective heat and moisture transfer coefficients were applied for the different indoor environmental conditions. The objective of the investigations (1 and 2) was to determine minimum and maximum hygrothermal conditions, which were likely to occur in the building component and the building zone. The objective of studying the conditions using a standard value for the convective surface heat transfer coefficient (conditions 3 and 4) was to compare the influences of the convective surface heat transfer coefficient and the surface moisture transfer coefficient separately. The hygrothermal response of the building was simulated using the values presented for the convective surface transfer coefficients, applied to the presented building components (Figure 14 and Figure 15). The specific values which have been applied for the surface transfer coefficients are presented in Table 7. It should be noticed that CHAMPS-Multizone [16] does not allow the separate modelling of convective and radiative heat transfer in the room. Therefore, the convective and radiative surface heat transfer coefficients have been treated as combined surface heat transfer coefficients.

For the convective surface transfer coefficients of other components, such as the floor and ceiling, values based on Beausoleil-Morrison [48] were applied, corresponding to a combined surface heat transfer coefficient of respectively 6 W m^{-2}K^{-1} and 10 W m^{-2}K^{-1}.

Table 7 : Convective heat and moisture transfer coefficients, which have been applied for the different indoor environmental conditions.

Cases	Conditions	Combined surface transfer coefficient	Convective surface heat transfer coefficient	Convective surface moisture transfer coefficient
		$\alpha = \alpha_c + \alpha_r$ [W m^{-2}K^{-1}]	α_c [W m^{-2}K^{-1}]	β_c [10^{-7} s m^{-1}]
1 Lower limits	Radiation, no convection	3	1	0.1
2 Upper limits	Radiation, forced convection	15	8	1
3 Lower limit β_c and standard α_c	Radiation, natural convection	8	3.5	0.1
4 Higher limit β_c and standard α_c	Radiation, mixed convection	8	3.5	1

3.2 Results

In this section the simulation results are presented. The predicted surface conditions on the walls and interior conditions in the room have been analyzed. Section 3.2.1 presents the predicted hygrothermal conditions on the surface of the building components. In Section 0, the predicted hygrothermal conditions in the building zone are presented. A discussion of the simulation results is presented in Section 3.2.3.

3.2.1 Hygrothermal conditions on building components

We give here the predicted hygrothermal conditions on the internal surface of the components (see Figure 14 and Figure 15). First of all, the surface temperature and relative humidity on the wall elements (Figure 14) during 2 days are presented. Second, weekly averaged surface conditions on the presented components were analyzed by presentation in an isopleth. Since the results obtained from the simulation of the timber frame wall are comparable to the results for the lightweight concrete wall, only the results obtained from the lightweight concrete wall simulations are presented. Third, the surface temperature and relative humidity in the corner of the thermal bridge (Figure 15) are shown.

Wall elements

Figure 16 shows the surface temperature, the surface relative humidity and the partial vapour pressure at the internal surface of the lightweight concrete wall during 2 days (May 27-28). The selected period is representative for the entire year. Figure 16 shows that a notable difference is present between the lower limit (1) and the higher limit (2). Comparing the surface conditions for the average surface heat transfer coefficient and lower and higher limits for the surface moisture transfer coefficient (conditions (3) and (4)), Figure 16 presents a relatively small deviation. Moreover, analysis of the partial vapour pressure shows, that a relatively small difference between the investigated limits is observed. From this observation, it may be concluded that the influence of the convective surface heat transfer coefficient on the hygrothermal performance is relatively large compared to the influence of the convective surface moisture transfer coefficient.

Figure 17 shows the surface conditions on the lightweight concrete wall predicted over the entire year from an analysis using an isopleth. The isopleth was based on daily averaged values for the surface temperature and relative humidity. Figure 17 shows that the difference between the observed conditions when applying lower (1) and higher limits (2) for the surface transfer coefficients is limited. When applying lower limits (1) for the surface transfer coefficients compared to the application of higher limits (2), the histograms show a comparable distribution. The number of days during which the surface conditions exceed 70% RH is relatively similar for both cases.

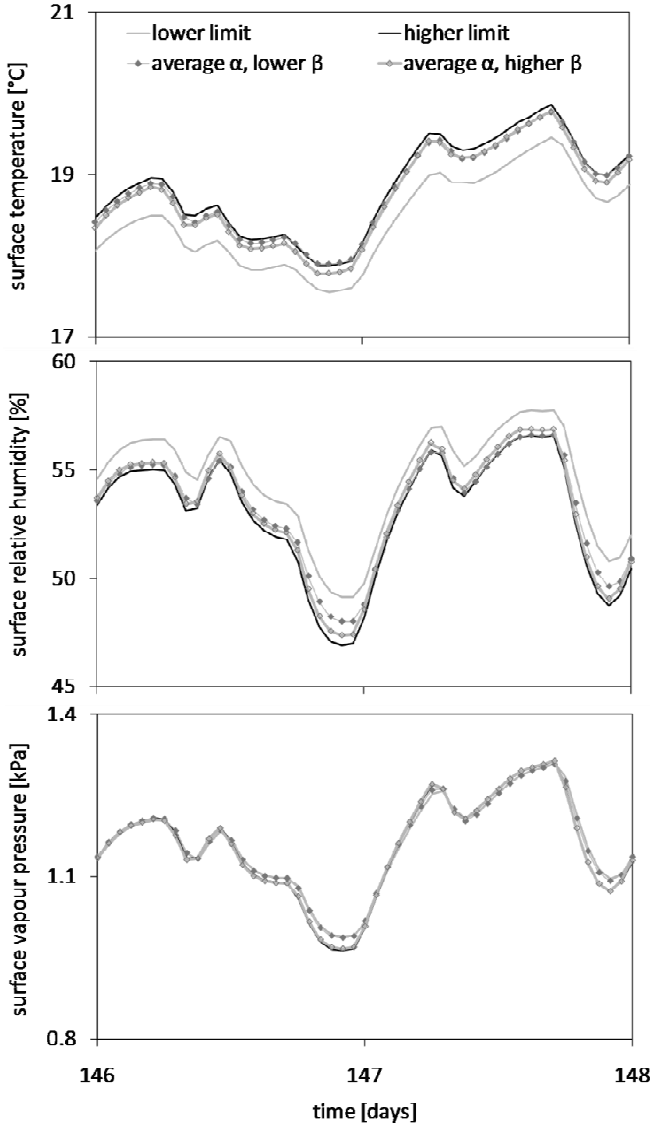

Figure 16: Surface temperature, relative humidity and vapour pressure at the internal side of the light weight concrete wall.

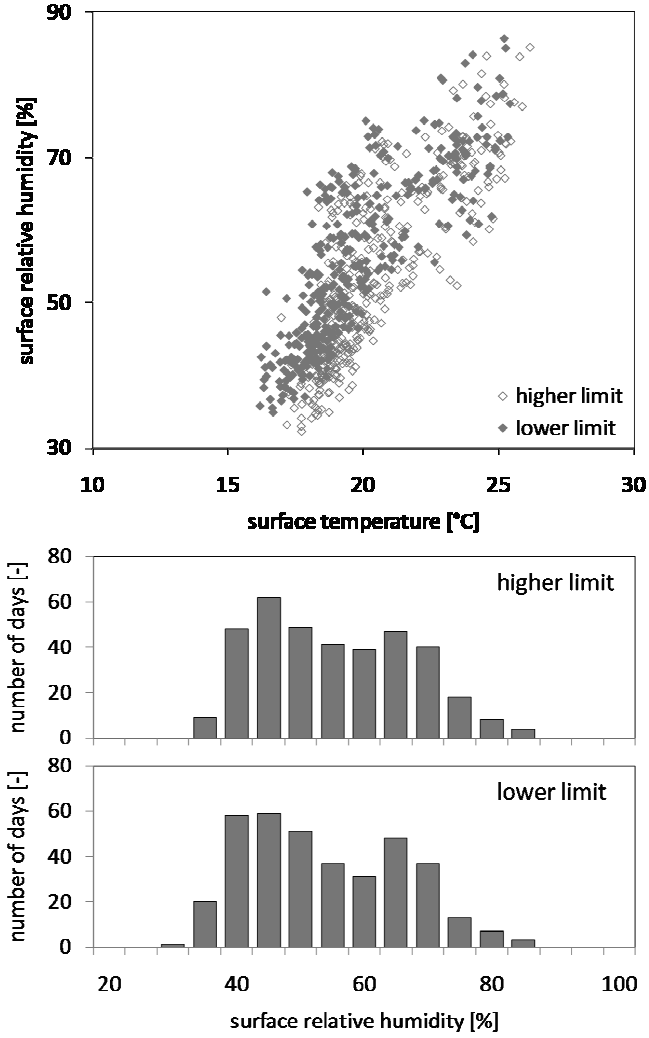

Figure 17: Predicted surface conditions for the lightweight concrete wall using lower (1) and higher limits (2) for the surface transfer coefficients. Isopleth representation of the daily averaged surface conditions during one year. Histogram of the observed daily averaged surface relative humidity as a function of the number of days.

Building corner

Figure 18 presents the temperature, the relative humidity and the partial vapour pressure in the corner of the building component during 2 days (May 27-28.). The figure shows that a relatively large difference is present between the lower limit (1) and the higher limit (2). Moreover, considering the hygrothermal conditions between the standard surface heat transfer coefficient and lower and higher limits for the surface moisture transfer coefficient (conditions (3) and (4)), the difference is significant.

Comparing the simulation results of the components and the thermal bridge for the standard surface heat transfer coefficient and lower and higher limits for the surface moisture transfer coefficient (conditions

(3) and (4)), the surface moisture transfer coefficient is shown to be more important when considering the thermal bridge. At the same time, the reader should realize that while the surface moisture coefficient has a larger influence here, the influence of the surface heat transfer coefficient is still dominant. Analysis of the relative humidity (Figure 18) shows that values of the predicted relative humidity, when assuming an average heat transfer coefficient (conditions (3) and (4)), lie closer to each other compared to the conditions with lower limits (1) and higher limits (2).

Figure 19 presents the temperature and relative humidity in the corner of the building component. The predicted conditions when applying lower limits (1) and higher limits (2) for the surface transfer coefficients have been compared. The daily averaged temperatures and relative humidities are presented in the isopleth. Comparing the simulation results for the wall elements (Figure 17) and the thermal bridge (Figure 19), the results show that the difference in the predicted hygrothermal conditions is relatively large for the thermal bridge.

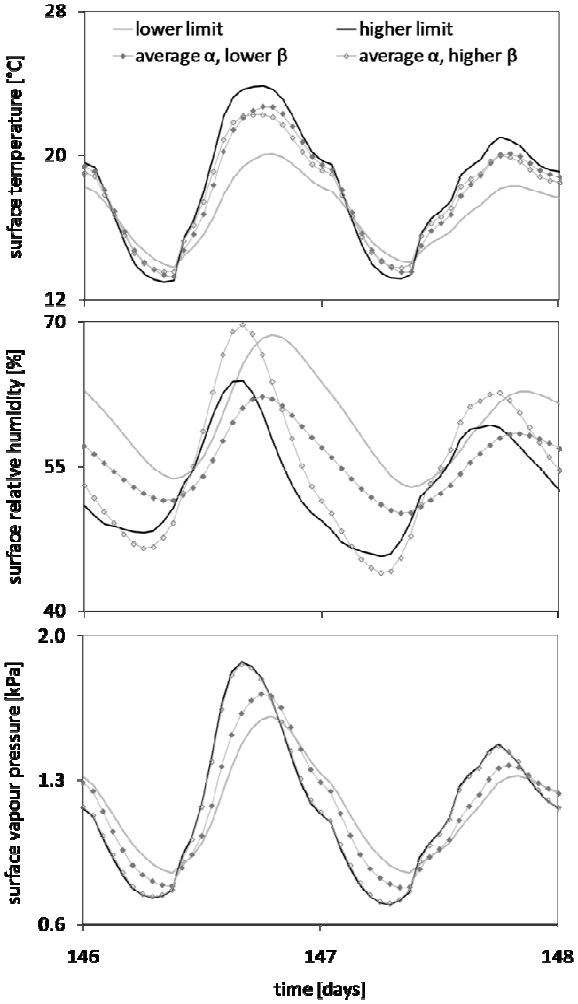

Figure 18: Surface temperature and relative humidity in the corner of the building component. The different conditions, i.e. lower limits, higher limits and average values for the surface transfer coefficients corresponding.

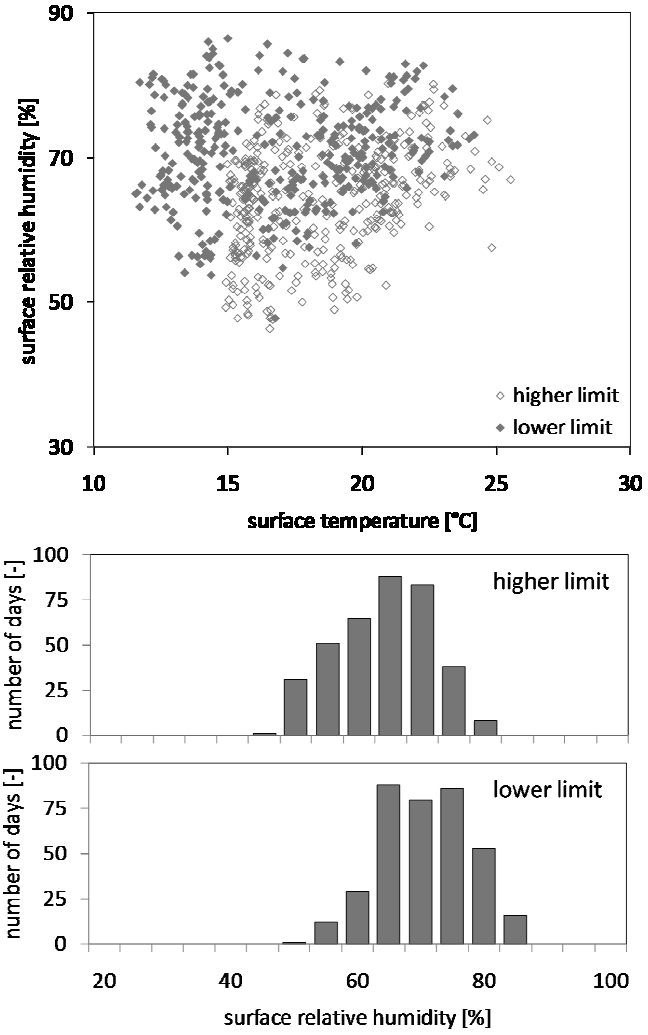

Figure 19: Temperature and relative humidity in the corner of the thermal bridge using lower (1) and higher limits (2) for the surface transfer coefficients. Isopleth representation of the daily averaged surface conditions during one year. Histogram of the observed daily averaged surface relative humidity as a function of the number of days.

3.2.2 Hygrothermal conditions in building zones

In this section, the influence of the surface heat and mass transfer coefficients on the hygrothermal conditions in the building zone is presented. Figure 20 shows the average indoor air temperature and relative humidity in the building zone for timber frame wall (TF) and the lightweight concrete wall (LC) with lower (1) and higher limits (2) for the surface transfer coefficients during 2 days (May 27-28). The simulation results show that the influence of both the surface heat transfer coefficient and the surface moisture transfer coefficient on the indoor environmental conditions is relatively large. Assuming standard values for the surface transfer coefficients may introduce relatively large errors in the prediction of the heat and moisture fluxes to and from the indoor environment and the prediction of the indoor environmental conditions.

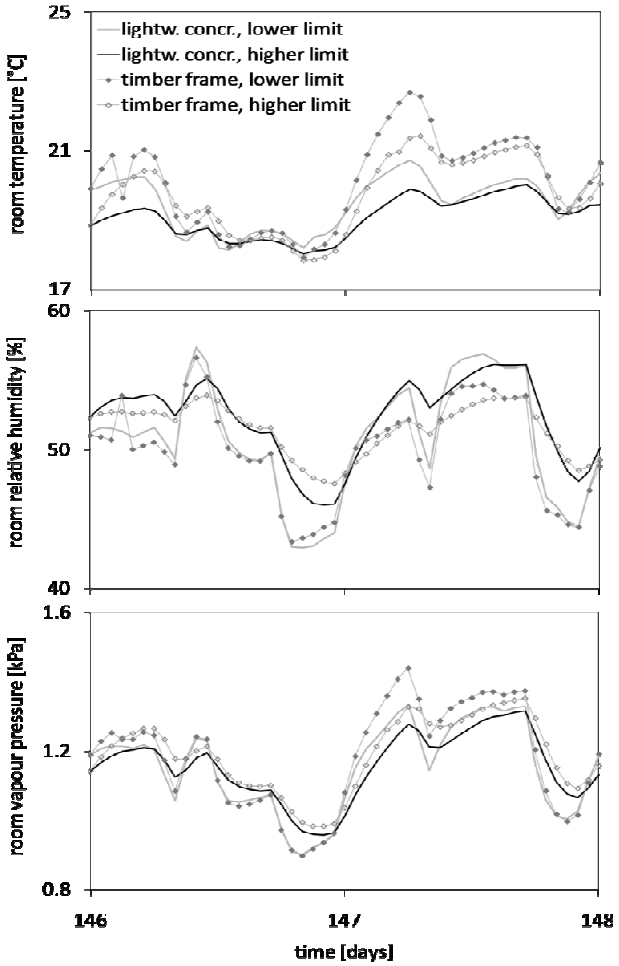

Figure 20: Average indoor air temperature and relative humidity in the room during 2 days (May 27-28). The results obtained from the simulations of the timber frame wall and the lightweight concrete wall with lower (1) and higher limits (2) for the surface transfer coefficients are compared.

In Figure 21, the amplitude of the indoor air temperature for both walls using lower (1) and higher limits (2) is presented. The amplitude is defined by Eq. (23).

$$\Delta T = \left| T_{\max} - T_{avg} \right| \tag{23}$$

where T_{avg} [°C] is the daily averaged indoor air temperature, and T_{max} [°C] is the maximum indoor air temperature of that day. Comparing the amplitudes of the indoor air temperature, Figure 21 shows that the lightweight concrete wall's ability to buffer heat is relatively large compared to the timber frame wall, resulting in relatively small amplitudes. Moreover, the figure shows that the surface heat transfer coefficient has a relatively large influence on the heat buffering of the component.

Similarly the amplitude of the hourly relative humidity of the indoor air, defined by Eq. (24), for both walls is presented in Figure 22. Figure 22 shows that the moisture buffering capacity of both walls is comparable.

$$\Delta RH = \left| RH_{\max} - RH_{avg} \right| \tag{24}$$

Analyzing the influence of the surface transfer coefficients on the indoor air temperature and relative humidity (Figure 21 and Figure 22), the range of predicted indoor air temperature and relative humidity is relatively narrow, when applying higher limits (2). This means that peaks are reduced and instantaneous increases or decreases in indoor air temperature and relative humidity are levelled out.

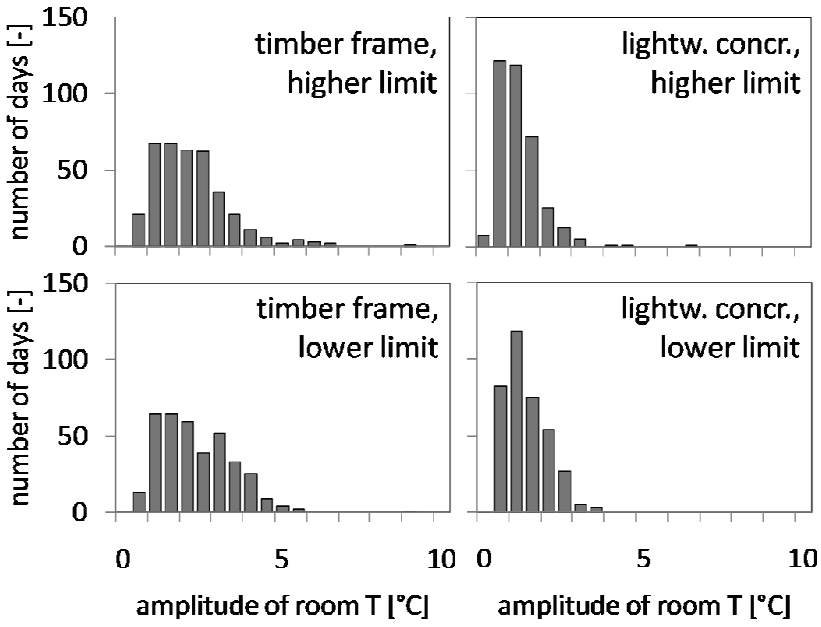

Figure 21: Amplitude of the indoor air temperature in the room, defined by Eq. (23), obtained from the simulations of the timber frame wall and the lightweight concrete wall with lower and higher limits for the surface transfer coefficients are compared.

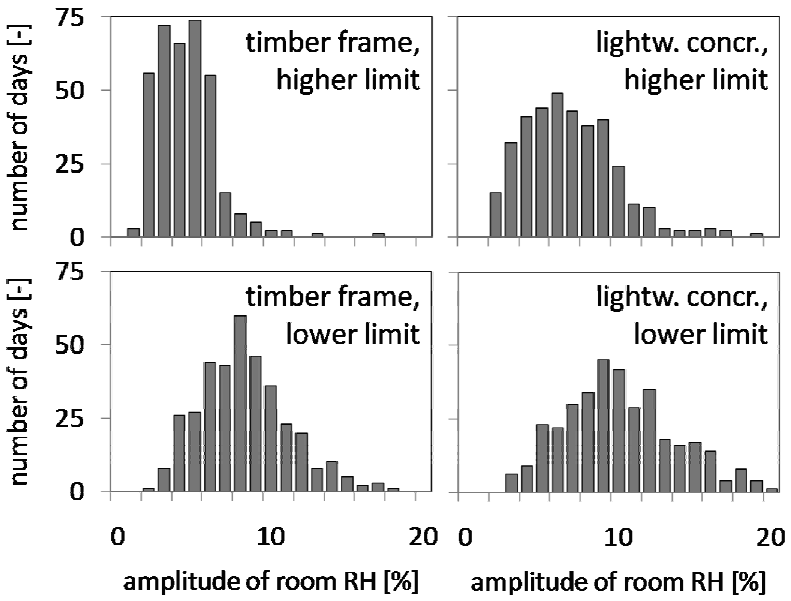

Figure 22: Amplitude of the indoor relative humidity (Eq. (24)) in the room obtained from the simulations of the timber frame wall and the lightweight concrete wall with lower and higher limits for the surface transfer coefficients are compared.

3.2.3 Discussion

Analysis of the simulation results showed that the influence of the convective surface heat transfer coefficient on the hygrothermal conditions on the building component (Figure 16 and Figure 18) was relatively large compared to the influence of the convective surface mass transfer coefficient. An explanation for this could be obtained by analyzing the material and surface resistances for heat and moisture transport.

Analyzing the building components (Figure 14) the thermal resistance of the building materials is approximately 4 $m^2K\ W^{-1}$, while the surface heat transfer resistances lie between 0.33 $m^2K\ W^{-1}$ down to 0.061 $m^2K\ W^{-1}$. For heat transfer hence, the magnitude of the surface resistance is approximately 5% of the material's thermal resistance. Regarding the thermal bridge, the resistance of approximately 30 cm of concrete is approximately 0.2 $m^2K\ W^{-1}$, resulting in a relatively larger influence of the surface transfer resistance compared to the material's thermal resistance.

Focussing on the moisture transfer, the moisture transfer resistances of the building materials are approximately $6 \cdot 10^9$, $13 \cdot 10^9$, and $29 \cdot 10^9$ m s^{-1} for the timber frame wall, the lightweight concrete wall, and the thermal bridge respectively. Comparing these resistances to the surface transfer resistances varying between $0.01 \cdot 10^9$ - $0.1 \cdot 10^9$ m s^{-1} shows that the surface moisture transfer resistance is negligible (less than 1%) compared to the material's resistance. Thus, the influence of the thermal surface resistance on the behaviour of component and the thermal bridge should be larger compared to the influence of the hygric surface resistance.

Under transient conditions, the penetration depth d_p and the related material layer's heat and moisture capacity are best able to quantify the potential for materials to damp changes in indoor temperature and humidity respectively. The active thickness of a material for heat and moisture exchange is estimated using the penetration depth, represented by Eq. (25) and Eq. (26) [71].

$$d_{p,H} = \sqrt{\frac{\lambda t_p}{\rho c_p \pi}} \tag{25}$$

$$d_{p,M} = \sqrt{\frac{\delta p_{vsat} t_p}{\xi \pi}} \tag{26}$$

where d_p is the penetration depth [m], λ the thermal conductivity [W m^{-1}K^{-1}], ρ the density [kg m^{-3}], c_p the heat capacity [J kg^{-1}K^{-1}], δ is the vapour permeability of the material [s], ζ the moisture capacity of the material [kg m^{-3}], and t_p is the period of time of the moisture production cycle [s]. The active thickness and the moisture capacity of the materials used on the internal side of the walls and the thermal bridge are presented in Table 8.

The ratio between the influence of the surface resistance and the material resistance on the heat and moisture transport is described by the Biot number. Eq. (27) and Eq. (28) present the Biot numbers for heat and moisture transfer respectively.

$$Bi_H = \frac{\alpha_c L_H}{\lambda} \tag{27}$$

$$Bi_M = \frac{\beta_c L_M}{\delta} \tag{28}$$

where α_c is the convective surface heat transfer coefficient [W m^{-2}K^{-1}], β_c is the convective surface moisture transfer coefficient, and L_H and L_M are the characteristic lengths for heat and moisture transfer [m]. Considering the porous wood fibre board, the reader should notice that the characteristic length (L_M) is equal to half of the active thickness of the material ($d_{p,M}$), while the characteristic length for heat transfer (L_H) is equal to half of the thickness of the material (d), since the material thickness is lower than the thermal penetration depth.

Table 8 presents the corresponding Biot numbers for heat and moisture transfer for the timber frame wall, the lightweight concrete wall, and the thermal bridge. The table shows that, focusing on the heat transport, the Biot numbers (Bi_H) of all materials are smaller than 0.1 and within the same order of magnitude. Since the Biot numbers for heat transfer of both materials are smaller than 0.1, this indicates that the surface transfer resistance has a relatively large influence on the thermal behaviour of the building component.

With respect to the moisture transport (Bi_M), the Biot numbers of the components are larger than 0.1, and in this case a lumped system analysis is not applicable, indicating that changes in the surface transfer coefficient will have a relatively smaller influence on the hygric behaviour of the component, as the internal resistance to moisture transport is also significant.

In conclusion, the analysis of the material and surface resistances for heat and moisture transport confirmed the observations that the influence of the convective surface heat transfer coefficients is relatively large compared to the influence of the convective surface moisture transfer coefficient on the hygrothermal response of the building components.

The convective surface transfer coefficients were also shown to have an influence on the hygrothermal conditions in the building zone via the thermal and hygric buffering of the building components, i.e. the amplitudes of the indoor air temperature and relative humidity in the room. Analysis of the thermal and hygric effusivity, which represent the measure of the material's ability to exchange heat and moisture with its surroundings is done using Eq. (29) and Eq. (30).

$$e_H = \sqrt{\lambda \rho c_p} \tag{29}$$

$$e_M = \sqrt{\xi \delta / p_{vsat}} \tag{30}$$

where λ is the thermal conductivity [W m^{-1}K^{-1}], ρ the density [kg m^{-3}], c_p the heat capacity [J kg^{-1}K^{-1}], δ is the vapor permeability of the material [s], and ξ the moisture capacity of the material [kg m^{-3}Pa^{-1}].

Focusing on the indoor air temperature in the room, Figure 20 and Figure 21 show that the lightweight concrete wall has a larger heat buffering capacity compared to the timber frame wall, i.e. the peaks in the indoor air temperature are reduced. Moreover, the range of indoor temperatures when applying the lightweight concrete wall is relatively narrow compared to the timber frame wall. Comparing the relative humidity in the room (Figure 20 and 10), the results show that the hygric buffering capacity of both walls is relatively similar.

However, comparison of the effusivities for both materials, Table 8 showed that the ability of the lightweight concrete to buffer both heat and moisture is relatively large compared to the ability of the timber frame wall. The reader should notice that the specific values for the surface transfer coefficient which are applied in the simulation influence the heat and moisture buffering capacity of the wall indirectly and determine the predicted indoor environmental conditions.

Table 8: Material properties

	Porous wood fibre	Lightweight concrete	Concrete
d [mm]	13	50	300
$d_{p,M}$ [mm]	1.5	3.4	1.1
$d_{p,H}$ [mm]	56.4	97.1	150
λ [W m^{-1} K^{-1}]	0.13	0.45	1.5
ρ [kg m^{-3}]	450	1250	2200
c_p [J kg^{-1} K^{-1}]	2500	1050	840
δ [s]	$4.5 \cdot 10^{-12}$	$1.8 \cdot 10^{-11}$	$2 \cdot 10^{-12}$
ξ [kg m^{-3} Pa^{-1}]	0.0507	0.044	0.046
Bi_H	0.05	0.06	0.02
Bi_M	1.74	0.93	2.73
e_H	382	769	1665
e_M	$4.8 \cdot 10^{-7}$	$8.9 \cdot 10^{-7}$	$3.0 \cdot 10^{-7}$

3.3 Conclusions

This section presents the conclusions from the parameter study and the consequences of the investigations for hygrothermal component performance analysis. The influence of the surface heat and moisture transfer coefficients on the hygrothermal conditions on building components and in the building zone has been analysed. A literature study was undertaken to obtain an overview of the previous research on the on the modelling of the local indoor environmental conditions and the hygrothermal conditions in a building component. Lower and upper limits for the convective surface transfer coefficients (α_c and β_c) were assigned. A parameter study was used to investigate how the magnitude of the surface transfer coefficients - resulting from the air velocity near the surface of a building component – varied with the hygrothermal conditions in the building component and the indoor environment. Three building component configurations (calculation objects) were selected for analysis. Different values for the surface heat and moisture transfer coefficients were applied and the hygrothermal response of the building was simulated. The simulated conditions resulted in minimum and maximum hygrothermal conditions in the building component and in the building zone.

From this work we concluded that:

- while the influence of the convective surface transfer coefficients on the HAM conditions on the surface of the insulated walls was limited, this influence was relatively large when considering a thermal bridge. Different surface temperature, relative humidity and vapour pressures were predicted when different airflow conditions near a component resulted in different convective surface transfer coefficients. In consequence, when performing a hygrothermal performance analysis and simulation, it is important to take the local airflow velocity near the component into account.
- when focusing on the hygrothermal performance of the walls, the influence of the convective surface heat transfer coefficient on the hygrothermal performance is relatively large compared to the influence of the convective surface moisture transfer coefficient. With respect to the analysed building components, the investigations showed that assuming an average value for the convective surface moisture transfer coefficient is acceptable, while assuming an average value for the convective surface heat transfer coefficient is not acceptable. The study showed that the influence on the surface relative humidity is limited. However, an influence on the exchange with the interior environment is still present.
- with respect to the hygrothermal performance of the thermal bridge, the influence of both the convective surface heat and moisture transfer coefficient on the hygrothermal performance is relatively large. The analysis showed that assuming an average value for these coefficients is not acceptable.
- the influence of both the surface heat transfer coefficient and the surface moisture transfer coefficient on the heat and vapour exchange between the building component and the indoor environment as well as the buffering capacity of the building component is relatively large. Assuming average values for the surface transfer coefficients may introduce relatively large errors in the prediction of these fluxes and the prediction of the indoor environmental conditions.

Building researchers and designers should be aware that the appropriate indoor environmental conditions should be applied when performing a hygrothermal component simulation and analysis. The local airflow conditions near the component have a relatively large influence on the predicted hygrothermal conditions on the surface of the component. It is recommended that, for example in a design stage, different local airflow conditions are investigated to predict the influence of these conditions on the hygrothermal performance of the specific component.

Future research should focus on the prediction of the local air velocity near interfaces and on the analysis and determination of the relationship between the local air velocity and the convective surface heat transfer coefficient. A more detailed description and prediction of the interaction between the indoor environment and the hygrothermal conditions in the building component is desirable. The quality of such an

analysis would be improved by providing guidelines and relationships between the convective surface heat transfer coefficient and the local air velocity near the building component.

4 Numerical Modelling

In this thesis, the applicability of sub-zonal airflow modelling for the prediction of the local environmental conditions and surface transfer coefficients is investigated. It is the objective to obtain an accurate assessment of the heat, air and moisture conditions in the building component and the building zone. In Chapter 2, it has been demonstrated that two options for the modelling of the local indoor environmental conditions near the component are applicable: sub-zonal modelling and computational fluid dynamics (CFD). The literature review showed that both approaches served as a valuable tool for predicting temperature and relative humidity distributions in enclosed environments. While CFD is capable of providing detailed information regarding the airflow in a room and the local surface transfer coefficients, the capability of the sub-zonal model to predict these has currently not been investigated. However, sub-zonal models may be an alternative for the use of CFD models, which are strongly limited by computer capacity. The ability of the sub-zonal model to provide a relatively accurate prediction of the local conditions in a room as well as the short computation time makes the application of the sub-zonal model attractive for the transient simulation of heat, air and moisture in buildings.

This study intends to develop an efficient and flexible model, which is suitable for the assessment of the heat, air and moisture transport in the indoor environment and within the building envelope as well as for the analysis of the interaction between both domains. The applicability of the sub-zonal model to predict local temperature and relative humidity in a room is studied. Moreover, surface transfer coefficient models are evaluated for the prediction of the local convective surface transfer coefficients in a room. Three test cases for respectively natural, forced and mixed convection in a room have been analyzed. The sub-zonal models have been compared to the CFD models regarding efficiency, accuracy, computational effort (or simulation time), and flexibility. Section 4.1 presents the methodology that has been applied for the modelling of the indoor environmental conditions and the local convective surface transfer coefficients in the test cases. Section 4.2 presents the numerical details and considerations considering the modelling of the indoor environmental conditions using sub-zonal airflow modelling. In Section 4.3, the modelling of the local convective surface transfer coefficients is presented.

4.1 Methodology

Three test cases for respectively natural, forced and mixed convection in a room have been defined. For natural convection, experimental results from CETHIL's MINIBAT test cell that has been presented by Inard *et al.* [35] have been used. The test cell consists of a (three-dimensional) room where it is possible to analyze the natural convective airflow under laboratory conditions. The forced convective airflow in a (two-dimensional) room has been studied based on the Annex 20 Benchmark described by Nielsen [81]. The experimental data obtained from [81] and the numerical results obtained from [82] have been used for comparison and analysis. For mixed convection, the airflow in a (two-dimensional) rectangular room described by Steeman [13] has been investigated. The experimental and numerical data sets that were available for each test case have been used for verification and validation of the results obtained from the present study.

For each test case, several sub-zonal airflow models have been developed and simulated to predict the heat and moisture flows in the room and the flows between the room and the building components. Section 4.1.2 presents the methodology that has been applied with respect to the sub-zonal airflow models.

With respect to the surface transfer coefficient models, the results from the sub-zonal airflow model have been used for the prediction of the local convective surface transfer coefficients along the building components. Section 4.1.3 presents the methodology regarding the application of the surface transfer coefficient models for the prediction of the local convective surface heat and moisture transfer coefficients.

Similarly, CFD simulations have been carried out for the prediction of the indoor environmental conditions and surface transfer coefficients in each test case. The CFD simulations have been performed within the framework of the present study and carried out along the lines of the best practice guidelines that were presented by Steeman [13]. Section 4.1.1 presents a brief summary of the methodology that has been

applied for the modelling and simulations of the CFD models. For additional information and specific details the reader is referred to [13].

The reader should notice that long-wave radiation among the surfaces in the room has neither been considered in the CFD models nor in the sub-zonal airflow models. The modelling of thermal radiation in CFD and sub-zonal models would require the implementation and application of two different radiation models. In general, CFD software incorporates standard models for thermal radiation, while other models are available for the implementation in sub-zonal models. The use of different radiation models may result in deviations between the CFD results and the sub-zonal model's results, which are caused by the radiation models. Since it is not the objective of the present study to investigate the performance of the different radiation models, this analysis is not included in this thesis.

4.1.1 CFD modelling

The results obtained from CFD simulation serve as an important reference for comparison of the results obtained from the sub-zonal models. In Chapter 2, it was already mentioned that while CFD is a valuable tool for predicting air distribution in enclosed environments [29], there are many factors influencing the results predicted. Different users may obtain different results for the same problem even with the same computer program. The accuracy of the simulation heavily depends on a user's knowledge of fluid dynamics, experience and skills using numerical techniques. Among various influential factors proper selection of a turbulence modelling method is a key issue that will directly affect simulation accuracy and efficiency.

Steeman [13] presented an intensive study on the use of CFD simulation for indoor airflow analysis in buildings. The author's [13] experience and knowledge has been applied to develop a CFD model for each test case, which is able to produce reliable results. All CFD models that have been developed within the framework of the present study have been defined along the guidelines that were presented by Steeman [13]. The commercial CFD software FLUENT has been used. For additional information and specific details the reader is referred to [13].

The following methodology has been applied for the CFD simulations:

- CFD model:
    - Definition of the geometry.
    - Definition of the grid.
    - Definition of the material properties: Density variations of the air in the room have been modelled using the incompressible ideal gas relationship. Other relationships used to model the fluid properties include the mass weighted mixing law for the determination of the heat capacity and the ideal gas mixing law for the calculation of the thermal conductivity and the dynamic viscosity.
    - Applying the boundary conditions for the airflow, temperature and relative humidity in the room.
- Numerical model:
    - Selection of the numerical scheme: A second order upwind scheme has been applied for the discretisation of the convective terms in the transport equations in order to reduce numerical diffusion. The PRESTO! scheme is applied for the discretisation of the pressure and the SIMPLE algorithm is used for pressure-velocity coupling.
    - Selection of the turbulence model: As the interest of the study lies in the heat and moisture fluxes to the walls it is important to represent the near wall behaviour of the flow correctly. A low Reynolds number (LRN) k-ω model is applied for the simulation of the airflow in the room combined with a sufficiently refined grid near the wall.
    - Simulation
- Grid sensitivity study
    - The grid sensitivity of the simulation has been studied by refining the computational grid with a factor 2 and a factor 4 in all dimensions and checking the influence on the heat flow through

the wall. A structured grid with relatively dense cells close to the wall has been applied, while the cell size increases gradually further from the wall.

- Verification and comparison
  - Simulation and comparison of the CFD model with experimental and numerical results.
- Analysis of efficiency, accuracy, computational effort (or simulation time), and flexibility.

The CFD results obtained from the present study have been compared with the experimental results presented by Inard *et al.* [35] and Nielsen [47], and the numerical results presented by Steeman [13] and Chen [82]. Since it is not the objective of the current study to investigate the performance and quality of these CFD simulations in detail, the validation of these simulations is not documented intensively in this thesis.

4.1.2 Sub-zonal airflow modelling

Several sub-zonal airflow and surface transfer coefficient models have been developed and simulated to predict the heat and moisture flows in the room and between the room and the building components. For each test case the following general methodology has been applied.

- Sub-zonal airflow model:
  - Definition of the geometry.
  - Definition of the grid, selection and implementation of the relationships describing the corresponding flow elements.
  - Definition of the material properties: Density variations of the air in the room have been modelled using the incompressible ideal gas relationship.
  - Applying the boundary conditions for the airflow, temperature and relative humidity in the room.
  - Applying the convective surface transfer coefficients obtained from CFD simulation.
- Simulation
- Grid sensitivity study
  - Densification of the grid by factor 2 and 4 until a grid independent solution is obtained.
- Verification and comparison
  - Simulation and comparison of the indoor environmental conditions obtained from the sub-zonal airflow model with experimental and numerical results.
- Analysis of efficiency, accuracy, computational effort (or simulation time), and flexibility.

For additional information and numerical details regarding the sub-zonal airflow modelling, the reader is referred to Section 4.2.

The presented methodology with respect to the sub-zonal airflow modelling shows that the results from CFD simulation part of the sub-zonal model, i.e. the surface transfer coefficients obtained from CFD simulation are applied in the sub-zonal airflow model. The reader should notice that the temperature and relative humidity distribution in the room predicted by the sub-zonal model is dependent of both the ability of the airflow model to describe the airflow in the room as well as the convective surface transfer coefficients which are applied in the model. In order to distillate the influences of the convective surface transfer coefficients on the predicted temperature and humidity distributions from the influences of the sub-zonal airflow model on these distributions, similar convective surface transfer coefficients are used in both the CFD model and the sub-zonal model. In this way, it is investigated to what extent the sub-zonal airflow model is able to predict the temperature and relative humidity distribution in the room, when applying similar convective surface transfer coefficients as used in the CFD model.

In the methodology presented in the following section, different convective surface transfer coefficients are applied in the sub-zonal airflow model and the CFD model. This enables a more detailed investigation of the specific influence of the convective surface transfer coefficients on the predicted indoor environmental conditions in the room.

4.1.3 Surface transfer coefficient modelling

For each test case, the results from the sub-zonal airflow model have been used for the prediction of the local convective surface transfer coefficients along the building components. The following methodology has been applied:

- Surface transfer coefficient model:
  - Selection of an appropriate sub-zonal airflow model, based on the simulation results from the sub-zonal airflow model, to model the indoor environmental conditions in the room (Section 4.1.2).
  - Selection and implementation of different models for the correct representation of the local convective surface transfer coefficients.
- Simulation
- Verification and comparison of the convective surface transfer coefficient models with numerical results.
  - The numerically obtained convective surface transfer coefficients are compared with numerical data resulting from CFD.

For additional information and numerical details regarding the modelling of the surface transfer coefficients, the reader is referred to Section 4.3.

4.2 Sub-zonal airflow modelling

For each test case, the methodology that is presented in Section 4.1.2 has been applied to predict the local temperature and relative humidity field in the room. In this section, the numerical details of the sub-zonal airflow modelling are presented.

The airflow in the rooms has been modelled using a sub-zonal airflow model. The room is sub-divided into a relatively small number of discrete control volumes. Within a sub-zone, the temperature and relative humidity are considered to be fairly uniform. In the subdivided rooms, two types of subzones are used: standard sub-zones and flow element (or mixed) sub-zones.

Standard sub-zones

Standard subzones are assumed to have a representative air temperature and relative humidity which does not differ markedly from their immediate neighbouring subzones. The important characteristic of these subzones is that flow velocity (and momentum) differences between them are small and primarily driven by pressure differences. Mass flows between adjacent sub-zones are calculated in different ways for horizontal and vertical interfaces.

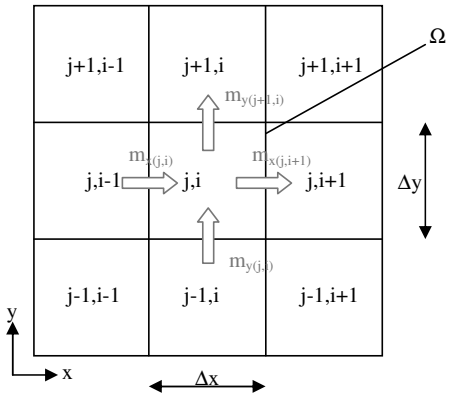

Figure 23: Discretization

Starting from the general transport equation (Eq. (31)) for property Φ, property Φ is replaced by the fluid's density ρ [kg m^{-3}] for mass continuity describing that the rate at which mass enters a system is equal to the rate at which mass leaves the system. Assuming that the process is steady-state and the fluid is incompressible, Eq. (31) reduces to the volume continuity equation, represented by Eq. (32).

$$\frac{\partial \Phi}{\partial t} + (\underline{u} \bullet \nabla)\Phi - \Gamma_\phi \nabla^2 \Phi = S_\phi \tag{31}$$

$$\int_\Omega \left\{ \rho(\nabla \bullet \underline{u}) + S_\rho \right\} d\Omega = 0 \tag{32}$$

where Ω represents the volume of the subzone [m^3] (Figure 23), t is the time [s], ρ is the fluid's density [kg m^{-3}], $\underline{u}$ is the velocity vector [m s^{-1}], and S_ρ is the source term [kg m^{-3} s^{-1}]. (Density variations of the air have been modelled using the incompressible ideal gas relationship).
For each sub-zone, a two-dimensional discretization has been applied, and the mass conservation is described by Eq. (33).

$$\sum m_{j,i} + S_M = 0 \tag{33}$$

where $m_{j,i}$ is the mass flow [kg s^{-1}] between the volumes i and j, and S_M is a mass source term [kg s^{-1}]. Using a two-dimensional discretisation and assuming that the source term $S_M = 0$, the mass conservation is represented by Eq. (34). For standard sub-zones the power-law relation is used to describe the differential mass flow, as presented in Section 2.4.

$$m_{x(j,i)} - m_{x(j,i+1)} + m_{y(j,i)} - m_{y(j+1,i)} = 0 \tag{34}$$

where m_x and m_y represent the mass flow in x- and y-direction respectively, described by the power-law relation, presented in Table 9:

Table 9: Air mass flow in x- and y-direction

$m_{x(j,i)}$	$C_d \rho_{(j,i)} A_{(j,i)} \left\lvert p_{(j,i-1)} - p_{(j,i)} \right\rvert^n \frac{p_{(j,i-1)} - p_{(j,i)}}{\left\lvert p_{(j,i-1)} - p_{(j,i)} \right\rvert}$
$m_{x(j,i+1)}$	$C_d \rho_{(j,i+1)} A_{(j,i+1)} \left\lvert p_{(j,i)} - p_{(j,i+1)} \right\rvert^n \frac{p_{(j,i)} - p_{(j,i+1)}}{\left\lvert p_{(j,i)} - p_{(j,i+1)} \right\rvert}$
$m_{y(j,i)}$	$\left\lvert p_{(j-1,i)} - p_{(j,i)} - \frac{1}{2}\rho_{y(j,i)} g (h_{(j-1,i)} + h_{(j,i)}) \right\rvert^n \frac{p_{(j-1,i)} - p_{(j,i)} - \frac{1}{2}\rho_{y(j,i)} g (h_{(j-1,i)} + h_{(j,i)})}{\left\lvert p_{(j-1,i)} - p_{(j,i)} - \frac{1}{2}\rho_{y(j,i)} g (h_{(j-1,i)} + h_{(j,i)}) \right\rvert}$
$m_{y(j+1,i)}$	$\left\lvert p_{(j,i)} - p_{(j+1,i)} - \frac{1}{2}\rho_{y(j+1,i)} g (h_{(j,i)} + h_{(j+1,i)}) \right\rvert^n \frac{p_{(j,i)} - p_{(j+1,i)} - \frac{1}{2}\rho_{y(j+1,i)} g (h_{(j,i)} + h_{(j+1,i)})}{\left\lvert p_{(j,i)} - p_{(j+1,i)} - \frac{1}{2}\rho_{y(j+1,i)} g (h_{(j,i)} + h_{(j+1,i)}) \right\rvert}$

where C_d is an empirical 'permeability' constant, analogous to the orifice discharge coefficient, that is, assumed to have a value less than 1.0. In literature [40], it has been concluded that a value of 0.83 m s^{-1} Pa^{-n} is most appropriate. The power-law exponent n is often taken as $n = 0.5$ which corresponds to the orifice equation and ρ refers to the density of the incoming air [kg m^{-3}].

A numerical solution for the airflow field in the room is obtained by solving the mass conservation equation (Eq. (33)) for each sub-zone.

Flow element sub-zones

If a sub-zone is under direct influence of a flow driver, for example a fan or a heater, the flow in the sub-zone is modelled as a flow element. Flow elements are treated as isolated volumes where the air movement is controlled by a restricted number of parameters, and the air movement is fairly independent of the general flow in the enclosure. Often, the mathematical equations governing the airflow in flow elements are based on empirical relationships [35] [41] [83]. In this study, three types of flow elements have been used: a boundary layer model, a two-dimensional isothermal ceiling jet, and a wall turbulent non-isothermal jet.

The thermal boundary layer model is based on experimental work that has focussed on the analysis of the thermal boundary layer along flat plates. When a surface in a room is poorly insulated or the surface is exposed to solar radiation, the surface temperature is different from the surroundings and there is free convection between the surface and the surrounding air. In this case, the thickness of the boundary layer is zero at the top of the vertical surface, and increases in the downward direction due to entrainment of room air (Figure 24). If the surface is located in calm surroundings, the boundary layer flow at the top of the surface will be laminar, and at a certain distance from the top it will become turbulent. The ratio between the buoyancy and viscous (friction) forces is expressed by the Grashof number (Eq. (35)). Depending on whether the airflow in the boundary layer of a cold wall is laminar or turbulent, Eq. (36) and Eq. (38), or Eq. (37) and Eq. (39) are applied for the boundary layer thickness and the flow through the boundary layer respectively.

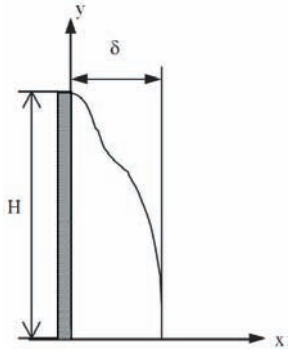

Figure 24: Thermal boundary layer flow along a cold vertical surface [41]

$$Gr(y) = \frac{g\beta\Delta T(H-y)^3}{\nu^2} \tag{35}$$

$$\delta(y) = 0.048(H-y)^{1/4}\Delta T^{1/4} \tag{36}$$

$$\delta(y) = 0.11(H-y)^{7/10}\Delta T^{-1/10} \tag{37}$$

$$\phi(y) = 0.0024(H-y)^{3/4}\Delta T^{1/4}L \tag{38}$$

$$\phi(y) = 0.0021(H-y)^{6/5}\Delta T^{2/5}L \tag{39}$$

where g is the gravitational acceleration [m s^{-2}], β is the thermal expansion coefficient of air [K^{-1}], ν is the kinematic viscosity of air [m^2 s^{-1}], δ is the boundary layer thickness [m], ϕ is the volume flow rate through the boundary layer [m^{3}s^{-1}], H is the height of the wall [m], L is the width of the wall [m], ΔT is the temperature difference between the wall surface and the average temperature in the room [K], and y is the vertical coordinate [m].

If the air in a room is under the direct influence of an isothermal jet, for example due to the vicinity of an inlet opening, the airflow at different distances from the inlet opening is determined by Eq. (40) [84].

$$\phi(x) = 0.25\varphi_0\sqrt{\frac{x}{b_0}} \tag{40}$$

where ϕ_0 is the airflow rate at the inlet [m^3 s^{-1}], b_0 is the thickness of the diffuser [m], and x the horizontal coordinate [m]. The corresponding height of the sub-zone is determined by the height of the jet (Eq. (41)).

$$h(x) = 0.16x \tag{41}$$

For a non-isothermal jet, the airflow rate can also be calculated by Eq. (40) [85].

Temperature and Relative Humidity Field

Conservation of energy in a flow in volume Ω, with velocity components $\underline{u}$ [m s^{-1}]in a fluid of density ρ [kg m^3] at temperature T [K], is expressed by:

$$\int_\Omega \left\{ \frac{\partial(\rho cT)}{\partial t} + \nabla\cdot(\rho c_p T\underline{u}) - \nabla\cdot(\lambda\nabla T) + S_T \right\} d\Omega = 0 \tag{42}$$

where c_p is the specific heat capacity [J kg^{-1}K^{-1}], λ is the thermal conductivity of the fluid [W m^{-1}K^{-1}], while S_T represents any heat sources [W m^{-3}] in the fluid.

Considering a steady-state situation where the flow does not change in time, Eq. (42) reduces to

$$\int_\Omega \left\{ \nabla\cdot(\rho c_p T\underline{u}) - \nabla\cdot(\lambda\nabla T) + S_T \right\} d\Omega = 0 \tag{43}$$

After applying Gauss's divergence theorem and the control volume method for discretisation of the volume Ω the system results in Eq. (44), and the convective and diffusive fluxes are represented by Eq. (45) and Eq. (46) respectively.

$$\int_S n\cdot(\rho cT\underline{u})dS - \int_S n\cdot(\lambda\nabla T)dS + \int_\Omega S_T d\Omega = 0 \tag{44}$$

$$\begin{aligned}\int_S n\cdot(\rho c\underline{u}T)dS &= \int(\rho cuT)_{x(j,i+1)}dy - \int(\rho cuT)_{x(j,i)}dy + \int(\rho cvT)_{y(j+1,i)}dx - \int(\rho cvT)_{y(j,i)}dy \\ &= \rho cuT\Big|_{x(j,i)}^{x(j,i+1)}\Delta y + \rho cvT\Big|_{y(j,i)}^{y(j+1,i)}\Delta x\end{aligned} \tag{45}$$

$$\begin{aligned}\int_S n\cdot(\lambda\nabla T)dS &= \int\lambda\frac{\partial T}{\partial x}\Big|_{x(j,i+1)}dy - \int\lambda\frac{\partial T}{\partial x}\Big|_{x(j,i)}dy + \int\lambda\frac{\partial T}{\partial y}\Big|_{y(j+1,i)}dx - \int\lambda\frac{\partial T}{\partial y}\Big|_{y(j,i)}dx \\ &= \lambda\frac{\partial T}{\partial x}\Big|_{x(j,i)}^{x(j,i+1)}\Delta y + \lambda\frac{\partial T}{\partial x}\Big|_{y(j,i)}^{y(j+1,i)}\Delta x\end{aligned} \tag{46}$$

while the subscripts *x(j,i+1)*, *x(j,i)*, *y(j+1,i)*, and *y(j,i)* represent the quantities and fluxes on the Eastern, Western, Northern and Southern surfaces of the control volumes. The discrete model has been completed using second order Taylor series expansion for the approximation of the values of T and the flux ($\partial T/\partial x$) at the cell faces in terms of the values of T at the cell centres. The resulting convective (F) and diffusive (D) fluxes are presented in Table 10, where the width and the height of the subzone is represented by respectively Δx and Δy [m]. Furthermore, an upwind scheme has been applied.

Table 10: Convective (F)and diffusive (D) coefficients

	x(j,i)	x(j,i+1)	y(j,i)	y(j+1,i)
F	$\rho c u_{x(j,i)} \Delta y$	$\rho c u_{x(j,i+1)} \Delta y$	$\rho c v_{y(j,i)} \Delta x$	$\rho c v_{y(j+1,i)} \Delta x$
D	$-\lambda \frac{\Delta y}{\Delta x}$	$-\lambda \frac{\Delta y}{\Delta x}$	$-\lambda \frac{\Delta x}{\Delta y}$	$-\lambda \frac{\Delta x}{\Delta y}$

With respect to the boundary conditions, the heat transfer to and from the building component to the air perpendicular to the component is represented as a source term (Eq. (47)).

$$\int_{\Omega} S_T d\Omega = \int_{S} \{n \bullet (\alpha_c (T_{air} - T_{wall}))\} dS \tag{47}$$

where α_c is the convective surface heat transfer coefficient [W m^{-2}K^{-1}], T_{air} and T_{wall} are the air temperature in the centre of the control volume and the wall surface temperature [K] respectively, and S is the surface [m], corresponding to the height or the width of the control volume.

Similarly, the steady-state equation governing the conservation of vapour in the sub-zones is presented by Eq. (48).

$$\int_{\Omega} \{\nabla \cdot (\rho \underline{u} X) = \nabla \cdot (\rho D_v \nabla X) + S_V\} d\Omega = 0 \tag{48}$$

where $\underline{u}$ is the velocity in of the fluid with density ρ [kg m^{-3}], D_v is the vapour diffusivity [m^2 s^{-1}], and X is the vapour content per kg dry air [kg kg^{-1}]. Vapour sources in the room are represented by the source term S_v [kg m^{-3}]. A similar analysis and upwind scheme as for the energy equation has been applied. The resulting convective (F) and diffusive (D) fluxes are presented in Table 11.

Table 11: Convective (F_i) and diffusive (D_i) coefficients

	x(j,i)	x(j,i+1)	y(j,i)	y(j+1,i)
F	$\rho c u_{x(j,i)} \Delta y$	$\rho c u_{x(j,i+1)} \Delta y$	$\rho c v_{y(j,i)} \Delta x$	$\rho c v_{y(j+1,i)} \Delta x$
D	$-\rho D_v \frac{\Delta y}{\Delta x}$	$-\rho D_v \frac{\Delta y}{\Delta x}$	$-\rho D_v \frac{\Delta x}{\Delta y}$	$-\rho D_v \frac{\Delta x}{\Delta y}$

The boundary conditions for vapour transfer to and from the building component to the air perpendicular to the component are represented as a source term (Eq. (49))

$$\int_{\Omega} S_M d\Omega = \int_{S} \{n \bullet (\beta^X (X_{air} - X_{wall}))\} dS \tag{49}$$

where β^X is the surface moisture transfer coefficient [m s^{-1}], $m_{v,air}$ and $m_{v,wall}$ are moisture content of the air in the centre of the control volume and at the wall surface [kg kg^{-1}] respectively, and S is the surface [m^2], corresponding to the height of the width of the control volume.

Numerical Solution

The resulting system consists of discrete equations describing the air mass, energy and vapour mass balance for each sub-zone (Eq. (50) – Eq. (52)).

$$\sum m_{(i,j)} + S_M = 0 \tag{50}$$

$$\sum q_{(i,j)} + S_T = 0 \tag{51}$$

$$\sum \phi_{v(i,j)} + S_V = 0 \tag{52}$$

where $m_{j,i}$ is the air mass flow [kg s^{-1}] between the volumes i and j, S_M is a air mass source term [kg s^{-1}], q represents the energy fluxes [W m^{-3}], S_T represents the heat sources [W m^{-3}] in the fluid, ϕ_v the vapour fluxes [kg m^{-3} s^{-1}], and S_V represents the moisture sources [kg m^{-3} s^{-1}].

The airflow model has been implemented in the CHAMPS-BES program [78], which is an envelope model for the coupled simulation of heat, air, moisture, and pollutant transport in building components. The software incorporates an efficient solver for large, sparse systems [86] . For every subzone, the conservation equations are written in the form:

$$F(\underline{s}) = 0 \tag{53}$$

$$F : R^N \rightarrow R^N$$

$$F : R^N \rightarrow R^N$$

F is represented by the system of mass balances and $\underline{u}$ is the solution vector, containing the pressures, temperatures and vapour contents in the centre of the subzones $\underline{s} = \{p_{1,1}, p_{2,1}, \ldots p_{N-1,N}, p_{N,N}, T_{1,1}, T_{2,1}, \ldots T_{N-1,N}, T_{N,N}, m_{v1,1}, m_{v2,1}, \ldots m_{vN-1,N}, m_{vN,N}\}$. The nonlinear algebraic system in real N-space is solved using the Newton method (which has been implemented in the KINSOL solver [86]).

Depending on the linear solver used, KINSOL employs either an Inexact Newton method or a Modified Newton method. At the highest level, kinsol implements the following iteration scheme:

1. Set s_0 = an initial guess
2. For n = 0, 1, 2,…. until convergence do:
3. Solve $\mathbf{J}(s_n)\delta_n = -F(s_n)$
4. Set $s_{n+1} = s_n + \lambda_n \delta_n \quad 0 < \lambda < 1$
5. Test for convergence

Here, s_n is the nth iterate to s, and $J(s) = F'(s)$ is the system Jacobian. At each stage in the iteration process, a scalar multiple of the step δ_n, is added to s_n to produce a new iterate, s_{n+1}. A test for convergence is made before the iteration continues.

For solving the linearized system represented by Eq. (53), a sparse system solver is used [86] . Two methods of applying a computed step δ_n to the previously computed solution vector are implemented. The first and simplest is the standard Newton strategy using λ set to 1. The other method is a global strategy, which attempts to use the direction implied by δ_n in the most efficient way for furthering convergence of the nonlinear problem. This technique is implemented in the second strategy, called Linesearch.

Moreover, a backtracking algorithm to find first the value λ, such that $s_n+\delta_n$ satisfies the sufficient decrease condition represented by Eq. (54).

$$F(s_n + \delta_n) \leq F(s_n) + \alpha \nabla F(s_n) \lambda \delta_n \tag{54}$$

where $\alpha = 10^{-4}$. Although backtracking in itself guarantees that the step is not too small, the solver secondly relaxes¸ to satisfy the condition described by Eq. (55).

$$F(s_0 + \lambda\delta_n) \geq F(s_n) + \beta\nabla F(s_n)\lambda\delta_n \tag{55}$$

where β = 0.9. During this second phase, λ is allowed to vary in the interval [λ_{min}, λ_{max}] where λ_{min} is described by Eq. (56) [86] .

$$\lambda_{\min} = \frac{\text{steptol}}{\left\|\bar{\delta}_n\right\|_\infty} \tag{56}$$

$$\bar{\delta}_n^j = \frac{\delta_n^j}{1/D_s^j + s^j} \tag{57}$$

and λ_{max} corresponds to the maximum feasible step size at the current iteration (typically λ_{max} = *stepmax*/ $\|\delta_n\|D_u$. Here, s^j indicates the jth component of a vector *s*.

Stopping criteria for the Newton method are applied to both of the nonlinear residual and the step length. For the former, the Newton iteration must pass a stopping test (Eq. (58))

$$\left\|F(s_n)\right\|_{D_F,\infty} < \text{Ftol} \tag{58}$$

where Ftol is an input scalar tolerance with a default value of $S^{1/3}$, and S is the unit roundoff. For the latter, the Newton method will terminate when the maximum scaled step is below a given tolerance.

$$\left\|\lambda\delta_n\right\|_{D_s,\infty} < \text{steptol} \tag{59}$$

where steptol is an input scalar tolerance with a default value of $S^{2/3}$. Only the first condition (small residual) is considered a successful completion of kinsol. The second condition (small step) may indicate that the iteration is stalled near a point for which the residual is still unacceptable.

As a user option, KINSOL permits the application of inequality constraints, $s^i > 0$ and $s^i < 0$, as well as $s^i \geq 0$ and $s^i \leq 0$, where s^i is the ith component of *s*. Any such constraint may be imposed on each component. The KINSOL solver reduces step lengths in order to ensure that no constraint is violated. Speciffically, if a new Newton iterate will violate a constraint, the maximum step length (over all i) along the Newton direction that will satisfy all constraints is found and δ_n (Equation (10)) is scaled to take a step of that length.

When using a Modified Newton method (i.e. when a direct linear solver, for example the banded solver, is used), in addition to the strategy described below for the update of the Jacobian matrix, kinsol also provides an optional nonlinear residual monitoring scheme to control when the system Jacobian is updated. Specifically, a Jacobian update also occurs when **mbsetsub**= 5 [86] nonlinear iterations have passed since the last update and

$$\left\|D_s F(s_n)\right\|_2 > \omega\left\|D_s F(s_m)\right\|_2 \tag{60}$$

where u_n is the current iterate and u_m is the iterate at the last Jacobian update. The scalar ω is given by

$$\omega = \min(\omega_{\min} e^{\max(0,\beta-1)}, \omega_{\max}) \tag{61}$$

with β defined by Eq. (62).

$$\beta = \frac{\left\| D_s F(s_n) \right\|_2}{\text{Ftol}} \tag{62}$$

and Ftol is the input scalar tolerance discussed before. Optionally, a constant value ω_{const} can be used for the parameter ω. The constants controlling the nonlinear residual monitoring algorithm can be changed from their default values through optional inputs to kinsol. These include the parameters ω_{min} and ω_{max}, the constant value ω_{const}, and the threshold **mbsetsub**.

With the direct dense and band methods, the Jacobian may be supplied by a user routine, or approximated by difference quotients, at the user's option. In the latter case, the usual approximation is used Eq.(63)).

$$\mathbf{J}^{ij} = \left[F^i(s + \sigma_j e^j) - F^i(s) \right] / \sigma_j \tag{63}$$

and the increments σ_j are given by

$$\sigma_j = \sqrt{S} \max \left\{ \left| s^j \right|, 1 / D_s^j \right\} \tag{64}$$

where S is the unit roundoff. In the band case, the columns of **J** are computed in groups, by the Curtis-Powell-Reid algorithm [86] , with the number of F evaluations equal to the bandwidth. Convergence of the Newton method is maintained as long as the value of σ remains appropriately small.

While the airflow model is capable of obtaining a solution for the airflow, temperature, and relative humidity field in a room, a model for the prediction of the convective surface transfer coefficients is needed to get a reliable prediction for the heat and moisture fluxes to/from the building components. Next section presents different models for the convective surface transfer coefficients.

4.3 Local convective surface transfer coefficient modelling

For each test case, the sub-zonal airflow model has been simulated, resulting in the local indoor environmental conditions in the room and information regarding the airflow pattern in the room, such as the air mass fluxes through the faces of the sub-zones. This information provided by the sub-zonal model is used as input data for the surface transfer coefficient models. For each test case, the methodology that is presented in Section 4.1.3 has been applied to predict the convective surface transfer coefficients. Different models for the local convective surface heat and moisture transfer coefficients have been applied. In Chapter 2, previous research on the determination and modelling of the convective surface transfer coefficients has been described. The relationships have been determined analytically, experimentally, or numerically. In this section, the numerical details of the different surface transfer coefficient models are presented. The models are characterized by the different flow regimes in a room. First of all, the study focuses on the convective surface heat transfer coefficient (CHTC) (Section 4.3.1). Second, the modelling of the convective surface moisture transfer coefficient (SMTC) is analyzed (Section 4.3.2).

4.3.1 Convective surface heat transfer coefficient modelling

Models for the local convective surface heat transfer coefficients have been developed. The models are based on the relationships that resulted from a review of the literature on convective surface heat transfer coefficient modelling. The models are characterized by the different flow regimes in a room.

Natural convection

With respect to the theoretical determination of the convective surface heat transfer coefficient (CHTC), Section 2.5.1 showed that the boundary layer theory [50] describing the flow along a vertical flat plate with uniform temperature may be applicable for establishing a relationship for the local CHTC based on the conditions in the room. The local CHTC (α_c [W m^{-2}K^{-1}]) is then defined by Eq. (65).

$$\alpha_c = \frac{Nu_x \lambda}{x} \tag{65}$$

where Nu_x is the local Nusselt number along the building component, describing the ratio of convective to conductive heat transfer across the boundary, λ is the thermal conductivity of the fluid [W m^{-1}K^{-1}], and x is the coordinate along the component [m].

The CHTC is directly dependent of the local Nusselt number along the component. Table 12 shows that the flat plate analogy (1) distinguishes a laminar and a turbulent region, determined by the local Grashoff number (Eq. (35)). For Grashoff numbers smaller than $1{\cdot}10^9$, the flow is considered to be laminar, while a turbulent flow is assumed for Grashoff numbers larger than $1{\cdot}10^{10}$. The region between Grashoff numbers $1{\cdot}10^9$ and $1{\cdot}10^{10}$ is considered to be a transition region.

Table 12: Local CHTC Models for natural convection

CHTC Model	Source		
1Flat plate [50]	Theory	Laminar ($Gr_y < 1{\cdot}10^9$)	$Nu_x = \frac{0.676\,\mathrm{Pr}^{1/2}}{(0.861+\mathrm{Pr})^{1/4}}\left(\frac{Gr_x}{4}\right)^{1/4}$
		Turbulent ($Gr_y > 1{\cdot}10^{10}$)	$Nu_x = 0.0295(Gr_x)^{2/5}(Pr)^{7/15}(1+0.494Pr^{2/3})^{-2/5}$
2 Turner *et al.* [87]	Exp.	$3.5{\cdot}10^6 < Ra < 5.5{\cdot}10^9$	$Nu_x = 0.524(Gr_x)^{0.26}$
3 Bohn *et al.* [88]	Exp.	$3{\cdot}10^9 < Ra < 6{\cdot}10^{10}$	$Nu_x = 0.62(Ra_x)^{1/4}$

Regarding the experimentally developed CHTC relationships, Khalifa *et al*. published an intensive review of CHTC's for natural convection on isolated vertical and horizontal surfaces with special interest in their application to building geometries [52], and on surfaces in two- and three-dimensional enclosures [53] . From this review, two relationships have been selected based on the analogy between the test setup, which have been used for determination of the CHTC, and the conditions in the rooms. Turner *et al*. (2) [87] determined the CHTC in a two-dimensional air cavity with one heated wall and a concentrated cooling strip on the opposing wall, while the top and bottom surfaces were adiabatic. The model of Bohn *et al*. (3) [88] has been determined in a cube filled with water, while the vertical walls were at different temperatures, and adiabatic horizontal walls. The models have been implemented and the predicted CHTC's have been compared with CFD predictions and average convective surface transfer coefficients obtained from literature [9].

Forced convection

Similarly as for natural convection, relationships for the local CHTC based on the boundary layer theory [50] describing forced convection along a vertical flat plate with uniform temperature are available. In general, the relationships are defined by the local Nusselt number (Eq. (65)). However, in contradiction with the relationships for natural convection, the Nusselt number is based on the local Reynolds number along the plate.

Several correlations are available for forced convection. Correlations for laminar forced convection along a vertical plate with a uniform surface temperature have been developed by Churchill [50], and Rose [50]. Those correlations have been determined for local Reynolds numbers smaller than the critical Reynolds

number of 50000. Churchill and Ozoe [60] extended these correlations for transitional and turbulent boundary layers.
Table 13 presents an overview of the relationships that have been applied in the present study, where Re_x is the local Reynolds number along the plate, and Pr is the Prandtl number.

Table 13: Local CHTC models for forced convection

CHTC Model		
1Flat plate (Churchill) [50]	Laminar	$Nu_x = \frac{0.3387\,\mathrm{Re}_x^{0.5}\,\mathrm{Pr}^{0.33}}{\left[1+\left(\frac{0.0468}{\mathrm{Pr}}\right)^{0.667}\right]^{0.25}}$
2 Flat plate (Rose) [50]		$Nu_x = \frac{\mathrm{Re}_x\,\mathrm{Pr}^{0.5}}{\left[27.8+75.9\,\mathrm{Pr}^{0.306}+657\,\mathrm{Pr}\right]^{0.1667}}$
3 Flat plate (Churchill and Ozoe) [60]	Laminar $Re_x<Re_{cr}$	$Nu_x = \frac{0.886\,\mathrm{Re}_x^{0.5}\,\mathrm{Pr}^{0.33}}{\left[1+\left(\frac{\mathrm{Pr}}{0.0207}\right)^{0.667}\right]^{0.25}}$
	Transition $Re_{cr}<Re_x<10^7$	$Nu_x = 0.0296\,\mathrm{Re}_x^{0.8}\,\mathrm{Pr}^{0.33}$
	Turbulent $Rex>10^7$	$Nu_x = 1.596\,\mathrm{Re}_x(\ln(\mathrm{Re}_x))^{-2.584}\,\mathrm{Pr}^{0.33}$
4 Local Beausoleil-Morrison [9]		$Nu_x = \frac{x}{\lambda}\left(\frac{T_s-T_f}{\Delta T}\right)\cdot\left[-0.199+0.19(ACH\cdot(\frac{\Delta h}{H}))^{0.8}\right]$

First of all, it should be noticed that these correlations have been determined in laboratory conditions for specific boundary conditions, such as a uniform surface temperature, and assumptions. These relationships may have limitations with respect to the applications to building components, where the airflow is also influenced by the geometry of the enclosure, for example corners.

Second, the presented correlations require knowledge of the local Reynolds number along the building component. The performance of the sub-zonal model in predicting local Reynolds numbers is currently not known and these correlations may fail to give an accurate prediction of the local convective surface transfer coefficients. Therefore, the study focussed on alternative methods to obtain a reliable prediction of the convective surface transfer coefficients.

In an ideal situation, correlations for the local surface transfer coefficients based on global conditions in the room would be preferred. The main advantage of such a correlation would be that the correlation itself does not depend on the accuracy of the sub-zonal model. However, a literature study showed that such relationships have not been documented. Correlations for average (global) surface transfer coefficients for an entire building component have only been reported by Beausoleil-Morrison [9]. Within the framework of this study, several methods and approaches have been investigated. The method that generally gives the most accurate prediction of the convective surface transfer coefficients for forced convection along a building component is presented in this thesis. The approach is based on the relationships developed by Beausoleil-Morrison [9].

The relationships developed by Beausoleil-Morrison [9] have been applied locally by means of an alternative approach. For an entire building surface, the global CHTC for forced convection ($\alpha_{c,f}$) is represented by Eq. (66).

$$\alpha_{c,f} = \left(\frac{T_s - T_f}{\Delta T} \right) \cdot \left[-0.199 + 0.19(ACH)^{0.8} \right] \tag{66}$$

where $\alpha_{c,f}$ is the convective surface transfer coefficient for forced convection [W m^{-2}K^{-1}], T_s is the surface temperature [K], T_f is the temperature of the air in the room [K], ΔT is the absolute temperature difference between the air in the room and the building surface [K], and ACH is the air change rate of the room [h^{-1}]. The correlation presented by Eq. (66) has been 'localized' by scaling for application to a single sub-zone. Instead of using the air change rate of the room and the corresponding temperature differences between the room air and the entire building component, the air change rate of the specific sub-zone and local temperature differences are used. Further, the length scale of the CHTC has been adapted using the relative difference between the height of the specific sub-zone and the height of the component, resulting in Eq. (67). This approach avoids the requirement of the local Reynolds number and may lead to a more accurate prediction of the local CHTC compared to using an average CHTC obtained from Beausoleil-Morrison [9].

$$\alpha_{c,f} = \left(\frac{T_{x,s} - T_{x,f}}{\Delta T} \right) \cdot \left[-0.199 + 0.19(ACH \cdot (\frac{\Delta h}{H}))^{0.8} \right] \tag{67}$$

where $\alpha_{c,f}$ is the local convective surface transfer coefficient for forced convection [W m^{-2}K^{-1}], $T_{x,s}$ is the local surface temperature [K] of the building component, $T_{x,f}$ is the local temperature of the air in the room [K] near the component, ΔT is the absolute temperature difference between the air in the room and the building surface [K], ACH is the air change rate of the subzone [h^{-1}], Δh is the height of the sub-zone [m], and H is the height of the building component or room height [m]. Rewriting Eq. (67), the equation can be expressed in terms of the local Nusselt number (Eq. (68)). The reader should notice that the relationship presented by Eq. (68) has been developed empirically based on the investigations presented in Chapter 5.

$$Nu_x = \frac{x}{\lambda} \left(\frac{T_s - T_f}{\Delta T} \right) \cdot \left[-0.199 + 0.19(ACH \cdot (\frac{\Delta h}{H}))^{0.8} \right] \tag{68}$$

4.3.2 Convective surface moisture transfer coefficient (SMTC) modelling

The moisture fluxes (Eq. (69)) between the room and the building component have been modelled using the Chilton-Colburn analogy (Eq. (70)), which relates the heat and mass transfer coefficients directly.

$$g = \beta^X (X_s - X_\infty) \tag{69}$$

$$\frac{\alpha_c}{\beta^X} = \rho c_p \left(\frac{Sc}{Pr} \right)^{2/3} = \rho c_p \left(\frac{\alpha}{D} \right)^{2/3} = \rho c_p Le^{2/3} \tag{70}$$

where g represents the mass flux [kg m^{-2} s^{-1}] at the interface between the gas and liquid or solid, , X the mass fraction of the vapour (species mass per mixture mass), and the subscripts 's' and '∞' respectively represent the surface and free stream conditions. Furthermore, α_c and β^X are the convective surface heat and moisture transfer coefficients [W m^{-2} K^{-1}],[m s^{-1}] respectively, ρ the density of the fluid [kg m^{-3}], c_p the fluid's thermal capacity [J kg^{-1} K^{-1}] and Le is the Lewis number, defined as the ratio of thermal diffusivity α [m^{2}s^{-1}] to mass diffusivity D [m^{2}s^{-1}].

Local convective surface heat transfer coefficients are obtained from the models presented in Section 4.3.1, resulting in local convective surface moisture transfer coefficients. Applying Eq. (69), results in the prediction of the corresponding moisture fluxes to/from the building component.

The model for the local convective surface transfer coefficients is based on the Chilton-Colburn analogy [59] for heat and mass transfer. The validity of the heat and mass analogy for airflows inside buildings has been studied by Steeman [13]. Despite the frequent use of the heat and mass transfer analogy, the author investigated whether the relationship is applicable for the determination of average and local convective surface mass transfer coefficients inside buildings, where natural and mixed convection occurs over complex geometries. For the scenarios with simultaneous heat and mass transfer, the research [13] produced good results and proved the capability of the heat and mass transfer analogy to accurately predict mass transfer coefficients for natural and mixed convection in these cases. Steeman also showed that problems can arise due to the choice of the reference condition, especially considering the cases with non-analogous boundary conditions for heat and mass transport.

In practical cases, the requirement that all boundary conditions for heat and mass transfer inside buildings should be analogous is rarely fulfilled. If the boundary conditions are not analogous, the accurate prediction of local mass fluxes using the analogy is no longer guaranteed when one single reference value is used. A more intensive examination of the study [13] showed that it is not necessarily required to discard the Chilton-Colburn analogy, but, hence, use computational fluid dynamics to choose the correct reference condition for the analogy. In this way, the determination of local surface mass transfer coefficient in case of non-analogous boundary conditions by means of the Chilton-Colburn analogy is applicable, but should be done carefully. For additional information on the validity of the Chilton-Colburn analogy in buildings, the reader is referred to Chapter 2 and the work presented by Steeman [13].

4.4 Conclusion

The methodology and models for the modelling of the indoor environmental conditions and the surface transfer coefficients have been presented. The indoor environmental conditions in the room are modelled using the sub-zonal airflow model and CFD modelling. While the CFD model is able to compute the local convective surface transfer coefficients directly, a sub-zonal airflow model is combined with a surface transfer coefficient model to calculate the local convective surface heat and moisture transfer coefficients in the room.

Regarding the model for the local surface heat transfer coefficients, three models are applied for natural convection, while four models are applied for forced convective airflow. Analytical models based on the boundary layer theory for the flow over a flat plate and experimental relationships resulting from a literature study have been applied. The analysis showed that the applicability of the boundary layer theory may be limited. Furthermore, the validity and assumptions should be considered carefully when applying these correlations in building enclosures. With respect to the convective surface moisture transfer coefficients, the Chilton-Colburn analogy is applied. This analogy usually produces good predictions of the local surface mass transfer coefficients for the scenarios with simultaneous heat and mass transfer. If the boundary conditions are not analogous, the analogy should be applied carefully.

In the next section, the performance of the sub-zonal airflow and surface transfer coefficient models is evaluated based on efficiency, accuracy, computational effort (or simulation time), and flexibility of the models. Furthermore, the results are compared with experimental results and numerical results obtained from CFD.

5 Airflow and Convective Surface Transfer Coefficient Modelling

The research presented in Chapter 3, showed that the local surface transfer coefficients near the building component have a relatively large influence on the predicted hygrothermal conditions on the surface of the component and the heat and moisture buffering capacity of the building envelope. The correct modelling of the heat and moisture fluxes between the building envelope and the indoor environment is important. As mentioned previously, these heat and moisture fluxes are dependent of the local temperature and relative humidity distribution of the air near the building component as well as the local surface transfer coefficients.

In this thesis, the applicability of the sub-zonal model to predict local temperature, and relative humidity in a room is studied. Moreover, surface transfer coefficient models are evaluated for the prediction of the local convective surface transfer coefficients in a room. This section comprises the simulation of the temperature and relative humidity in a room for various flow regimes using sub-zonal airflow models combined with different surface transfer coefficient models. The main objective of the research presented in this section is to assess the applicability of sub-zonal models to get a qualitatively accurate prediction of the local temperature and relative humidity distribution near the building component and the corresponding local convective surface transfer coefficients.

Section 5.1 presents a brief description of the test cases for respectively natural, forced and mixed convection in a room. In Section 5.2, detailed information regarding the studied test case and the simulation results for natural convection in a room are presented. Similarly, Sections 5.3 and 5.4 present more detailed information and the simulation results for respectively the test cases for forced and mixed convection. In Section 5.5, alternatives, which may be also attractive for the transient simulation of heat, air and moisture transfer in buildings, are discussed. Section 5.6 presents the conclusions of the study.

5.1 Test cases

Three test cases for respectively natural, forced and mixed convection in a room are analyzed. The methodology that has been applied as well as the specific details regarding the modelling of the indoor environmental conditions and convective surface transfer coefficients have been presented in Chapter 4. First of all, the natural convective airflow in the CETHIL's MINIBAT test cell that has been presented by Inard *et al.* [35] is analyzed. Second, the Annex 20 Benchmark described by Nielsen [81] has been used as a test case for forced convective airflow. Third, results from a computational fluid dynamics model presented by Steeman [13], have been used for the investigation of the airflow for mixed convection in a two-dimensional enclosure. Table 14 presents the investigated cases ordered by flow regime.

Table 14: Analyzed cases

Case	**Flow regime**
MINIBAT case [35]	Natural convection
Annex 20 Benchmark case [81]	Forced convection
CFD case [13]	Mixed convection

For each test case, several sub-zonal airflow models have been developed and simulated to predict the heat and moisture flows in the room and the flows between the room and the building components. With respect to the surface transfer coefficient models, the results from the sub-zonal airflow model have been used for the prediction of the local convective surface transfer coefficients along the building components. Similarly, CFD simulations have been carried out for the prediction of the indoor environmental conditions and surface transfer coefficients in each test case. The CFD simulations have been performed within the framework of the present study and carried out along the best practice guidelines that were presented by Steeman [13]. The results from the CFD simulations as well as experimental and numerical results from literature have been used for comparison.

In order to avoid any ambiguity regarding the work that has been carried out within the framework of this study, the investigations are briefly summarized. Table 15 presents the investigated cases that are presented in this thesis. The first column presents the investigated test case, while the second and the third column describe the flow regime in the room and the corresponding air change rate of the room. The fourth and the fifth column present the results that have been used for comparison, validation and verification. The fourth column presents the numerical results which are obtained from the models that have been simulated within the framework of this study. The fifth column presents the experimental and numerical results from measurements and simulations, which have not been carried out within the present study, but have served as reference data for the validation and verification of the results obtained in this study.

Table 15: Investigations within the present study

Test case	**Flow regime**	**ACH [h^{-1}]**	**Results**	
			Present study	**Literature**
MINIBAT case	Natural convection	0	- Sub-zonal model results - CFD results	- Experimental data [35] - Sub-zonal model results [35]
Annex 20 Benchmark case	Forced convection	14	- Sub-zonal model results - CFD results	- Experimental data [81] - CFD results [82]
Steeman CFD Case	Mixed (dominating natural convection)	11	- Sub-zonal model results	- CFD results [13]
Steeman CFD Case	Mixed (dominating natural convection)	2	- Sub-zonal model results - CFD results	- CFD results [13]

The indoor environmental conditions in the test cases presented in Table 15 have been simulated using different sub-zonal models and surface transfer coefficient models. Moreover, the results are compared with the experimental results and CFD results. The results from the sub-zonal models have been compared to the CFD models' results regarding efficiency, accuracy, computational effort (or simulation time), and flexibility.

5.2 MINIBAT case

The natural convective airflow, heat and moisture flows in the CETHIL's MINIBAT test cell that has been presented by Inard *et al.* [35] are analyzed. The MINIBAT test cell consists of a 24 m^3 (3.1 x 3.1 x 2.5m) single volume of which the temperature is controlled and kept constant on the faces. The MINIBAT test cell is a room that has been designed to study the airflow in the room under laboratory conditions. A detailed description of the MINIBAT test cell can be found in [89]. The temperatures of the Northern and Southern walls, as well as the floor and ceiling temperatures have been kept constant at 33.0°C, 16.9°C, 26.9°C, and 28.5°C respectively. The temperature of the Western and Eastern walls is approximately 27 °C. Since a similar surface temperature is applied on the Western and Eastern walls, the airflow in centre of the room is considered to be two-dimensional. The analysis focuses on the symmetry plane. Figure 25 presents a two-dimensional slice of the room along the symmetrical centre, the corresponding geometry and boundary conditions. The relative humidity on both walls is 50%RH, while the floor and ceiling are considered to be vapour tight.

Inard *et al.* [35] carried out measurements in the room to investigate the natural convective airflow in the room in order to validate and verify numerical results from a sub-zonal model. Detailed experimental information regarding the airflow pattern and temperature distribution in the MINIBAT test cell under specific conditions is available. The data has been used for comparison with the results obtained in the present study.

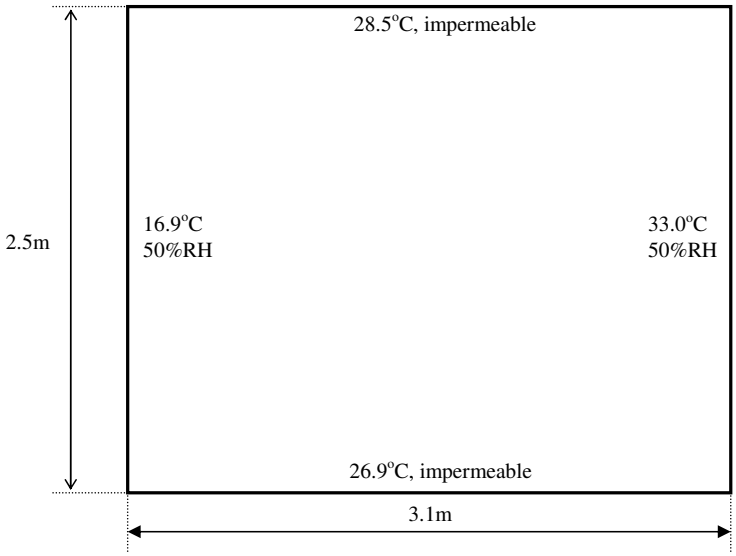

Figure 25: Geometry and boundary conditions for the MINIBAT case [35]

5.2.1 Results

The MINIBAT case has been simulated with and without a model describing the flow in the boundary layer near the walls. The implementation of a boundary layer model requires a relatively large effort and advanced programming. Therefore, a simulation of the sub-zonal model without thermal boundary layer model may lead to a model that is more robust and relatively user-friendly, implementation wise. The literature study showed that this model can be considered to be the state-of-the-art, i.e. this model is usually applied in building simulation based on sub-zonal models.

Table 16 presents an overview of the simulated sub-zonal models and computational grids that have been used. As already has been presented in the methodology (Chapter 4) a grid sensitivity study has been carried out for each case, which ensures that the obtained results are grid independent. The results from the three different sub-zonal airflow models are compared to the experimental and CFD results. The results from the CFD simulation have been verified and validated based on the work published by Inard *et al.* [35]. The results from the CFD simulations gave a good resemblance with the experimental results. As it is not the focus of the current work to give an intensive validation of the CFD simulation, a detailed verification of the CFD results is omitted.

Table 16: Sub-zonal airflow models

Model	**Airflow model**	**STC**	**Grid (x . y)**
(a)	No thermal boundary layer model	CFD	50 x 62
(b)	Thermal boundary layer model	CFD	8 x 10
(c)	Thermal boundary layer model	CFD	16 x 20

Airflow field

Figure 26 shows the streamlines of the air mass flow predicted by the sub-zonal airflow model (b) and predicted by the CFD model. The figure shows that both models predict a descending airflow (from ceiling to the floor) near the Western wall, while an ascending airflow (from the floor towards the ceiling) is predicted near the Eastern wall. Moreover, Figure 26 shows that the sub-zonal model is less capable of predicting local recirculation regions in the room. Deviations between the sub-zonal model and the CFD model are observed, especially near the floor and in the lower left and upper right corner. These deviations may be caused by the characteristics of the sub-zonal model and the application of a relatively coarse grid compared to CFD.

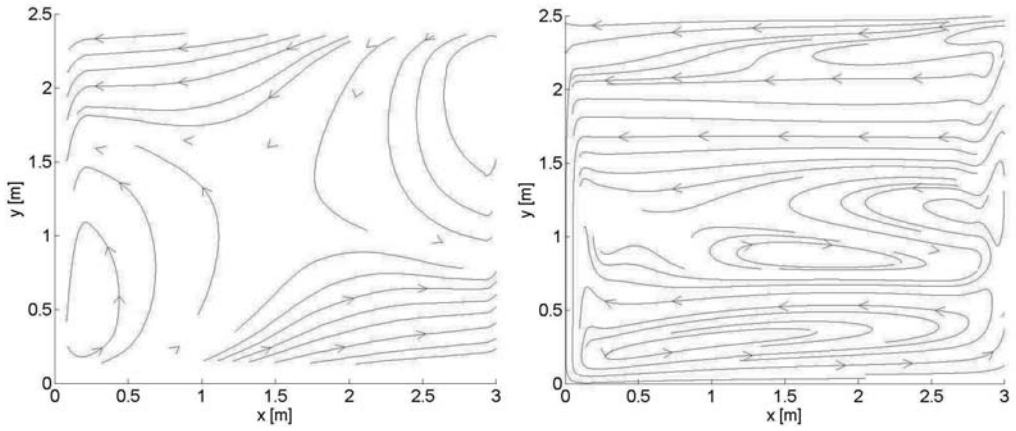

Figure 26: Streamlines of the air mass flow predicted by the sub-zonal airflow model (b) (left), and predicted by the CFD model (right).

It may be difficult to compare the resulting airflow patterns obtained from the sub-zonal model and CFD quantitatively based on Figure 26. Figure 27 presents the air mass flow through the horizontal and vertical faces between the sub-zones. The air mass flows resulting from respectively the sub-zonal model used by Inard *et al*. [35], the CFD model, and the sub-zonal model with the thermal boundary layer model (model (b)), are presented. Only the results from sub-zonal model (b) are presented in the figure, since these agree best with the results from CFD and literature. Moreover, because the CFD simulation has been performed on a relatively dense grid, the mass flow through each surface has been determined by averaging.

The presented air mass flows in Figure 27 should be interpreted as follows: Blue numbers/arrows represent the air mass flow in vertical y-direction, while red numbers/arrows represent the air mass flow in horizontal x-direction. Negative numbers represent air mass flows in opposite x- or y-directions. The direction of the arrows results from the airflow pattern predicted by CFD. Furthermore, the quantitative air mass flow is represented by three numbers per arrow: The first number represents the mass flow predicted by the sub-zonal model by Inard *et al*. [35]. The second number represents the air mass flow calculated by the CFD model, while the third number represents the predictions from the sub-zonal airflow model.

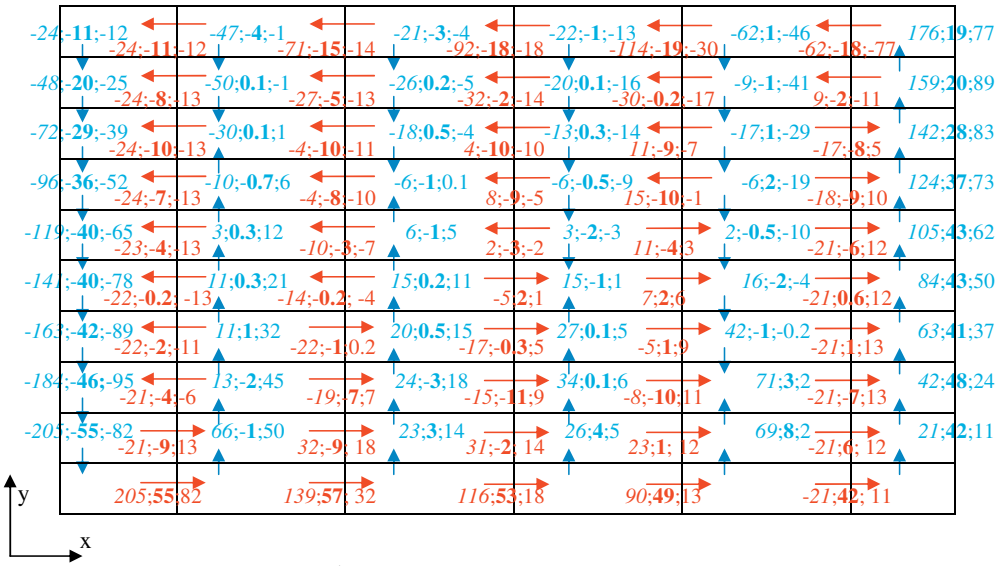

Figure 27: Predicted mass flows [kg h^{-1}] resulting from Inard *et al*. [35], CFD, and sub-zonal model (b) (*Literature*;**CFD**;(c)). Blue arrows/numbers represent vertical air mass flows, red arrows/numbers represent horizontal air mass flows

Comparing the air mass flows near the walls, floor and ceiling, the models predict a similar flow direction, however, the magnitude of the flows may vary significantly. In general, the mass flow near the walls predicted by sub-zonal model (b) and CFD lie in the same order of magnitude. It should be noticed that the near-wall grid that has been used in the CFD simulation is dense, and is able to represent opposite flow directions within one sub-zone. The depicted average values do not represent such opposite flow directions. Furthermore, the model presented by Inard *et al*. [35] gives a larger over-prediction of the mass flow in the layer near the walls. In principle, this leads to an over-prediction of the air mass flows in the entire room, which makes it difficult to compare the airflows quantitatively.

Focusing on the airflow in the centre part of the room, both the flow direction and the air mass flow predicted by the sub-zonal model (c) and CFD may be different. It is difficult to get a general impression about the accuracy of the sub-zonal model based on Figure 27. However, the simulation results show that the applied thermal boundary layer model is capable of predicting (the direction of) the airflow near the wall.

Temperature and vapour content field

Figure 28 presents the measured temperature distribution [35], while the results obtained from CFD are shown in Figure 29. Figure 30 presents the temperature and vapour content distributions in the room for the sub-zonal models (a), (b), and (c). Figure 31 and Figure 32 present a comparison of the temperatures and vapour contents at respectively x=0.62m, x=1.55m, and x=2.69m, and at x=0.15 and x=2.95m, as a function of the height (y) of the room.

Comparing the numerical models with the experimental results, the figures show that the predicted temperature and vapour content distributions are comparable. The results from the CFD simulations give a relatively close resemblance with the experimental results, while the sub-zonal models only give a relatively rough prediction of the temperature and vapour content patterns in the room. However, a qualitative comparison of the simulation results based on the temperature and vapour content distributions presented in Figure 28, Figure 29 and Figure 30 is difficult. Therefore, the results presented in Figure 31 and Figure 32 are shown. The evaluation starts with a comparison on a global scale and then focuses on the qualitative prediction of the indoor environmental condtions.

Comparing the results from the sub-zonal model with the experimental and numerical results from CFD, the following observations are presented:

- *Global temperature distribution*: The predicted temperature and vapour content distribution resulting from models (b) and (c), which include a thermal boundary layer model, are relatively similar, while model (a) shows a different pattern. Local differences are also observed. The main difference between sub-zonal model (a) and the other sub-zonal models is that the highest temperatures are observed in the upper right corner of the room, compared to the upper left corner, predicted by the other models. Further, model (a) predicts a relatively large gradient perpendicular to the wall. This might be explained by the fact that, due to the absence of a thermal boundary layer model, the buoyancy is not represented correctly. In essence, sub-zonal model (a) only accounts for thermal diffusion near the walls, i.e. there is only thermal diffusion from the wall to the indoor air. Similarly, sub-zonal models (b) and (c) may over-predict the convective heat transfer in the centre part of the room, causing the highest temperatures to lie in the upper left corner, instead of the upper right.
- *Local quantities*: it should be noticed that a qualitative comparison of the measured temperature and the resulting temperature from CFD shows clear deviations. Figure 31 and Figure 32 show a difference of approximately 1^{o}C between the experimental and numerical data. It is assumed that this systematic deviation is caused by the experimental accuracy of the investigations. When this systematic deviation is neglected, CFD is best capable of predicting the temperature distribution in the room. Furthermore, Figure 31 shows that sub-zonal model (b) is best capable of giving a relatively accurate qualitative prediction of the temperature and vapour content in the room. The deviation between the CFD results and the quantities predicted by model (b) lies between 10% and 15%. Figure 31 also shows a deviation of 25% and higher regarding sub-zonal model (a).
- *Near wall distribution*: while the models are capable of predicting a stratified pattern in the room, Figure 32 clearly show that sub-zonal model (a) is not capable of predicting the distribution close to the walls. Moreover, Figure 32 shows that sub-zonal model (b) is capable of giving a prediction with in general a deviation between 10-15% for the temperature and vapour content near the walls.
- *Temperature and vapour content gradient*: Figure 31 and Figure 32 show a sudden increase in the temperature and the vapour content at the evaluated locations between approximately 0.75m and 1.75m. A sharp gradient of the temperature and vapour content at these locations is observed. The slope is indirectly caused by the thermal boundary layer model that is implemented and can be explained as follows: The thermal boundary layer model determines the buoyant airflow near the walls. Figure 27 shows that the sub-zonal model gives an over-prediction of the air mass flows (of factor 2) and higher at the bottom of the left wall and at the top of the right walls compared to the results in CFD. This means that a relatively large amount of cold air is transferred to the bottom of the room, resulting in a lower temperature here. Similarly, a large amount of hot air is transported to the top of the room, resulting in a higher temperature there, and an increased temperature gradient in the

centre of the room between respectively y=0.75m and 1.75m. A similar phenomenon has been observed for the vapour content distribution.
The following assumption should be mentioned: the thermal boundary layer model (Chapter 4, Section 1.2) assumes that the thermal boundary layer starts developing from the beginning of the wall. In essence, the boundary layer thickness is assumed to be zero at the beginning, resulting in a zero air mass flux through the thermal boundary layer, while the air mass flux through the boundary layer increases along the wall with increasing boundary layer thickness. For building enclosures, such as a room, this assumption might be discussable because of the presence of the corners. In practice, the flow in the corner is influenced by the geometry of the room, and the airflow in the room, which may result in a thermal boundary layer thickness and corresponding air mass flow that is larger than the thickness and air mass flow assumed by the model.

- *Grid densification*: Given the similarity in the predicted temperature field by models (b) and (c), a densification of the grid does not influence the simulation results significantly. Additionally, applying a denser grid does not improve the predicted results. For example, Figure 32 shows that the dense grid, applied in model (c), gives a larger deviation of the vapour content at x=0.15m compared to the coarser grid in model (b). It is also observed that the influence of the thermal boundary model (flow element sub-zones) might be relatively large compared to the influence of the standard sub-zones, provided that the discretisation of the standard sub-zones is dense enough to represent the airflow pattern in the room. Of course, if the discretisation of the zone is too coarse, the quality of the simulation results is poor.

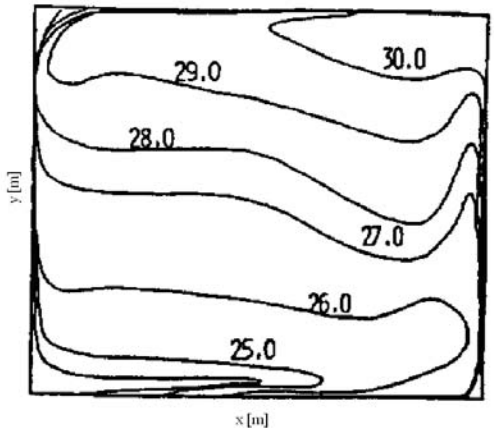

Figure 28: Measured temperature distribution [°C] in the room.

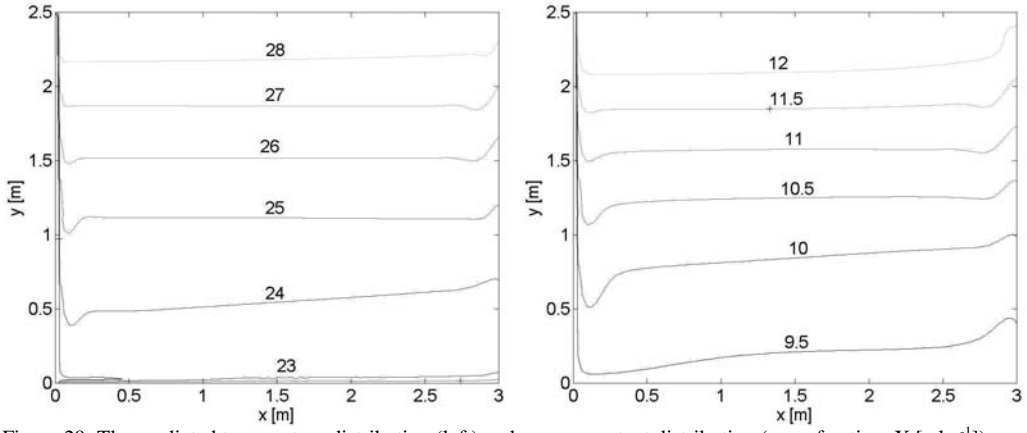

Figure 29: The predicted temperature distribution (left) and vapour content distribution (mass fraction, X [g kg^{-1}]) (right) in the room obtained from CFD.

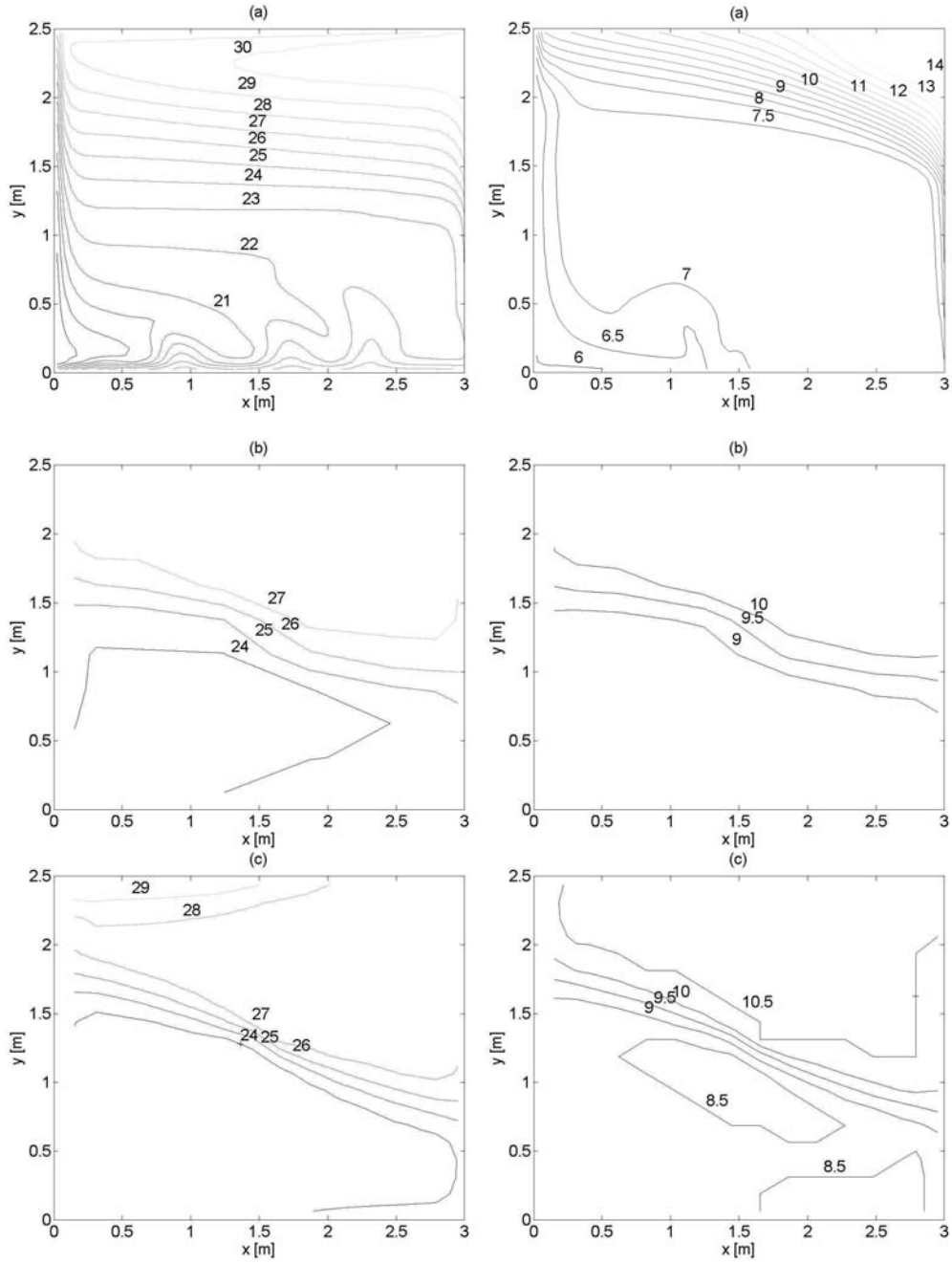

Figure 30: Temperature distribution [^{o}C] (left) and vapour content distribution [g kg^{-1}] (right) predicted by the sub-zonal models (a), (b), and (c) (Table 16).

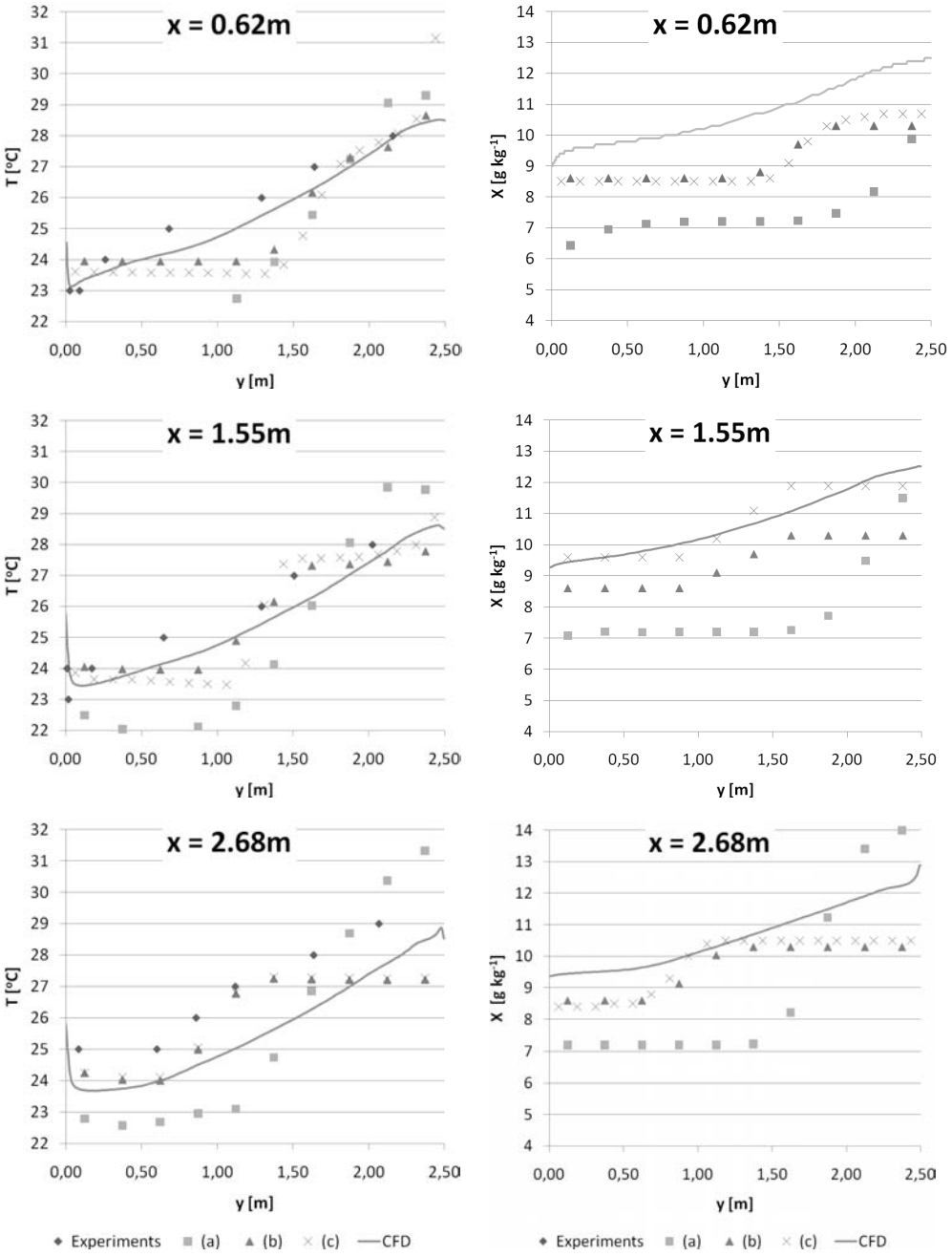

Figure 31: Temperature [°C] and vapour content distribution [g kg^{-1}] at different locations in the room (x=0.62, 1.55, and 2.68m).

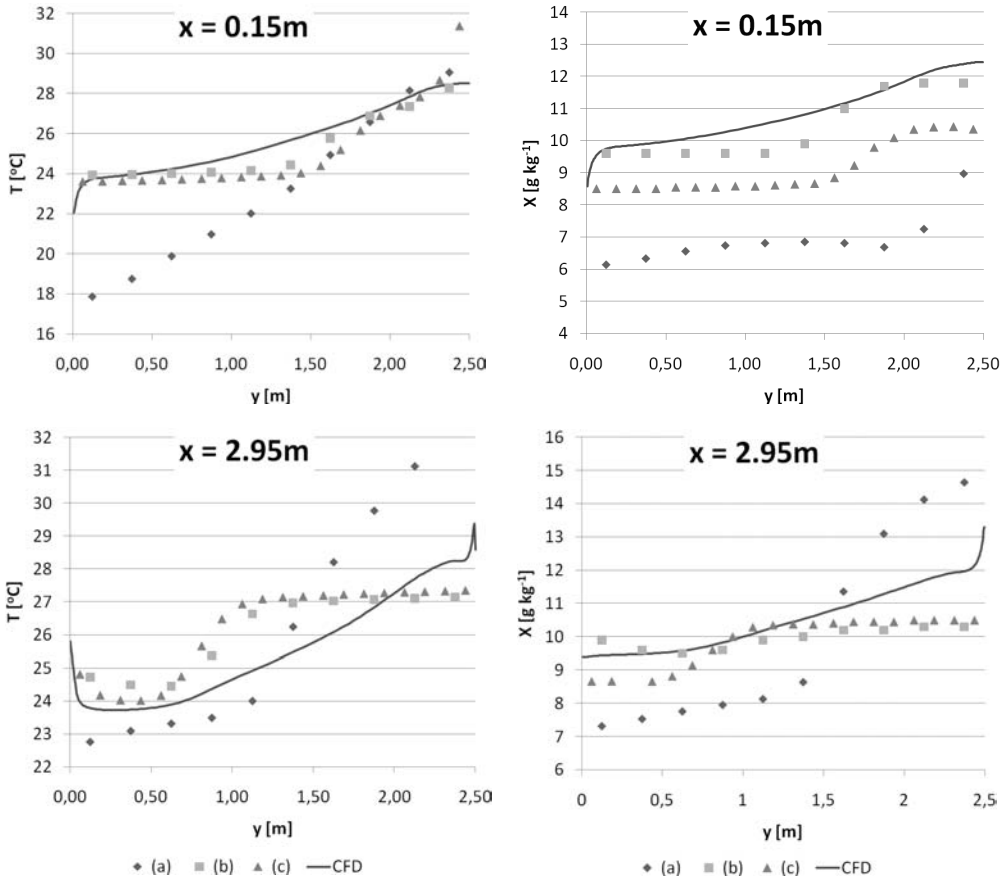

Figure 32: Temperature [°C] and vapour content [g kg^{-1}] distribution at different locations in the room (x=0.15,and 2.95m).

The comparison of the results obtained from the sub-zonal models with the experimental and CFD results showed that the sub-zonal airflow model is able to predict the local temperature and vapour content in the room with a maximum relative deviation between approximately 10% and 15%. A similar deviation has been observed for the local temperature and vapour content near the walls. However, the sub-zonal model showed not to be applicable for the prediction of the air mass flows and local velocities in the room. Deviations of a factor 2 and more with respect to the predicted air mass flow have been observed. Based on the natural convective airflow that has been modelled by Mora et al.[46], he similarly concluded that the sub-zonal model was not suitable for the prediction of the air velocities in the room, while the sub-zonal model gave good results for the temperature distribution.

Furthermore, a densification of the grid did not change the predicted temperature and vapour content distribution significantly. Investigations carried out by other researchers, for example Wurtz et al. [44], illustrated that a densification of the grid by a factor two did barely change the results. In addition, the influence of the thermal boundary layer model on the predicted temperature and vapour content distribution in the room is relatively large. As has been mentioned previously, this is caused by the thermal boundary layer model that determines the airflow along the wall. However the thermal boundary layer model has been presented as a general model for the thermal boundary layer along a wall [41] , the limitations for the applications for building enclosures and corresponding geometrical effects due to corners have not been

discussed in literature. Other authors [90] used thermal boundary layer models that have been developed for the specific conditions in the room using experimental facilities. Tuning of the thermal boundary layer model for this specific case, for example by using experimental data or numerical results, might improve the results, though it may limit the general application of the sub-zonal model.

Convective surface transfer coefficients

The analysis showed that the sub-zonal model with a thermal boundary layer model implemented is capable of giving a relatively accurate prediction of the temperature and vapour content distribution in a room where natural convection is dominant. Furthermore, the model showed to be applicable to give a prediction of the local temperature and vapour content near the walls. Besides the local temperature and vapour content, the convective surface transfer coefficients are important for the prediction of the heat and moisture flows between the room and the walls.

The sub-zonal model (Table 16: model (b)) with thermal boundary layer model has been used to model the natural convective airflow in the room. The results obtained from the sub-zonal airflow model have been used as input data for the surface transfer coefficient models. The predicted convective surface heat and moisture transfer coefficients (CHTC and SMTC) along the walls resulting from the surface transfer coefficient models and the CFD model have been compared. Table 17 presents an overview of the simulated surface transfer coefficient models and computational grids that have been used.

Table 17: Surface transfer coefficient models

MODEL	STC	Grid (x . y)
(ref)	Beausoleil-Morrison [9]	8 x 10
(a)	Flat plate	8 x 10
(b)	Turner *et al.* [87]	8 x 10
(c)	Turner *et al.* [87]	16 x 20
(d)	Bohn *et al.* [88]	8 x 10

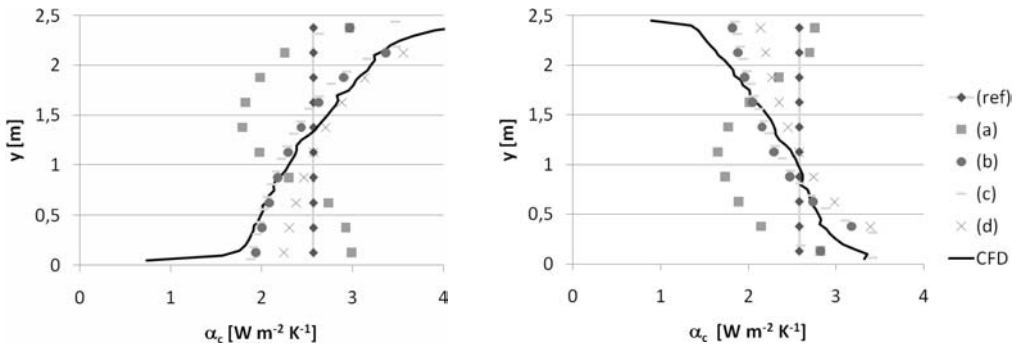

Figure 33: Convective surface heat transfer coefficient (α_c [W m^{-2} K^{-1}]) for the Western wall (left) and the Eastern wall (right).

Figure 33 and Figure 34 present a comparison of the local convective surface heat and moisture transfer coefficients resulting from the different surface transfer coefficient models (Table 17) and the values obtained from the CFD simulation. With respect to the coefficients predicted by model (a), based on the flat plate analogy, the figures show an under-prediction in the region from the leading corner down/up to the centre of the wall (y=1.25m) and an over-prediction of the coefficients further from the centre (y=1.25). Comparison of the results with the CFD results showed that the main reason for the under/over prediction is that the size of the laminar region is over-predicted by the model, resulting in smaller surface transfer coefficients, while the size of the turbulent region is under predicted.

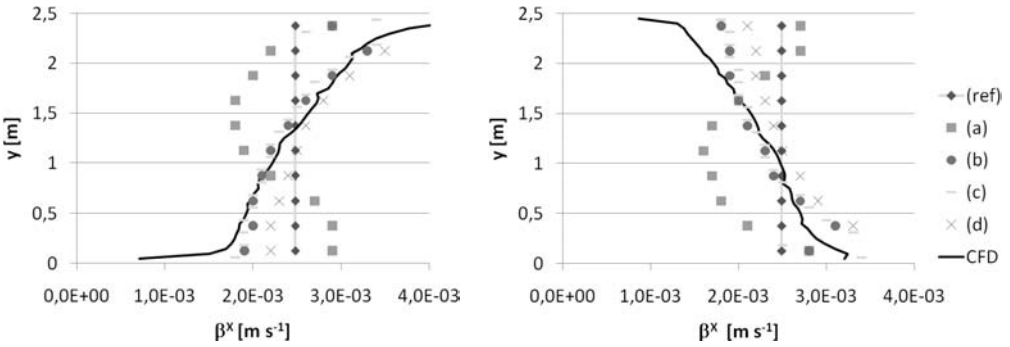

Figure 34: Convective surface moisture transfer coefficient (SMTC) for the Western wall (left) and the Eastern wall (right).

Regarding the results predicted by model (b), (c), and (d), the resulting local surface transfer coefficients are comparable with the coefficients predicted by CFD. The STC's predicted by model (b) and (c), based on Turner *et al* [87], give the best agreement, while the deviation is less than 10%. Model (d) Bohn *et al*. [88] gives a slight over-prediction and a maximum relative deviation of approximately 25%. This relatively high deviation might be caused by the dissimilarity between the simulated case and the conditions that have been used for the determination of the relationships. Bohn *et al*. [88] determined the CHTC for a cube, with a rib length of 0.3m, in water, and Rayleigh range between $3 \cdot 10^9$ and $6 \cdot 10^{10}$, while Turner *et al* [87] determined the CHTC's for various rectangular boxes in air, and a Rayleigh range between $3.5 \cdot 10^6$ and $5.5 \cdot 10^9$. The Rayleigh number in the studied room varied between $2.5 \cdot 10^6$ and $18 \cdot 10^9$.

The investigations showed that the surface transfer coefficient model based on the flat plate analogy is not suitable for the prediction of the convective surface transfer coefficients in the room. As has been discussed earlier, the specific assumptions of the boundary layer theory for flat plates, for example regarding the boundary conditions, geometrical influences, entrance velocity and leading edges, and surface roughness, are not (entirely) valid in building enclosures. Similar observations have been reported by Khalifa *et al.* [52] and the authors concluded that a correlation obtained for an isolated flat plate is not suitable for a surface in a real sized enclosure, especially for buildings. This conclusion has been confirmed by the present investigations. Furthermore, the boundary layer model that has been developed based on measurements of the global indoor environmental conditions for natural convection in a room, such as the model developed by Turner *et al* [87], are suitable for the prediction of the convective surface transfer coefficients, provided similar Rayleigh numbers are observed as in the experimental conditions on which the correlation is based.

5.2.2 Conclusion

The investigations showed that the sub-zonal airflow model is able to predict the natural convective airflow in a room, provided an appropriate thermal boundary layer model and surface transfer coefficient model are applied. Comparison of the sub-zonal model and CFD showed that the models predicted in general similar flow directions. However, the sub-zonal model showed not to be applicable for the prediction of the air mass flows and local velocities in the room. Deviations of a factor 2 and more with respect to the predicted air mass flow have been observed. The sub-zonal model gives a prediction of the temperature and vapour content distribution in the room, with a maximum relative deviation between approximately 10% and 15%. While the predicted distributions are only slightly influenced by a densification of the grid, the influence of the thermal boundary layer model on the predicted temperature and vapour content distribution in the room showed to be relatively large.

Regarding the prediction of the convective surface transfer coefficients, the model based on the flat plate analogy was not suitable. The specific assumptions of the boundary layer theory for flat plates, especially focussing on the boundary conditions, geometrical influences, entrance velocity and leading edges, and surface roughness, are not (entirely) valid in building enclosures. The experimentally determined

surface transfer coefficient model based on the natural convective airflow in a rectangular enclosure gave the best results.

5.3 Annex 20 Benchmark case

Within the framework of the International Energy Agency project, ECBCS, Annex 20 (‘‘Air flow patterns within buildings’’), a two dimensional test case, for which detailed experimental data is available, has been specified in [47]. The test case represents both isothermal flow and summer cooling.

The configuration of the room is shown in Figure 35. The room is specified by the room height H = 3.0m. The other dimensions are expressed in terms of L/H = 3.0, h/H = 0.056, and t/H = 0.16. At the inlet the Reynolds number is 5000 and the turbulence intensity 4, which corresponds to an inlet velocity of 0.455 m/s and inlet temperature of 15°C. The room is ventilated with an air change rate of 14 h^{-1}. Nielsen [81] carried out experiments in the facility and this data set has been used for the validation and verification of CFD results by Chen [82]. Experimental data with respect to the airflow field and the temperature distribution in the Annex 20 Benchmark case are available. The experimental investigations from Nielsen [47] showed that the airflow in the centre of the enclosure at z = 0.5W can be considered to be two-dimensional. This assumption has been applied in the present study.

Isothermal and non-isothermal investigations have been carried out. With respect to the isothermal investigations, the study focused on the prediction of the air velocity and especially the recirculation of the airflow in the room. Furthermore, the non-isothermal Annex 20 Benchmark case was changed to meet the requirements for the analysis of the heat and moisture flows in the room. Regarding the non-isothermal investigations, the original boundary conditions that have been applied in the original Annex 20 Benchmark case were changed: the temperature and relative humidity at the surface of the left and right walls (respectively at x= 0 and x = L) are 20°C and 50%, and 30°C and 50% respectively. The ceiling and floor are assumed to be adiabatic and impermeable for vapour transport.

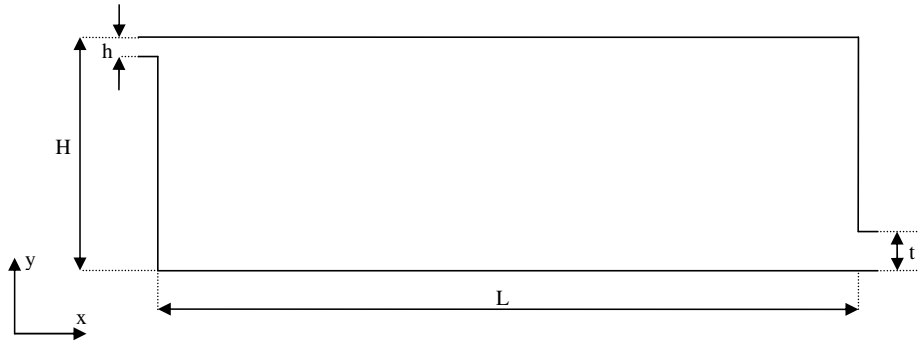

Figure 35: Geometry of the Annex 20 Benchmark case [47]

CFD simulations were carried out to obtain a reliable prediction of the vapour content distribution and the local convective surface transfer coefficients. This data set has been used for comparison with the results from the sub-zonal models. The results from the CFD simulation have been verified and validated based on the work published by Chen [82] and by Nielsen [47]. The results from the CFD simulations gave a good resemblance with the experimental results. While it is not the focus of the current work to give an intensive validation of the CFD simulation, a detailed verification of the CFD results is omitted.

5.3.1 Results

Table 18 presents an overview of the simulated sub-zonal models and computational grids that have been used. As already has been presented in the methodology (Chapter 4) a grid sensitivity study has been carried out for each case, which ensures that the obtained results are grid independent. A standard sub-zonal airflow model without a jet model (model (a)) and a standard sub-zonal airflow model with a specific model describing the jet near the ceiling (model (b)) have been developed. Furthermore, a densification of the grid was carried out (model (c)).

Table 18: Sub-zonal airflow models

Model	Airflow model	STC	Grid (x . y)
(a)	Sub-zonal without jet	CFD	6 x 9
(b)	Sub-zonal + Jet-model	CFD	6 x 9
(c)	Sub-zonal + Jet-model	CFD	12 x 18

Airflow field

Figure 36 presents the air mass flow streamlines in the room predicted by CFD. The predicted airflow field resulting from sub-zonal models without and with a jet model, respectively models (a), (b), and (c), and the results obtained from the CFD models have been compared. Figure 37 presents the streamlines of the air mass flow predicted by the sub-zonal models in the room. A comparison with the CFD results shows that the model without the jet model (a) is not capable of predicting any recirculation in the room. While sub-zonal models (b) and (c) are capable of predicting recirculation, a considerable difference between the resulting airflow patterns consists. Since sub-zonal model (a) is not able to predict any recirculation of the airflow in the room and the results deviate a lot from the CFD results, sub-zonal model (a) is not suitable for the prediction of the indoor environmental conditions in the room and the results are not discussed further. Only the results from sub-zonal models (b) and (c) are compared with the CFD results and discussed.

Comparing sub-zonal airflow models (b) and (c) with the CFD results, differences regarding the size of the recirculation region and the location of the region's centre have been observed. Moreover, deviations are observed in the lower left corner and the upper right corner of the room. The differences between the sub-zonal model's results and the CFD results may be caused by the characteristics of the sub-zonal model, and the empirical jet model that has been implemented.

As has been mentioned in the literature review, the sub-zonal models do not take the surface drag into account, i.e. the power law sub-zonal model implicitly demands that all changes in kinetic energy in a control volume are dissipated. This assumption corresponds to a static fluid, which is not a reasonable assumption in ventilated rooms. The model is not able to take into account the transfer of shear stress near wall surfaces. The momentum transfer is especially important when (small) recirculation regions of the airflow, for example near corners, are observed. Since the model is not able to describe the transfer of momentum, the standard sub-zonal airflow model is not able to predict recirculation. This limitation of the sub-zonal model has been observed by other authors [38] [43]as well. Generally, two possible solutions are available: the implementation of flow element sub-zones [41] or a sub-zonal model, which is based on a surface-drag flow relation [43]. Both options have been intensively discussed in Chapter 2, and the reader is referred to this section, if additional information is required.

The inlet jet is modelled as an empirical jet model based on the jet height, and local volume flow through the control volume's face [41]. The model determines the pressure drop over the sub-zone and the airflow through the sub-zone's face based on the jet height and the local volume flow at the jet inlet. However, the model does not take other influences into account, such as the inlet temperature and geometrical influences. The model that has been applied is a general model for non-isothermal jets. Discrepancies between the momentum transfer predicted by the jet model and the CFD model, which solves the Navier-Stokes equations, are likely. To improve the simulation results, especially the recirculation of the airflow, it might be an option to develop a jet model for the specific conditions in the room, by for example using experimental facilities. Tuning of the jet model for this specific case, for example by using

experimental data or numerical results, might improve the results, though it may limit the general application of the sub-zonal model.

A densification of the computational grid that has been applied in sub-zonal model (b) by factor two has been applied in model (c). Figure 37 shows that the densification did not change the simulation results significantly, i.e. the airflow is relatively similar and the centre of the recirculation region lies around 7m.

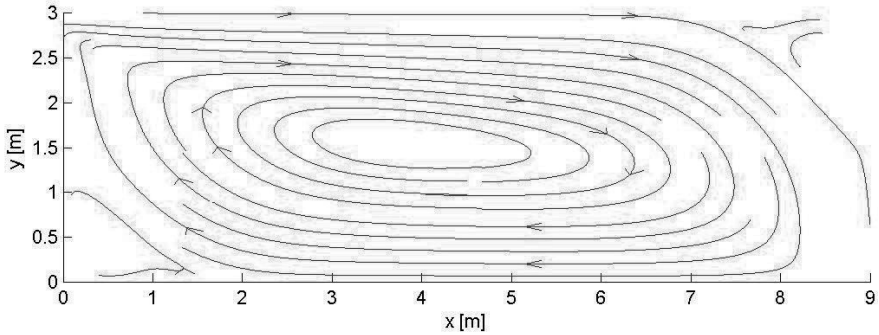

Figure 36: Air mass flow streamlines [kg s^{-1}] resulting from the CFD simulation.

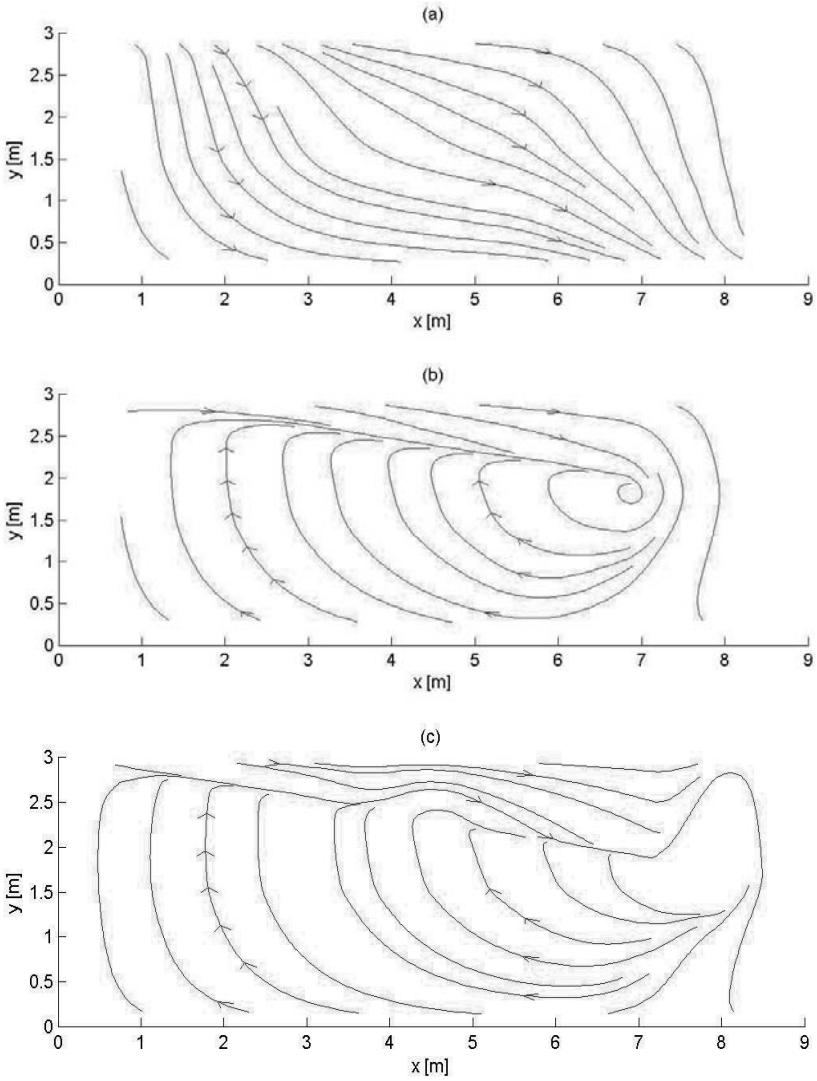

Figure 37: Air mass flow streamlines [kg s^{-1}] resulting from the sub-zonal model (a) without a jet model and models (b) and (c) with a jet model.

Figure 38 shows a quantitative comparison of the air mass fluxes through the sub-zone faces computed by the sub-zonal model and CFD. The presented air mass flows in Figure 38 should be interpreted as follows: Blue numbers/arrows represent the air mass flow in vertical y-direction, while red numbers/arrows represent the air mass flow in horizontal x-direction. Negative numbers represent air mass flows in opposite x- or y-directions. The direction of the arrows results from the airflow pattern predicted by CFD. Furthermore, the quantitative air mass flow is represented by two numbers per arrow: The first number represents the mass flow predicted by the CFD model. The second number represents the air mass flow calculated by the sub-zonal airflow model (b).

The figure shows that in the main part of the room sub-zonal model (b) and CFD predict similar directions of the airflow. A (minor) discrepancy is observed due to the differences in the predicted size of the recirculation region. Regarding the prediction of the magnitude of the airflows a relatively large discrepancy between both models has been observed, i.e. deviations between a factor 2 and 3 shown. The sub-zonal model generally gives a smaller prediction of the air mass flows compared to the CFD results. The differences are mainly caused by the characteristics of the sub-zonal model, and the empirical jet model that has been implemented. These specific characteristics, i.e. sub-zonal models do not take the surface drag into account, and the influences of the empirical jet model on the airflow field in the room have been discussed earlier. Moreover, the discrepancies might have a large influence on the predicted temperature and vapour content field in the room, as well as on the predicted convective surface transfer coefficients. The study proceeds with the analysis of the predicted local temperature, vapour content and convective surface transfer coefficients in the room.

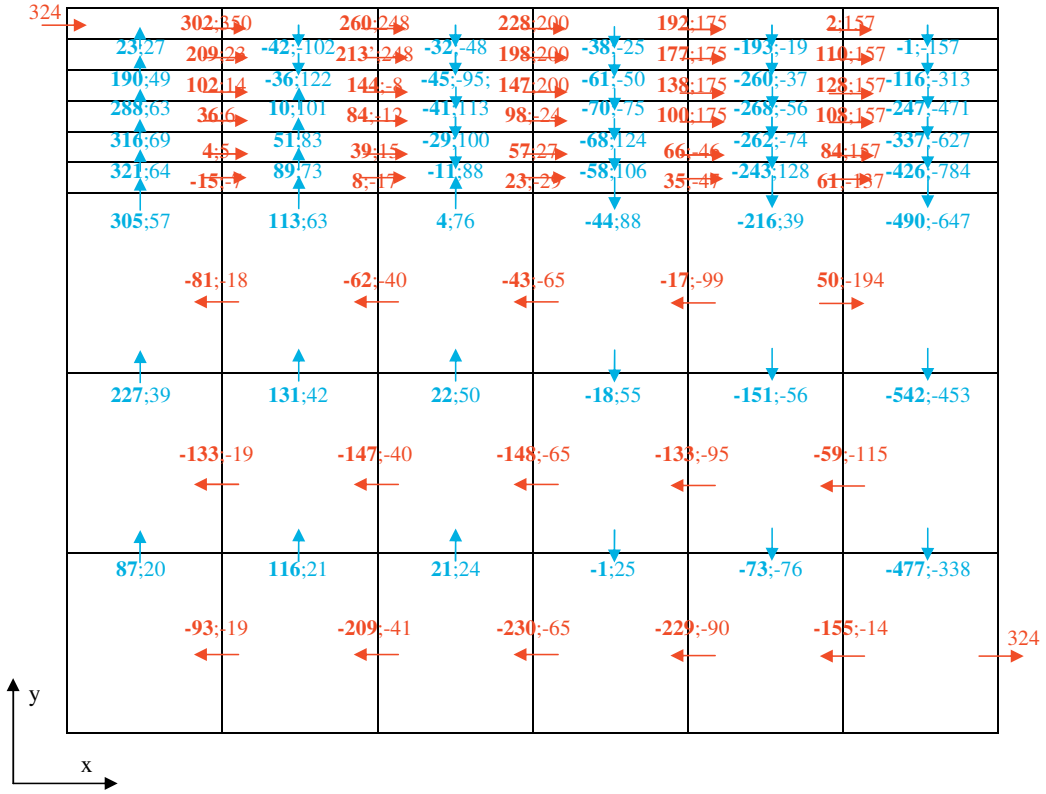

Figure 38: Predicted mass flows [kg h^{-1}] resulting from CFD and the sub-zonal airflow model (b) (CFD;(b)).

Temperature and vapour content field

Figure 39 and Figure 40 show the temperature and vapour content distribution in the room predicted by the CFD model. Figure 41 presents the temperature field in the room predicted by sub-zonal models. The corresponding vapour contents predicted by the sub-zonal models are presented in Figure 42 Regarding the results obtained from the sub-zonal models, only results from the model which includes a jet model are shown, since a sub-zonal model without a jet model showed not to be able to predict the airflow in the room

correctly. Moreover, a comparison of the local temperature and vapour content distributions at 0.125m from the walls is shown in Figure 43 and Figure 44.

Comparing the results from the sub-zonal model with the experimental and numerical results from CFD, the following observations are presented:

- *Global temperature and vapour content distribution*: Figure 41 and Figure 42 show that the sub-zonal is capable of giving a rough prediction of the global temperature and vapour content distribution in (the centre of) the room. Considering the predicted temperature in the centre of the room the sub-zonal model predicts 15.5°C compared to 15.1°C by CFD, while the vapour content in the centre predicted by both models is approximately 4.6 kg/kg. However, discrepancies between the sub-zonal models and CFD with respect to the recirculation of the air are observed. Figure 39 and Figure 40 show a uniform temperature and vapour content distribution in the main part of the room, where a large recirculation region of the air is observed. In the corners, where small recirculation is present slightly higher temperatures are predicted. The sub-zonal models, though, predict a relatively uniform temperature and vapour content distribution in the entire room, since they are not able to capture the recirculation.
- *Local quantities*: Comparing Figure 41 and Figure 39, as well as Figure 42 and Figure 40, the sub-zonal model is not able to predict the temperature distribution very close to the walls (represented by a white region along the edges of Figure 41 and Figure 42). The CFD model is capable of giving a prediction of the local quantities very close to the walls. Based on the global distributions in the rooms it is difficult to compare the models quantitatively. Therefore the local temperature and vapour content distribution at 0.125m from the walls is presented in Figure 43 and Figure 44. Figure 43 shows that the temperature in the centre of the walls is predicted with a maximum deviation of 10%. However, close to the floor and the ceiling, the relative deviation between the sub-zonal airflow model and CFD increases up to 25%. Especially in the lower left corner and the upper right corner deviations of 2°C and more are observed. Similarly, Figure 44 shows that the relative deviation increases up to 30% with respect to the local vapour content in the corners, while comparing the sub-zonal airflow models and CFD. The local recirculation of the airflow shows to be a problem with respect to the local quantities in the room.
- *Grid densification*: Given the similarity in the predicted temperature field by models (b) and (c), Figure 41 and Figure 42 showed that a densification of the grid did not influence the simulation results significantly. Both the global temperature and vapour content distributions (Figure 41 and Figure 42) as well as the local patterns (Figure 43 and Figure 44) did not change significantly when applying a densification of the grid with a factor 2.

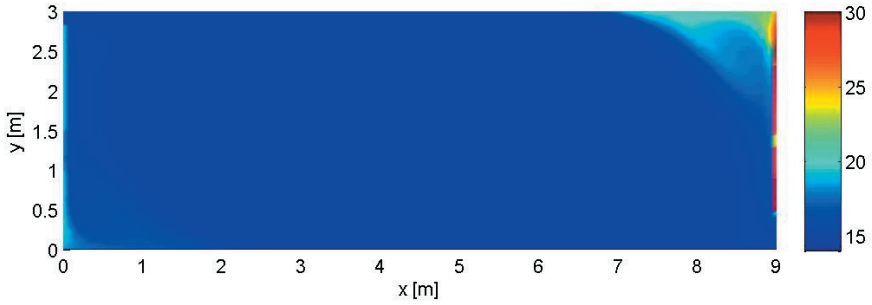

Figure 39: Temperature distribution [°C] predicted by CFD.

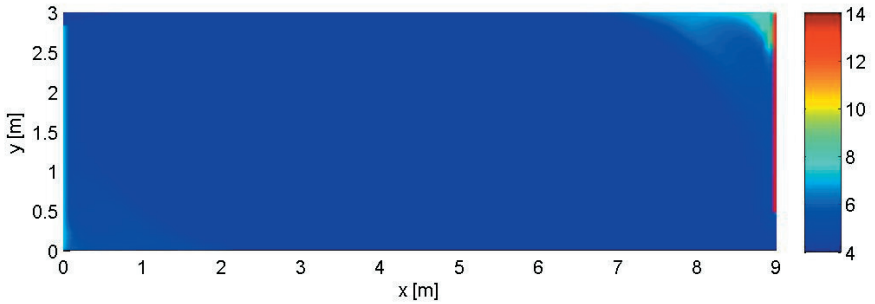

Figure 40: Vapour content (mass fraction, X [g kg^{-1}]) distribution predicted by CFD

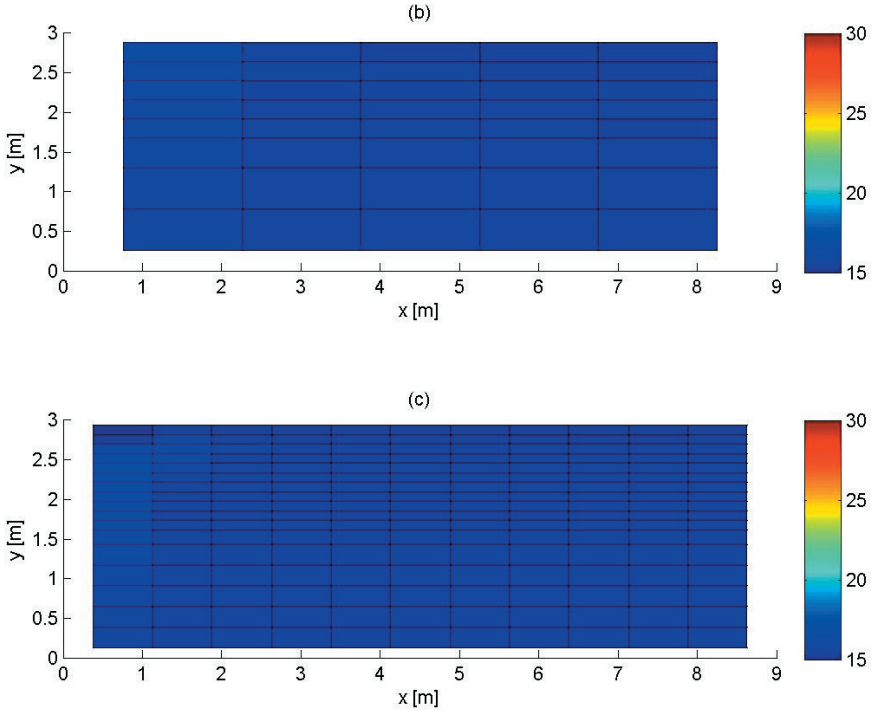

Figure 41: Temperature distribution [°C] predicted by the sub-zonal models (b) and (c).

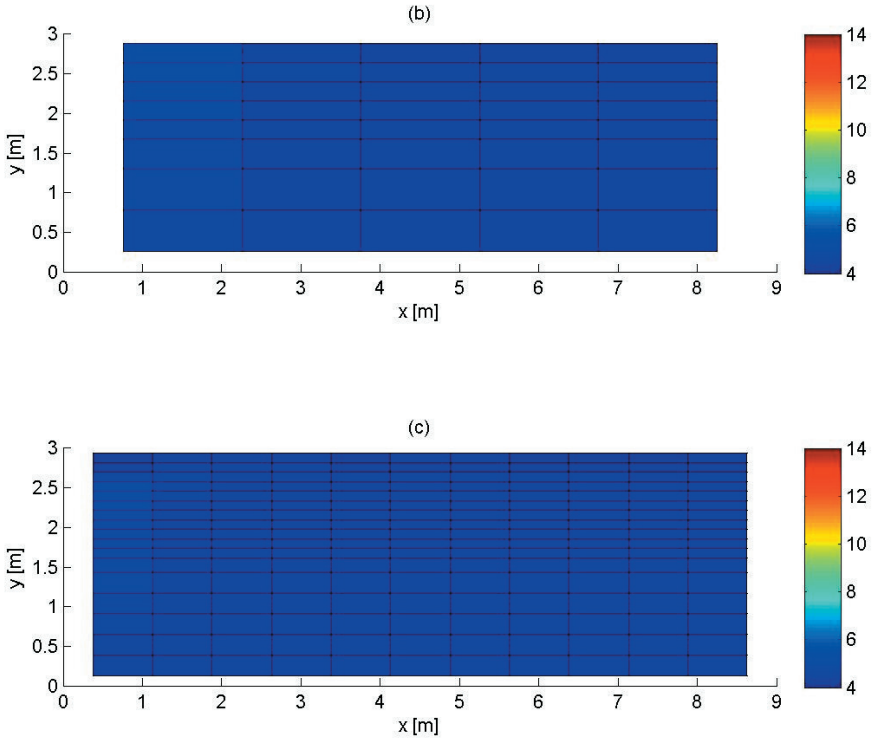

Figure 42: Vapour content (mass fraction, X [g kg^{-1}]) distribution predicted by the sub-zonal models (b) and (c).

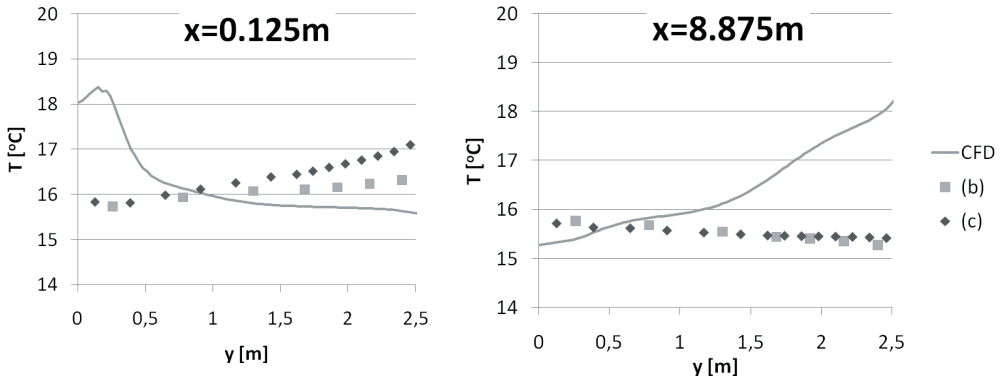

Figure 43: Temperature distribution [°C] at 0.125m from the walls at respectively x=0.125m, and 8.875m.

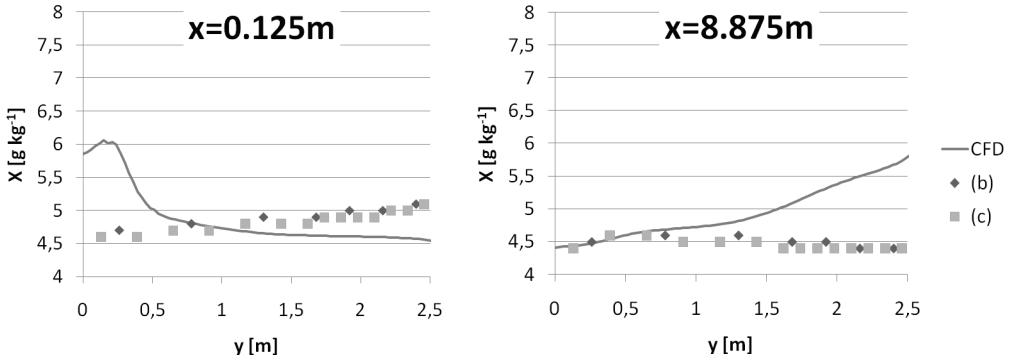

Figure 44: Vapour content (mass fraction, X [g kg^{-1}]) distribution at 0.125m from the walls at respectively x=0.125m, and 8.875m

The comparison of the results obtained from the sub-zonal models with the CFD results showed that the sub-zonal airflow model is able to predict the global temperature and vapour content in the room with a maximum relative deviation of approximately 10%. However, with respect to the prediction of the local indoor environmental quantities, the presence of local recirculation regions of the airflow in the corners showed to be problematic. Close to the floor and the ceiling, the relative deviation between the sub-zonal airflow model and CFD increases up to 25% for the local temperature and 30% for the local vapour content. Furthermore, the sub-zonal model showed not to be applicable for the prediction of the air mass flows and local velocities in the room. Deviations of a factor 2 and more with respect to the predicted air mass flow have been observed.

Other authors [37] [38] [43] [46] similarly indicated that the sub-zonal model is capable of giving a rough prediction of the forced convective airflow in the room provided an appropriate flow element model, describing the jet in the room, is implemented. In the research presented by Wurtz [37], the isothermal Annex 20 Benchmark case has been analyzed too. He concluded that sub-zonal models give a satisfactory estimate of airflow patterns only with specific laws to model momentum added to the air by the jet. Sub-zonal models give a rough estimate of the structure of the recirculation in the room.

Though, the study presented by Wurtz [37] did not focus on smaller local recirculation regions of the air, for example in a corner of the room. This study demonstrated that the sub-zonal airflow model is not capable of capturing such smaller recirculation regions, resulting in a deviation of the local temperature and vapour content that increases up to 30%. In addition, the study [37] did not consider the prediction of the local temperature and vapour content near the building component specifically. While Wurtz [37] did not experience any problems with respect to the prediction of the local temperature in the room and observed that only small discrepancies between the sub-zonal model and experimental data were observed, larger deviations have been observed in the present study.

Convective surface transfer coefficients

The analysis showed that the sub-zonal model with a jet model implemented is capable of giving a relatively rough prediction of the temperature and vapour content distribution in a room where force convective airflow is dominant. Furthermore, the sub-zonal model showed to be capable of giving a prediction of the local temperature and vapour content near the walls. Provided local recirculation regions are not present, the maximum relative deviation with respect to the indoor environmental quantities in the room lies between 5% and 10%. If a recirculation region is present near the wall, for example in a corner, the model is not capable of giving an accurate prediction of the local quantities in that region and the relative deviation increases up to 30%.

Besides the local temperature and vapour content, the convective surface transfer coefficients are important for the prediction of the heat and moisture flows between the room and the walls. The predicted

convective surface heat and moisture transfer coefficients (CHTC and SMTC) along the walls resulting from the sub-zonal models and the CFD have been compared. Table 19 presents an overview of the simulated surface transfer coefficient models and computational grids that have been used. With respect to the airflow model, the sub-zonal model (Table 18: Model (b)) with thermal boundary layer model has been used to model the forced convective airflow in the room.

Table 19: Surface transfer coefficient models

MODEL	STC	Grid (x . y)
(a)	Beausoleil-Morrison [9]	6 x 9
(b)	1Flat plate (Churchill) [50]	6 x 9
(c)	2 Flat plate (Rose) [50]	6 x 9
(d)	3 Flat plate (Churchill and Ozoe) [60]	6 x 9
(e)	Local Beausoleil-Morrison [9]	6 x 9

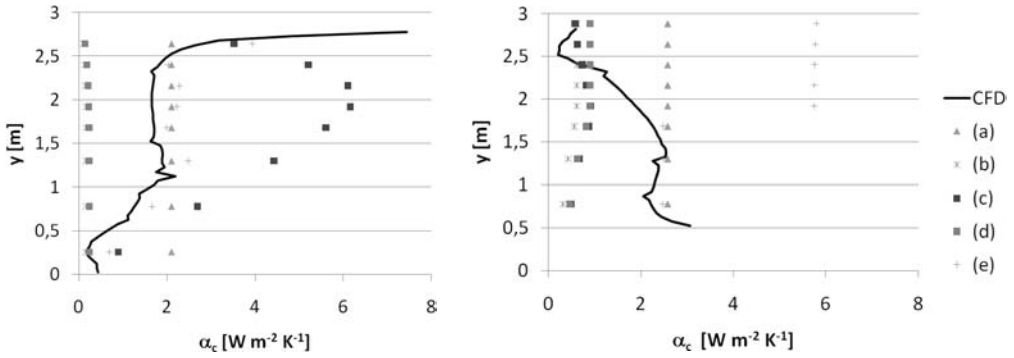

Figure 45: Convective surface heat transfer coefficient (α_c [W m^{-2} K^{-1}]) for the Western wall (left) and the Eastern wall (right).

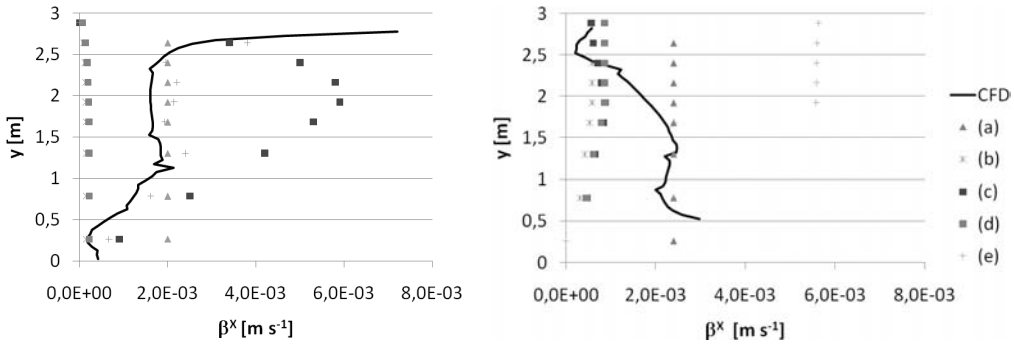

Figure 46: Convective surface moisture transfer coefficient (h_m [m s^{-1}]) for the Western wall (left) and the Eastern wall (right).

Figure 45 and Figure 46 present a comparison of the local convective surface heat and moisture transfer coefficients resulting from the different surface transfer coefficient models (Table 19) and with the values obtained from the CFD simulation.

First of all, the figures show that the relationships for average surface transfer coefficients obtained from Beausoleil-Morrison [9], i.e. model (a), are not applicable, since these result in an over-prediction of factor 2 and more in the lower region of the Western wall and the upper region of the Eastern wall.

Second, the figure shows that the models based on the flat plate relationships obtained by Churchill [50], model (b), and Churchill and Ozoe [60], model (d), are not capable of predicting the convective surface heat transfer coefficient along both walls. The models give an under-prediction of a factor 10 and more. With respect to the flat plate based correlation reported by Rose [50], the predictions for the Western wall result in an over-prediction of the CFD results of a factor 2 and higher, while the correlation does neither give good results for the Eastern wall.

The main reasons for the erroneous prediction of the local convective surface transfer coefficient by the surface transfer coefficient models based on the flat plate analogy may be, first of all, found in the fact that these models are based on relationships that have been determined for isolated flat plates instead of real building components. This issue has been discussed previously in Section 2.5.1 and Section 4.3 and it was demonstrated that the specific assumptions of the boundary layer theory for flat plates, for example regarding the boundary conditions, geometrical influences, entrance velocity and leading edges, and surface roughness, are not (entirely) valid in building enclosures.

Second, the models require the accurate prediction of the local Reynolds and Nusselt numbers near the wall. Previously, it has been observed that the sub-zonal model is not able to give an accurate prediction of the air mass flux through the faces of the sub-zones. In the model, average Reynolds and Nusselt numbers are calculated for each face of the sub-zones parallel to the wall based on the average air mass flux through these faces. In principle, both the local Reynolds and Nusselt numbers are based on the local air mass fluxes. This means that an erroneous prediction of the air mass flux automatically results in an erroneous prediction of the Reynolds and Nusselt numbers and thus erroneous convective surface transfer coefficients.

As an alternative to the use of the correlations based on forced convection over a flat plate, the correlations from Beausoleil-Morrison have been applied locally (Chapter 4: Surface heat transfer coefficients). Figure 45 and Figure 46 present the calculated convective surface heat and moisture transfer coefficients from sub-zonal model (e). With respect to the Western wall, the figures show that the model is able to predict the surface transfer coefficients in the same order of magnitude compared to CFD, while the relative deviation is approximately 30%. Similarly, the model (e) is able to give a prediction of the surface transfer coefficients in the lower part of the Eastern wall with a relatively small deviation of 30%, while a deviation of factor 3 and more is observed towards the ceiling. An explanation for these deviations might be found in the presence of a recirculation region in the upper right corner. As has been mentioned earlier, the sub-zonal model is not able to predict this recirculation of the air in the corner and this may therefore result in erroneous convective surface transfer coefficients.

5.3.2 Conclusion

The investigations showed that the sub-zonal airflow model is able to give a prediction of the forced convective airflow in a room, provided an appropriate jet model is implemented and an appropriate surface transfer coefficient model is applied. Comparison of the sub-zonal model and CFD showed that the models predicted in general similar flow directions. Differences regarding the size of the recirculation region and the location of the region's centre have been observed. The sub-zonal model clearly has problems with the accurate prediction of the airflow in regions where recirculation takes place. Regarding the prediction of the magnitude of the airflows relatively large discrepancies of factor 2 and more between sub-zonal and CFD models has been observed. Similarly, the sub-zonal model showed to be applicable to give a rough prediction of the global temperature and vapour content distribution in the room with a maximum relative deviation of approximately 10%. However, if local recirculation of the airflow, for example in a corner, is present, the model is not capable of giving an accurate prediction in these regions, while the relative deviation increases up to 25% for the local temperature and 30% for the local vapour content.

Regarding the prediction of the convective surface transfer coefficients, the models based on the flat plate analogy showed to be not applicable. Deviations of the predicted local surface heat and moisture transfer coefficients of factor 2 and more have been observed, when applying these models. Two main problems regarding the models based on the flat plate analogy have been observed: first of all, the models are based on relationships that have been determined for isolated flat plates instead of real building components.

Second, the models require the accurate prediction of the local Reynolds number and air mass flux along the wall. Since the sub-zonal model is not able to predict these numbers accurately, this results automatically in deviations of the convective surface transfer coefficients.

As an alternative to the use of the correlations based on forced convection over a flat plate, The surface transfer coefficient model that is based on the locally applied correlations from Beausoleil-Morrison gave relatively good results for regions where recirculation does not take place, while the relative deviation is approximately 30%. The model cannot be applied in regions where local recirculation of the airflow takes place.

5.4 Steeman CFD Case

A two-dimensional case with simultaneous heat and moisture transfer in a rectangular room with dimensions of 2.5m x 2.5m is analyzed. Figure 47 presents the geometry and the boundary conditions that have been applied for the studied test case.

The boundary conditions are as follows: constant temperature and relative humidity of 20°C, 50%RH, and 30°C, 50%RH, have been applied at the Western and Eastern walls respectively. The floor and ceiling are considered to be adiabatic and impermeable to water vapour. The room is ventilated with a constant air change rate. The inlet with a height of 0.1m is located at the top of the Western wall, while an outlet with a height of 0.2m is situated at the bottom of the Eastern wall..

Results from computational fluid dynamics simulations carried out by Steeman [13], have been used for the investigation of the airflow, heat and moisture flows in the enclosure. Steeman [13] analyzed the airflow in a room under four different flow regimes: dominating forced convection, mixed convection, dominating natural convection, and natural convection. Table 20 presents the scenario's that have been investigated by Steeman [13] and the corresponding air change rates per hour. With respect to the present study, only the results from the dominating natural convection case are analyzed. In buildings, air change rates of respectively 114 h^{-1} and 36 h^{-1} are less common. Therefore, these scenarios are excluded from this investigation. Furthermore, the natural convection case has been excluded, since experimental data obtained from measurements in the MINIBAT test case has been used for the analysis of natural convective airflow in a room (Section 5.2).

For the investigated flow scenario, i.e. dominating natural convection, numerical results of the airflow, temperature, and relative humidity field in the room, as well as the local convective surface transfer coefficients are available. For additional information and details regarding the CFD simulation and validation of the results the reader is referred to [13].

In addition, the air change rate of 11.4 h^{-1} is relatively large and might be less common in buildings. To investigate the airflow distribution and the heat and moisture flows under conditions that are more common in buildings, the test case presented in Figure 47 been simulated with an air change rate of 2 h^{-1}. This scenario can be considered as an additional investigation within the framework of the present study. Numerical results obtained from a CFD simulation have been used for comparison of the sub-zonal models' and surface transfer coefficient models' results.

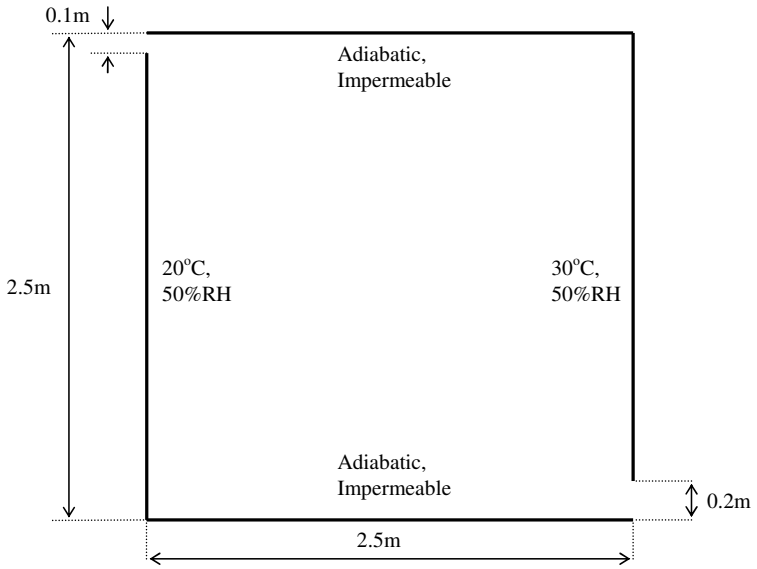

Figure 47: Geometry and boundary conditions for the CFD case [13]

Table 20: Investigated flow scenario's by Steeman [13]

Scenario	1	2	**3***	4
Flow regime	Dominating forced convection	Mixed convection	**Dominating natural convection**	Natural convection
Air change rate [h^{-1}]	114	36	**11 and 2**	0

*only this scenario is analyzed within the present study

5.4.1 Results

The Steeman CFD case has been simulated for two mixed convective airflow regimes in the room: dominating natural convection at an air change rate of 11 h^{-1}, and dominating natural convection at an air change rate of 2 h^{-1}. In a first part, the results for the ventilation rate of 11 h^{-1} are presented. The results obtained for dominating natural convective airflow in the room at an air change rate of 2 h^{-1} are presented in a second part. Results from computational fluid dynamics simulations carried out by Steeman [13], have been used for the investigation of the airflow, heat and moisture flows in the enclosure.

5.4.1.1 Dominating natural convection: ACH 11 h^{-1}

Table 21 presents an overview of the simulated sub-zonal models and computational grids that have been used. Compared to the other cases that have been analyzed, presented in respectively Sections 5.2 and 5.3, the modelling of the indoor environmental conditions using a sub-zonal model is less straightforward. In general, three options are available: the first option is a standard sub-zonal model which assumes that the natural convection in the room is dominating the airflow field (model (a)). This means that the sub-zonal model includes a thermal boundary layer model to describe the buoyancy driven airflow near the walls. Moreover, sub-zonal model (b) is based on a similar assumption on a dense grid. Second, another option is a standard sub-zonal model assuming that the airflow in the room is dominated by forced convection (model (b)). This option consists of a sub-zonal airflow model with a specific airflow model describing the jet near the ceiling. A third option consists of a combination of the previous two options which means that a

standard sub-zonal airflow model with both a thermal boundary layer model and specific airflow model describing the jet near the ceiling are applied (model (d)).

The investigations showed that natural convection plays an important role in the room. Therefore only the options where natural convection is taken into account, respectively models (a), (b) and (d), are further investigated, while the analysis of the results obtained model (c) is omitted. Moreover, for both options different assumptions have been applied: When only applying a thermal boundary layer model (model (a) and (b)), it is assumed that natural convection in the room is dominating the forced convective airflow. The thermal boundary layer model describes the airflow due to the buoyancy effects that take place near the walls. The model is implemented as has been described in (Chapter 4). Moreover, fresh air is supplied along the ceiling (Section 5.2) and it is assumed that the momentum of the airflow is relatively small, i.e. the supply airflow is diffuse. Because the momentum of the fresh supplied fresh air is relatively small, no specific model has been implemented to describe this airflow. In case of applying the jet model, that describes the airflow along the ceiling, it is assumed that the ceiling jet dominates the airflow in the room. While natural convection is still present in the room, a thermal boundary layer model has been applied as well in order to model the influence of buoyancy.

As already has been mentioned in the methodology (Chapter 4) a grid sensitivity study has been carried out for each case, which ensures that the obtained results are grid independent. The results from the three different sub-zonal airflow models (Table 21) are compared to the CFD results [13].

Table 21: Sub-zonal airflow models

Model	Airflow model	STC	Grid (x . y)
(a)	Standard sub-zonal airflow model and thermal boundary layer model	CFD	8 x 10
(b)	Standard sub-zonal airflow model and thermal boundary layer model	CFD	16 x 20
(c)	Standard sub-zonal airflow model and jet model	CFD	10 x 20
(d)	Standard sub-zonal airflow model including a thermal boundary layer model and a jet model	CFD	10 x 20

Airflow

The predicted airflow field in the room resulting from sub-zonal models (a) and (d), respectively the sub-zonal model including only a thermal boundary layer model, and the model including both a thermal boundary layer model and a jet model, and the results obtained from the CFD models have been compared. A densification of the computational grid that has been applied in sub-zonal model (a) by factor two has been applied in model (b). The densification did not change the simulation results significantly. The results obtained from model (a) are not presented explicitly.

Figure 49 presents the streamlines of the air mass flow predicted by the sub-zonal models in the room. Both sub-zonal models give a different prediction of the airflow pattern in the room. While sub-zonal model (d) predicts a relatively large influence from the jet, which results from the specific jet model that was implemented, is the influence of the supplied air predicted by model (b) limited. A comparison with the CFD results (Figure 48) showed that indeed the influence of the supplied air on the airflow in the room is limited and natural convection along the walls of the room is dominating the airflow pattern. Based on the predicted airflow pattern, the model (d) with the jet model seems not to be capable of predicting the airflow pattern in the room, since the influence of the jet is overestimated.

A qualitative comparison (based on Figure 48 and Figure 49) between the airflow fields predicted by the sub-zonal models and the CFD results illustrated that sub-zonal model (b) is best capable of predicting the airflow in the room. Model (b) predicts similar flow directions along the Western and Eastern walls compared to CFD. However, in the centre of the room deviations are observed. The sub-zonal model (b)

predicts direct streamlines from the inlet to the outlet of the room, while CFD predicts a strong circulation due to natural convection. The prediction of the direct streamlines is caused by the characteristics of the sub-zonal model, i.e. the model predicts the airflow pattern based on the pressure difference between inlet and outlet. Moreover, this pressure difference is dominating the airflow pattern in the room, while the pressure difference imposed by the thermal boundary layer model is relatively small. In principle, the airflow between the inlet and outlet is dominating the natural convection.

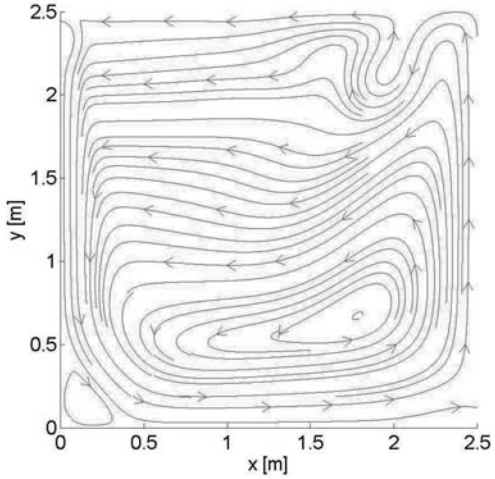

Figure 48: mass flow streamlines [kg s^{-1}] resulting from the CFD simulation.

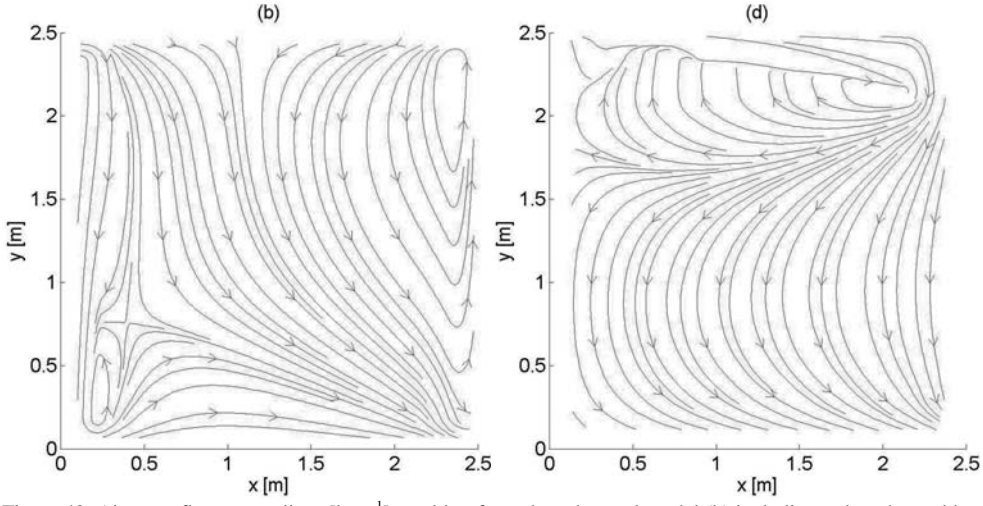

Figure 49: Air mass flow streamlines [kg s^{-1}] resulting from the sub-zonal model (b) including only a thermal boundary layer model, and model (d) including both a thermal boundary layer model and a jet model.

A quantitative comparison of the air mass fluxes between sub-zonal model (a) and CFD shows that the magnitudes of the flows vary significantly. Analysis of the regions along the walls, where the flow directions are similar, illustrated that differences between a factor two and three are observed. It is difficult to

get a general impression about the accuracy of the sub-zonal model based on

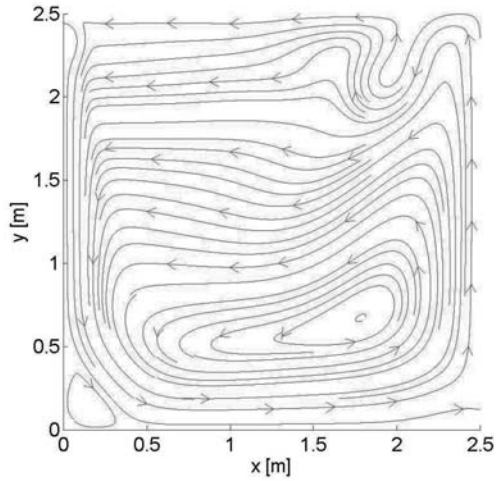

Figure 48: mass flow streamlines [kg s^{-1}] resulting from the CFD simulation.

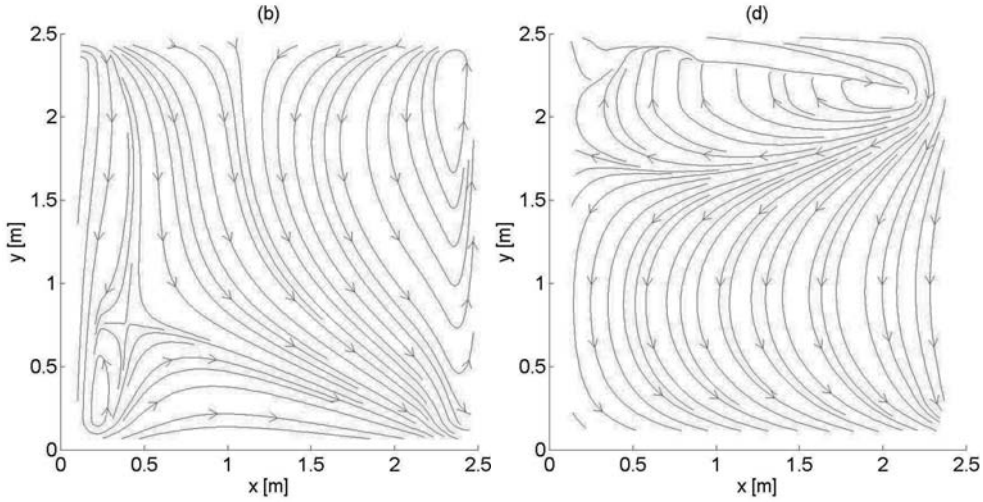

Figure 49. Moreover, the quality of the predictions regarding the airflow pattern and the corresponding air mass fluxes may have a significant influence on the prediction of the local temperature and vapour content in the room as well as the convective surface transfer coefficients. The analysis proceeds with the comparison of the local indoor environmental conditions in the room.

Temperature and vapour content field

Figure 50 shows the temperature and vapour content distribution in the room predicted by the CFD model. Figure 51 presents the temperature field in the room predicted by sub-zonal models. Regarding the results obtained from the sub-zonal models, only results from the models (b) and (d) are shown. The corresponding vapour contents predicted by the sub-zonal models are presented in Figure 52. Moreover, a comparison of the local temperature and vapour content (mass fraction, X [g kg^{-1}]) distribution in the centre of the room (x=1.25m) and at 0.125m from the walls, at respectively x=0.125m, and 2.375m, are presented in Figure 53.

Comparing the results from the sub-zonal model with the experimental and numerical results from CFD, the following observations are presented:

- *Global temperature and vapour content distribution*: The CFD model (Figure 50) predicts the relatively cold air at the inlet to descend along the Western wall while the air is warmed up until it reaches the floor of the room. From the floor, the air is heated along the Eastern wall until the airflow reaches the ceiling. Moreover, the CFD results show that a stratified temperature and vapour content distribution is observed in the room. In Figure 51, the temperature distributions obtained from sub-zonal airflow models (b) and (d) are presented. Similarly, Figure 52 shows the predicted vapour content distributions. The figures show that both sub-zonal models are not capable of predicting the stratification of the temperature and vapour content in the room.
  Regarding model (d), the sub-zonal model predicts a more or less uniform temperature and vapour content distribution in the room. The predicted patterns are dominated by the forced convective contribution due to the implementation of the jet model. With respect to model (b), the sub-zonal model gives a prediction that is better capable of predicting the natural convective influences, while a relatively cold region is observed in the upper left part of the room, and relatively cold and warmer temperatures are observed respectively near the floor and the ceiling. However, still relatively large discrepancies are observed. The analysis proceeds with the quantification of these discrepancies, focussing on prediction of the local quantities in the room.

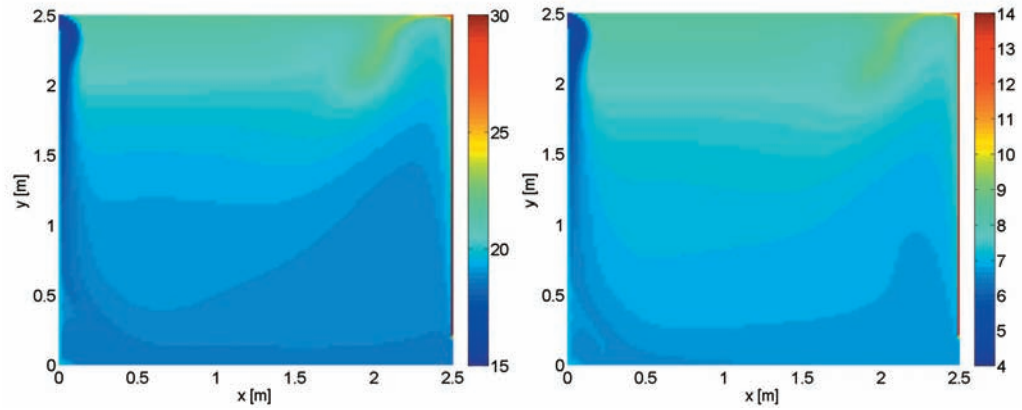

Figure 50: Temperature (left) and vapour content (right) distribution predicted by CFD.

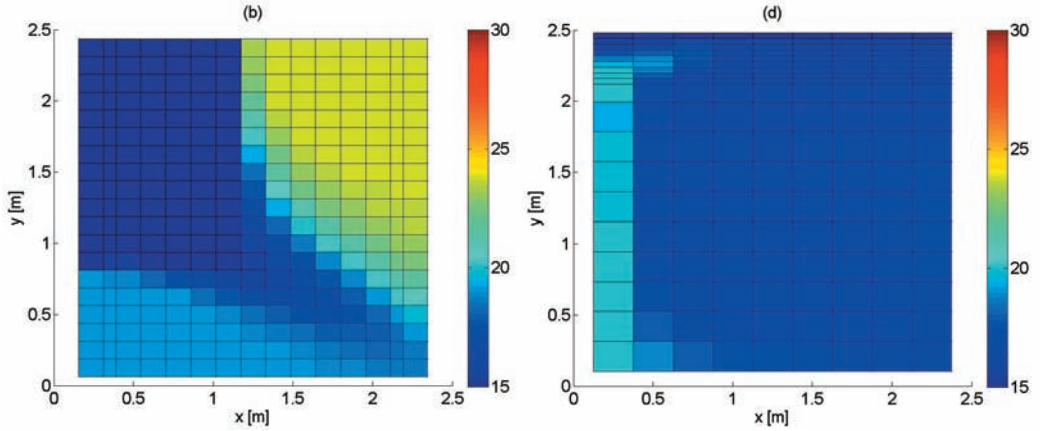

Figure 51: Temperature distribution predicted by sub-zonal model (b) (left), and model (d) (right).

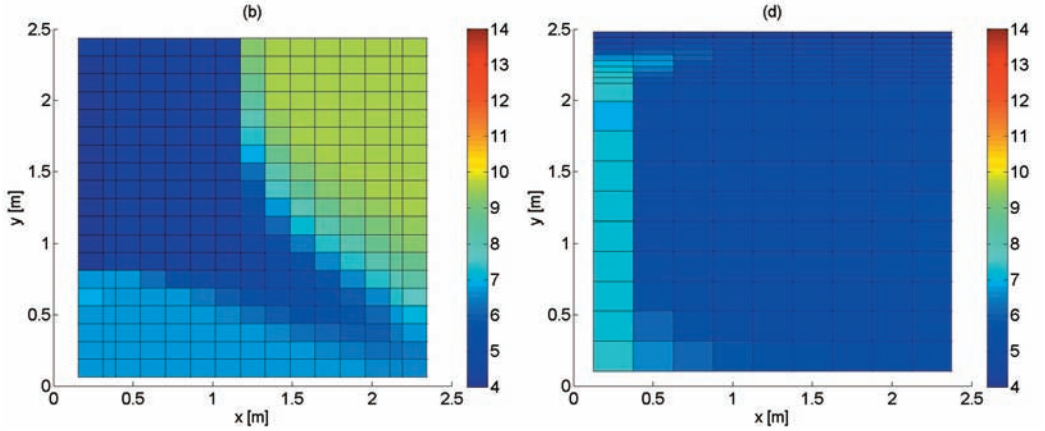

Figure 52: Vapour content distribution predicted by sub-zonal model (b) (left), and model (d) (right).

- *Local quantities*: Figure 53 shows the local temperature and vapour content (mass fraction, Y [g kg^{-1}]) distribution in the centre of the room (x=1.25m) and at 0.125m from the walls, at respectively x=0.125m, and 2.375m. With respect to the predictions in the centre of the room, the CFD models predicts stratified distributions with relatively low temperatures and vapour contents near the floor, while the temperature and vapour content increases towards the ceiling. Sub-zonal model (d) predicts a relatively uniform temperature of 16°C and a vapour content of 5 g kg^{-1}. Moreover, sub-zonal models (a) and (b) give a temperature and vapour content profile in the centre of the room that does not resemble the stratified profile predicted by CFD. Focussing on the distributions close to the walls, both models are not able to give an acceptable prediction of the local quantities. Deviations between 20% and 30% for the local temperature near the walls and between 30% and 40% for the local vapour content near the walls are observed.
- *Grid densification*: Given the similarity in the predicted temperature field by models (a) and (b), Figure 51, Figure 52and Figure 53 showed that a densification of the grid did not influence the simulation results significantly. Both the global temperature and vapour content distributions as well

as the local patterns did not change significantly when applying a densification of the grid with a factor 2.

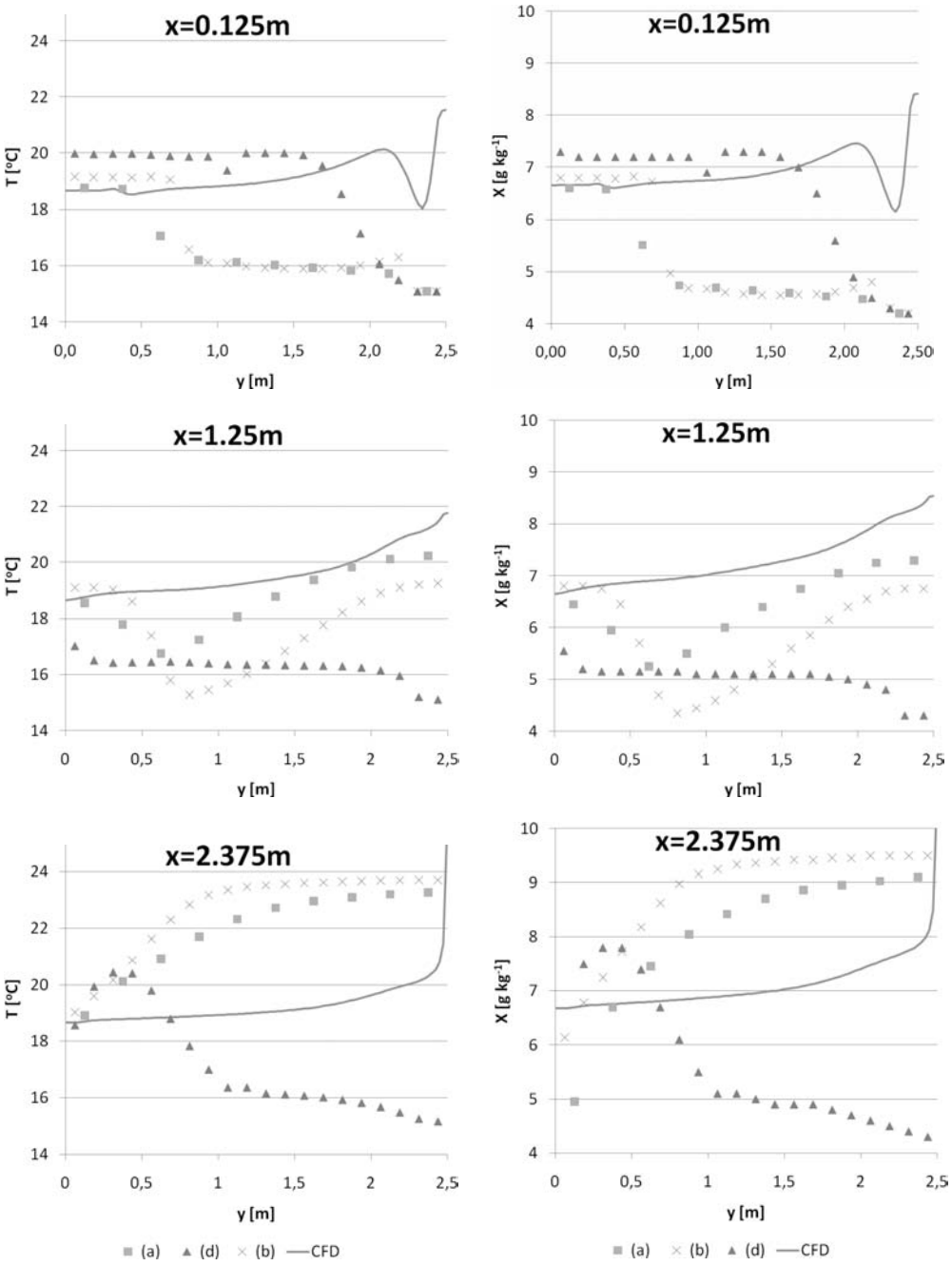

Figure 53: Temperature and vapour content (mass fraction, X [g kg^{-1}]) distribution in the centre of the room (x=1.25m) and at 0.125m from the walls, at respectively x=0.125m and 2.375m.

The comparison of the results obtained from the sub-zonal models with the CFD results showed that compared to the other cases presented in Section 5.2and5.3, the sub-zonal airflow model has relatively large problems regarding the prediction of the indoor environmental conditions in the room. Relatively large deviations with respect to both the global and local conditions in the room have been observed. Three sub-zonal airflow models have been studied. A sub-zonal model including a thermal boundary layer model gave the best performance. However, the sub-zonal model predicted the local temperature and vapour content in the room with a maximum relative deviation between approximately 20% and 40%, while the models were not able to predict the stratified temperature distribution predicted by CFD. Moreover, completely different distributions of the temperature and vapour content resulting from the sub-zonal models and CFD were shown. Compared to the MINIBAT case and the Annex 20 Benchmark case the results of the sub-zonal airflow model were poor. First of all, the analysis focuses on these performance problems. Second, the literature related to these problems is discussed and possible limitations and solutions are mentioned.

The main problem with respect to the modelling of the mixed convective airflow in a room is the ratio between natural and forced convection. For the modelling of natural convection, a thermal boundary layer model is applicable, while for the modelling of forced convection experimental jet models are suitable. However, in this case study, the influence of forced convection on the airflow field in the room is relatively limited, in such a way, that the experimental jet model is inapplicable. Moreover, the supplied air is modelled as a diffuse inlet, assuming that the momentum of the inlet air is dissipated in the sub-zone that is assigned to the inlet. The sub-zonal model only includes a thermal boundary layer model, which describes the natural convective airflow along the wall. Though, since the model is applicable for natural convection along a wall, the model might not be applicable in this case. The results from the sub-zonal model are determined by the pressure balance imposed by the pressure difference between the inlet and the outlet of the room, and the pressure difference imposed by the thermal boundary layer model. In this mixed convection case with an air change rate of 11 h^{-1}, the pressure difference between inlet and outlet is dominating the airflow in the room, resulting in direct streamlines between the inlet and the outlet, while the influence of natural convection is under-estimated.

A review of the literature showed that most authors used sub-zonal airflow models for the modelling of the indoor environmental condition in cases of natural convection [44] [46] or mixed convection, while forced convection was dominant [37] [38] [43][46]. In general, the authors reported that sub-zonal models give a satisfactory estimate of the indoor environmental conditions. The investigations presented in this paragraph showed that the modeling of mixed convective airflow in a room, where natural convection is dominant, lies outside the application domain of the sub-zonal airflow models. The sub-zonal airflow model seems not to be able to calculate the indoor environmental conditions correctly when taking into account the pressure difference between inlet and outlet and the pressure difference caused by the thermal boundary layer model. Furthermore, the thermal boundary layer model might only be applicable for natural convection in an enclosure.

In this section, it was illustrated that the mixed convection case study might lie outside the application domain of current sub-zonal modeling. However, improvements of the results might be obtained by tuning of the thermal boundary layer model for this specific case, for example by using experimental data or numerical results. On the other hand, tuning of the model may limit the general application of the sub-zonal model. To complete the analysis, the investigations proceeds with the study of the surface transfer coefficient models with respect to the prediction of the local convective surface transfer coefficients in the room.

Convective surface transfer coefficients

The analysis showed that the sub-zonal model with a thermal boundary layer model implemented is capable of giving a prediction of the temperature and vapour content distribution in a room where natural convection is dominating forced convection. However the quality of the predictions with respect to the indoor environmental conditions is questionable, the results from the sub-zonal airflow model are applied for the prediction of the local convective surface transfer coefficients. In such a way, it is investigated how accurate the input, i.e. the results from the sub-zonal airflow model, should be to obtain a reliable prediction of the convective surface transfer coefficients in the room.

The sub-zonal model (Table 21: model (b)) with thermal boundary layer model has been used to model the mixed convective airflow in the room. The results obtained from the sub-zonal airflow model have been used as input data for the surface transfer coefficient models. The predicted convective surface heat and moisture transfer coefficients (CHTC and SMTC) along the walls resulting from the surface transfer coefficient models and the CFD model have been compared. Table 22 presents an overview of the simulated surface transfer coefficient models and computational grids that have been used.

Table 22: Surface transfer coefficient models

MODEL	STC	Grid (x . y)
(ref)	Beausoleil-Morrison [9]	16 x 20
(a)	Turner *et al.* [87]	16 x 20
(b)	Bohn *et al.* [88]	16 x 20
(c)	1Flat plate (Churchill) [50]	6 x 9
(d)	2 Flat plate (Rose) [50]	6 x 9
(e)	3 Flat plate (Churchill and Ozoe) [60]	6 x 9
(f)	Local Beausoleil-Morrison	6 x 9

The local convective surface heat and moisture transfer coefficients resulting from the different surface transfer coefficient models (Table 22) and with the values obtained from the CFD simulation are compared. It should be mentioned that the relatively large deviations, between 20% and 40%, with respect to both the global and local conditions in the room, that have been predicted by the sub-zonal airflow model might lead to deviations in the predicted convective STC's. These deviations might not necessarily be caused by the surface transfer coefficient model itself. Therefore, a thorough evaluation of the applied surface transfer coefficient models may not be possible at this point.

Figure 54 and Figure 55 present the convective surface heat and moisture transfer coefficients along the Western and Eastern walls in the room. Figure 54 shows that CFD predicts the convective surface heat transfer coefficient along the Western wall to be approximately factor 50 times larger compared to the CHTC resulting from the sub-zonal model. Since the deviation is present for all sub-zonal models' predictions, the deviations may be caused by the relatively poor prediction of the indoor environmental conditions by the sub-zonal model. Similar deviations of the SMTC are presented in Figure 55.

In addition, one remark should be made here. Regarding the predicted average convective surface heat transfer coefficients based on the relationships from Beausoleil-Morrison [9], these relationships result in an under prediction of the average CHTC of the Western wall. When applying the relationships [9] combined with the average conditions in the room obtained from CFD, the convective surface heat transfer coefficient for natural convection is approximately 2.2 W $m^{-2}K^{-1}$, while the average CHTC for forced convection is approximately 1.2 W $m^{-2}K^{-1}$. This results in a total average convective surface heat transfer coefficient of 2.31 W $m^{-2}K^{-1}$ for the Western wall. However, the average convective surface heat transfer coefficient calculated by CFD is approximately 15 W $m^{-2}K^{-1}$. The relationships from Beausoleil-Morrison [9] may not be applicable for the prediction of the average convective surface heat transfer coefficient of the Western wall.

Figure 54 also presents the convective surface heat transfer coefficient of the Eastern wall. Compared to the predicted convective surface heat transfer coefficients for the Western walls, the predicted coefficients for the Eastern walls lie in the same order of magnitude. However, considerable differences are observed. The figure shows that the model based on the flat plate relationship obtained by Churchill and Ozoe [60], model (e), is not capable of predicting the convective surface heat transfer coefficient along the wall. The model gives an under-prediction between a factor 2 and 10. The flat plate based correlations reported by Churchill [50] (model (c)), and Rose [50] (model (d)) gave similar deviations with respect to the predicted CHTC's for the Eastern wall. (The results from these models are not presented in Figure 54 and Figure 55).

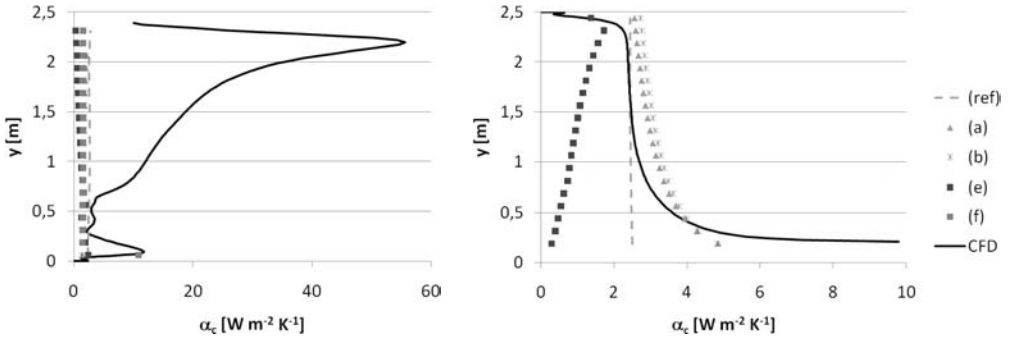

Figure 54: Convective surface heat transfer coefficient (α_c [W m^{-2} K^{-1}]) for the Western wall (left) and the Eastern wall (right).

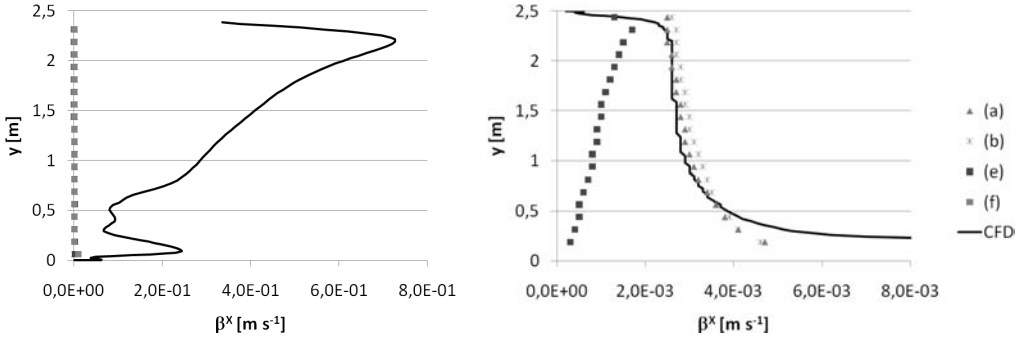

Figure 55: Convective surface moisture transfer coefficient (SMTC) for the Western wall (left) and the Eastern wall (right).

The convective surface transfer coefficients predicted by models (a) and (b), based on respectively Turner *et al* [87], and Bohn *et al*. [88] give the best agreement. While both relationships have been determined for natural convection in an enclosure, the relationships seem to be applicable for the prediction of the local convective surface heat transfer coefficient along the Eastern wall. The maximum relative deviation of the convective surface transfer coefficient based on Turner *et al* [87] is approximately 20%, while the maximum relative deviation based on the relationship from Bohn *et al*. [88] is approximately 25%. The deviation between the results predicted based on Turner *et al* [87], and Bohn *et al*. [88] increases towards the floor. This may be influenced by the outlet of the room which is located near the floor.

The applicability of the models based on natural convection in an enclosure may demonstrate that natural convection is dominating the forced convective heat transfer along the wall. The Richardson number (Eq. (71)) which describes the ratio between buoyancy and inertial forces is analyzed. Typically, the natural convection is negligible when Ri < 0.1, forced convection is negligible when Ri > 10.

$$Ri = \frac{Gr}{\mathrm{Re}^2} = \frac{g\beta(T_s - T_{ref})L}{V^2} \tag{71}$$

where Gr is the Grashof number, describing the ratio of the buoyancy to viscous force acting on a fluid, Re is the Reynolds number, a measure of the ratio of inertial forces to viscous forces, while g is the gravitational acceleration [m s^{-2}], β the thermal expansion coefficient [K^{-1}], T_s the surface temperature [K], T_{ref} the reference temperature [K], L is the characteristic length [m], and V is the velocity [m s^{-1}].

Calculation of the Richardson number in the room showed that the Richardson number is equal to 10, illustrating that natural convection is dominating the forced convection in the room. However, the CFD results also show that the local velocity of the airflow near the Western wall is relatively large, resulting in locally dominating forced convection.

In summary, a comparison of the results obtained from the sub-zonal models with the CFD results showed that the sub-zonal airflow model has problems with respect to the accurate prediction of the indoor environmental conditions in the room. Relatively large deviations regarding both the global and local conditions in the room have been observed. The sub-zonal model which was best capable of predicting the indoor environmental conditions included a thermal boundary layer model to model the natural convective airflow along the walls. No specific model was added to account for forced convection. The analysis of the case study showed that the ratio between natural and forced convection in the room is an important issue when modelling the indoor environmental conditions in the room. Similarly, this ratio is important for the modelling of the local convective surface transfer coefficients in the room. It was possible to give a relatively accurate prediction of the local convective surface transfer coefficients along the Eastern wall with a maximum relative deviation of 20% using relationships based on natural convective airflow in enclosures. However, with respect to the Western wall, where forced convective airflow was dominating, it was not feasible to predict the local surface transfer coefficients, while deviations between factor 20 and 50 have been observed.

5.4.1.2 Dominating natural convection: ACH 2 h^{-1}

As mentioned previously, the Steeman CFD case has also been simulated for dominating natural convective airflow in the room at a constant air change rate of 2 h^{-1}. Table 23 presents an overview of the simulated sub-zonal models and computational grids that have been used. In Section 5.4.1.1, it was illustrated that three options for the modelling of the indoor environmental conditions using a sub-zonal model are available. For this case and under these indoor environmental conditions, similar options as presented in Section 5.4.1.1 have been investigated. For additional details, related information and assumptions with respect to the models presented in Table 23 the reader is referred to Section 5.4.1.1. Furthermore, a grid sensitivity study has been carried out for each case, which ensures that the obtained results are grid independent.

Table 23: Sub-zonal airflow models

Model	Airflow model	STC	Grid (x . y)
(a)	Standard sub-zonal airflow model and thermal boundary layer model	CFD	8 x 10
(b)	Standard sub-zonal airflow model and thermal boundary layer model	CFD	16 x 20
(c)	Standard sub-zonal airflow model and jet model	CFD	10 x 20
(d)	Standard sub-zonal airflow model including a thermal boundary layer model and a jet model	CFD	10 x 20

Airflow

The predicted airflow field in the room resulting from sub-zonal models (b) and (d), respectively the sub-zonal model including only a thermal boundary layer model, and the model including both a thermal boundary layer model and a jet model, and the results obtained from the CFD models have been compared. A densification of the computational grid that has been applied in sub-zonal model (a) by factor two has been applied in model (b). The densification did not change the simulation results significantly. The results obtained from model (a) are not presented explicitly.

Figure 57 presents the streamlines of the air mass flow predicted by the sub-zonal models in the room. Both sub-zonal models give a different prediction of the airflow pattern in the room. While sub-zonal model (d) predicts a relatively large influence from the jet, which results from the specific jet model that was implemented, is the influence of the supplied air predicted by model (b) limited. A comparison with the CFD results (Figure 56) showed that indeed the influence of the supplied air on the airflow in the room is limited and natural convection along the walls of the room is dominating the airflow pattern. Based on the predicted airflow pattern, the model (d) with the jet model seems not to be capable of predicting the airflow pattern in the room, since the influence of the jet is overestimated.

Comparing Figure 57 and Figure 56, sub-zonal model (b) is best capable of predicting the airflow in the room. Model (b) predicts similar flow directions along the Eastern walls compared to CFD. However, along the Western wall, the sub-zonal model predicts a local recirculation in the corner, while this recirculation is not predicted by CFD. Deviations are also observed in the centre of the room. Compared to the scenario presented in Section 5.4.1.1, the sub-zonal model (b) similarly predicts direct streamlines from the inlet to the outlet of the room, while CFD predicts a strong circulation of the airflow due to natural convection. As already has been discussed in Section 5.4.1.1, the prediction of the direct streamlines is caused by the characteristics of the sub-zonal model, since the model predicts the airflow pattern based on the pressure difference between inlet and outlet. Quantitatively, the air mass fluxes between sub-zonal model (a) and CFD showed that the magnitudes of the flows vary significantly. Along the walls, differences between a factor two and three have been observed. The quality of the predictions regarding the airflow pattern and the corresponding air mass fluxes may have a significant influence on the prediction of the local temperature and vapour content in the room as well as the convective surface transfer coefficients. The analysis proceeds with the comparison of the local indoor environmental conditions in the room.

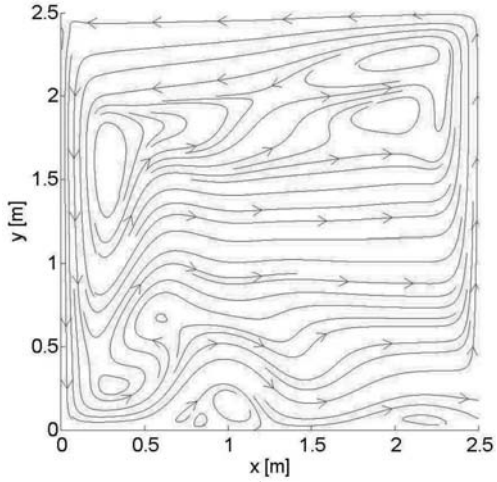

Figure 56: mass flow streamlines [kg s^{-1}] resulting from the CFD simulation.

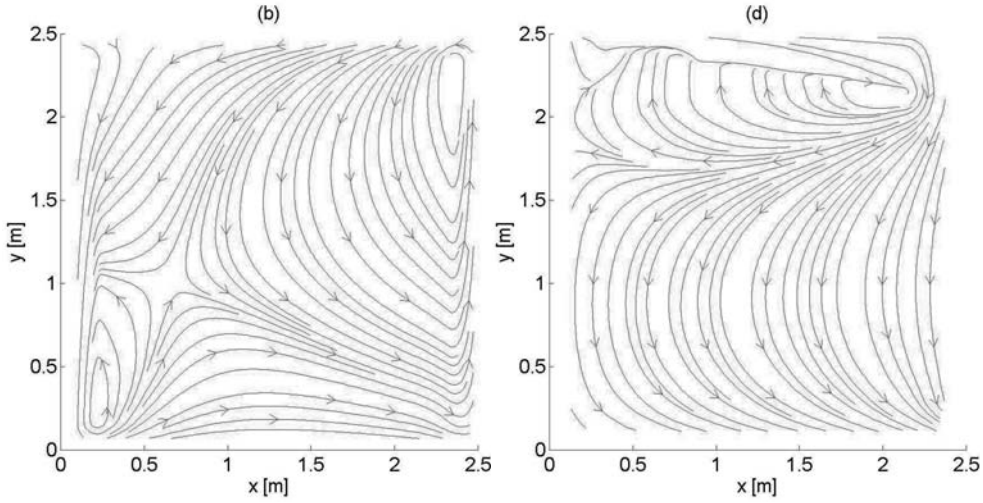

Figure 57: Air mass flow streamlines [kg s^{-1}] resulting from the sub-zonal model (b) including only a thermal boundary layer model, and model (d) including both a thermal boundary layer model and a jet model.

Temperature and vapour content field

Figure 58 shows the temperature and vapour content distribution in the room predicted by the CFD model. Figure 59 presents the temperature field in the room predicted by sub-zonal models. Regarding the results obtained from the sub-zonal models, only results from the models (b) and (d) are shown. The corresponding vapour contents predicted by the sub-zonal models are presented in Figure 60. Moreover, a comparison of the local temperature and vapour content (mass fraction, X [g kg^{-1}]) distribution in the centre

of the room (x=1.25m) and at 0.125m from the walls, at respectively x=0.125m, and 2.375m, are presented in Figure 61.

Comparing the results from the sub-zonal model with the experimental and numerical results from CFD, the following observations are presented:

- *Global temperature and vapour content distribution*: The CFD model (Figure 58) predicts the relatively cold air at the inlet to descend along the Western wall while the air is warmed up until it reaches the floor of the room. From the floor, the air is heated along the Eastern wall until the airflow reaches the ceiling. Moreover, the CFD results show a stratified temperature and vapour content distribution in the room. The stratification indicates that natural convection in the room is dominating the forced convection. In Figure 59, the temperature distributions obtained from sub-zonal airflow models (b) and (d) are presented. Similarly, Figure 60 shows the predicted vapour content distributions. The figures show that only sub-zonal model (b) is capable of predicting the stratification of the temperature and vapour content in the room.
  Regarding model (d), the sub-zonal model predicts relatively large temperatures and vapour contents in the centre of the recirculation region, while the temperature and vapour content reduces towards the Western wall, floor and the ceiling. The predicted patterns are dominated by the forced convective contribution due to the implementation of the jet model. With respect to model (b), the sub-zonal model gives a prediction that is better capable of predicting the natural convective influences, while a relatively cold region is observed in the lower part of the room, and a warmer region is observed near the ceiling.

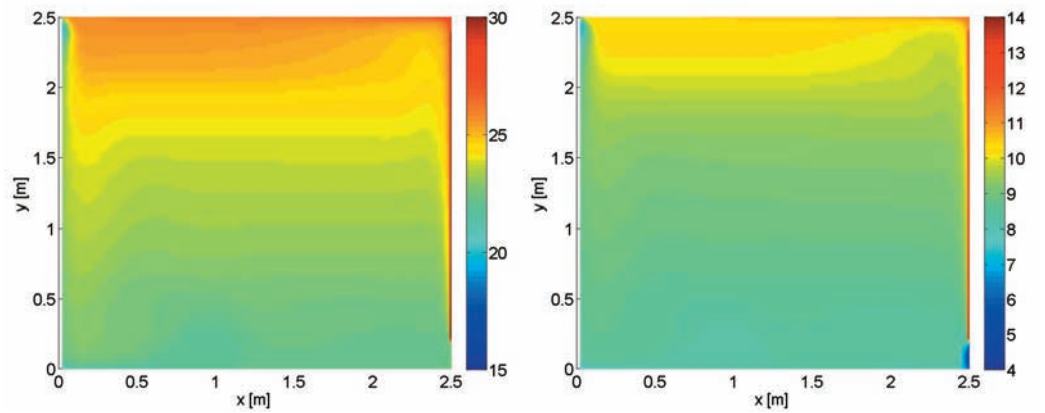

Figure 58: Temperature (left) and vapour content (right) distribution predicted by CFD.

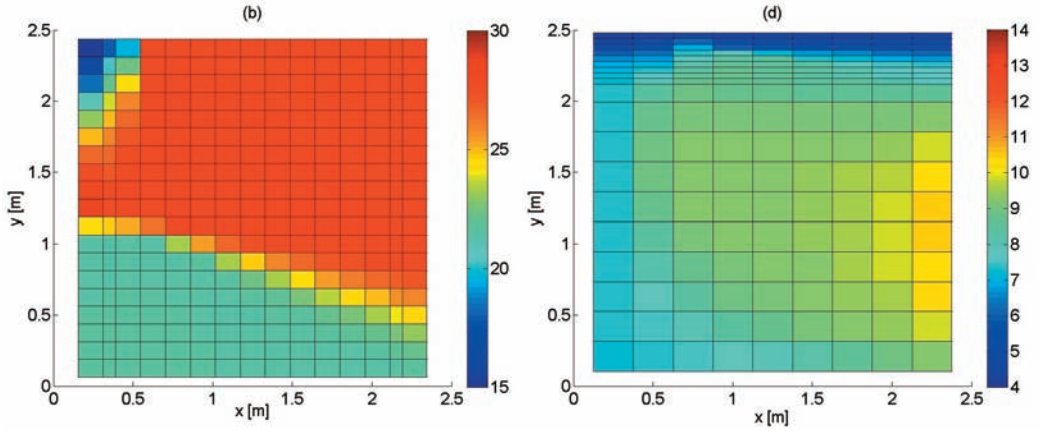

Figure 59: Temperature distribution predicted by sub-zonal model (b) (left), and model (d) (right).

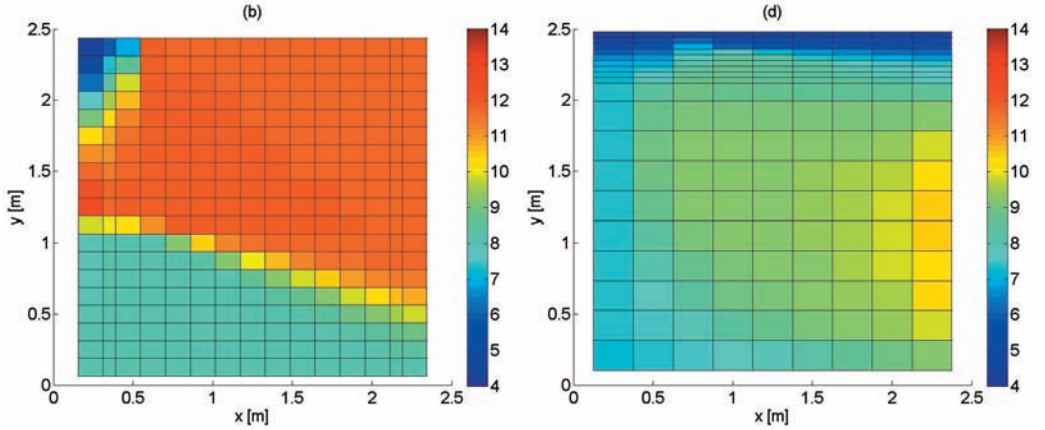

Figure 60: Vapour content distribution predicted by sub-zonal model (b) (left), and model (d) (right).

- *Local quantities*: Figure 61 shows the local temperature and vapour content (mass fraction, Y [g kg^{-1}]) distribution in the centre of the room (x=1.25m) and at 0.125m from the walls, at respectively x=0.125m, and 2.375m. With respect to the predictions in the centre of the room, the CFD models predicts stratified distributions with relatively low temperatures and vapour contents near the floor, while the temperature and vapour content increases towards the ceiling. Sub-zonal model (d) predicts a relatively large temperature of approximately 22°C, and a vapour content of 9 g/kg near the floor, while the temperature decreases towards the ceiling. The deviations are mainly caused by the implementation of the jet model, and the over-prediction of forced convection in the room. Sub-zonal model (b) gives a stratified temperature and vapour content profile in the centre of the room. However, the profiles do not resemble the predictions by CFD, since a large gradient is present at approximately 0.75m from the floor. Focussing on the distributions close to the walls, both models are not able to give an acceptable prediction of the local quantities. Relative deviations up to 40% for the local temperature near the walls and up to 50% for the local vapour content near the walls have been observed.

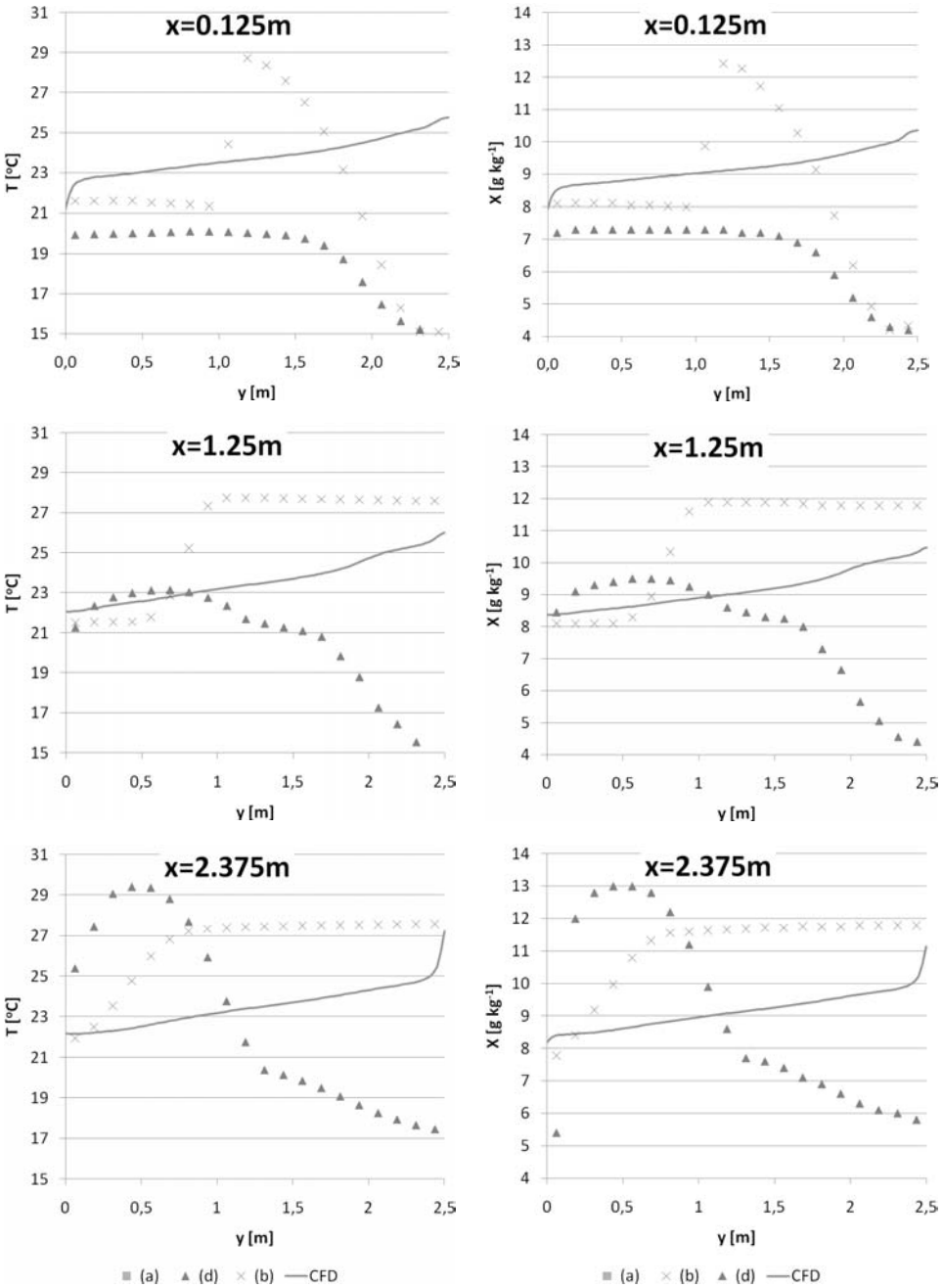

Figure 61: Temperature and vapour content (mass fraction, X [g kg^{-1}]) distribution in the centre of the room (x=1.25m) and at 0.125m from the walls, at respectively x=0.125m and 2.375m.

The comparison of the results obtained from the sub-zonal models with the CFD results showed that compared to the scenario with an air change rate of 11 h^{-1} (Section 5.4.1.1) , the sub-zonal airflow model has problems regarding the prediction of the indoor environmental conditions in the room. Deviations up to 40% with respect to both the global and local conditions in the room have been observed. Three sub-zonal airflow models have been studied. A sub-zonal model including a thermal boundary layer model gave the best performance. However, the sub-zonal model predicted the local temperature and vapour content in the room with a maximum relative deviation between approximately 30% and 50%. As already has been illustrated in Section 5.4.1.1, the main problem with respect to the modelling of the mixed convective airflow in a room is the ratio between natural and forced convection. Application of sub-zonal airflow modelling for mixed convection might lie outside the application domain. The investigations proceeds with the study of the surface transfer coefficient models with respect to the prediction of the local convective surface transfer coefficients in the room.

Convective surface transfer coefficients

The analysis showed that the sub-zonal model with a thermal boundary layer model implemented is capable of giving a prediction of the temperature and vapour content distribution in a room where natural convection is dominating forced convection. However the quality of the predictions with respect to the indoor environmental conditions is questionable, the results from the sub-zonal airflow model are applied for the prediction of the local convective surface transfer coefficients. In such a way, it is investigated how accurate the input, i.e. the results from the sub-zonal airflow model, should be to obtain a reliable prediction of the convective surface transfer coefficients in the room.

The sub-zonal model (Table 23: model (b)) with thermal boundary layer model has been used to model the mixed convective airflow in the room. The results obtained from the sub-zonal airflow model have been used as input data for the surface transfer coefficient models. The predicted convective surface heat and moisture transfer coefficients (CHTC and SMTC) along the walls resulting from the surface transfer coefficient models and the CFD model have been compared. Table 24 presents an overview of the simulated surface transfer coefficient models and computational grids that have been used.

Table 24: Surface transfer coefficient models

MODEL	STC	Grid (x . y)
(ref)	Beausoleil-Morrison [9]	16 x 20
(a)	Turner *et al.* [87]	16 x 20
(b)	Bohn *et al.* [88]	16 x 20
(c)	1Flat plate (Churchill) [50]	6 x 9
(d)	2 Flat plate (Rose) [50]	6 x 9
(e)	3 Flat plate (Churchill and Ozoe) [60]	6 x 9
(f)	Local Beausoleil-Morrison	6 x 9

The local convective surface heat and moisture transfer coefficients resulting from the different surface transfer coefficient models (Table 24) and with the values obtained from the CFD simulation are compared. It should be mentioned that the relatively large deviations, between 30% and 50%, with respect to both the global and local conditions in the room, that have been predicted by the sub-zonal airflow model might lead to deviations in the predicted convective STC's. These deviations might not necessarily be caused by the surface transfer coefficient model itself. Therefore, a thorough evaluation of the applied surface transfer coefficient models may not be possible at this point.

Figure 62 and Figure 63 present the convective surface heat and moisture transfer coefficients along the Western and Eastern walls in the room. Figure 62 shows that CFD predicts the convective surface heat transfer coefficient along the Western wall to be approximately factor 2 to 3 times larger compared to the CHTC resulting from the sub-zonal models. Regarding the predicted average convective surface heat transfer coefficients based on the relationships from Beausoleil-Morrison [9], these relationships result in an under prediction of the average CHTC of the Western wall. When applying the relationships [9] combined with the average conditions in the room obtained from CFD, the convective surface heat transfer coefficient for natural convection is approximately 1.9 W $m^{-2}K^{-1}$, while the average CHTC for forced convection is

approximately 0.35 W $m^{-2}K^{-1}$. Applying the appropriate correlations [9], this results in a total average convective surface heat transfer coefficient of 1.9 W $m^{-2}K^{-1}$ for the Western wall. However, the average convective surface heat transfer coefficient calculated by CFD is approximately 4.3 W $m^{-2}K^{-1}$. The relationships from Beausoleil-Morrison [9] may not be applicable for the prediction of the average convective surface heat transfer coefficient of the Western wall.

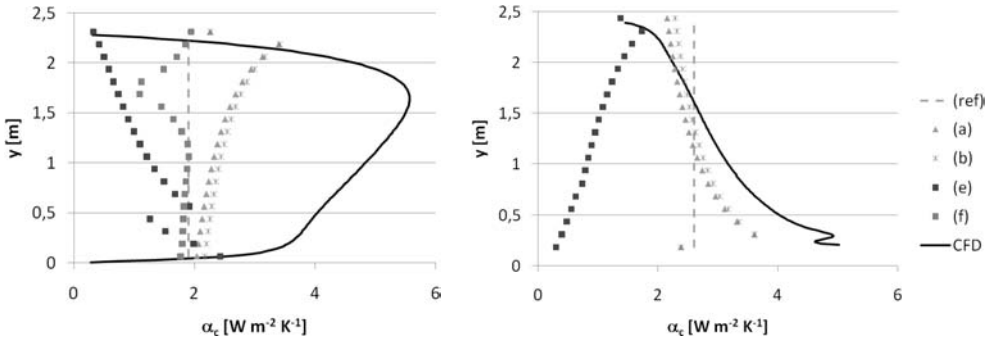

Figure 62: Convective surface heat transfer coefficient (α_c [W m^{-2} K^{-1}]) for the Western wall (left) and the Eastern wall (right).

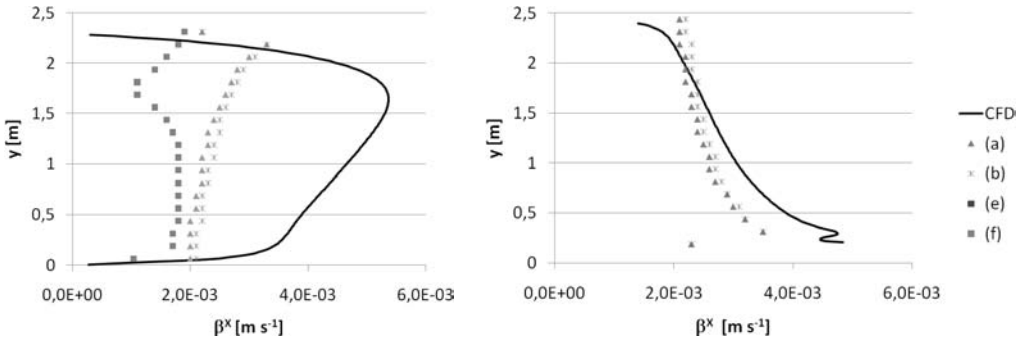

Figure 63: Convective surface moisture transfer coefficient (β^X [m s^{-1}]) for the Western wall (left) and the Eastern wall (right).

Figure 62 also presents the convective surface heat transfer coefficient of the Eastern wall. Compared to the predicted convective surface heat transfer coefficients for the Western walls, the predicted coefficients for the Eastern walls lie in the same order of magnitude. However, considerable differences are observed. The figure shows that the model based on the flat plate relationship obtained by Churchill and Ozoe [60], model (e), is not capable of predicting the convective surface heat transfer coefficient along the wall. The model gives an under-prediction between a factor 2 and 10. The flat plate based correlations reported by Churchill [50] (model (c)), and Rose [50] (model (d)) gave similar deviations with respect to the predicted CHTC's for the Eastern wall. (The results from these models are not presented).

The convective surface transfer coefficients predicted by models (a) and (b), based on respectively Turner *et al* [87], and Bohn *et al*. [88] give the best agreement. While both relationships have been determined for natural convection in an enclosure, the relationships seem to be applicable for the prediction of the local convective surface heat transfer coefficient along the Eastern wall. The maximum relative deviation of the convective surface transfer coefficient based on Turner *et al* [87] is approximately 30%,

while the maximum relative deviation based on the relationship from Bohn *et al*. [88] is approximately 25%. The deviation between the results predicted based on Turner *et al* [87], and Bohn *et al*. [88] increases towards the floor and towards the ceiling. This may be caused by local influences from the outlet of the room which is located near the floor, and from the corners.

In conclusion, the analysis showed that, also for this case study, the ratio between natural and forced convection in the room is an important issue when modelling the surface transfer coefficients in the room. It was possible to give a relatively accurate prediction of the local convective surface transfer coefficients along the Eastern wall with a maximum relative deviation of 25% using relationships based on natural convective airflow in enclosures. However, with respect to the Western wall, where the airflow is more influenced by forced convection, it was not feasible to predict the local surface transfer coefficients, while deviations between factor 2 and 10 have been observed.

5.4.2 Conclusion

The investigations showed that the application of a sub-zonal airflow model to predict the indoor environmental conditions and surface transfer coefficients for mixed convection in a room, ventilated at an air change rate of 11 h^{-1} and 2 h^{-1} is limited. A comparison of the results obtained from the sub-zonal models with the CFD results showed that the sub-zonal airflow model has problems with respect to the accurate prediction of the indoor environmental conditions in the room. Relatively large deviations up to 40% regarding both the global and local conditions in the room have been observed. The sub-zonal model which was best capable of predicting the indoor environmental conditions included a thermal boundary layer model to model the natural convective airflow along the walls. No specific model was added to account for forced convection.

The analysis of the case study at an air change rate of 11 h^{-1} and 2 h^{-1} showed that the ratio between natural and forced convection in the room is an important issue when modelling the indoor environmental conditions in the room. The sub-zonal airflow model was able to give a slightly better prediction of the indoor environmental conditions for the case with a relatively small air change rate of 2 h^{-1}, since natural convection was dominating the airflow pattern in the room. Similarly, this ratio is important for the modelling of the local convective surface transfer coefficients in the room. For both ventilation regimes, it was possible to give a relatively accurate prediction of the local convective surface transfer coefficients along the Eastern wall with a maximum relative deviation of 20% using relationships based on natural convective airflow in enclosures. However, with respect to the Western wall, where forced convective airflow was dominating locally, it was not feasible to predict the local surface transfer coefficients, while deviations up to factor 2 and higher have been observed.

5.5 Discussion

In this thesis, it has been demonstrated that the sub-zonal model combined with an appropriate surface transfer coefficient model is able to provide a satisfactory estimate of the local indoor environmental conditions and local convective surface transfer coefficients in a room. The quality of the results showed to be dependent of the airflow regime in the room. The main advantage of the sub-zonal model is a significant reduction in computational effort compared to CFD. The ability of the sub-zonal model to provide a relatively accurate prediction of the local conditions in a room as well as the short computation time makes the application of the sub-zonal model attractive for the transient simulation of heat, air and moisture transfer in buildings.

Currently, alternatives, which may be also attractive for the transient simulation of heat, air and moisture transfer in buildings, are available, such as computational fluid dynamics simulations on a relatively coarse or rough grid, computational fluid dynamics using a zero-equation turbulence models, and the use of proper orthogonal decomposition (POD) for airflow simulations in buildings. In this section, the advantages and disadvantages of these approaches are discussed based on the literature and compared with the sub-zonal airflow model.

As has been mentioned previously, CFD models are capable of predicting the local temperature and relative humidity near a building component as well as the local surface transfer coefficients. However, detailed airflow models cannot easily and quickly solve time-dependent hygrothermal interactions across the boundaries of a building model. In practice, only steady-state simulations of the airflow in a single room at a specific time are feasible. And, since these steady-state calculations are relatively computationally intensive, transient calculations over a longer period of time are currently not possible. In this section, alternatives to the use of sub-zonal models and CFD simulations are presented.

5.5.1 CFD on a coarse grid

In order to reduce the computation time of a CFD simulation, the size of the computational grid that is used for the CFD simulation can be reduced. Mora *et al*. [46] modelled the forced convective airflow in the Annex 20 Benchmark case (Section 5.3) using a standard k-ε turbulence model on a relatively coarse grid of 10x10 cells. Based on their investigations, the authors [46] concluded that coarse-grid k-ε CFD can be a satisfactory alternative to sub-zonal methods where more accurate details are required, for predicting airflows and contaminant transport in large indoor spaces connected to a complex multi-zone building.

In the framework of this study, a CFD simulation of the airflow in the Annex 20 Benchmark case (Section 5.3) using a standard k-ε turbulence model on a relatively coarse grid of 10x10 cells has been carried out using the commercial CFD software FLUENT. Based on the simulation results, two main problems have been observed. First of all, the CFD solution does not converge, i.e. the residual of the solution does not decrease until the convergence criteria for mass and energy conservation are reached. After a certain number of iterations the solver is manually interrupted and the problem is considered to be solved. Though, it should be noticed that mass and energy are not conserved. Second, while the resulting air velocity and temperature fields in the room are satisfactory, the convective surface heat transfer coefficients are over-predicted with a factor 10 and higher. Applying the guidelines for CFD simulations that were presented by Steeman [13], the results obtained from such a CFD simulation using a standard k-ε turbulence model on a relatively coarse grid are not reliable. A similar approach for the test cases with natural and mixed convection in the room resulted in similar observations. The main reason for the relatively poor results and non-convergence of the solution is that the requirements for the modelling of the turbulence are not valid when applying a standard k-ε model on a relatively coarse grid.

5.5.2 Zero-equation turbulence models

As an alternative to the use of a standard k-ε turbulence model, Chen et al. [91] used a zero-equation turbulence model to simulate three-dimensional distributions of air velocity, temperature, and contaminant concentrations in rooms. The model has been used to predict natural convection, forced convection, mixed convection, and displacement ventilation in a room. The authors [91] concluded that the results agree reasonably with experimental data and the results obtained by the standard k-ε model. The zero-equation model uses less computer memory and a computation time of at least 10 times faster was reported compared to the standard k-ε model. The grid size can often be reduced so that the computing time needed for a case can be a few minutes on a PC [91].

The performance of the zero-equation turbulence model for the simulation of indoor airflow has been evaluated by Zhang [33]. Zhang [33] investigated the quality of the simulation results for natural, mixed and forced convective airflow in a room, as well as for strong buoyancy airflow. Regarding mixed convective airflow regimes, the zero-equation turbulence model performs better compared to the sub-zonal airflow models, while the maximum relative deviation of the temperature in most of the cells is approximately 10%, compared to 40% for the sub-zonal airflow model. For natural convective airflow, the performance of the zero-equation turbulence model is relatively poor, while the maximum relative deviation of the temperature in the room lies between 20% and 30%, compared to 10-15% regarding the sub-zonal airflow model. For

forced convective airflow conditions, both models perform similar with a maximum relative deviation of the temperature in the room between 20% and 30%.

The main advantage of the zero-equation turbulence model is that the model is capable of giving a better qualitative prediction of the local air velocity in the room compared to the sub-zonal model. Moreover, the zero-equation model is better able to predict recirculation of the airflow in a room. However, a disadvantage with respect to the zero-equation model is that performance of the model has not been investigated regarding the prediction of the local convective surface transfer coefficients in the room.

Comparing the zero-equation turbulence model and the sub-zonal model, the main issue to be addressed is the implementation of the models. Since both models are not available in a commercial software package, this means that the user is required to implement both models. The implementation of a sub-zonal airflow model is relatively straightforward compared to the implementation of a zero-equation turbulence model. However, the zero-equation turbulence model may be more generally applicable, since it does not require the implementation of specific flow elements, as this is necessary in sub-zonal airflow models.

5.5.3 Proper orthogonal decomposition (POD) for airflow simulations in buildings

Currently, CFD models are too time-consuming for the transient simulation of heat, air and moisture transport in buildings. A reduced airflow model might be applied to reduce the computational effort. In mixed convection, when the air temperature has negligible variations, the velocity field may be considered fixed. In this case, the size of a CFD model may be reduced by solving only the energy balance equation. The equations describing conservation of mass and momentum are written in the form of a linear state-space system and the order is reduced by proper orthogonal decomposition (POD).

In [76] for example, this algorithm was applied for the modelling of the airflow in a room equipped with a fan coil. First of all, CFD simulations are performed for the whole operating range and are considered as reference data. Second, airflow patterns are considered and a fixed flow field hypothesis is used to build a high-order model for each airflow pattern. Four fixed airflow fields, corresponding to negligible air temperature variation, were considered, resulting in four airflow patterns. After that, the model of each fixed air velocity field is reduced by using POD. Finally, these reduced models are interpolated to form a complete model for the whole range of variation of the inlet air temperature. The reduced model obtained from these airflow patterns was validated by comparison with CFD results.

The performance of the reduced order modelling of the airflow in the room has not been compared to experimental data. Moreover, the approach has not been evaluated regarding the prediction of the local convective surface transfer coefficients in the room. However the computational effort is relatively low, with a simulation of the airflow field taking a few minutes per time step, the accuracy of the reduced order model may be discussible. The main limitation of the model is the fixed flow field hypothesis, where it is assumed that the temperature in the room has negligible variations. Such an assumptions may be true under forced convective airflow and air change rates in a room, but is definitely a problem when considering mixed convection in for example a naturally ventilated room subjected to varying boundary conditions.

In this section, the alternatives for the modelling of the indoor environmental conditions and local convective surface transfer coefficients in a room have been discussed. It is concluded that while the application of all alternatives for the transient simulation of heat, air and moisture transfer in buildings may result in a reduction of computational effort, the quality of the predictions decreases as well.

5.6 Conclusion

In this Section, the applicability of the sub-zonal airflow model to predict local temperature, relative humidity in a room was studied. Moreover, surface transfer coefficient models have been evaluated for the prediction of the local convective surface transfer coefficients in a room. Three test cases for respectively natural, forced and mixed convection in a room were analyzed. For each test case, several sub-zonal airflow models have been developed and simulated to predict the heat and moisture flows in the room and the flows between the room and the building components. With respect to the surface transfer coefficient models, the results from the sub-zonal airflow model have been used for the prediction of the local convective surface transfer coefficients along the building components. Similarly, CFD simulations have been carried out for the prediction of the indoor environmental conditions and surface transfer coefficients in each test case. The CFD simulations have been performed within the framework of the present study and carried out along the lines of the best practice guidelines that were presented by Steeman [13]. The results from the sub-zonal models are compared to the CFD models' results regarding, accuracy, efficiency computational effort (or simulation time), and flexibility.

Table 25 presents a summary of the case studies that have been investigated. The table focuses on the accuracy with respect to the prediction of the local indoor environmental conditions and surface transfer coefficients. Furthermore, the observations from this study with respect to the efficiency, computational effort and flexibility are discussed regarding the modelling of the hygrothermal interaction between the building component and the indoor environment.

Table 25: Case studies

Case	**Flow regime**	**ACH [h^{-1}]**	**Sub-zonal airflow model**	**STC model**	**Maximum relative deviation**	
					Indoor environmental conditions	Convective surface transfer coefficients
MINIBAT case	Natural convection	0	Thermal boundary layer	Turner *et al.*	10-15%	< 10%
Annex 20 Benchmark case	Forced convection	14	Jet model	Local Beausoleil-Morrison	5-10% < 30% [1)]	30%
CFD case	Mixed (dominating natural) convection	11	Thermal boundary layer	Turner *et al.* [3)]	40%	20% [3)]
	Mixed (dominating natural) convection	2	Thermal boundary layer	Turner *et al.* [3)]	40%	20% [3)]

[1)] In a recirculation region
[2)] If no local recirculation
[3)] Only for local natural convection

In Table 25, the three case studies that have been analyzed are presented. The table shows that for the modelling of natural and mixed convection in the rooms a thermal boundary layer model has been applied to describe the airflow in the thermal boundary near the walls, while a jet model has been applied to describe the ceiling jet in the forced convection case. Regarding the MINIBAT case and the Annex 20 Benchmark case the implementation of the sub-zonal airflow model was straightforward.

Regarding the MINIBAT case, the application of a thermal boundary layer model was obvious and resulted in a relatively accurate prediction of the indoor environmental conditions with a maximum relative

deviation of 10-15%. Other researchers [44] [46] also observed that the sub-zonal airflow model gave an accurate prediction of the temperature distribution for natural convection in a room. With respect to the prediction of the local convective surface transfer coefficients the model based on the experimental correlations for natural convection in an enclosure developed by Turner *et al.* [87] gave prediction with a maximum relative deviation up to 10%.

With respect to the Annex 20 Benchmark case, the sub-zonal model including a jet model also resulted in a relatively accurate prediction of the local indoor environmental conditions in the room with a maximum deviation between 5-10% outside local recirculation regions. Other authors similarly indicated [37] [38] [43][46] that the sub-zonal model is capable of giving a rough prediction of the forced convective airflow in the room provided an appropriate flow element model, describing the jet in the room, is implemented. However, in the present study it was observed that, if local recirculation of the airflow in the room is present, for example in a corner, the relative deviation of the predicted indoor environmental conditions increases up to 30%. The study presented by Wurtz [37] did not focus on smaller local recirculation regions.

With respect to both case studies, it may be difficult to generalize the observations for natural and forced convection in a room. The present study and other researchers [37] [38] [43][46] showed that sub-zonal models are suitable to obtain a relatively rough prediction of the indoor environmental conditions compared to CFD. The present study also illustrated that for airflows dominated by natural or forced convection, sub-zonal models combined with an appropriate surface transfer coefficient model are applicable for the prediction of the local convective surface transfer coefficients in a room.

Regarding the modelling of the indoor environmental conditions and local surface transfer coefficients under mixed convective conditions, Table 25 shows that the maximum relative deviation with respect to the indoor environmental conditions is approximately 40%. In addition, the study showed that it was not possible to model the local convective surface transfer coefficients near a wall where forced convection is dominating with a combination of a sub-zonal airflow model and a surface transfer coefficient model. In contrary, near a wall where natural convection is dominating, it is possible to model the local convective surface transfer coefficients with a maximum relative deviation of 20%. The modelling of mixed convective internal airflows might lie outside the application domain of sub-zonal modelling, since the flow elements, such as a thermal boundary layer model and a jet model, are not suitable for the application under mixed convective conditions. Moreover, the surface transfer coefficient models might be rarely able to predict the local convective surface transfer coefficients under these conditions.

In conclusion, sub-zonal models combined with an appropriate surface transfer coefficient model are able to give a prediction of the indoor environmental conditions in a room under natural or forced convective conditions. However, one important remark should be made. In the case studies, reference conditions, for example experimental data or numerical results from CFD, have been used for the development of a reliable sub-zonal airflow model. The availability of such reference conditions is a prerequisite for the development of a reliable sub-zonal model and surface transfer coefficient model.

The main advantage of the sub-zonal model is a significant reduction in computational effort compared to CFD. The computation time of a sub-zonal airflow model with a surface transfer coefficient model implemented generally varies between a few seconds up to 20 seconds. The sub-zonal airflow model is solved on a relatively coarse grid, while only three equations, i.e describing the conservation of mass, energy, and vapour, are solved per time step. The computational effort of the CFD simulations that have been carried out is relatively large. The computation time of a CFD simulation varies between several hours up to a few days. Furthermore, the stability of the sub-zonal model showed to be relatively large compared to CFD, resulting in only a few iterations for solving the airflow and the temperature and vapour content fields. The relatively short computation time and flexibility makes the application of the sub-zonal model attractive for the transient simulation of heat, air and moisture in buildings.

6 Coupling HAM – Airflow

In this thesis, the applicability of sub-zonal airflow modelling for the prediction of the local environmental conditions and surface transfer coefficients has been investigated. The main objective is to obtain a more accurate assessment of the heat, air and moisture conditions in the building component and the zone by modelling and coupling a sub-zonal airflow model, which describes the varying, non-uniform indoor airflow near a building component with a HAM component model. Since both systems, i.e. the room air and the building envelope, have a different characteristic time, both models should be coupled in an efficient way, regarding efficiency, accuracy, computational effort (or simulation time), and flexibility. Strategies, approaches, and guidelines have been analyzed.

In this section, an efficient and flexible model, which is applicable for the assessment of the heat, air and moisture transport in the indoor environment and in the building envelope as well as the interaction between both domains is developed. The model should provide detailed information of the local environmental conditions in the building zone near the building component, i.e. the local air temperature, and relative humidity, of the local conditions in the building component, and detailed information regarding the local convective surface transfer coefficients. Moreover, the model should be suitable for transient heat, air and moisture simulations of the component-indoor air interaction, provided the computation time is relatively short. The simulation results from the coupled simulation are compared with a HAM component simulation where different values for the surface heat and moisture transfer coefficients are applied.

Section 6.1 presents the methodology that has been applied to investigate the hygrothermal performance of a building zone and building envelope using a coupled whole-building HAM simulation. In Section 6.2, the building component and building zone that were investigated are presented. The different models, which have been applied for the modelling of the indoor environmental conditions and the convective surface transfer coefficients, are presented in Section 6.3. Section 6.4 describes the coupling strategy and data exchange method that was used for the coupled HAM building simulation. The simulation results are presented in Section 6.5. A discussion of the results and the conclusions are presented in respectively Section 6.6 and Section 6.7.

6.1 Methodology

The hygrothermal performance of a building zone and building envelope has been investigated using a coupled whole-building HAM simulation. The room can be considered to be located in a building consisting of rooms with a length and height of 3.1m and 2.5m respectively. The (conceptual) two-dimensional geometry of the building is presented in Figure 64. The rooms are separated by lightweight concrete internal walls and a lightweight concrete floor. Furthermore, each room is connected to the outdoor environment with an external wall.

First of all, the geometry of a room which is defined along the lines of the CETHIL's MINIBAT test cell that has been presented by Inard *et al.* [35]. The building zone is coupled to the building components. The specific details with respect to the building zone and the component are presented in the following section.

Second, the geometry of the room was defined in the sub-zonal airflow model. The geometry of the building component is defined in CHAMPS-BES [78], which is an envelope model for the coupled simulation of heat, air, moisture and pollutant transport in a building component. Both models are coupled in order to solve the governing equations in the different domains, i.e. in the zone and in the component, iteratively.

Third, external boundary conditions were applied using the Test Reference Year (TRY) for Danish (Copenhagen) outdoor climatic conditions and the indoor environmental conditions were applied for the internal surfaces. Different values for the surface heat and moisture transfer coefficients were calculated based on the results obtained from the sub-zonal airflow model.

Regarding the indoor climate in the room, no heat and moisture sources and no indoor controls are taken into account, contrary to the simulation case presented in Chapter 3. In Section 2.5.2, it has been shown that the Chilton-Colburn relationship may not be valid when heat/moisture sources are present in the room. The study presented by Steeman [13] showed that problems can arise due to the presence of heat/moisture sources in the room. In order to avoid the introduction of any errors in the convective surface transfer coefficients, heat and moisture sources and indoor controls have been omitted.

Then, an initial temperature and relative humidity of 20 °C and 50% RH respectively were applied throughout the entire building. The hygrothermal performance of the building was simulated for one year. The investigations showed that a transition period may be neglected using these initial conditions of 20 °C and 50% RH, which are average conditions, representative for the entire year.

The simulation results obtained from the coupled hygrothermal simulation of the building zone and the building component are compared with the results from a HAM component simulation. In the HAM component simulation, the indoor environmental conditions in the room and the convective surface transfer coefficients are considered to be uniform, i.e. the building zone is defined as a multizone/network model.

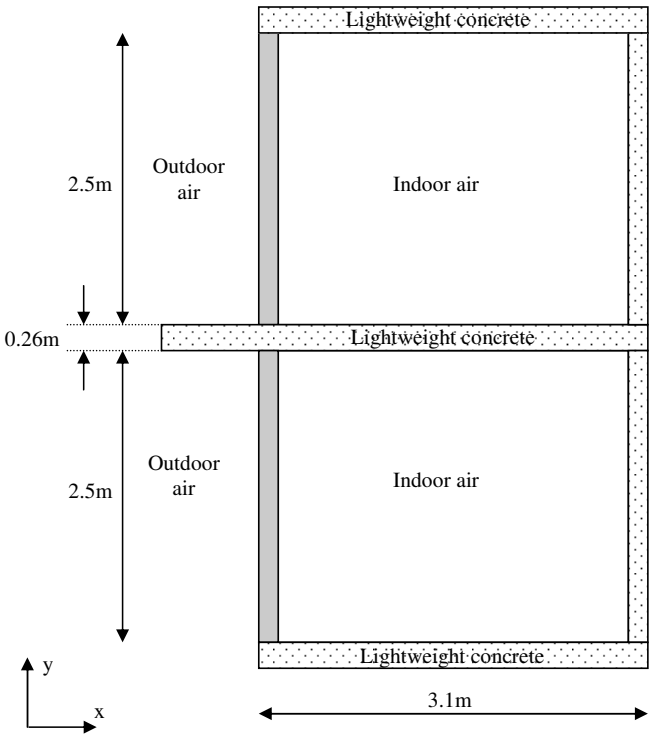

Figure 64: Building geometry

6.2 Building configuration

This section presents the building component and building zone that were investigated. The composition of the wall element is presented in Table 26. A floor penetrating the external wall of a building was analysed. Two rooms (on top of each other) were connected by a concrete floor. Both rooms were connected to the outdoor climate by the lightweight concrete wall, consisting of a plywood cladding, a wind barrier, mineral wool insulation and a lightweight concrete layer. The construction is presented in Figure 65. Moreover, a two-dimensional model in CHAMPS-BES [78] has been used to simulate the HAM transport in the building corner. The two-dimensional CHAMPS-BES model is coupled to the sub-zonal airflow model.

It was our objective to investigate the influence of the convective surface transfer coefficients on the hygrothermal performance of the component and on the surface conditions of the component when considering a thermal bridge, such as a balcony.

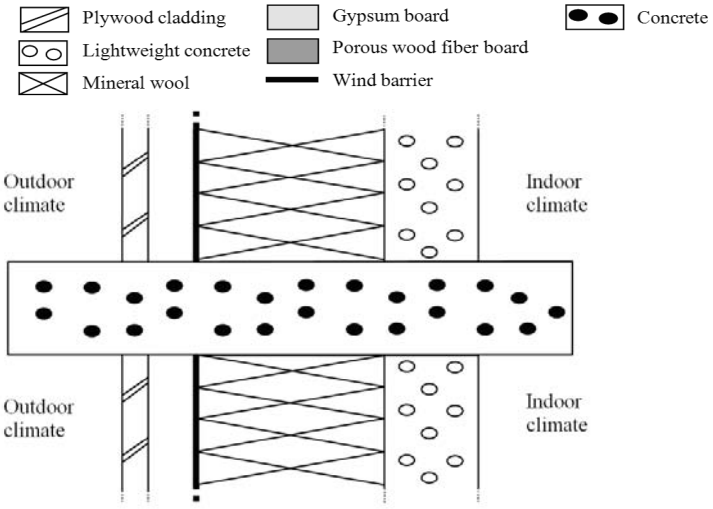

Figure 65: Building component selected for analysis.

Table 26: Wall elements

Lightweight concrete wall element	Number of calculation nodes
▪ 15 mm plywood cladding	10 x 7
▪ 25 mm vented cavity	10 x 6
▪ wind barrier	-
▪ 100 mm glass wool	10 x 24
▪ 50 mm lightweight concrete	10 x 12

The building component is connected to the indoor climate in the rooms. Since the geometry and the conditions in the room are considered to be similar, only the indoor environmental conditions in one room have been analysed. The geometry of the room has been defined along the lines of the MINIBAT test cell. A detailed description of the MINIBAT test cell can be found in Allard et *al*. [89]. The room consists of a 24 m^3 (3.1 x 3.1 x 2.5m) single volume of which the temperature is controlled and kept constant on the floor, ceiling and Eastern wall.

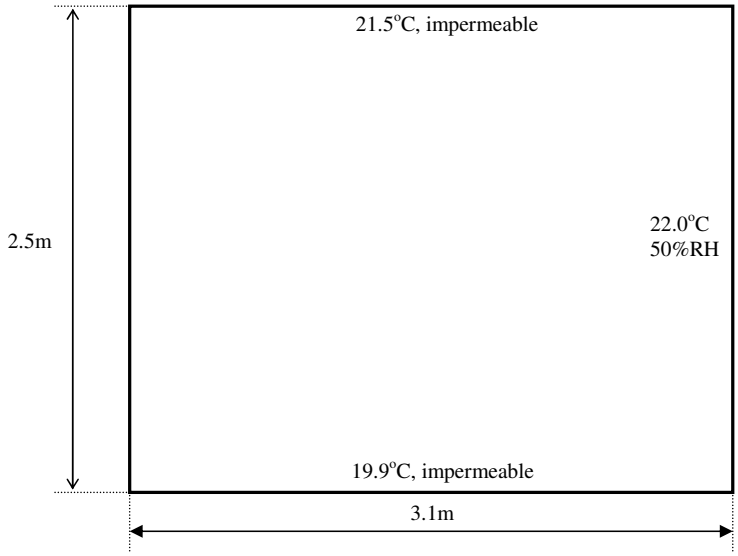

Figure 66: Geometry and boundary conditions for the MINIBAT case [35]

The temperature of the Eastern wall, the floor and ceiling is respectively 22.0°C, 19.9°C, and 21.5°C respectively. Furthermore, the geometry of the room is three dimensional. Assuming symmetrical boundary conditions for the Northern and Southern walls, the airflow in centre of the room is considered to be two-dimensional. The relative humidity of the Eastern wall is kept constant at 50%RH, while the floor and ceiling are considered to be vapour tight. The boundary conditions on the Western wall are retrieved from the HAM component simulation.

The airflow in the room is analyzed under natural convective conditions, which means that the room is not ventilated. In practice, such a scenario might be less realistic. However, the reader should notice that this configuration has been chosen to illustrate the application of sub-zonal airflow models for the analysis of whole building heat, air and moisture transport.

6.3 Airflow and surface transfer coefficient modelling

Several models have been applied to model the indoor environmental conditions in the room. Table 27 presents an overview of the models that have been applied. It should be noticed that the convective surface transfer coefficient models have been applied for the modelling of the transport between the building zone and the building component. For the convective surface transfer coefficients of other components, such as the floor and ceiling, values based on Beausoleil-Morrison [48] were applied.

First of all, a sub-zonal airflow model was used to model the temperature and relative humidity in the room. The airflow in the room has been modelled using a sub-zonal airflow model. A thermal boundary layer model has been implemented in order to model the buoyancy driven airflow near the walls. In Section 5.2, it was demonstrated that a sub-zonal model with a thermal boundary layer model on a 8x10 grid gave satisfactory results for the airflow in a room under natural convective conditions. The local convective surface transfer coefficients were modelled based on the relationships developed by Turner *et al* [87] for natural convection in an enclosure. The Chilton-Colburn analogy [59] has been applied for the modelling of the local convective surface moisture transfer coefficient. Radiant heat exchange among the surfaces inside the room takes place by long-wave radiation. Walton's method [92] is used to calculate long-wave exchange among these surfaces. In Walton's method the internal surface of each wall is assumed to radiate to a

fictitious surface which area, emittance and temperature provides the same heat transfer from the room surface as in the actual multi-surface case. The main advantage of Walton's method is that this method reduces the number of interchange equations considerably.

Second, a nodal model has been used to predict the indoor environmental conditions in the room. The model assumes that the indoor environmental conditions are uniform. Moreover, average convective surface heat transfer coefficients are calculated based on the relationships developed by Beausoleil-Morrison [9]. The Chilton-Colburn analogy [59] has been applied for the modelling of the average convective surface moisture transfer coefficient. Walton's method [92] is used to calculate long-wave exchange among the surfaces in the room.

Third, a simulation has been performed with minimum and maximum values for the convective heat and moisture transfer coefficients for the different indoor environmental conditions. The objective of the investigations was to determine the influence of the minimum and maximum hygrothermal conditions, which were likely to occur in the building component and the building zone on the heat and moisture conditions in the building component and in the building zone. For additional information regarding the specific values and conditions with respect to the simulations with lower and higher limits, the reader is referred to Chapter 3.

Table 27: Indoor environmental models

Indoor Environment	Radiation	Convective surface heat transfer coefficient	Convective surface moisture transfer coefficient
(1) Sub-zonal airflow model	Walton's method	Turner	Chilton-Colburn
(2) Nodal model	Walton's method	Beausoleil-Morrison	Chilton-Colburn
(3) Lower limits	3	1	0.1
(4) Upper limits	15	8	1

6.4 Coupling HAM and Sub-zonal airflow model

The sub-zonal airflow model has been coupled to the HAM component model. However, coupling of the building zone and the component is not straight-forward. While the characteristic time with respect to the HAM flows in a building component is relatively long, usually between a few hours up to a few days, the characteristic time of the airflow in a room varies between a few minutes and a few hours. The difference between these characteristic times of the systems may result in an inefficient transient simulation of both systems at the same time. While the airflow simulation requires the model to take relatively small time steps, calculation of the heat and moisture flows in the building component at these steps would result in small deviations of these flows over time, and in principle in unnecessary computations. Or, in other words, the airflow simulation must be performed over a long period for the hygrothermal performance of the building envelope, but it must use a small time-step to account for the room air characteristics. Therefore, the room model and the component model should be coupled in such a way that a simulation can be carried out efficiently. The efficiency, accuracy, computational effort (or simulation time), and flexibility of the data exchange methods between the envelope and room model are important.

In Chapter 2, coupling strategies for the coupling of airflow simulation and HAM component simulation have been reviewed. Several strategies were discussed. Based on the literature study, quasi-dynamic coupling has been selected and implemented in the model. The coupling algorithm is presented in Figure 67. First of all, the heat and moisture transport in the building component is simulated in CHAMPS-BES [78]. The temperature and relative humidity on the surface of the building component is provided to the sub-zonal airflow model. Second, the sub-zonal airflow model is simulated until convergence is reached. The resulting convective heat and moisture transfer coefficients are provided to the CHAMPS-BES component model. Moreover, the differences between the air temperature in the first sub-zone adjacent to the component and the surface component temperature and the corresponding differences in relative humidity are provided to the CHAMPS-BES component model. The boundary conditions for the component model are updated and the time-step is increased. Then the HAM component solver is re-started at the next time step and simulated

until convergence is reached. The resulting surface temperatures and relative humidities are provided to the sub-zonal model and the sub-zonal airflow model is simulated in order to provide updated indoor environmental conditions.

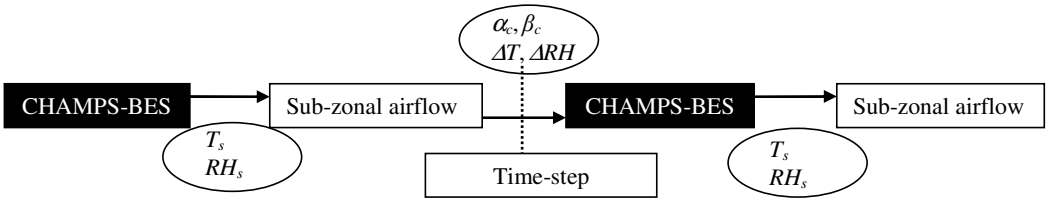

Figure 67: Quasi-dynamic coupling

Quasi-dynamic coupling was preferred above full-dynamic coupling, because of the software structure of the CHAMPS-BES component model and the efficiency of the strategy [70]. The current CHAMPS-BES software structure does not allow the iteration between two domains for a couple of times at each time-step to reach a converged solution. This means that full-dynamic coupling is not applicable. Furthermore, full dynamic coupling is computational intensive and may result in a relatively long computation time.

Regarding the accuracy of the results and the stability of the solution, two important issues are discussed: the data exchange method and the coupling/interfacing time-step. First of all, in Chapter 2, data exchange methods have been evaluated based on Zhai [72]. It was demonstrated that the method, which transfers enclosure interior surface temperatures (T_{surf}) from the energy simulation to the airflow simulation and returns convective heat transfer coefficients (α_c) and indoor air temperature gradients (ΔT) from the airflow domain to the energy simulation unconditionally satisfies the convergence condition when the heat transfer coefficient is larger than zero. Furthermore, the computational effort of the method showed to be relatively low. Based on Zhai [72], this data exchange method has been implemented in the current model.

Second, Nicolai et *al*. [16] showed that another critical parameter for coupling an airflow model and a HAM component model was found to be the coupling/interfacing time step. By selecting proper time steps for exchanging interface quantities, satisfactory accuracy can be achieved, even if only one round of integration for each exchange time step in the airflow and envelope models (i.e., without iteration) is used. Based on the case that was analyzed [16], the authors required time steps below one hour. Yet, for performance reasons, the interchange interval lengths should be above 15 minutes. An exchange time step between 30 minutes and one hour showed to be a recommended compromise between performance and accuracy. Different time steps, of respectively 5 min, 15 min, 30min and 1 hour, have been applied for the simulation of the present case study. The maximum deviation of the simulation results showed to be below 5% for the time steps of 5 min, 15 min and 30 min, while the maximum deviation increases slightly up to 10%, if time steps of 1 hour are used.

6.5 Results

The building that has been presented in Figure 64 was simulated for 1 year. In this section the simulation results are presented. A coupling time step of 15 min has been used. The predicted surface conditions on the walls and interior conditions in the room are analyzed.

The predicted hygrothermal conditions on the internal surface of the building components are presented. First of all, the surface temperature and relative humidity in the corner of the thermal bridge (Figure 65) are shown during 2 days. Second, weekly averaged surface conditions on the presented components were analysed by presentation in an isopleth.

Figure 68 presents the temperature, the relative humidity and the partial vapour pressure in the corner of the building component during 2 days (May 27-28.). The figure shows that a relatively large relative difference up to approximately 10% is present between the lower limit (3) and the higher limit (4). Considering the hygrothermal conditions predicted by sub-zonal model (1) and the nodal model (2) smaller differences with a maximum relative difference of 5% are observed.

Figure 69 presents the temperature and relative humidity in the corner of the building component. The predicted conditions obtained from the sub-zonal airflow model and the nodal model are shown. The daily averaged temperatures and relative humidities are presented in the isopleth. The figure shows that the minimum temperature predicted by the nodal model is approximately 2^{o}C lower compared to the minimum temperature predicted by the sub-zonal model. This difference is caused by the model that is used for the prediction of the surface transfer coefficients. The nodal model, which predicts the average convective surface transfer coefficients based on the relationships based on Beausoleil-Morrison [48] is in general relatively small compared to the local convective surface transfer coefficients predicted by the model based on Turner *et al* [87].

Moreover, Figure 69 shows a comparison of the surface relative humidity in the corner of the building component predicted by the sub-zonal model, the nodal model, and the models with lower and higher limits for the convective surface transfer coefficients. The figure shows that differences with respect to the surface relative humidity are observed. While the model with lower limits for the convective surface transfer coefficients and the nodal model predict relative humidities above 70%, where mould growth may develop [93], the sub-zonal model and the model with higher limits for the convective surface transfer coefficients predict relative humidities below 70% during the entire year.

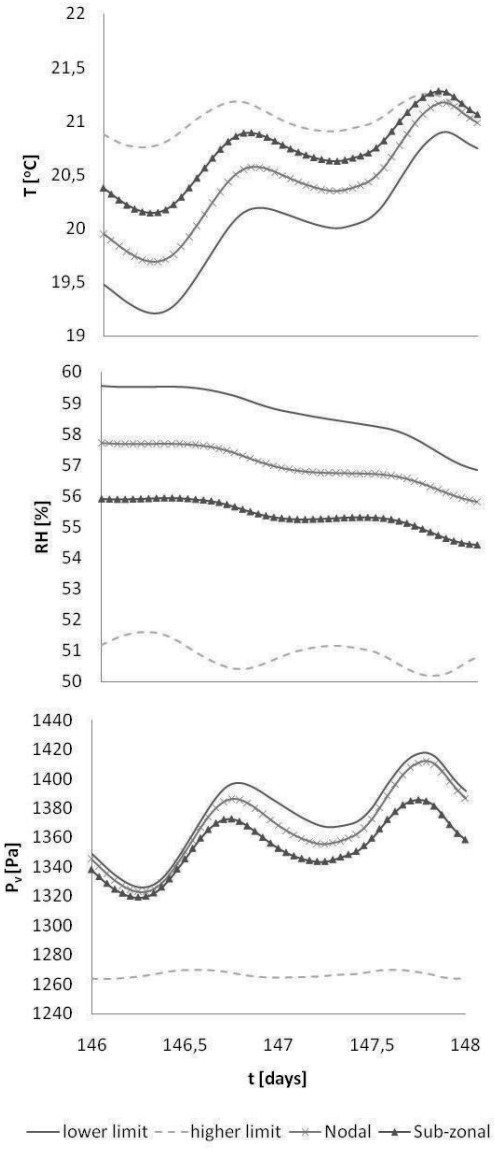

Figure 68: Surface temperature and relative humidity in the corner of the building component. The different models, i.e. the sub-zonal model, the nodal model, and the models with lower limits and higher limits for the convective surface transfer coefficients.

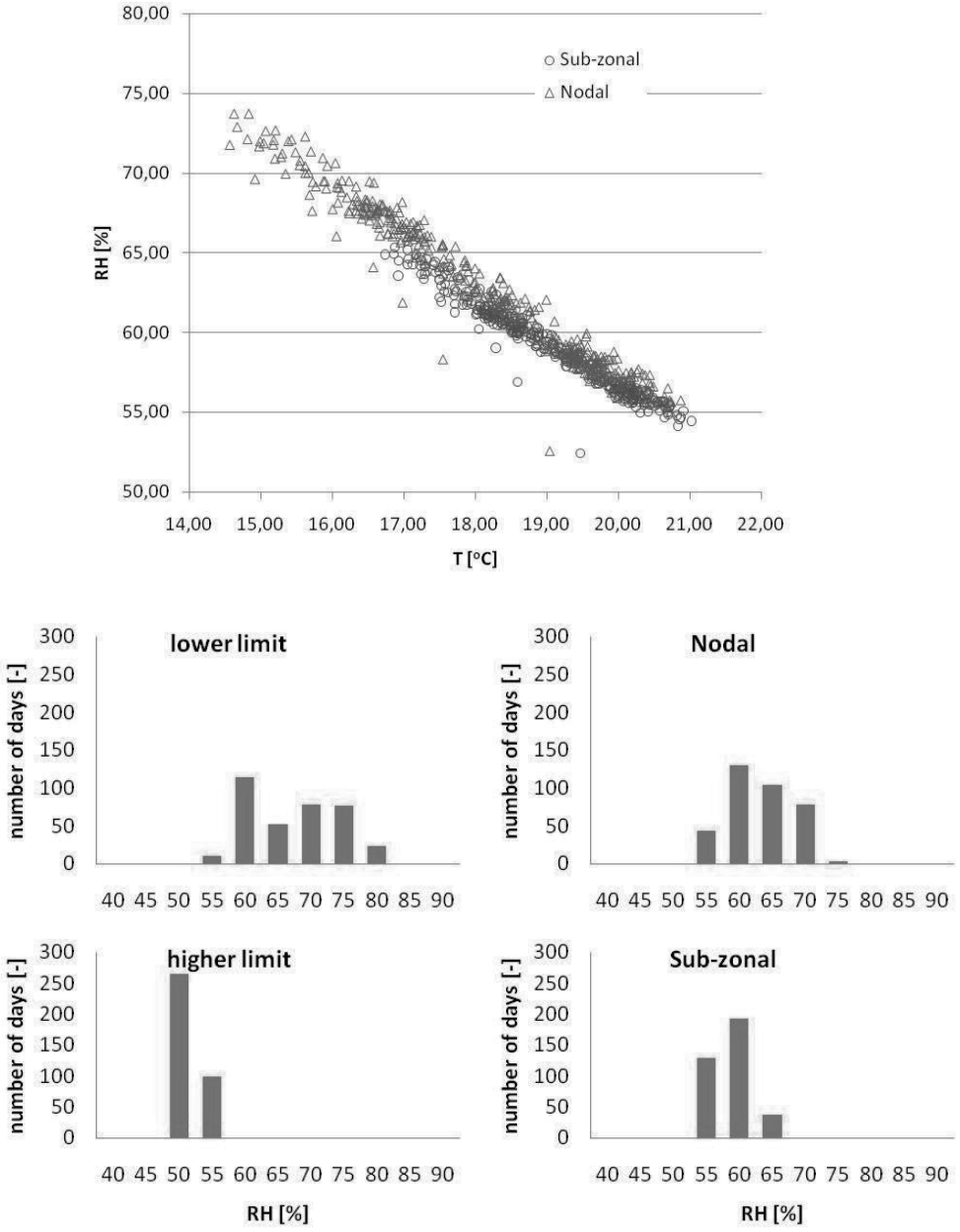

Figure 69: Temperature and relative humidity in the corner of the thermal bridge predicted by the sub-zonal model, the nodal model, and the models with lower limits and higher limits for the convective surface transfer coefficients. Isopleth representation of the daily averaged surface conditions during one year. Histogram of the observed daily averaged surface relative humidity as a function of the number of days.

6.6 Discussion

It should be noticed that the differences between the nodal model and the sub-zonal model are relatively small. The nodal model predicts a relative humidity of 70% and higher during 85 days, while the sub-zonal model predicts the relative humidity to lie below 70% during the entire year. Moreover, differences in the surface conditions in the corner predicted by the sub-zonal model and the nodal model are relatively small. The relatively small differences between both models are partly caused by the restrictions due to the choice of the boundary conditions in the room and partly due to the limited size of the room, the ventilation regime in the room, and the absence of heat and moisture sources in the room.

First of all, fixed surface temperatures between 19.9°C and 22 °C have been imposed on the internal surfaces in the room. Moreover, the ceiling and the floor are impermeable for vapour transport, while a fixed surface relative humidity of 50% is imposed on the Eastern wall. Second, the room is relatively small, resulting in a relatively small hygrothermal active surface. The airflow regime in the room is considered to be natural convective, while the room is not ventilated. Furthermore, the absence of heat and moisture sources results in relatively stable indoor environmental conditions in the room.

In Chapter 5, it has been demonstrated that the sub-zonal airflow model performs well for the given indoor environmental conditions and is able to give satisfactory results. However, the restrictions regarding the indoor environmental conditions result in an indoor climate with only small deviations over time. The HAM component conditions are only subjected to larger excitations of the outdoor environmental conditions. Therefore, the case study is less suitable to demonstrate the influence of the varying local indoor environmental conditions and surface transfer coefficients on the hygrothermal conditions on the surface of and in the building component.

Regarding the performance of the coupled simulation, the computation time is approximately 20 minutes for a 1 year simulation and respectively 35040 time steps of 15 minutes. Compared to a computational fluid dynamics simulation of the natural convective airflow in the room, which takes approximately a few hours up to a few days per time step, the developed model is flexible and suitable for the assessment of the heat, air and moisture transport in the indoor environment and within the building envelope as well as the interaction between both domains.

6.7 Conclusions

In this section, the hygrothermal performance of a building zone and building envelope has been investigated using a coupled whole-building HAM simulation. The model has been used to analyze the heat, air and moisture transport in the indoor environment and within the building envelope as well as the interaction between both domains. A case study has been used for analysis. The case study consists of two rooms (on top of each other), separated by a concrete floor including a thermal bridge, and connected to the outdoor climate by the lightweight concrete wall. The influence of the local indoor environmental conditions and local surface transfer coefficients on the hygrothermal performance of the component was investigated. The airflow in the room is analyzed under natural convective conditions.

Four models have been applied to model the indoor environmental conditions and the convective surface transfer coefficients in the room: a coupled HAM component and sub-zonal airflow model combined with a surface transfer coefficient model based on the relationships developed by Turner *et al* [87], a coupled HAM component and nodal model combined with average convective surface transfer coefficients, calculated based on the relationships developed by Beausoleil-Morrison [9], and two separate HAM component models with respectively lower and upper limits for the convective surface transfer coefficients.

The predicted hygrothermal conditions on the internal surface of the building components predicted by the different models have been compared. Based on the investigations it is concluded that:

- Regarding the surface temperature and relative humidity on the surface of the building component, a relatively large relative difference up to approximately 10% has been observed between the separate HAM component models with lower and upper limits for the convective surface transfer coefficients.

- Considering the hygrothermal conditions predicted by the coupled HAM component and sub-zonal model and the coupled HAM component and nodal model smaller differences with a maximum relative difference of 5% have been observed.

It is concluded that the coupled HAM component model and sub-zonal model provided detailed information of the local environmental conditions in the building zone near the building component, i.e. the local air temperature, and relative humidity, of the local conditions in the building component, and detailed information regarding the local convective surface transfer coefficients. Moreover, the model showed to be suitable for transient heat, air and moisture simulations of the component-indoor air interaction. Regarding the performance of the coupled simulation, the computation time is approximately 20 minutes for a 1 year simulation and respectively 35040 time steps of 15 minutes. However, the differences between the nodal model and the sub-zonal model showed to be relatively small, since the surface conditions on the building component are restricted by the indoor environmental conditions in the room and, in principle, are mainly subjected to the varying outdoor environmental conditions.

This case study showed to be less suitable for demonstrating the influence of the varying local indoor environmental conditions and surface transfer coefficients on the hygrothermal conditions on the surface of and in the building component. Therefore, it is recommended for future research to apply the coupled HAM component model and sub-zonal airflow model for investigations considering larger and ventilated enclosures, where moisture sources are present, which results in a larger excitation of the indoor environmental conditions.

7 General Conclusions and Discussion

In this thesis, the current software for the simulation of the heat, air, and moisture conditions in a building has been categorized in three classes. It is common to subdivide these tools based on the spatial discretisation or granularity of the model. Focusing on the room-component interaction, the accurate prediction of this interaction depends on the local near-component conditions, and the convective surface transfer coefficients. The prediction of the local conditions and surface transfer coefficients is directly influenced by the airflow model that describes the indoor airflow in the building near the component. It has been shown that while several options are available with respect to the modelling of the airflow in a room, only computational fluid dynamics and sub-zonal airflow models are capable of providing a prediction of the local temperature and relative humidity in a room.

The literature review showed that CFD applications for indoor airflow simulation have achieved considerable successes and serve as a valuable tool for predicting airflow, temperature and relative humidity distributions in enclosed environments as well as the local convective surface transfer coefficients. However, there are many factors influencing the results predicted. CFD results should be analyzed with care, and validation with experimental results is always required. Nevertheless, detailed airflow models cannot easily and quickly solve time-dependent hygrothermal interactions across the boundaries of a building model. In practice, only steady-state simulations of the airflow in a single room at a specific time, and/or transient simulations over a relatively short period of time, for example a diurnal cycle, are feasible. And, since these calculations are relatively computational intensive, transient calculations over a longer period of time are currently not possible.

As an alternative for the use of CFD models, which are strongly limited by computer capacity, sub-zonal airflow models can be used. A review of the literature demonstrated that the sub-zonal modelling approach can be a suitable method to estimate temperature and relative humidity fields in a room with reasonable accuracy. However, studies on the ability of sub-zonal airflow models to give an accurate prediction of the local indoor environmental conditions near a building component and of the local convective surface transfer coefficients have not been reported so far.

In this thesis, the applicability of sub-zonal airflow modelling for the prediction of the local environmental conditions and convective surface transfer coefficients is investigated. The main objective is to obtain a more accurate assessment of the heat, air and moisture conditions in the building component and the zone by modelling and coupling a sub-zonal airflow model, which describes the varying, non-uniform indoor airflow near a building component with a HAM component model. Since both systems, i.e. the room air and the building envelope, have a different characteristic time, both models should be coupled in an efficient way, regarding efficiency, accuracy, computational effort (or simulation time), and flexibility. In the study, strategies, approaches, and guidelines have been analyzed.

In a first part of the thesis, the investigations focused on the magnitude of the surface heat and moisture transfer coefficients, and it was investigated how the magnitude of these coefficients may affect the hygrothermal performance of building components and building zones. Second, the applicability of the sub-zonal model to predict local temperature and relative humidity in a room was studied. Moreover, convective surface transfer coefficient models have been evaluated for the prediction of the local convective surface transfer coefficients in a room. In a third part, an efficient and flexible model, which is applicable for the assessment of the heat, air and moisture transport in the indoor environment and within the building envelope as well as the interaction between both domains has been developed.

7.1 Influence of Interactions

A parameter study was used to investigate how the hygrothermal conditions in the building component and the indoor environment varied with the magnitude of the surface transfer coefficients resulting from the air velocity near the surface of a building component. Three building component configurations (calculation

objects) were selected for analysis. Different values for the surface heat and moisture transfer coefficients were applied and the hygrothermal response of the building was simulated. The simulated conditions resulted in minimum and maximum hygrothermal conditions in the building component and in the building zone.

From this work, it is concluded that:

- while the influence of the convective surface transfer coefficients on the HAM conditions on the surface of the insulated walls was limited, this influence was relatively large when considering a thermal bridge. Different surface temperature, relative humidity and vapour pressures were predicted when different airflow conditions near a component resulted in different convective surface transfer coefficients. In consequence, when performing a hygrothermal performance analysis and simulation, it is important to take the local airflow velocity near the component into account.
- when focusing on the hygrothermal performance of the walls, the influence of the convective surface heat transfer coefficient on the hygrothermal performance is relatively large compared to the influence of the convective surface moisture transfer coefficient. With respect to the analysed building components, the investigations showed that assuming an average value for the convective surface moisture transfer coefficient is acceptable, while assuming an average value for the convective surface heat transfer coefficient is not acceptable. The study showed that the influence on the surface relative humidity is limited. However, an influence on the exchange with the interior environment is still present.
- with respect to the hygrothermal performance of the thermal bridge, the influence of both the convective surface heat and moisture transfer coefficient on the hygrothermal performance is relatively large. The analysis showed that assuming an average value for these coefficients is not acceptable.
- the influence of both the surface heat transfer coefficient and the surface moisture transfer coefficient on the heat and vapour exchange between the building component and the indoor environment as well as the buffering capacity of the building component is relatively large. Assuming average values for the surface transfer coefficients may introduce relatively large errors in the prediction of these fluxes and the prediction of the indoor environmental conditions.

Building researchers and designers should be aware that the appropriate indoor environmental conditions should be applied when performing a hygrothermal component simulation and analysis. The local airflow conditions near the component have a relatively large influence on the predicted hygrothermal conditions on the surface of the component. A more detailed description and prediction of the interaction between the indoor environment and the hygrothermal conditions in the building component is desirable.

7.2 Airflow and Convective Surface Transfer Coefficient Modelling

The applicability of sub-zonal models to get a qualitatively accurate prediction of the local temperature and relative humidity distribution near the building component and the corresponding local convective surface transfer coefficients has been assessed based on three test cases. Test cases for respectively natural, forced and mixed convection in a room have been defined. CFD simulations have been carried out for the prediction of the indoor environmental conditions and surface transfer coefficients in each test case. For each test case, several sub-zonal airflow models have been developed and simulated to predict the heat and moisture flows in the room and the flows between the room and the building components. With respect to the surface transfer coefficient models, the results from the sub-zonal airflow model have been used for the prediction of the local convective surface transfer coefficients along the building components. The results obtained from the present study have been compared with experimental results and numerical results.

Regarding the different test cases, respectively natural, forced and mixed convections, the following has been concluded from this work:

Natural convection

- The sub-zonal airflow model is able to predict the natural convective airflow in a room, provided an appropriate thermal boundary layer model and surface transfer coefficient model are applied. The sub-

zonal model gives a prediction of the temperature and vapour content distribution in the room, with a maximum relative deviation between approximately 10% and 15% compared to the temperatures and vapour contents predicted by CFD. (The relative maximum deviation is defined as the maximum deviation between a quantity predicted by the sub-zonal model and the quantity predicted by CFD, divided by the quantity predicted by the CFD model). While the predicted distributions are only slightly influenced by a densification of the grid, the influence of the thermal boundary layer model on the predicted temperature and vapor content distribution in the room showed to be relatively large.

- Regarding the prediction of the local convective surface transfer coefficients, the model based on the flat plate analogy was not suitable. The specific assumptions of the boundary layer theory for flat plates, especially focussing on the boundary conditions, geometrical influences, entrance velocity and leading edges, and surface roughness, are not (entirely) valid in building enclosures. The surface transfer coefficient model based on the experimentally determined convective surface transfer coefficients natural convective airflow in a rectangular enclosure gave the best results.

Forced convection

- The sub-zonal airflow model is able to give a prediction of the forced convective airflow in a room, provided an appropriate jet model is implemented and an appropriate surface transfer coefficient model is applied. The model showed to be applicable to give a rough prediction of the global temperature and vapour content distribution in the room with a maximum relative deviation of approximately 10%. However, if local recirculation of the airflow, for example in a corner, is present, the model is not capable of giving an accurate prediction in these regions, while the relative deviation increases up to 25% for the local temperature and 30% for the local vapor content.
- Regarding the prediction of the convective surface transfer coefficients, the models based on the flat plate analogy showed to be not applicable. Deviations of the predicted local surface heat and moisture transfer coefficients of factor 2 and more have been observed, when applying these models. Two main problems regarding the models based on the flat plate analogy have been observed: first of all, the models are based on relationships that have been determined for isolated flat plates instead of real building components. Second, the models require the accurate prediction of the local Reynolds number and air mass flux along the wall. Since the sub-zonal model is not able to predict these numbers accurately, this results automatically in deviations of the convective surface transfer coefficients.
- The surface transfer coefficient model that is based on the locally applied correlations from Beausoleil-Morrison gave relatively good results for regions where recirculation does not take place, while the relative deviation is approximately 30%. The model cannot be applied in regions where local recirculation of the airflow takes place.

Mixed convection

- The application of a sub-zonal airflow model to predict the indoor environmental conditions and surface transfer coefficients for mixed convection in a room, ventilated at an air change rate of 11 h^{-1} and 2 h^{-1} is limited. Relatively large deviations up to 40% regarding both the global and local indoor environmental conditions in the room have been observed. The sub-zonal model which was best capable of predicting the indoor environmental conditions included a thermal boundary layer model to model the natural convective airflow along the walls. No specific model was added to account for forced convection.
- The ratio between natural and forced convection in the room is an important issue when modelling the indoor environmental conditions in the room. The sub-zonal airflow model was able to give a slightly better prediction of the indoor environmental conditions for the case with a relatively small air change rate of 2 h^{-1}, since natural convection was dominating the airflow pattern in the room.
    - For both ventilation regimes, it was possible to give a relatively accurate prediction of the local convective surface transfer coefficients with a maximum relative deviation of 20%, based on relationships for natural convective airflow in enclosures, in the part of the room where natural convection was dominating locally. However, with respect to the Western wall, where forced convective airflow was dominating locally, it was not feasible to predict the local surface transfer coefficients, while deviations up to factor 2 and higher have been observed.

While sub-zonal airflow models are definitely not capable for the prediction of the indoor environmental conditions with an accuracy which is comparable with that of CFD, sub-zonal models can give a satisfactory estimate of the local indoor environmental conditions in the room depending on the airflow regime in the room. Moreover, the local conditions predicted by the sub-zonal model are useful for the prediction of the local convective surface transfer coefficients. However, one important remark should be made. In the case studies, reference conditions, for example experimental data or numerical results from CFD, have been used for the development of a reliable sub-zonal airflow model. The availability of such reference conditions is a prerequisite for the development of a reliable sub-zonal model.

7.3 HAM-Airflow coupling

The hygrothermal performance of a building zone and building envelope has been investigated using a coupled whole-building HAM simulation. The model was used to analyze the heat, air and moisture transport in the indoor environment and within the building envelope as well as the interaction between both domains. A case study consisting of two rooms (on top of each other), separated by a concrete floor including a thermal bridge, and connected to the outdoor climate by a lightweight concrete wall was investigated. The influence of the local indoor environmental conditions and local surface transfer coefficients on the hygrothermal performance of the component has been analyzed. The airflow in the room is analyzed under natural convective conditions.

Four models have been applied to model the indoor environmental conditions and the convective surface transfer coefficients in the room. The predicted hygrothermal conditions on the internal surface of the building components predicted by the different models have been compared. Based on the investigations it is concluded that:

- Regarding the surface temperature and relative humidity on the surface of the building component, a relatively large relative difference up to approximately 10% has been observed between the separate HAM component models with lower and upper limits for the convective surface transfer coefficients.
- Considering the hygrothermal conditions on the surface of the building component predicted by the coupled HAM component and sub-zonal model and the coupled HAM component and nodal model smaller differences with a maximum relative difference of 5% have been observed.

The differences between the nodal model and the sub-zonal model showed to be relatively small, since the surface conditions on the building component are restricted by the indoor environmental conditions in the room and, in principle, are mainly subjected to the varying outdoor environmental conditions. The case study showed to be less suitable for demonstrating the influence of the varying local indoor environmental conditions and surface transfer coefficients on the hygrothermal conditions on the surface of and in the building component. Therefore, it is recommended for future research to apply the coupled HAM component model and sub-zonal airflow model for investigations considering larger and ventilated enclosures, where moisture sources are present, which results in a larger excitation of the indoor environmental conditions.

Based on the analyzed case, it is concluded that the coupled HAM component model and sub-zonal model provided detailed information of the local environmental conditions in the building zone near the building component, i.e. the local air temperature, and relative humidity, of the local conditions in the building component, and detailed information regarding the local convective surface transfer coefficients. Moreover, the model showed to be suitable for transient heat, air and moisture simulations of the component-indoor air interaction.

8 References

1. Intergovernmental Panel on Climate Change, 2001, Climate Change: The Scientific Basis, Cambridge University Press.
2. de Wilde, P., Rafiq, Y. & Beck, M., 2008, Uncertainties in predicting the impact of climate change on thermal performance of domestic buildings in the UK, Build. Serv. Eng. Res. Technol. 29, 7-26, Sage Publications.
3. Danish Building Defects Fund (Byggeskadefonden), 2008, Annual Report 2008 (Årsberetning 2008), Danish Building Defects Fund (Byggeskadefonden), Copenhagen.
4. Building Damage Fund for Building Renewal (Byggeskadefonden vedrørende Bygningsfornyelse) 2008, *Annual Report 2008 (Årsberetning 2008)*, Copenhagen.
5. International Energy Agency, Energy Conservation in Buildings and Community Systems programme, Annex 41, 2005, Whole building heat, air and moisture response.
6. Woloszyn, M.; Rode, C., 2008, Tools for performance simulation of heat, air and moisture conditions of whole buildings, Building Simulation, 1, 5-24, Tsinghua Press.
7. Holm, A., 2001, Ermittlung der Genauigkeit von instationären hygrothermischen Bauteilberechnungen mittels eines stochastischen Konzeptes, PhD thesis, TU Munich.
8. Janssen, H., Blocken, B., Carmeliet, J., 2007, Conservative modelling of the moisture and heat transfer in building components under atmospheric excitation, International Journal of Heat and Mass Transfer, vol. 50, no. 5-6, pp. 1128-1140.
9. Beausoleil-Morrison, I., 2000, The adaptive coupling of heat and air flow modeling within dynamic whole-building simulation, PhD thesis, University of Strathclyde.
10. Mortensen, L.H., 2007, Hygrothermal Microclimate on Interior Surfaces of the Building Envelope, PhD thesis, Technical University of Denmark.
11. Roels, S.; Janssen, H., 2006, A comparison of the Nordtest and Japanese test methods for the moisture buffering performance of building materials, Journal of Building Physics, vol. 30, pp. 137-161.
12. Abuku, M.; Janssen, H.; Roels, S., 2009, Impact of wind-driven rain on historic brick wall buildings in a moderately cold and humid climate: Numerical analyses of mould growth risk, indoor climate and energy consumption, Energy & Buildings, vol. 41, pp. 101-110.
13. Steeman, H.J., 2008, Modelling Local Hygrothermal Interaction between Airflow and Porous Materials for Building Applications, PhD thesis, Universiteit Gent.
14. Steskens, P. W. M. H., Janssen, H., Rode, C., 2009, Influence of the Convective Surface Transfer Coefficients on the Heat, Air, and Moisture (HAM) Building Performance, Indoor and Built Environment, 18, 245-256, SAGE Publications.
15. Kunzel, H. M., Holm, A., Zirkelbach, D., Karagiozis, A. N., 2005, Simulation of indoor temperature and humidity conditions including hygrothermal interactions with the building envelope, Solar Energy, vol. 78, pp. 554-561.
16. Nicolai, A.; Zhang, J. S.; Grunewald, J. Nicolai, A., Zhang, J.S., Grunewald, J., 2007, Coupling strategies for combined simulation using multizone and building envelope models, Proceedings of the 10th International Building Performance Simulation Association (IBPSA) Conference, pp. 1506-1513.
17. Djunaedi, E., 2005, External coupling between building energy simulation and computational fluid dynamics, PhD thesis, Eindhoven University of Technology.
18. Zhai, Z. J., Chen, Q., 2006, Sensitivity analysis and application guides for integrated building energy and CFD simulation, Energy and Buildings, vol. 38, no. 9, pp. 1060-1068.
19. Neale, A., Derome, D., Blocken, B., Carmeliet, J., 2007, Coupled Simulation of Vapor between Air and a Porous Material, Buildings X Conference Proceedings, American Society of Heating, Refrigerating and Air-Conditioning Engineers, Inc.
20. Mirsadeghi, M., Blocken, B.,Hensen, J., 2009, Application of Externally-coupled BES-CFD in HAM Engineering of the Indoor Environment, Eleventh International IBPSA Conference (Building Simulation 2009).

21. International Standards Organisation (ISO), 2001, Hygrothermal performance of building components and building elements – Internal surface temperature to avoid critical surface humidity and interstitial condensation – Calculation methods 2001, ISO 13788.
22. Kuenzel, H. M., Zirkelbach, D., Karagiozis, A. N., Holm, A., Sedlbauer, K., 2008, Simulating Water Leaks in External Walls to Check the Moisture Tolerance of Building Assemblies in Different Climates, Durability of Building Materials and Components 11, vol. 3, pp. 1379-1368.
23. Peuhkuri, R., Viitanen, H., Ojanen, T., 2008, Modelling of mould growth in building envelopes, IEA ECBCS Annex 41, Closing Seminar.
24. Blocken, B. J. E., Janssen, H., Carmeliet, J. E., 2005, On the modelling of runoff of driving rain on a capillary active surface., Proceedings of the 11th Symposium of Building Physics, vol. 1, pp. 400-409.
25. Crawley, D. B., Hand, J. W., Kummert, M., Griffith, B. T., 2008, Contrasting the capabilities of building energy performance simulation programs, Building & Environment, vol. 43, pp. 661-673.
26. Janssens, A., Rode, C., De Paepe, M., Woloszyn, M., Sasic-Kalagasidis, A., 2008, From EMPD to CFD - overview of different approaches for Heat Air and Moisture modelling, IEA ECBCS Annex 41 Closing Seminar, pp. 9-20.
27. Holm, A., Kuenzel, H. M., Sedlbauer, K., 2006, Raumklima Simulation—Methoden, Validierung, Anwendung, Wksb-Sonderheft, vol. 57, pp. 37-44.
28. Versteeg, H. K., Malalasekera, W., 2007, An Introduction to Computational Fluid Dynamics - The Finite Volume Method, Prentice Hall.
29. Zhai, Z., Zhang, Z., Zhang, W., Chen, Q., 2007, Evaluation of Various Turbulence Models in Predicting Airflow and Turbulence in Enclosed Environments by CFD: Part 1 -- Summary of Prevalent Turbulence Models, HVAC and R Research, vol. 13, pp. 853.
30. Jouvray, A., Tucker, P. G., Liu, Y. 2007, On nonlinear RANS models when predicting more complex geometry room airflows, International Journal of Heat and Fluid Flow, vol. 28, pp. 275-288.
31. Jouvray, A., Tucker, P. G., 2005, Computation of the flow in a ventilated room using non-linear RANS, LES and hybrid RANS/LES, International Journal for Numerical Methods in Fluids, vol. 48, pp. 99-106.
32. Chen, Q., 1995, Comparison of different k-varepsilon models for indoor air flow computations, Numerical Heat Transfer, Part B (Fundamentals), vol. 28, pp. 353-369.
33. Zhang, Z., Zhang, W., Zhai, Z., Chen, Q., 2007, Evaluation of Various Turbulence Models in Predicting Airflow and Turbulence in Enclosed Environments by CFD: Part 2 -- Comparison with Experimental Data from Literature, HVAC and R Research, vol. 13, pp. 871.
34. Lebrun, J., 1970, Exigences physiologiques et modalities physiques de la climatisation par source statique concentrée, PhD thesis, University de Liège.
35. Inard, C., Bouia, H., Dalicieux, P., 1996, Prediction of air temperature distribution in buildings with a zonal model, Energy and Buildings, vol. 24, pp. 125-132.
36. Mendonça, K.C., 2004, Modelisation thermo-hydro-aeraulique des locaux climatises selon l'approche zonale, PhD thesis, Université de La Rochelle.
37. Wurtz, E., Mora, L., Inard, C., 2006, An equation-based simulation environment to investigate fast building simulation, Building and Environment, vol. 41, pp. 1571-1583.
38. Teshome, E. J., Haghighat, F., 2004, Zonal Models for Indoor Air Flow - A Critical Review, International Journal of Ventilation, vol. 3, pp. 119.
39. Megri, A. C., 2007, Zonal Modeling for Simulating Indoor Environment of Buildings: Review, Recent Developments, and Applications, HVAC R research, vol. 13, pp. 887.
40. Wurtz, E., 1995, Modèlisation tridimensionnelle des transferts thermiques et aérauliques dans le bâtiment en environnement oriente objet, PhD thesis, Ecole nationale des ponts et chausses, Lyon, France.
41. Stewart, J., Ren, Z., 2006, COwZ-A subzonal indoor airflow, temperature and contaminant dispersion model, Building and Environment, vol. 41, pp. 1631-1648.
42. Jiru, T. E., Haghighat, F., 2006, A new generation of zonal models, ASHRAE Transactions, vol. 112 PART 2, pp. 163-174.
43. Axley, J. W., 2001, Surface drag flow relations for zonal modeling, Building and Environment, vol. 36, pp. 843-850.

44. Wurtz, E., Nataf, J., Winkelmann, F., 1999, Two- and three-dimensional natural and mixed convection simulation using modular zonal models in buildings, International Journal of Heat and Mass Transfer, vol. 42, pp. 923-940.
45. Haghighat, F., Wurtz, E., Haghighat, F., Mora, L., Maalouf, C., Bourdoukan, P., Mendonça, K. C., Coogan, J., Zhao, H., 2006, An integrated zonal model to predict transient indoor humidity distribution, ASHRAE Transactions, vol. 112, PART 2, pp. 175-186.
46. Mora, L., Gadgil, J., Wurtz, E., 2003, Comparing zonal and CFD model predictions of isothermal indoor airflows to experimental data, Indoor Air, vol. 13, pp. 77-85.
47. Nielsen, P. V., 1990, Specification of a Two-Dimensional Test Case, University of Aalborg, Aalborg.
48. Beausoleil-Morrison, I., 2002, The adaptive simulation of convective heat transfer at internal building surfaces, Building and Environment, vol. 37, pp. 791-806.
49. Erhorn, H., Szerman, M., 1992, Überprüfung der Wärme- und Feuchteübertragungskoeffizienten in Außenwanddecken von Wohnbauten, Gesundheits-Ingenieur, vol. 113, pp. 177-186.
50. Schlichting, H., Gersten, K., 2003, Boundary layer theory,8th edition, Springer, pp. 799.
51. Wallentén, P., 2001, Convective heat transfer coefficients in a full-scale room with and without furniture, Building and Environment, vol. 36, pp. 743-751.
52. Khalifa, A. N., 2001, Natural convective heat transfer coefficient - a review: I. Isolated vertical and horizontal surfaces, Energy Conversion and Management, vol. 42, pp. 491-504.
53. Khalifa, A. N., 2001, Natural convective heat transfer coefficient - a review: II. Surfaces in two- and three-dimensional enclosures, Energy Conversion and Management, vol. 42, pp. 505-517.
54. Alamdari, F., Hammond, G. P., 1983, Improved Data Correlations for Buoyancy-Driven Convection in Rooms, Building Services Engineering Research and Technology, vol. 4, pp. 106-112.
55. Fisher, D. E., 1995, An Experimental Investigation of Mixed Convection Heat Transfer in a Rectangular Enclosure, PhD thesis, University of Illinois.
56. Fohanno, S., Polidori, G., 2006, Modelling of natural convective heat transfer at an internal surface Energy & Buildings, vol. 38, pp. 548-553.
57. Awbi, H. B., Hatton, A., Natural convection from heated room surfaces, Energy & Buildings, vol. 30, pp. 233-244.
58. International Standards Organisation (ISO), 2004, Hygrothermal performance of building components and building elements—assessment of moisture transfer by numerical simulation, ISO15026.
59. Chilton, T. H., Colburn, A. P., 1934, Mass transfer (absorption) coefficients, Industrial and engineering chemistry, vol. 26, pp. 1183-1187.
60. Cengel, Y. A., 2003, Heat Transfer: A Practical Approach, McGraw-Hill.
61. Schwarz, B., 1972, Die Wärme- und Stoffübertragung an Außenwandoberflächen, PhD thesis, Univ. Stuttgart, Institut für Bauphysik der Fraunhofer-Gesellschaft Aussenstelle, Holzkirchen.
62. Bednar, T., Dreyer, J., 2003, Determination of moisture surface transfer coefficients under transient conditions, International Building Physics Conference II, Leuven.
63. Mortensen, L. H., Rode, C., Peuhkuri, R., 2006, Effect of airflow velocity on moisture exchange at surfaces of building materials, International Building Physics Conference III, Montreal.
64. Talev, G., Gustavsen, A., Næss, E., 2008, Influence of the velocity, local position, and relative humidity of moist air on the convective mass transfer coefficient in a rectangular tunnel - Theory and experiments, Journal of Building Physics, vol. 32, pp. 155-173.
65. Worch, A., 2004, The behaviour of vapour transfer on building material surfaces: The vapour transfer resistance, Journal of Thermal Envelope and Building Science, vol. 28, pp. 187-200.
66. Iskra, C. R., Simonson, C. J., 2007, Convective mass transfer coefficient for a hydrodynamically developed airflow in a short rectangular duct, International Journal of Heat and Mass Transfer, vol. 50, pp. 2376-2393.
67. Paepe, M. De, 2008, Surface transfer coefficients in Annex 41 Whole building Heat, Air, Moisture Response. Boundary Conditions and Whole Building HAM Analysis, vol. 3, Chapter 3, p 65.
68. Mortensen, L. H., Woloszyn, M., Rode, C., Peuhkuri, R., 2007, Investigation of Microclimate by CFD Modeling of Moisture Interactions between Air and Constructions, Journal of Building Physics, vol. 30, pp. 279.

69. Chen, Q., Peng, X., van Paassen, A. H. C., 1995, Prediction of room thermal response by CFD technique with conjugate heat transfer and radiation models, ASHRAE Transactions, vol. 101, pp. 50-60.
70. Zhai, Z., Chen, Q., Haves, P., Klems, J.H., 2002, On approaches to couple energy simulation and computational fluid dynamics programs, Building and Environment, vol. 37, pp. 857-864.
71. Cunningham, M. J., 1992, Effective penetration depth and effective resistance in moisture transfer, Building and Environment, vol. 27, pp. 379-386.
72. Zhai, Z., Chen, Q., 2003, Solution characters of iterative coupling between energy simulation and CFD programs, Energy and Buildings, vol. 35, pp. 493-505.
73. Clovis, R. M., 2001, Issues on the integration of CFD to building simulation tools, Proceedings of the Seventh International IBPSA Conference, Rio de Janeiro, vol. 1, pp. 29-40.
74. Zhang, J. S.; Christianson, L. L.; Wu, G. J.; Riskowski, G. L., 1992, Detailed measurements of room air distribution for evaluating numerical simulation models, ASHRAE Transactions, vol. 98, pp. 58-65.
75. Zhai, Z., Chen, Q., Klems, J. H.; Haves, P., 2001, Strategies for coupling energy simulation and computational fluid dynamics programs, Proceedings of the Seventh International IBPSA Conference, Rio de Janeiro, Brazil.
76. Sempey, A., Inard, C., Ghiaus, C., Allery, C., 2009, Fast simulation of temperature distribution in air conditioned rooms by using proper orthogonal decomposition, Building and Environment, vol. 44, pp. 280-289.
77. Rode, C., Woloszyn, M., 2004, Common Exercise 1 (Whole building heat, air and moisture analysis), International Energy Agency, Energy Conservation in Buildings and Community Systems programme, Annex 41 - Subtask 1.
78. Nicolai, A., Grunewald, J. 2006, CHAMPS-BES Program for Coupled Heat, Air, Moisture and Pollutatant Simulations in Building Envelope Systems (User Manual), BEESL - Building Energy and Environmental Systems Laboratory, Department of Mechanical and Aerospace Engineering, Syracuse University, NY, Syracuse, NY.
79. Wit, M. H. de, 2006, HAMBASE - Heat Air and Moisture model for Buildings and Systems Evaluation, Eindhoven University Press, Eindhoven, the Netherlands.
80. Hens, H.S.L.C., 2007, Building Physics - Heat, Air and Moisture - Fundamentals and Engineering Methods with Examples and Exercises, Ernst & Sohn, Wiley.
81. Nielsen, P. V., 1976, Flow in Air Conditioned Rooms. Model experiments and numerical solution of the flow equations, PhD thesis, Technical University of Denmark.
82. Chen, Q., 1991, Simulation of Simple Test Cases, Energy Conservation in Buildings and Community Systems programme, Annex 20 Air flow patterns within buildings, Subtask 1: Room Air and Contaminant Transport.
83. Rajaratnam, N., 1976, Turbulent Jets, Elsevier Scientific Publishing Company, Amsterdam - Oxford - New York.
84. Rajaratnam, N., 1976, Plane turbulent wall jets (Chapter 10), Turbulent Jets, Elsevier Scientific Publishing Company, Amsterdam - Oxford - New York.
85. Ren, Z., 2002, Enhanced modeling of indoor airflows, temperatures, pollutant emission and dispersion by nesting sub-zones within a multizone model, PhD thesis, Queen's University of Belfast.
86. Collier, A. M., Hindmarshm, A. C., Serban, R., Woodward, C. S., 2006, User Documentation for KINSOL v.2.5.0, Centre for Applied Scientific Computing, Lawrence Livermore National Laboratory.
87. Turner, B. L., Flake, L. D., 1980, The experimental measurement of natural convection heat transfer in rectangular enclosures, ASME Transactions, Journal of Heat Transfer, vol. 102, pp. 236-241.
88. Bohn, M. S., Kirkpatrik, A. T., Olson, D. A., 1984, Experimental study of three-dimensional natural convection and high Rayleigh numbers, ASME Transactions, Journal of Heat Transfer, vol. 106, pp. 339-384.
89. Allard, F., Brau, J., Inard, C., Pallier, J. M., 1987, Thermal experiments of full-scale dwelling cells in artificial climatic conditions, Energy and Buildings, vol. 10, pp. 49-58.
90. Allard, F., Inard, C., Simoneau, J. P., Phénomènes convectifs intérieurs dans les cellules d'habitation. Approches expérimentales et numériques, Revue Générale de Thermique, vol. 29, pp. 216-225.

91. Chen, Q., Xu, W., 1998, A zero-equation turbulence model for indoor airflow simulation, Energy and Buildings, vol. 28, pp. 137-144.
92. Walton, G. N., 1980, A new algorithm for radiant exchange in room loads calculations, ASHRAE Transactions, vol. 86, pp. 190-208.
93. Sedlbauer, K., Krus, M., Breuer, K., 2003, Mould growth prediction with a new biohygrothermal method and its application in practice, Polska Konferencja Naukowo-Techniczna Fizyka Budowli Teorii i Praktyce.

Bibliography

Journal Papers

Steskens, P.W.M.H., Janssen, H., Rode, C., (2009), *Influence of the convective surface transfer coefficients on the Heat, Air, and Moisture (HAM) building performance*, Indoor and Built Environment, vol:18, issue: 3, pages: 245-256, Sage Science Press (UK)

Conference Papers

Steskens, P.W.M.H., Janssen, H., Rode, C., (2009), *Modeling Local Hygrothermal Interactions: Local Surface Transfer Coefficients*, Healthy Buildings Conference 2009, Syracuse, NY.

Steskens, P.W.M.H., Janssen, H., Rode, C., (2008), *Influences of the Indoor Environment on Heat, Air, and Moisture Conditions in the Component: Boundary conditions modelling*, Proceedings of the 8th Symposium on Building Physics in the Nordic Countries, pages: 653-660, 2008, Danish Society of Engineers, IDA, Copenhagen

Steskens, P.W.M.H., Janssen, H., Rode, C., (2008), *Influences of the Indoor Environment on Heat, Air and Moisture Conditions in the Building Component: Boundary Conditions Modelling*, Durability of Building Materials and Components, Globality and Locality in Durability, pages: 1433-1440, 2008, Istanbul Technical University, Istanbul

Other contributions

Steskens, P.W.M.H., Janssen, H., Rode, C., (2009), *Model for Multidimensional Heat, Air, and Moisture Conditions in Building Envelope Components*, CHAMPS Seminar, Syracuse University, Syracuse, NY.

Steskens, P.W.M.H., Janssen, H., Rode, C., (2008), *Coupled Modeling of Indoor Environment and HAM Response*, CHAMPS Seminar, University of La Rochelle, La Rochelle.

Steskens, P.W.M.H., Janssen, H., Rode, C., (2007), *Model for Multidimensional Heat, Air, and Moisture Conditions in Building Envelope Components*, CHAMPS Seminar, 12th Symposium for Building Physics, Dresden University of Technology, Dresden.

List of Symbols

A	Surface	[m^2]
ACH	Air change rate	[h^{-1}]
b_0	Diffuser thickness	[m]
Bi	Biot number	[-]
c_p	Thermal capacity	[J kg^{-1} K^{-1}]
C	Gas contaminant concentration	[mol mol^{-1}]
C_d	Emperical permeablility constant	[m s^{-1} Pa^{-n}]
d	Thickness	[m]
d_p	Penetration depth	[m]
D	Mass diffusivity	[m^2s^{-1}]
D_v	Vapour diffusivity	[m^2s^{-1}]
e	Effusivity	[-]
g	Gravitational acceleration	[m s^{-2}]
g	mass flux	[kg m^{-2} s^{-1}]
Gr_x	Local Grashof number	[-]
h	Height	[m]
H	Height	[m]
L	Length	[m]
L_H	Characteristic length for heat transfer	[m]
L_M	Characteristic length for moisture transfer	[m]
Le	Lewis number	[-]
m	Mass flux	[kg s^{-1}]
m_v	vapour content per kg dry air	[kg kg^{-1}]
n	Power-law exponent	[-]
Nu_x	Local Nusselt number	[-]
p	Pressure	[Pa]
P_v	Partial vapour pressure	[Pa]
Pr	Prandtl number	[-]
q	Heat flux	[W m^{-2}]
Ra_x	Local Rayleigh number	[-]
Re_x	Local Reynolds number	[-]
RH	Relative humidity	[%]
Sc	Schmidt number	[-]
St	Stanton number	[-]
t	Time	[s]
t_p	period of time	[s]
T	Temperature	[K]
$\underline{u}$	Velocity	[m s^{-1}]
v	Velocity	[m s^{-1}]
x	Coordinate	[m]
X	Mass fraction (species mass per mixture mass)	[kg kg^{-1}]
y	Coordinate	[m]
Z	Mole fraction (moles of species per mole mixture)	[mol mol^{-1}]

Greek symbols

α	Thermal diffusivity	[m^2s^{-1}]
α	Surface heat transfer coefficient	[$W\ m^{-2}K^{-1}$]
α_c	Convective surface heat transfer coefficient	[$W\ m^{-2}K^{-1}$]
α_r	Radiative surface heat transfer coefficient	[$W\ m^{-2}K^{-1}$]
β	Thermal expansion coefficient	[K^{-1}]
β_c	Surface moisture transfer coefficient (related to the partial vapour pressure P_v)	[$s\ m^{-1}$]
β^ρ	Surface moisture transfer coefficient related to the vapour density ρ	[$m\ s^{-1}$]
β^X	Surface moisture transfer coefficient related to the vapour mass fraction X	[$m\ s^{-1}$]
β^P	Surface moisture transfer coefficient related to the partial vapour pressure P_v	[$s\ m^{-1}$]
β^Z	Surface moisture transfer coefficient related to the vapour mole fraction Z.	[$kg\ mol\ m^{-2}\ s^{-1}\ mol^{-1}$]
δ	Boundary layer thickness	[m]
δ	Vapour permeability	[s]
ϕ	Volume flow	[m^3s^{-1}]
ϕ_v	Vapour flux	[$kg\ m^{-3}\ s^{-1}$]
λ	Thermal conductivity	[$W\ m^{-1}K^{-1}$]
ν	Kinematic viscosity	[m^2s^{-1}]
ρ	Density	[$kg\ m^{-3}$]
ζ	Moisture capacity	[$kg\ m^{-3}$]

Subscripts

Avg	Average
c	Convective
c,f	Forced convective
f	Fluid
H	Thermal
Max	Maximum
M	Hygric
s	Surface
v	Vapour
∞	Infinity/Free stream